3GPP TR 38.812 V16.0.0 (2018-12)

Technical Report

3rd Generation Partnership Project;
Technical Specification Group Radio Access Network;
Study on Non-Orthogonal Multiple Access (NOMA) for NR
(Release 16)

Keywords

<New Radio, NOMA>

3GPP

Postal address

3GPP support office address

650 Route des Lucioles - Sophia Antipolis
Valbonne - FRANCE
Tel.: +33 4 92 94 42 00 Fax: +33 4 93 65 47 16

Internet

http://www.3gpp.org

Contents

Foreword

This Technical Report has been produced by the 3rd Generation Partnership Project (3GPP).

The contents of the present document are subject to continuing work within the TSG and may change following formal TSG approval. Should the TSG modify the contents of the present document, it will be re-released by the TSG with an identifying change of release date and an increase in version number as follows:

Version x.y.z

where:

- x the first digit:
  - 1 presented to TSG for information;
  - 2 presented to TSG for approval;
  - 3 or greater indicates TSG approved document under change control.
- y the second digit is incremented for all changes of substance, i.e. technical enhancements, corrections, updates, etc.
- z the third digit is incremented when editorial only changes have been incorporated in the document.

Introduction

The basic multiple access scheme for NR is orthogonal for both downlink and uplink data transmissions, e.g., time and frequency physical resources of different users are not overlapped. On the other hand, non-orthogonal multiple-access schemes recently gained wide interest.

Non-orthogonal transmission can be applied to both grant-based and grant-free transmission. The benefits of non-orthogonal multiple access, particularly when enabling grant-free transmission, may encompass a variety of use cases or deployment scenarios, including eMBB, URLLC, mMTC etc. In RRC_CONNECTED state, it saves the scheduling request procedure assuming UE is already uplink synchronized. In RRC_INACTIVE state, data can be transmitted even without RACH procedure or with 2-step RACH. The saving of the signalling naturally also saves UE's power consumption, reduces latency and increases system capacity.

1 Scope

This document is intended to gather all technical outcome of the study item "Study on non-orthogonal multiple access (NOMA) for NR" [2], and draw a conclusion on a way forward.

This activity involves the Radio Access work area of the 3GPP studies and has impacts both on the Mobile Equipment and Access Network of the 3GPP systems.

2 References

The following documents contain provisions which, through reference in this text, constitute provisions of the present document.

- References are either specific (identified by date of publication, edition number, version number, etc.) or non-specific.
- For a specific reference, subsequent revisions do not apply.
- For a non-specific reference, the latest version applies. In the case of a reference to a 3GPP document (including a GSM document), a non-specific reference implicitly refers to the latest version of that document *in the same Release as the present document*.

[1] 3GPP, TR 21.905: "Vocabulary for 3GPP Specifications".

[2] 3GPP, RP-181403, New Study Item proposal: Study on non-orthogonal multiple access (NOMA) for NR, RAN Plenary#80

[3] 3GPP, R1-1803615, Key processing modules at transmitter side for NOMA, ZTE, Sanechips, RAN1#92bis

[4] 3GPP, R1-1803663, Discussion on the design of SCMA, Huawei, HiSilicon, RAN1#92bis

[5] 3GPP, R1-1803770, PDMA transmitter side signal processing, CATT, RAN1#92bis

[6] 3GPP, R1-1803850, Discussion on NOMA transmitters, vivo, RAN1#92bis

[7] 3GPP, R1-1804396, Transmitter side signal processing schemes for NOMA, Samsung, RAN1#92bis

[8] 3GPP, R1-1804462, Considerations on NOMA transmitter, Nokia, Nokia Shanghai Bell, RAN1#92bis

[9] 3GPP, R1-1804573, Transmitter side signal processing schemes for NCMA, LG Electronics, RAN1#92bis

[10] 3GPP, R1-1804743, NOMA transmission scheme: LCRS, Intel Corporation, RAN1#92bis

[11] 3GPP, R1-1804823, Transmitter side signal processing schemes for NOMA, Qualcomm Incorporated, RAN1#92bis

[12] 3GPP, R1-1804859, Implementation Aspects of Low Code Rate NOMA Schemes, InterDigital, Inc., RAN1#92bis

[13] 3GPP, R1-1804941, Tx side processing for UL NOMA, NICT, RAN1#92bis

[14] 3GPP, R1-1805003, Signature design for NoMA, Ericsson, RAN1#92bis

[15] 3GPP, R1-1805065, Transmitter design for uplink NOMA, NTT DOCOMO, INC., RAN1#92bis

[16] 3GPP, R1-1805840, Key processing modules at transmitter side for NOMA, ZTE, RAN1#93

[17] 3GPP, R1-1806241, Signature design for NoMA, Ericsson, RAN1#93

[18] 3GPP, R1-1807223, Design Considerations for NOMA Transmitter, Convida Wireless LLC, RAN1#93

[19] 3GPP, R1-1809753, Discussion on the design of SCMA, Huawei, HiSilicon, RAN1#94

[20] 3GPP, R1-1808151, Transmitter side designs for NOMA, ZTE, RAN1#94

[21] 3GPP, R1-1808230, Discussion on NOMA transmitters, vivo, RAN1#94

[22] 3GPP, R1-1808331, Consideration on the transmitter side signal processing for NOMA, Sony, RAN1#94

[23] 3GPP, R1-1808386, NOMA transmitter side signal processing, CATT, RAN1#94

[24] 3GPP, R1-1808499, Transmitter side signal processing schemes for NCMA, LG Electronics, RAN1#94

[25] 3GPP, R1-1808677, NOMA transmission scheme, Intel Corporation, RAN1#94

[26] 3GPP, R1-1808760, Transmitter side signal processing schemes for NOMA, Samsung, RAN1#94

[27] 3GPP, R1-1808948, New Coding Scheme for NOMA with Traffic Control, Sequans Communications, RAN1#94

[28] 3GPP, R1-1808955, Discussion on general symbol-to-resource mapping for NR-NOMA, Fraunhofer HHI, Fraunhofer IIS, RAN1#94

[29] 3GPP, R1-1808968, Considerations on NOMA Transmitter, Nokia, Nokia Shanghai Bell, RAN1#94

[30] 3GPP, R1-1809148, Transmitter design for uplink NOMA, NTT DOCOMO, INC. , RAN1#94

[31] 3GPP, R1-1809434, Transmitter side signal processing schemes for NOMA, Qualcomm Incorporated, RAN1#94

[32] 3GPP, R1-1804169, CMA-OFDM with NR LDPC code for Uplink NOMA, HUGHES, RAN1#92bis

[33] 3GPP, R1-1802069, Signature generation and structure of LSSA, ETRI, RAN1#92

[34] 3GPP, TS38.211, Physical channels and modulation (Release 15)

[35] 3GPP, R1-1809499, Transmitter side signal processing schemes for NOMA, Samsung, RAN1#94

[36] Yang Hu; Chulong Liang; Jianhao Hu; Ping Li; "Low-cost Implementation Techniques for Interleave Division Multiple Access," IEEE Wireless Communications Letters, June 2018.

[37] Dhillon, I.S., Heath, R.W., Sustik, M.A., et al., "Generalized Finite Algorithms for Constructing Hermitian Matrices with Prescribed Diagonal and Spectrum," SIAM Journal on Matrix Analysis and Applications, 27(1):61-71, 2005.

[38] 3GPP, R1-1808205, NR-NOMA: Partially Asynchronous and Multi-layered transmission of ACMA, Hughes, RAN1#94

[39] 3GPP, R1-1811860, NOMA transmitter side signal processing, CATT, RAN1#94bis

[40] 3GPP, R1-1812095, Email discussion of more observations on LLS results, ZTE, RAN1#94bis

[41] 3GPP, R1-1814143, Performance summary of cases 32 through 35, Ericsson, RAN1#95

[42] 3GPP, R1-1814073, System level simulation results for NOMA, ZTE, Sanechips, RAN1#95

[43] 3GPP, R1-1813922, SLS evaluations and observations in mMTC, Huawei, HiSilicon, RAN1#95

[44] 3GPP, R1-1813997, Additional NOMA SLS evaluations, Huawei, HiSilicon, RAN1#95

[45] 3GPP, R1-1812969, Performance evaluation for NoMA, Samsung, RAN1#95

[46] 3GPP, R1-1813159, System Level evaluations for NOCA, Nokia, Nokia Shanghai Bell, RAN1#95

[47] 3GPP, R1-1814341, On NOMA mMTC SLS Evaluation, InterDigital, Inc. , RAN1#95

[48] 3GPP, R1-1813923, SLS evaluations and observations in uRLLC, Huawei, HiSilicon, RAN1#95

[49] 3GPP, R1-1812612, Link and system level evaluation results of NOMA, CATT, RAN1#95

[50] 3GPP, R1-1813924, SLS evaluations and observations in eMBB, Huawei, HiSilicon, RAN1#95

[51] 3GPP, R1-1814149, Link and system level evaluation for NOMA, Qualcomm Incorporated, RAN1#95

[52] 3GPP, R1-1814077, Evaluation results of UL NOMA, DCM, RAN1#95

[53] 3GPP, R1-1812190, Further discussion on NOMA evaluations, Huawei, HiSilicon, RAN1#95

[54] 3GPP, R1-1812189, Discussion on NOMA related procedures, Huawei, HiSilicon, RAN1#95

[55] 3GPP, R1-1812174, Procedures related to NOMA, ZTE, RAN1#95

[56] 3GPP, R1-1813900, System evaluation results for NOMA, ZTE, RAN1#95

[57] 3GPP, R1-1813307, NOMA related procedures, NTT DOCOMO, RAN1#95

[58] 3GPP, R1-1812611, Discussion on NOMA procedures, CATT, RAN1#95

[59] 3GPP, R1-1812296, Evaluations for NOMA, vivo, RAN1#95

[60] 3GPP, R1-1812477, NOMA related procedure, Intel Corporation, RAN1#95

[61] 3GPP, R1-1811194, Details of IDMA Transmitter Processing, InterDigital, RAN1#94b

[62] 3GPP, R1-1808763, Performance evaluation for NoMA, Samsung, RAN1#94

[63] 3GPP, R1-1813211, IDMA-based Multi-layer NOMA Transmission, InterDigital, RAN#95

[64] 3GPP, R1-1813858, Complexity analysis of NOMA receivers ZTE, Sanechips, RAN1#95

[65] 3GPP, R1-1813920, Discussion on the design of NOMA receiver, Huawei, HiSilicon, RAN1#95

[66] 3GPP, R1-1814043, NOMA receiver structure and complexity analysis, Intel Corporation, RAN1 #95

[67] 3GPP, R1-1813157, Receiver considerations for UL NOMA, Nokia, Nokia Shanghai Bell, RAN1#95

[68] 3GPP, R1-1813870, Receiver for uplink NOMA,NTT DOCOMO, INC, RAN1#95

[69] 3GPP, R1-1813160, Complexity Analysis of MMSE-based Hard IC Receiver, Nokia, Nokia Shanghai Bell, RAN1#95

[70] 3GPP, R1-1814315, Discussion on NOMA receivers, CATT, RAN1#95

[71] 3GPP, R1-1812967, Receivers for NoMA, Samsung, RAN1#95

[72] 3GPP, R1-1810623, Transmitter side signal processing of ACMA, HUGHES, RAN1#94bis

3 Definitions, symbols and abbreviations

3.1 Definitions

For the purposes of the present document, the terms and definitions given in 3GPP TR 21.905 [1] and the following apply. A term defined in the present document takes precedence over the definition of the same term, if any, in 3GPP TR 21.905 [1].

<defined term>: *<definition>.*

example: text used to clarify abstract rules by applying them literally.

3.2 Symbols

For the purposes of the present document, the following symbols apply:

<symbol> <Explanation>

3.3 Abbreviations

For the purposes of the present document, the abbreviations given in 3GPP TR 21.905 [1] and the following apply. An abbreviation defined in the present document takes precedence over the definition of the same abbreviation, if any, in 3GPP TR 21.905 [1].

BLER	BLock Error Rate
CP	Cyclic Prefix
DMRS	DeModulation Reference Signal
eMBB	enhanced Mobile BroadBand
EPA	Expectation Propagation Algorithm
ESE	Elementary Signal Estimator
FO	Frequency Offset
GP	Guard Period
IC	Interference Cancellation
MA	Multiple Access
IRC	Interference Rejection Combining
MAP	Maximum A Posteriori
MF	Matched Filter
MMSE	Minimum-Mean Squared Error
mMTC	massive Machine-Type Communication
MPA	Message-Passing Algorithm
NCP	Normal Cyclic Prefix
NOMA	Non-Orthogonal Multiple Access
NR	New Radio
OCC	Orthogonal Cover Code
OFDM	Orthogonal Frequency Division Multiplexing
PAPR	Peak to Average Power Ratio
PIC	Parallel Interference Cancellation
SIC	Successive Interference Cancellation
SINR	Signal to Interference plus Noise Ratio
SISO	Soft-Input-Soft-Output decoder
SNR	Signal to Noise Ratio
TO	Timing Offset
UE	User Equipment
URLLC	Ultra Reliable Low Latency Communication

4 Deployment scenarios

4.1 mMTC scenario

mMTC scenario is featured by massive number of connections with low control signalling overhead. Synchronous or asynchronous transmission are considered for the study [2]. The simulation assumptions for mMTC are included in Annex A.

4.2 URLLC scenario

URLLC requires both high reliability and low latency in the transmission. Synchronous transmission is considered for the study [2]. The simulation assumptions for URLLC are included in Annex A.

4.3 eMBB scenario

The transmission can be grant-based or grant-free. For grant-free, synchronous or asynchronous transmission are considered for the study [2]. The simulation assumptions for eMBB are included in Annex A.

5 Uplink NOMA transmission side processing

NOMA transmitter processing can be summarized as shown in the figure below, where the blocks in black and white reuse the current NR design, while new blocks with specification impact are highlighted in green. It should be noted that, the initialization seed for the legacy bit-scrambling sequence generation can be updated which may involve certain specification impact.

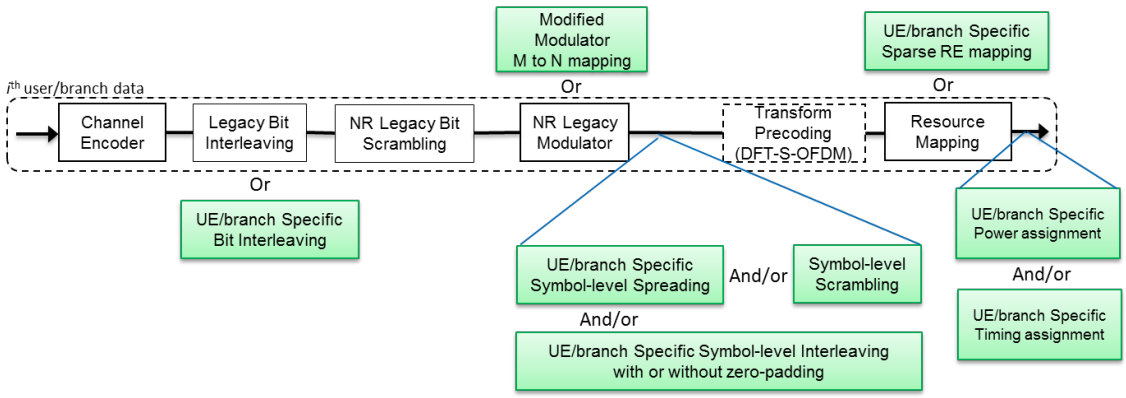

Figure 5.1: General structure of NOMA transmitter processing

NOMA transmission side processing is characterized by multiple access (MA) signature and auxiliary features. MA signature is typically used to differentiate users. In this subclause, MA signatures are described more from the perspective of traffic data.

5.1 Candidate MA signatures

5.1.1 Bit level processing based

The bit-level processing for NOMA achieves the user separation by randomizing the signals from other users [6][7][10] [12][13][18][22][32][35]. There are two ways of randomization, i.e. scrambling or interleaving.

UE-specific bit-level scrambling:

Bit-level scrambling based NOMA schemes such as LCRS [25] and NCMA [24] utilize the same transmitter processing procedure as Rel-15 NR PUSCH including channel encoding, rate matching, bit-level scrambling and then modulator, as shown in Figure 5.1-1.

Bit-level scrambling function defined in TS 38.211 Subclause 6.3.1.1 [34] can be the MA signature as it is defined in a UE-specific manner.

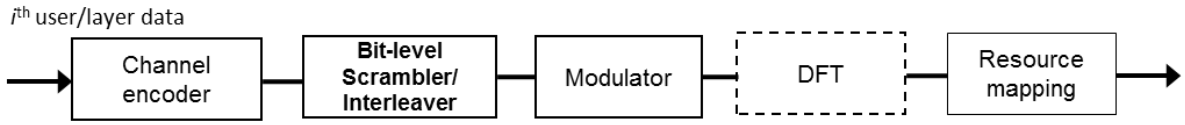

Figure 5.1-1: Transmitter procedure for bit-level processing (modules with dash blocks are optional).

UE-specific bit-level interleaving:

Bit-level interleaving based NOMA schemes such as IDMA [18][22][29] and IGMA [26][35] share the same transmitter processing at bit-level as in Figure 5.1-1. UE-specific interleaving pattern can be the MA signature. For example, UE specific interleaver based on NR LDPC block interleaver can replace the common block interleaver in rate matching module, i.e. the starting position of reading could be cyclically shifted with different offsets for different UEs as shown in Figure 5.1-2 [26][30].

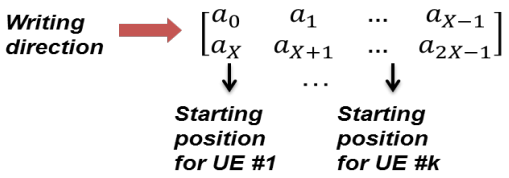

Figure 5.1-2: UE specific block interleaver design

Another example for the realization of user-specific interleaving is depicted in Figure 5.1-3, where a user-specific cyclic shift is introduced, allowing the same user-independent interleaving operation to be executed by K users. The combination of user-specific cyclic shift and non-user-specific interleaving is equivalent to user-specific interleaving [36].

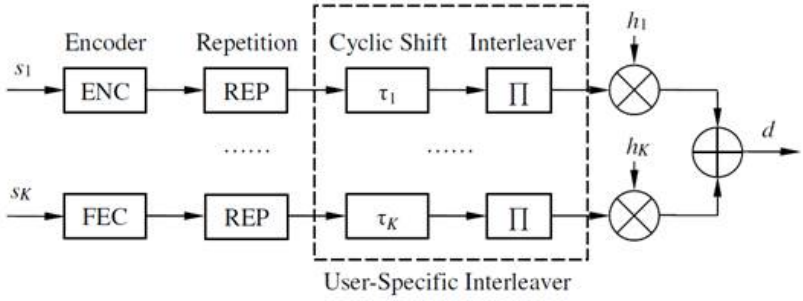

Figure 5.1-3: An example of user specific interleaving.

5.1.2 Symbol level processing

MA signatures applied at symbol level can have the following types: UE-specific spreading with NR legacy modulation, UE-specific spreading with modified modulation, scrambling, and UE-specific interleaving with zero-padding.

UE-specific symbol-level spreading with NR legacy modulation.

Symbol-level spreading sequences of low cross-correlation or low density are a type of MA signature and can be used to separate different users [3][4][5][8][9][11][14][15][27][33]. Symbols may be drawn from BPSK [21], QPSK, or higher

order QAM constellations to adjust spectral efficiency. For BPSK, e.g., {(1+j)/sqrt(2), (-1-j)/sqrt(2)}, it can be considered for CP-OFDM waveform. The transmitter processing procedure can be found in Figure 5.1-4.

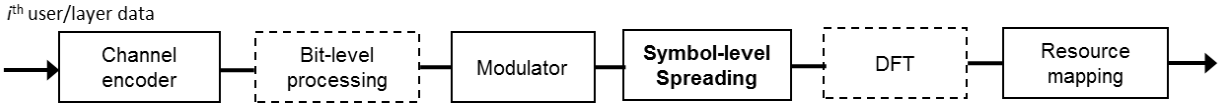

Figure 5.1-4: Transmitter procedure for symbol-level spreading with NR legacy modulation

Various designs of symbol-level spreading sequences are proposed for NOMA.

1) WBE sequences

In Welch bound equality (WBE) based spreading schemes such as WSMA [17] and RSMA [31], the design metric for the signature vectors is the total squared cross-correlation $T_c \triangleq \sum_{i,j} \| s_i^H s_j \|^2$. The lower bound on the total squared cross-correlation of any set of K vectors of length N, is $K^2/N \le T_c$. The WBE sequences are designed to meet the bound on the total squared cross-correlations of the vector set with equality $B_{Welch} \triangleq K^2/N$. Some examples of sequence generation method for the construction of WBE spreading sequences can be found in *Annex A.4.1* and *Annex A.4.2*.

2) Complex-valued sequences with quantized elements

The elements of spreading sequences can be drawn from quantized constellations as seen in MUSA [16]. Examples of QPSK and 9-QAM constellations are illustrated in Figure 5.1-5. The total numbers of sequences are 4^N and 9^N, respectively where N is the spreading factor. Example subsets of such sequences can be found in *Annex A.4.3*.

(a) 9-QAM (b) QPSK

Figure 5.1-5: Constellation of complex-valued spreading sequence.

3) ETF/Grassmannian sequences

A stricter Welch-bound equality is to minimize the maximum value of the cross-correlations among any of the two sequences, which is known as Equiangular Tight Frames (ETF) [17] or Grassmannian sequences, as seen in NCMA [24].

a) Grassmannian Sequence

i) Each complex spreading sequence of this sequence set is generated by Grassmannian line packing problem. Let the Grassmannian sequence set be defined by

$$G = \left[s^{(1)} \quad \dots \quad s^{(K)} \right] = \begin{bmatrix} s_1^{(1)} & \dots & s_1^{(K)} \\ \vdots & \ddots & \vdots \\ s_N^{(1)} & \dots & s_N^{(K)} \end{bmatrix}, G \subset C^{N \times K} \quad ,$$

where N is the spreading factor and K is the superposition factor, the sequence design problem can be posed as maximizing the minimum chordal distance between sequence pairs:

$$\min_{G}\left(\max_{1\le k<j\le K}\sqrt{1-\left|s^{(k)*}\cdot s^{(j)}\right|^2}\right),$$

where $s^{(k)*}$ is the conjugate sequence of $s^{(k)}$.

ii) Spreading sequence set: $G=\left[s^{(1)}\ \ \ldots\ \ s^{(K)}\right]$

b) M-QAM quantized Grassmannian Sequence

i) Each complex coefficient of this sequence (generated by the Grassmannian sequence) is quantized by M-QAM constellations. Then, the M-QAM quantized Grassmannian sequence set is defined by

$$\hat{G}=\left[\hat{s}^{(1)}\ \ \ldots\ \ \hat{s}^{(K)}\right]=\begin{bmatrix}\hat{s}_1^{(1)} & \ldots & \hat{s}_1^{(K)}\\ \vdots & \ddots & \vdots\\ \hat{s}_N^{(1)} & \ldots & \hat{s}_N^{(K)}\end{bmatrix}, G\subset C^{N\times K},$$

where *N* is the spreading factor and *K* is the superposition factor.

ii) Complex coefficient: $\hat{s}_i^{(j)}=c$, $i=1\le i\le N, i=1\le j\le K, c\in$ the set of M-QAM constellations

iii) Spreading sequence set: $\hat{G}=\left[\hat{s}^{(1)}\ \ \ldots\ \ \hat{s}^{(K)}\right]$

Some example of Grassmannian sequences can be found in *Annex A.4.4*.

4) GWBE sequences

Generalized welch-bound equality (GWBE) sequences are used as the MA signature, in the scheme of UGMA [30]. The cross-correlation between the received signals for multiple users is $R_x=S^H PS$, where $P=diag\{P_1,\ldots,P_K\}$ is a diagonal matrix whose diagonal elements are received powers of *K* users. Then, sequences satisfy

$$\min_{s_k^H s_k=1\,\forall\,k} R_x=\left\|S^H PS\right\|_F^2=\sum_{i=1}^{K}\sum_{j=1}^{K}P_iP_j\left|s_i^H s_j\right|^2,$$

where P_j is the received power of user *j*. In this case, sequences meeting the equality in generalized Welch-bound $\sum_{i=1}^{K}\sum_{j=1}^{K}P_iP_j\left|s_i^H s_j\right|^2\ge\frac{\left(\sum_{k=1}^{K}P_k\right)^2}{N}$ are selected, which are called as GWBE sequences. Some examples of GWBE sequences for 8, 12 and 16 users in two groups and 6dB SNR gap between the two groups can be found in *Annex A.4.5*. For any other given number of users *K*, spreading factor *N* and powers $\{P_1,\ldots,P_K\}$, the corresponding GWBE sequences can be generated by the algorithm in *Annex A.4.5*.

It should be noted that the elements of GWBE sequences are irregular complex values. Both the real and imaginary parts of GWBE sequences can be quantized into discrete values, e.g., $\{-1,0,1\}$ or $\{-1,1\}$ or $\{-2,-1,0,1,2\}$ etc. Some examples of quantized GWBE sequences are also provided in *Annex A.4.5*. For equal received power, GWBE sequences reduce to WBE sequences.

5) QPSK-based sequences

QPSK-based sequence applied in NOCA [29] which is same as DMRS sequence generation, $r_{u,v}(n)=\exp\left(\frac{j\varphi(n)\pi}{4}\right), 0\le n\le N-1$, where $\varphi(n)$ is given in *Annex A.4.6* for spreading factor equals to 4, 6 and 12 for each root u. It should be noted that the number of roots and the corresponding numer of sequences in *Annex A.4.6* is an example. Additional roots can be added as needed.

The sequences based on QPSK are obtained from computer search. The cross-correlations are 0 among sequences with the same root and different cyclic shifts, and low correlation among different root sequences.

Another example of symbol-level spreading where each modulated symbol is spread with different spreading sequence [29][31].

6) Sparse spreading patterns

Zeros are included in the spreading sequences with sparse spreading pattern.

a) Equal weighted such as SCMA [19]: the number of zeros is the same for each pattern. For example, the sparse patterns of sparse level 50% over the spreading block of size 4 are

$$\begin{bmatrix}1\\1\\0\\0\end{bmatrix},\begin{bmatrix}0\\0\\1\\1\end{bmatrix},\begin{bmatrix}1\\0\\1\\0\end{bmatrix},\begin{bmatrix}0\\1\\0\\1\end{bmatrix},\begin{bmatrix}1\\0\\0\\1\end{bmatrix},\begin{bmatrix}0\\1\\1\\0\end{bmatrix}.$$

b) Unequal weighted such as PDMA [23][39]: the numbers of zero and non-zero elements are flexible. The element of the spreading sequences can be selected from {0,1} or from {0,1,-1,j,-j}. More unequal weighted pattern matrix can be found in the *Annex A.4.7*.

7) MUI-qualified sequences

Another sequence generation method is to use the Multi-User Interference (MUI) parameter as a criterion [27]. Details can be found in *Annex A.4.8*.

UE-specific symbol-level spreading with modified modulation:

Transmitter side processing for symbol-level spreading with modified modulation is shown in Figure 5.1-6.

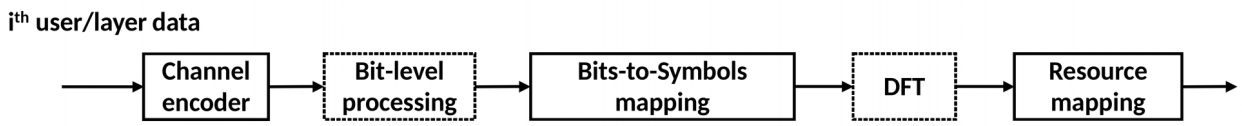

Figure 5.1-6: Transmitter procedure for symbol-level spreading with modified modulation

Joint spreading and modulation is proposed for SCMA [19]. *M* bits are first mapped to *N* symbols.

The *M*-bit to *N*-symbol mapping can be represented by a $N \times 2^M$ table in which each column represents the symbol sequence in term of an index of the input bit stream. The same mapping function can also be presented by a formula expressing the relation between the input bit stream **b** and the output symbol sequence **x**. For example, the formula of 8-point table is

$$x = \sqrt{\frac{2}{3}} \begin{bmatrix} \frac{-1}{\sqrt{2}} & j & 0 \\ \frac{-1}{\sqrt{2}} & 0 & j \end{bmatrix} (1-2b) \quad .$$

The output sequence **x** can be further multiplied by a UE-specific transform matrix **G** of size *N-by-N*, to obtain **y** = **Gx**. For instance of *N = 2*, this UE-specific 2-by-2 transform matrix **G** can be one of the following:

$$\begin{bmatrix}1 & 0\\0 & 1\end{bmatrix},\begin{bmatrix}1 & 0\\0 & -1\end{bmatrix},\begin{bmatrix}1 & 0\\0 & j\end{bmatrix},\begin{bmatrix}1 & 0\\0 & -j\end{bmatrix}$$

More bits-to-symbols mappings with different input bit lengths can be found in *Annex A.4.9*.

The output sequence **y** is then mapped to the corresponding non-zero element of the sparse spreading patterns as described in Subclause 5.1.3), to produce the sparse symbol sequence.

Symbol-level scrambling:

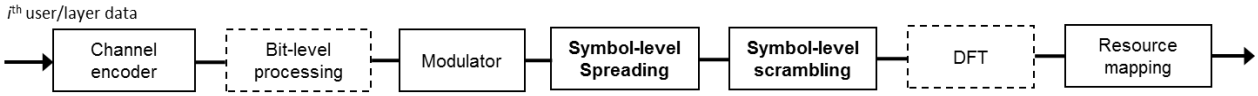

Figure 5.1-7: Transmitter procedure for hybrid symbol-level spreading and scrambling

Schemes like RSMA [31] use hybrid short code spreading and long code scrambling as the symbol-level MA signatures. The generation of scrambling sequences can be UE-group and/or cell specific, wherein the sequence ID of scrambling code is a function of cell ID and UE-group ID. One or multiple UE groups can be configured in a cell. The sequences used for scrambling code can be Gold sequences, Zadoff-Chu sequences, or a combination of the two, according to 3GPP TS 38.211.

UE-specific symbol-level interleaving with symbol-level zero padding:

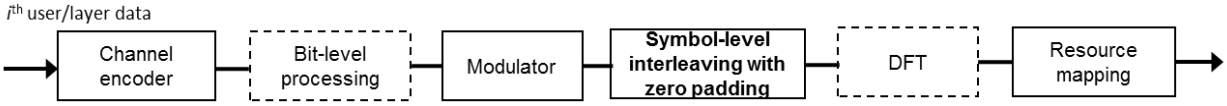

Figure 5.1-8: Transmitter procedure for symbol-level interleaving with symbol-level zero padding

In the proposed IGMA design [35], the symbol level operation is the grid mapping process. More specifically, it consists of zero padding and symbol level interleaving process, where in the end the sparse symbol-to-RE mapping can be achieved. The sparsity through grid mapping can be configurable.

For the k_{th} UE, via the resource configuration (size of the time-frequency resource) indicated by the gNB, the TB size and the MCS selected/configured for the transmission, a UE could derive the data matrix with the number of column as X and number of row as Y. Moreover, the density ρ_k and the zero-row indexes could be obtained by UE from gNB configuration, in which the ρ_k decides the ratio of the non-zero row of the data matrix and the zero-row indices tell the UE where to pad the zero rows. With "1" representing the data symbol row and "0" representing the zero row, the examples of zero patterns with Y = 4, ρ_k = 0.5 are given below.

$$\begin{bmatrix}1\\1\\0\\0\end{bmatrix},\begin{bmatrix}1\\0\\1\\0\end{bmatrix},\begin{bmatrix}1\\0\\0\\1\end{bmatrix},\begin{bmatrix}0\\1\\0\\1\end{bmatrix},\begin{bmatrix}0\\1\\1\\0\end{bmatrix},\begin{bmatrix}0\\0\\1\\1\end{bmatrix}.$$

After the zero padding and writing of the data symbols in corresponding row(s), the symbol sequence mapped to the REs could be further derived by reading the data from column direction of the data matrix. This symbol level interleaving is similar as block interleaving, i.e., the derived symbol sequence is $S'_k=[S_{k,0},0,S_{k,X},0,S_{k,1},0,S_{k,X+1},0.....S_{k,Y},0]$.

An exemplary interleaving with zero padding for sparse mapping is given below.

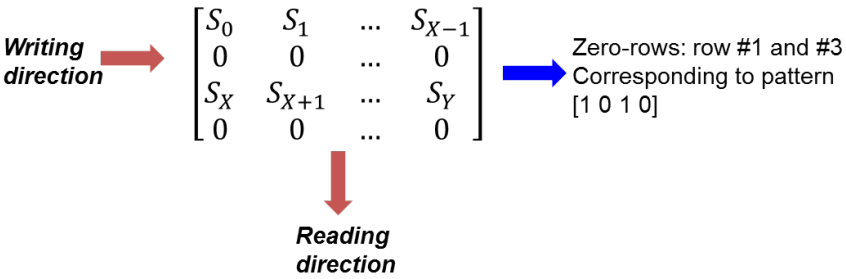

Figure 5.1-9: Illustration of symbol-level interleaving with zero padding

5.1.3 UE-specific sparse RE mapping

Sparse RE mapping is proposed as a type of MA signature in some NOMA schemes including SCMA [19], PDMA [23], and IGMA [26], where zeros are transmitted in some REs within the assigned PRBs.

It is noticed that in some cases, the sparse RE mapping can also be realized by applying sparse spreading sequences as shown in Subclause 2.2.1 [20][21][25][28].

For a NOMA system with regular-sparse resource mapping, where K users share N resources in a non-orthogonal fashion, design parameters are the sparsity of the signatures (number of non-zero elements as fraction of N). An example is depicted in Figure 5.1-10, where the explicit sparse resource mapping is represented as a binary matrix F. As an example shown in Figure 5.1-10, the rows correspond to the resources, and the columns represent the UE-specific signatures. In the example, 9 users in total are mapped to 6 resources, where 3 users access the same resource, and each user accesses 2 resources In the example shown as Figure 5.1-10, the construction has the property that the number of ones in each row, as well as the number of ones in each column, is fixed, and the overlap between the columns of F is at most 1 (i.e. the UE-specific signatures overlap at most one position).

$$\mathbf{F} = \begin{bmatrix} 1 & 0 & 0 & 0 & 0 & 1 & 0 & 1 & 0 \\ 0 & 1 & 0 & 1 & 0 & 0 & 0 & 0 & 1 \\ 0 & 0 & 1 & 0 & 1 & 0 & 1 & 0 & 0 \\ 1 & 0 & 0 & 0 & 1 & 0 & 0 & 0 & 1 \\ 0 & 1 & 0 & 0 & 0 & 1 & 1 & 0 & 0 \\ 0 & 0 & 1 & 1 & 0 & 0 & 0 & 1 & 0 \end{bmatrix}$$

Figure 5.1-10: An example of UE-specific sparse resource mapping.

5.1.4 OFDM symbol staggered transmission pattern

UE-specific starting transmission time is part of the MA signature in ACMA [38].

Staggered timing is shown in Figure 5.1-11, where the start time of each transmission is distributed over the OFDM symbols of the first N-1 time slots, or 14(N-1) OFDM symbols in a total time period of N time slots. At the end of slot N, all NOMA transmissions will have completed allowing other uses of the resources.

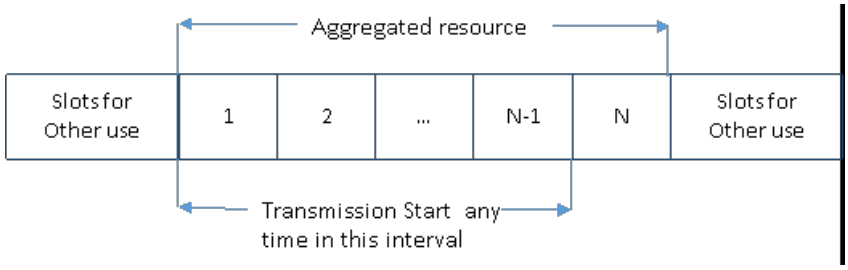

Figure 5.1-11: Time Staggered Transmission time in N aggregated time slots.

Figure 5.1-12 is a block diagram of the transmitter for a single-branch ACMA [38] which shows the use of time-staggered transmission in conjunction with bit or symbol-level scrambling.

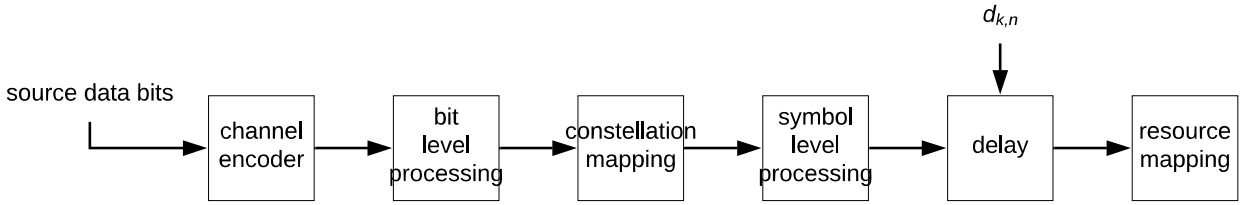

Figure 5.1-12: Block Diagram of ACMA transmit (single branch)

5.2 Auxiliary features related to MA signatures

5.2.1 Multi-branch transmission per UE

Multi-branch processing per user [19][20][22][23][26][30][31][63] can be operated before or after the channel encoder, as shown in Figure 5.2-1. UE-specific MA signature may be replaced by branch-specific MA signature, and these branch-specific MA signatures could be either orthogonal or non-orthogonal. Different branches could also share the same MA signature. Different weights can be applied to different branches.

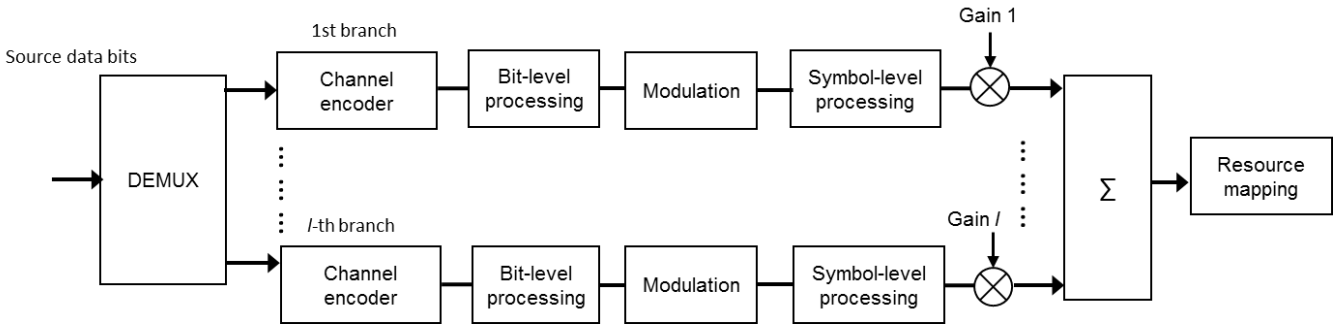

(a) Multi-branch transmission before the channel encoder

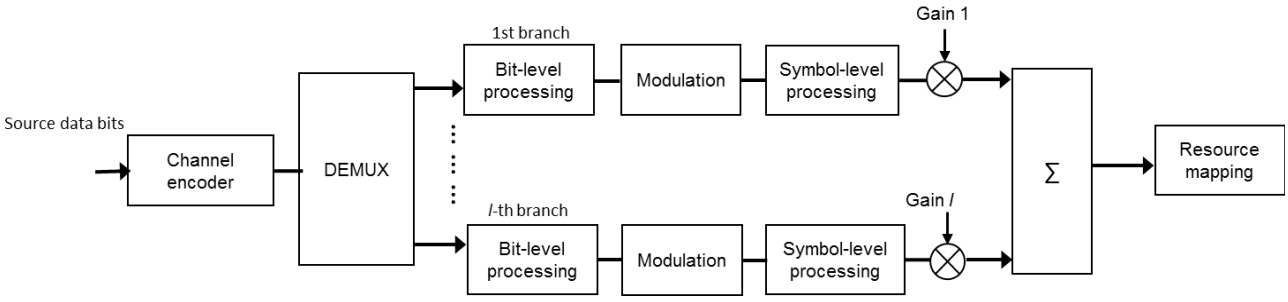

(b) Multi-branch transmission at bit-level after the channel encoder

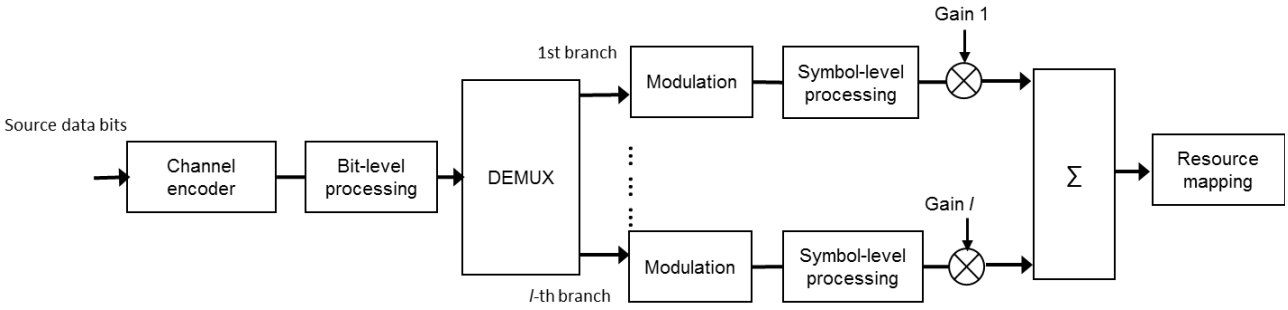

(c) Multi-branch transmission at symbol-level with legacy modulation.

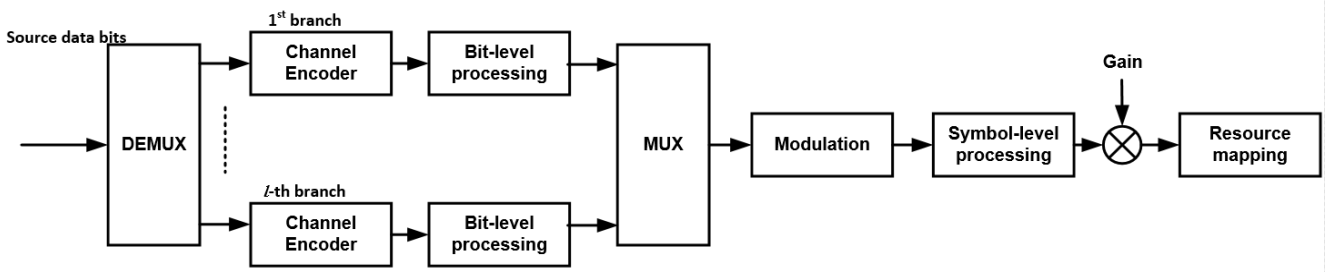

(d) Multi-branch transmission before the channel encoder and combined before modulation

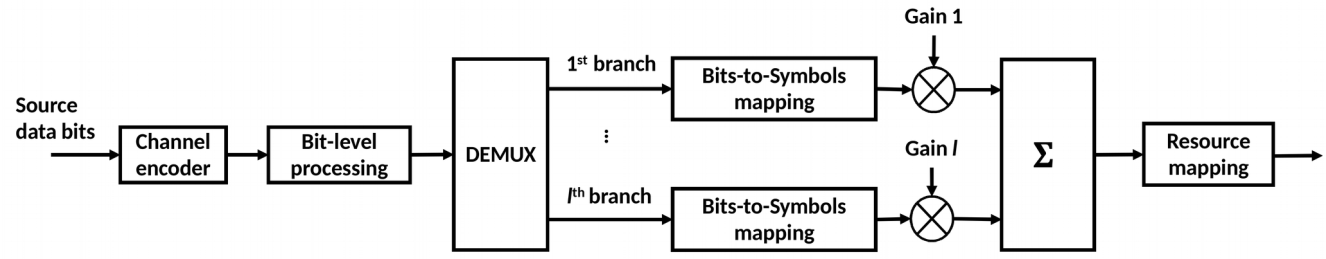

(e) Multi-branch transmission at symbol-level with modified modulation

Figure 5.2-1: Different operation modes for multi-branch transmission.

5.2.2 UE/branch-specific power assignment

For schemes such as GWBE sequences [30] and multi-branch transmission [20][31],power assignment is taken into account in the design of UE/branch-specific MA signatures.

The UE/branch-specific power can be assigned or selected for each user/layer independently from the MA signatures described above. The algorithms of sequence grouping can be found in *Annex A.4-12*.

6 Uplink NOMA receivers

The general block diagram of multi-user receiver for UL data transmissions is depicted in Figure 6.1-1.

- The algorithms for the detector block (for data) can be e.g. MMSE, MF, ESE, MAP, MPA, EPA.
- The interference cancellation can be hard, soft, or hybrid, and can be implemented in serial, parallel, or hybrid.
  - Note: the IC block may consist of an input of the received signal for some types of IC implementations
- The interference cancellation block may or may not be used.
  - Note: if not used, an input of interference estimation to the decoder may be required for some cases.
- The input to interference cancellation may come directly from the Detector for some cases

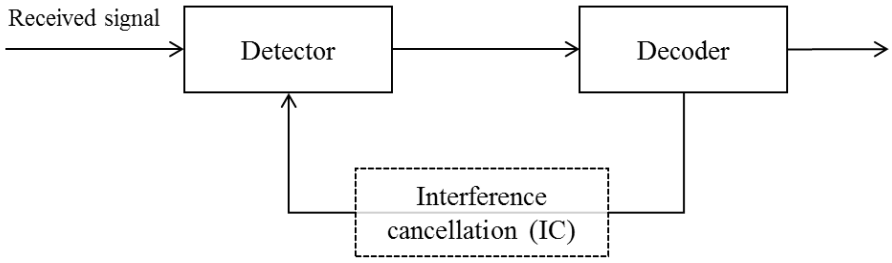

Figure 6-1. A high-level block diagram of multi-user receiver

6.1 Receivers for NOMA

Below are a few types of receivers for NOMA:

MMSE-IRC

Inter-cell interference is suppressed via MMSE detection, e.g., no interference cancellation is performed. In order to decode a user's data packet, MMSE detection and channel decoding are only performed once.

MMSE-hard IC

Interference cancellation is employed. "Hard" here means that the interference cancellation is based on the hard output of the decoder. The interference cancellation can be conducted successively, in parallel, or with hybrid process. In successive IC (SIC), each successfully decoded UE has its signal cancelled and removed from the pool of UEs to decode before processing the subsequent UEs. In parallel IC (PIC), iterative detection and decoding are employed, all UEs are decoded in parallel and successfully decoded UEs have their signal cancelled and are then removed from the pool of UEs to decode every iteration.

MMSE Soft IC

MMSE-soft IC cancellation differs from MMSE-hard IC in that the output of the decoder comprises soft information, which is used to reconstruct symbols and the interference cancellation is therefore soft. The interference cancellation can be conducted successively, in parallel, or with hybrid process. In successive IC, each decoded UE has its signal cancelled and successfully-decoded UEs are removed from the pool of UEs to decode before processing the subsequent UEs. In parallel IC, iterative detection and decoding are employed, all UEs are decoded in parallel their and signals are cancelled before proceeding to the next iteration, and successfully-decoded UEs can be removed from the pool of UEs to decode every iteration. A hybrid (soft-hard IC) receiver utilizes hard-IC to cancel successfully decoded UEs every iteration.

ESE + SISO

Iterative detection and decoding are employed. Statistics information, including mean and variance, is updated in each outer iteration for detector.

EPA + hybrid IC

Iterative detection and decoding are employed. Message passing between the factor nodes/resource elements (FN/RE) and the variable nodes (VN)/users is typically needed inside EPA for each outer iteration between the EPA and the channel decoder. The interference cancellation can be conducted successively, in parallel, or with hybrid process. Similar to the MMSE hybrid soft and hard IC, all UEs are decoded in parallel and successfully-decoded UEs are removed from the pool of UEs to decode every iteration.

6.2 Receiver complexity analysis

Approximate computation complexity analysis for each major receiver component for MMSE-IRC/Hard-IC and ESE-SISO receivers can be found in Table 6.2-1. Different options of complexity analysis for EPA-hybrid IC are listed in Table 6.2-2, 6.2-3, 6.2-4 respectively. In addition, the complexity analysis for linear MMSE receiver with hybrid IC can be found in the Appendix A.5.

Table 6.2-1: Computation complexity approximation formulae

Receiver component	Detailed component	Computation in O(.) analysis		
		MMSE-IRC/hard-IC	***ESE***	
			ESE+SISO	***Enhanced ESE+SISO***
Detector (complexity in #complex multi.)	UE detection	$O\left(N_{AP}^{DMRS}\cdot N_{\Re}^{DMRS}\cdot N\right.$	$O\left(N_{AP}^{DMRS}\cdot N_{\Re}^{DMRS}\cdot N_{\right.}$	$O\left(N_{AP}^{DMRS}\cdot N_{\Re}^{DMRS}\cdot N\right.$
	Channel estimation	$O\left(N_{UE}\cdot N_{\Re}^{CE}\cdot N_{\Re}^{DMR}\right.$	$O\left(N_{UE}\cdot N_{\Re}^{CE}\cdot N_{\Re}^{DMRS}\right.$	$O\left(N_{UE}\cdot N_{\Re}^{CE}\cdot N_{\Re}^{DMRS}\right.$
	Rx combining, if any			*O(* $N_{\Re}^{data}N_{UE}N_{rx}$ *)* *or O(* $N_{\Re}^{data}N_{UE}N_{rx}^{3}$ *)*
	Covariance matrix calculation, if any	Note 1		
	Demodulation weight computation, if any	Note 2		
	UE ordering, if any	Note 3		
	Demodulation, if any	$O\left(N_{iter}^{IC}\cdot N_{\Re}^{data}\cdot N_{rx}\right)$		
	Soft information generation, if any	$O\left(N_{iter}^{IC}\cdot N^{bit}\right)$		
	Soft symbol reconstruction, if any			
	Message passing, if any			
	Others			
Decoder (complexity in #addition/comparison)	LDPC decoding	A: $N_{iter}^{IC}\cdot N_{iter}^{LDPC}\cdot\left(d_v N^{bi}\right.$ C *:* $N_{iter}^{IC}\cdot N_{iter}^{LDPC}\cdot\left(2d_c-\right.$	A: $N_{iter}^{outer}\cdot N_{UE}\cdot N_{iter}^{LDPC}\cdot\left(\right.$ C *:* $N_{iter}^{outer}\cdot N_{UE}\cdot N_{iter}^{LDPC}\cdot\left(\right.$	A: $N_{iter}^{outer}\cdot N_{UE}\cdot N_{iter}^{LDPC}\cdot$ C *:* $N_{iter}^{outer}\cdot N_{UE}\cdot N_{iter}^{LDPC}\cdot$
Interference cancellation (complexity in #complex multi)	Symbol reconstruction(Including FFT operations for DFT-S-OFDM waveform), if any	$O\left(N_{UE}\cdot N_{\Re}^{data}\cdot N_{rx}\right)$		
	LLR to probability conversion, if any		$O\left(N_{iter}^{outer}\cdot N_{UE}\cdot N^{bit}\right)$	$O\left(N_{iter}^{outer}\cdot N_{UE}\cdot N^{bit}\right)$
	Interference cancellation		$O\left(6\cdot N_{iter}^{outer}\cdot N_{UE}\cdot N_{\right.}^{d}$	$O\left(6\cdot N_{iter}^{outer}\cdot\rho N_{UE}\cdot\right.$
	LDPC encoding, if any	Buffer shifting: $N_{UE}\cdot\left(N^{bit}-K^{bit}\right)/2$ Addition*:* $N_{UE}\cdot\left(d_c-1\right)\left(N^{bit}-\right.$		
	Others			

Note 1: Two options for covariance matrix calculation

Option 1: $O\left(N_{UE}\cdot N_{\Re}^{data}\cdot\left(N_{rx}\cdot N_{SF}\right)^2 ¿\, 2N_{\Re}^{adj}\right)$

Option 2: $N_{itr}\left(\frac{\left(N_{rx}N_{sf}\right)^2 N_{\Re}^{DMRS}}{2N_{sf}}+N_{UE}N_{Rx}N_{\Re}^{DMRS}\right)$ (option 2 is used to estimate the noise covariance matrix from inter-cell interferers, or unknown intra-cell interferers)

Note 2: Three options for demodulation weight calculation

Option 1: $O\left(\left(N_{\Re}^{data}\cdot\left(N_{rx}\cdot N_{SF}\right)^3+N_{iter}^{IC}\cdot N_{\Re}^{data}\cdot\left(N_{rx}\cdot N_{SF}\right)^2\right) ¿\, N_{\Re}^{adj}\right)$

Option2: $\frac{N_{itr}N_{\Re}^{Data}}{N_{\Re}^{adj}}\left(1.5\left(N_{rx}N_{sf}\right)^2 N_{UE}+\left(N_{rx}N_{sf}\right)^3\right)$, $N_{\Re}^{adj}=N\,N_{sf}$

Option 3:

$O\left(\left(N_{\Re}^{data}\cdot\left(N_{rx}\cdot N_{SF}\right)^3+N_{iter}^{IC}\cdot N_{\Re}^{data}\cdot\left(N_{rx}\cdot N_{SF}\right)^2+N_{\Re}^{data}\cdot N_{UE}\left(N_{UE}+1\right)\cdot\left(N_{rx}\cdot N_{SF}\right)^2/2\right) ¿\, N_{\Re}^{adj}\right)$

Note 3: Two options for UE ordering

Option 1: $O\left(N_{\Re}^{data}\cdot N_{rx}\cdot N_{SF}\cdot\left(N_{UE}\right)^2/N_{\Re}^{adj,SINR}\right)$

Option 2: $O\left(N_{\Re}^{data}\cdot N_{rx}\cdot N_{SF}\cdot\frac{\left(N_{UE}\right)^2}{N_{\Re}^{adj,SINR}}+\left(N_{UE}\right)^2\log\left(N_{UE}\right)/2\right)$

For ESE-SISO receiver,

The LLR probability and interference cancellation can be further elaborated as follows,

ESE-LLR: $5.5N_{itr}N_{UE}N_{\Re}^{Data}N_{Rx}$.

Mean-variance update: $2.5N_{itr}N_{UE}N_{\Re}^{Data}N_{Rx}+0.5N_{itr}N_{UE}N_{\Re}^{Data}$

Table 6.2-2: Computation complexity of EPA-hybrid IC receiver

Receiver component	Detailed component	Computation in O(.) analysis EPA-hybrid IC receiver
Detector (complexity in #complex multi. per user per resource element)	UE detection	$O\left(N_{AP}^{DMRS}\cdot N_{\Re}^{DMRS}\cdot N_{rx}\right)$
	Channel estimation	$O\left(N_{UE}\cdot N_{\Re}^{CE}\cdot N_{\Re}^{DMRS}\cdot N_{rx}\right)$
	Rx combining, if any	
	Covariance matrix calculation, if any	
	Matrix inversion	
	Equalization weight computation, if any	
	Demodulation weight computation, if any	
	UE ordering, if any	
	Equalization	
	Demodulation, if any	
	Soft information generation, if any	
	Soft symbol reconstruction, if any	$O\left(6\cdot N_{iter}^{outer}\cdot N_{iter}^{det}\cdot N_{UE}\cdot N_{\Re}^{data}\cdot d_u\cdot 2^{Q_m}/N_{SF}\right)$
	Message passing, if any	$O\left(8\cdot N_{iter}^{outer}\cdot N_{iter}^{det}\cdot N_{UE}\cdot N_{\Re}^{data}\cdot d_u/N_{SF}\right)$
	Others	
Decoder (complexity in #binary	LDPC decoding	A: $N_{iter}^{outer}\cdot N_{UE}\cdot N_{iter}^{LDPC}\cdot\left(d_v N^{bit}+2\left(N^{bit}-K^{bit}\right)\right)$

add/comp per user per coded bit)		C : $N_{iter}^{outer} \cdot N_{UE} \cdot N_{iter}^{LDPC} \cdot (2d_c - 1) \cdot (N^{bit} - K^{bit})$
Interference cancellation (complexity in #complex multi per user per resource element)	Symbol reconstruction(Including FFT operations for DFT-S-OFDM waveform), if any	Additional for DFT-s-OFDM: O($N_{iter}^{outer} \cdot N_{iter}^{det} \cdot N_{UE} \cdot N_{\Re}^{data} \cdot$ $log_2(N_{FFT})$)
	LLR to probability conversion, if any	$O\left(N_{iter}^{outer} \cdot N_{UE} \cdot N_{\Re}^{data} \cdot Q_m \cdot 2^{Q_m} / N_{SF}\right)$
	Interference cancellation	
	LDPC encoding, if any	
	Others	

Table 6.2-3: Computation complexity of EPA detector with hybrid soft and hard PIC

Receiver component	Detailed component	Computation in O(.) analysis Chip EPA+hybrid PIC
Detector (complexity in #complex multi.)	UE detection	$O\left(N_{AP}^{DMRS} \cdot N_{\Re}^{DMRS} \cdot N_{rx}\right)$
	Channel estimation	$O\left(N_{UE} \cdot N_{\Re}^{CE} \cdot N_{\Re}^{DMRS} \cdot N_{rx}\right)$
	Rx combining, if any	
	Covariance matrix calculation, if any	$O\left(\acute{N}_{iter}^{outer} \cdot N_{\Re}^{data} \left(\frac{1}{2} N_{rx}^2 d_f + N_{iter}^{det} \cdot \frac{1}{2} N_{rx} d_f\right)\right)$
	Demodulation weight computation, if any	$O\left(\acute{N}_{iter}^{outer} \cdot N_{\Re}^{data} \cdot N_{iter}^{det} \cdot \left(N_{rx}^3 + N_{rx}^2 d_f\right)\right)$
	UE ordering, if any	
	Demodulation, if any	$O\left(\acute{N}_{iter}^{outer} \cdot N_{\Re}^{data} \cdot N_{iter}^{det} \cdot 3 N_{rx} d_f\right)$
	Soft information generation, if any	
	Soft symbol reconstruction, if any	$O\left(3\acute{N}_{iter}^{outer} \cdot N_{iter}^{det} \cdot N_{UE} \cdot d_u \cdot \frac{Q_m \cdot N_{\Re}^{data}}{4 \cdot N_{SF}} + \acute{N}_{iter}^{outer} \cdot N_{UE} \cdot N^{bit} / 4\right)$
	Message passing, if any	$O\left(2 \cdot \acute{N}_{iter}^{outer} \cdot N_{iter}^{det} \cdot N_{UE} \cdot d_u \cdot \frac{N_{\Re}^{data}}{N_{SF}}\right)$
	Others	
Decoder (complexity in #addition/comparison)	LDPC decoding	A: $N_{iter}^{outer} \cdot N_{UE} \cdot N_{iter}^{LDPC} \cdot \left(d_v N^{bit} + 2\left(N^{bit} - K^{bit}\right)\right)$ C : $N_{iter}^{outer} \cdot N_{UE} \cdot N_{iter}^{LDPC} \cdot (2d_c - 1) \cdot (N^{bit} - K^{bit})$
Interference cancellation (complexity in #complex multi)	Symbol reconstruction(Including FFT operations for DFT-S-OFDM waveform), if any	$O\left(N_{UE} \cdot N_{\Re}^{data} \cdot N_{rx}\right)$
	LLR to probability conversion, if any	$O\left(\acute{N}_{iter}^{outer} \cdot N_{UE} \cdot \frac{2^{Q_m} N_{\Re}^{data}}{4 \cdot N_{SF}}\right)$
	Interference cancellation	

	LDPC encoding, if any	Buffer shifting: $N_{UE}\cdot\left(N^{bit}-K^{bit}\right)/2$ Addition: $N_{UE}\cdot\left(d_c-1\right)\left(N^{bit}-K^{bit}\right)$
	Others	

Table 6.2-4: Computation complexity of EPA-hybrid IC receiver

Detector	1: EPA-based detector for K users (**Rx combining, Covariance matrix calculation, Demodulation weight computation, Message passing**)	Initialize t = 1, $p^t\left(x_k=\alpha\right)=I_{\Delta\to k}\left(x_k=\alpha\right)$.	Marginal
		1.1: If $t > A_{\text{MUD,inner}}$, move to 2.1 Else, **VN Update:** For $k=1,\ldots,K$: For $l\in V\left(k\right)$: - Compute μ_{kl}^t and ξ_{kl}^t as $\mu_{kl}^t=\sum_{a\in X_k}p^t\left(x_k=\alpha\right)\alpha_l$ $p^t\left(x_k=\alpha\right)¿\alpha_l-\mu_{kl}^t\vee¿^2$ $\xi_{kl}^t=\sum_{a\in X_k}¿$ where α_l is l -th element of L -dimensional vector $\alpha\in X_k$. - Compute the mean $\mu_{k\to l}^t$ and variance $\xi_{k\to l}^t$ as $\frac{1}{\xi_{k\to l}^t}=\frac{1}{\xi_{kl}^t}-\frac{1}{\xi_{l\to k}^{t-1}}$ $\frac{\mu_{k\to l}^t}{\xi_{k\to l}^t}=\frac{\mu_{kl}^t}{\xi_{kl}^t}-\frac{\mu_{l\to k}^{t-1}}{\xi_{l\to k}^{t-1}}$	$N_{iter}^{outer}\cdot N_{iter}^{det}\cdot N_{\Re}^{data}\cdot$
		1.2: **FN Update:** For $l=1,\ldots,L$: a) Perform chip-by-chip MMSE as $m_l^{post}=m_l^{pri}+\Sigma_l^{pri}\acute{H}_l^H\left(\acute{H}_l\Sigma_l^{pri}\acute{H}_l^H+\sigma^2I\right)^{-1}\left(\acute{y}_l-\acute{H}_l\right.$ $\Sigma_l^{post}=\Sigma^{pri}-\Sigma_l^{pri}\acute{H}_l^H\left(\acute{H}_l\Sigma_l^{pri}\acute{H}_l^H+\sigma^2I\right)^{-1}\acute{H}_l\left(\Sigma_l^{pri}\right.$ where $m_l^{pri}=\left[\mu_{k\to l}^t\vee k\in F\left(l\right)\right]\in C^{d_f\times1}$ and $\Sigma_l^{pri}=diag\left(\left[\xi_{k\to l}^t\vee k\in F\left(l\right)\right]\right)\in C^{d_f\times d_f}$. b) For $k\in F\left(l\right)$: Given the posterior mean $\left[\hat{\mu}_{kl}^t\vee k\in F\left(l\right)\right]=m_l^{post}$ and variances $\left[\hat{\xi}_{kl}^t\vee k\in F\left(l\right)\right]=diag\left(\Sigma_l^{post}\right)$ of x_{kl} , compute the mean $\mu_{l\to k}^t$ and variance $\xi_{l\to k}^t$ as $\frac{1}{\xi_{l\to k}^t}=\frac{1}{\hat{\xi}_{kl}^t}-\frac{1}{\xi_{k\to l}^t}$ $\frac{\mu_{l\to k}^t}{\xi_{l\to k}^t}=\frac{\hat{\mu}_{kl}^t}{\hat{\xi}_{kl}^t}-\frac{\mu_{k\to l}^t}{\xi_{k\to l}^t}$	$N_{iter}^{outer}\cdot N_{iter}^{det}\cdot N_{\Re}^{data}\cdot$
		1.3: Update $p^t\left(x_k\right)$	

		$p^t(x_k=\alpha)=\frac{I_{\Delta\to k}(x_k=\alpha)\prod_{n\in V(k)}CN(x_{kn}=\alpha_n;\mu_n^t}{\sum_{a\in X_k}I_{\Delta\to k}(x_k=\alpha)\prod_{n\in V(k)}CN(x_{kn}=\alpha_n;}$ Update t = t +1 and repeat 1.1	$N_{iter}^{outer}\cdot N_{iter}^{det}\cdot N_{\Re}^{data}\cdot$
	2. Demodulation, i.e., **Soft information generation**	2.1: Calculate the LLR of coded bits of user *k* $LLR_{j,k}^{MUD,a}=\log\frac{\sum_{\alpha:x_{k,j}=1}p^t(x_k=\alpha)}{\sum_{\alpha:x_{k,j}=0}p^t(x_k=\alpha)}\forall k$	$N_{iter}^{outer}\cdot Q_m\cdot 2^{Q_m}\cdot N_U$
Decoder	3. **LDPC decoding**	3.1: LDPC decoding based on the LLR of MN_{RE}/SF coded bits obtained in 2.1 and obtain the LLR of coded bits $LLR_{j,k}^{DEC,a}$	$N_{iter}^{outer}\cdot N_{iter}^{LDPC}\cdot N_{UE}$
Interference cancellation	4. **LLR to probability conversion**	4.1: If $a > A_{PIC,outer}$, stop Else Calculate $I_{\Delta\to k}(x_k=\alpha)$ from $LLR_{j,k}^{DEC,a}$ as $I_{\Delta\to k}(x_k=\alpha)=\prod_{j=1}^{M}\frac{\exp(c_{j,k}LLR_{j,k}^{DEC,a})}{1+\exp(LLR_{j,k}^{DEC,a})}$, and repeat 1	$N_{iter}^{outer}\cdot Q_m\cdot 2^{Q_m}N_{UE}$

The following Table is for complexity analysis of MMSE-IRC receiver as the basic receiver.

Table 6.2-5: Computation complexity approximation formulae of basic MMSE IRC receiver

UE detection	$O\left(N_{AP}^{DMRS}\cdot N_{\Re}^{DMRS}\cdot N_{rx}\right)$
Channel estimation	$O\left(N_{UE}\cdot N_{\Re}^{CE}\cdot N_{\Re}^{DMRS}\cdot N_{rx}\right)$
Rx combining, if any	
Covariance matrix calculation, if any	$O\left(N_{UE}\cdot N_{\Re}^{data}\cdot\left(N_{rx}\right)^2 ¿ 2\,N_{\Re}^{adj}\right)$
Demodulation weight computation, if any	$O\left(\left(N_{\Re}^{data}\cdot\left(N_{rx}\right)^3+N_{\Re}^{data}\,N_{UE}\cdot\left(N_{rx}\right)^2\right) ¿ N_{\Re}^{adj}\right)$
Demodulation, if any	$O\left(N_{UE}\cdot N_{\Re}^{data}\cdot N_{rx}\right)$
Soft information generation, if any	$O\left(N_{UE}\cdot N^{bit}\right)$
LDPC decoding	A: $N_{UE}\cdot N_{iter}^{LDPC}\cdot\left(d_v N^{bit}+2\left(N^{bit}-K^{bit}\right)\right)$ C : $N_{UE}\cdot N_{iter}^{LDPC}\cdot\left(2d_c-1\right)\cdot\left(N^{bit}-K^{bit}\right)$

An example calculation is provided below.

Table 6.2-6: Example values of parameters for computation complexity calculation

Category	Parameter	Notation	Value
General	Number of receive antennas	N_{rx}	2 or 4
	Number of data resource elements	$N_{\Re}^{data}$	864
	Number of users	N_{UE}	12
MMSE and EPA related	Spreading length	N_{SF}	4
MMSE-hard IC specific	Number of decoding for MMSE-hard IC	N_{iter}^{IC}	$N_{iter}^{IC}=N_{UE}$ for IRC; $[1.5-3]\cdot N_{UE}=[$ for hard-IC
Channel coding related	Average column weight of LDPC PCM	d_v	3.43

Channel coding related Soft IC specific	Average row weight of LDPC PCM	d_c	6.55
	Number of information bits in a code block	K^{bit}	176
	Number of coded bits of a block	N^{bit}	432
	Number of inner iterations of LDPC decoding	N_{iter}^{LDPC}	20
	Number of outer iterations between detector and decoder	N_{iter}^{outer}	5 (for ESE), 3 (for EPA)
EPA specific	Number of inner iterations inside detector	N_{iter}^{det}	3
EPA specific User detection & channel estimation related	Number FN nodes (or resource elements) connected to each user	d_u	2
	Number of user connected to one resource element	d_f	6
	Modulation order	Q_m	3
	Maximal number of DMRS antenna ports	N_{AP}^{DMRS}	12
User detection & channel estimation related	Total number of DMRS REs for initially estimated channel	$N_{\Re}^{CE}$	12
	Total number of REs for DMRS, e.g., length of DMRS sequence	$N_{\Re}^{DMRS}$	24

Based on the exemplary values, the channel decoder complexity can be reflected in Table 6.2-7, and the overall detector plus IC complexity analysis for different options of each receiver type are collected in Figure 6.2-1 to 6.2-5.

Table 6.2-7: Ratio of decoding complexity of various receivers

Rx Types Decoding Complexity	MMSE IRC	MMSE hard-IC	ESE SISO	EPA-hybrid IC
Ratio by number of usages	1	1.5~3	5	2.6~3

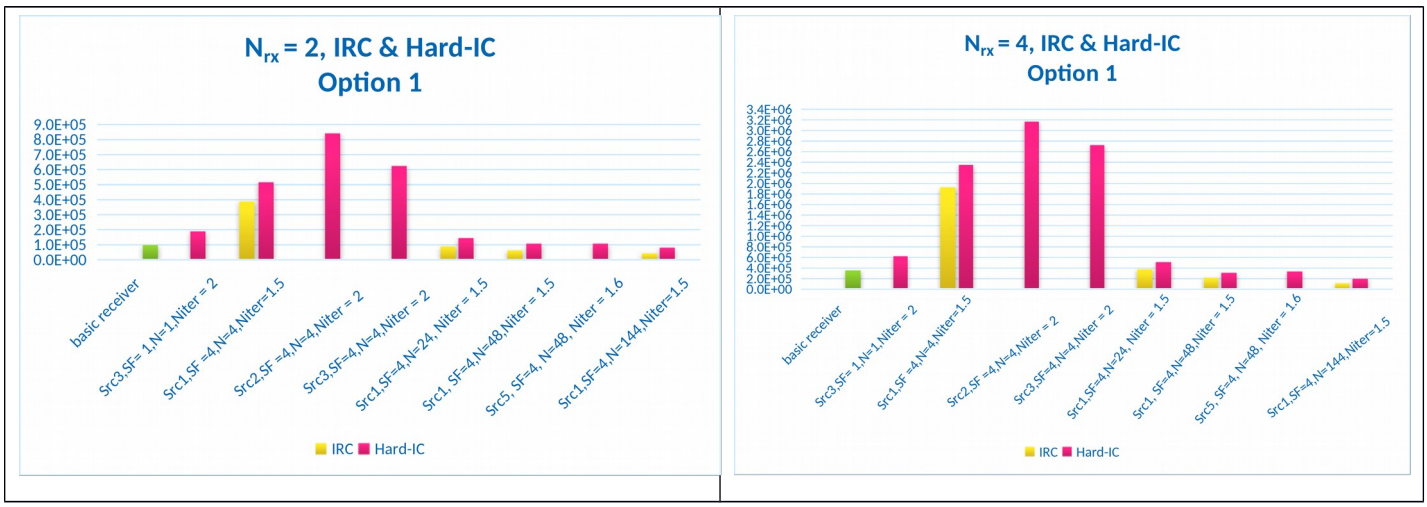

Figure 6.2-1: Option 1 complexity calculation of MMSE hard-IC based detector/IC

Note:

In the figures in this subclause, SF denotes for N_{sf}, N denotes for $N_{\Re}^{adj}$, and Niter denotes for N_{iter}^{IC} as used in Table 6.2-1.

For MMSE hard IC receiver, Source 1 [64] and Source 5 [68] assume $N_{\Re}^{adj,SINR}$ = 144, Source 2 [65] assumes $N_{\Re}^{adj,SINR}$ = 4. Source 3 [66] assumes $N_{\Re}^{adj,SINR}$ = 48.

For complexity of MMSE-IRC receiver provided by Source 1, the MMSE is implemented in joint code and spatial domain, and N_{iter}^{IC} is 1.

The impact of $N_{\Re}^{adj}$ on the BLER performance for MMSE hard IC receiver is analysed by Source 1 [64], Source 2 [65], Source 4 [69], and in [70] and [71]. Details can be found in Annex A.6.

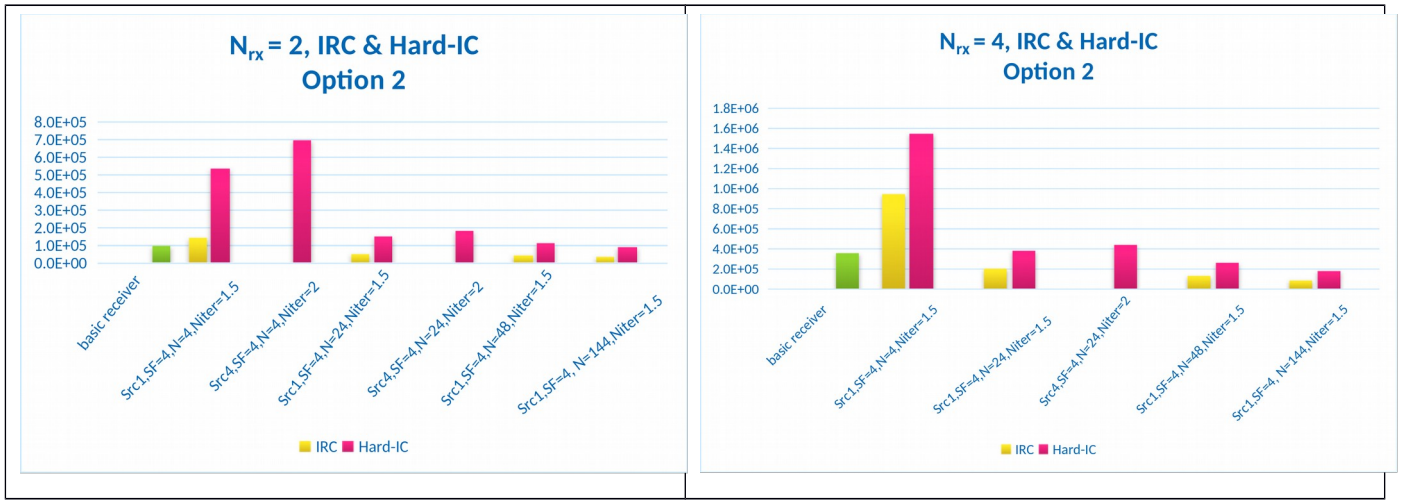

Figure 6.2-2: Option 2 complexity calculation of MMSE IRC/ hard-IC based detector/IC

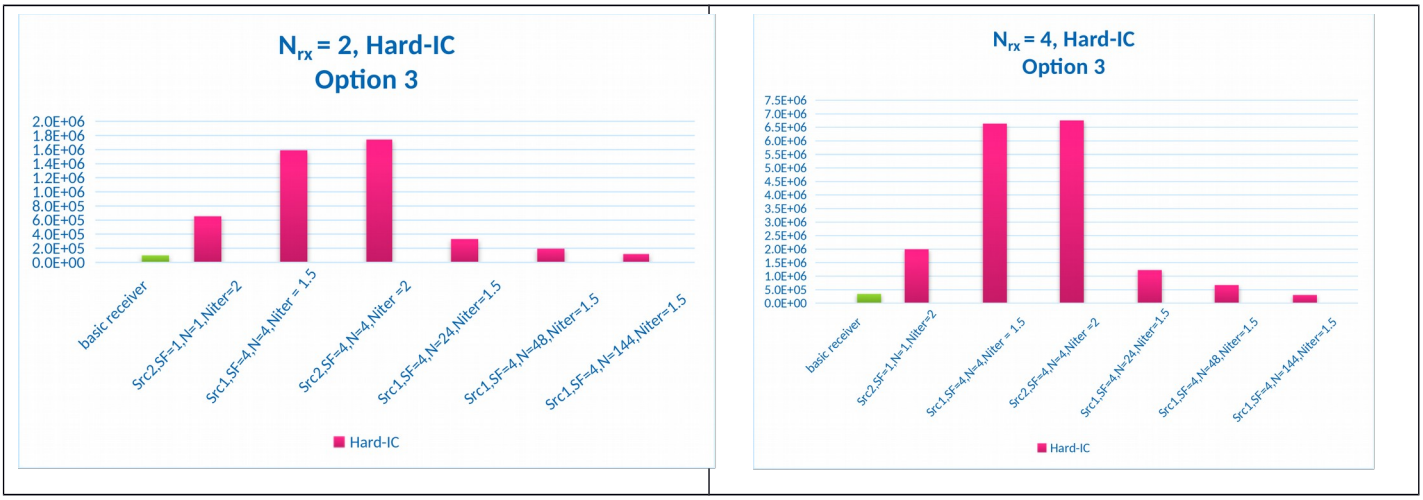

Figure 6.2-3: Option 3 complexity calculation of MMSE hard-IC receiver

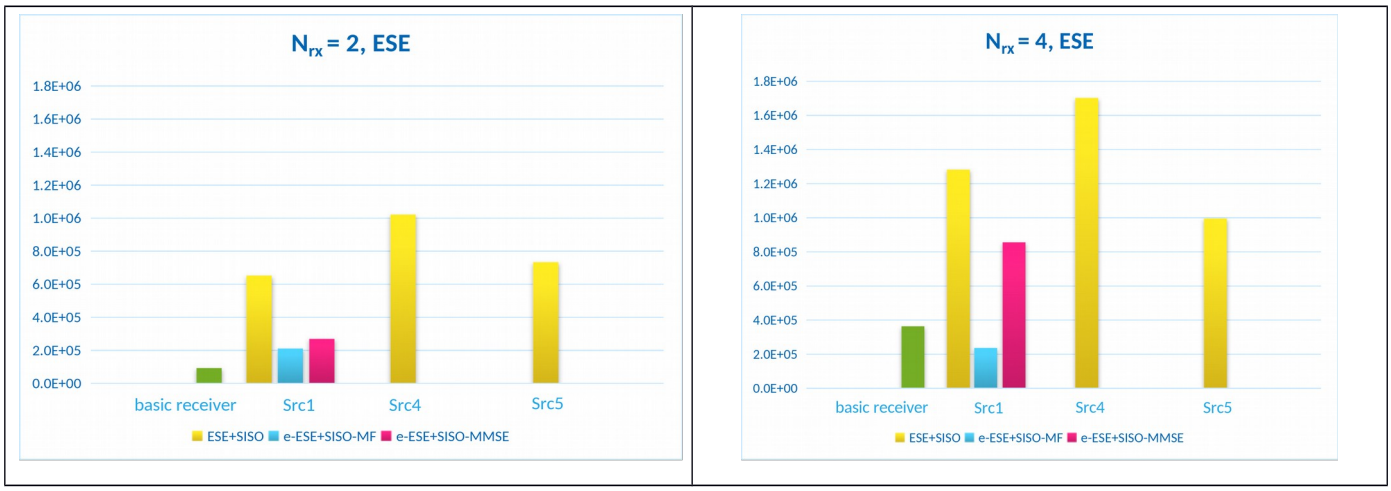

Figure 6.2-4: Complexity calculation of ESE/enhanced-ESE based detector/IC

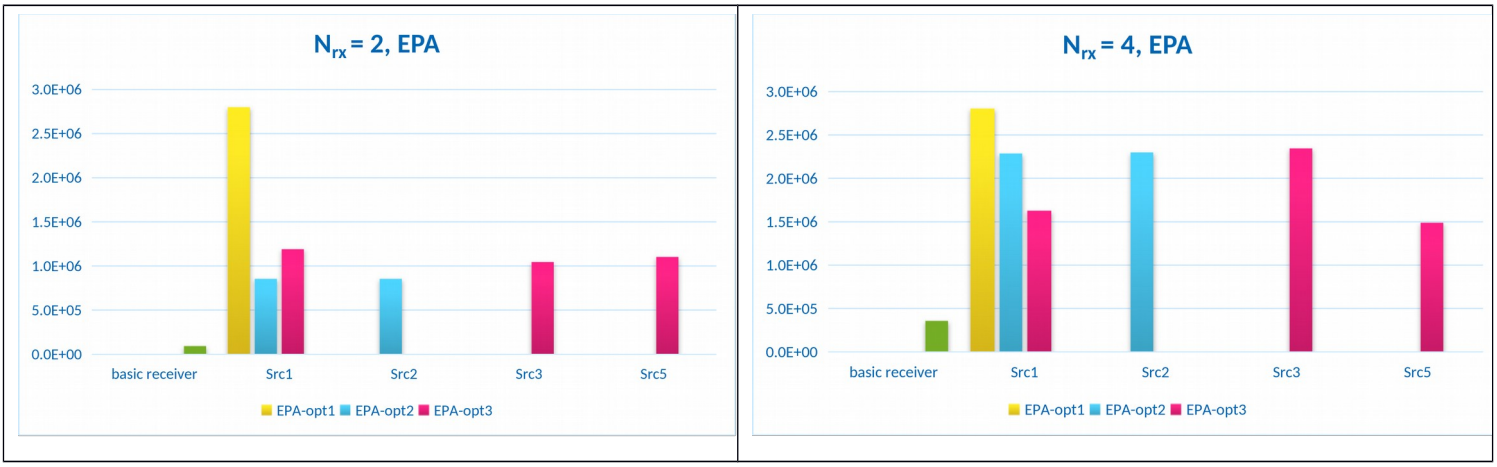

Figure 6.2-5: Complexity calculation of EPA based detector/IC

7 Procedures related to NOMA

UL data transmission and detection procedures of Rel-15 configured grant is the starting point for NOMA study. Synchronous UL data transmission should be the starting point.

This study also considers the asynchronous transmission, where timing offset is within [0, y] as starting point. y has two values at least for the purpose of evaluation: 1) NCP/2; 2) 1.5*NCP. Channel structure consisting of preamble and data can be considered for supporting the asynchronous transmission, where reusing Rel-15 NR preamble design can be considered as the starting point. Additional components can be included if necessary, e.g., the UL channel for assisting the UE detection or GP.

8 Link level performance evaluation

8.1 Performance and implementation related metrics

Performance metrics are at least:

- BLER vs. per UE SNR at a given pair of {per UE SE, # of UEs}
- Sum throughput vs. SNR at given BLER level, for a given pair of {per UE SE, # of UEs}
- MCL

Implementation related metrics are at least:

- PAPR/cubic metric
- RX complexity and processing latency

8.2 Evaluation results

Three templates were agreed to capture the link level simulation results of NOMA. In particular, Template 1 was formatted with the purpose to provide more detailed description of link performance, e.g., in terms of BLER vs. SNR curves. Total of 35 cases, together with the number of UEs to be simulated, are defined in Template 1. As complementary, more exhaustive combinations of scenarios, TBS, channel model, waveform, equal/unequal SNR, etc. can be found in Template 2 where a required SNR value for certain target BLER would be filled in for each case, instead of a BLER curve. Template 3 is used to collect PAPR statistics of different schemes/MA signatures.

8.2.1 Case-by-case evaluations on BLER vs. SNR

The 35 cases collected for the evaluation of BLER vs. SNR at link level are listed in Table 8.2-1.

Table 8.2-1: Simulated cases for BLER vs. SNR

Case #	Scenario	Freq	# Rx	SNR dist	waveform	Sign. alloc.	Chan. Model	TBS	#UEs	TO/FO	#curve	#comp.
1	mMTC	700M	2	equal	CP-ofdm	fixed	Tdl-A	10	12, 24	no	34	10
2	mMTC	700M	2	equal	CP-ofdm	fixed	Tdl-C	20	6, 12	no	36	11
3	mMTC	700M	2	equal	CP-ofdm	fixed	Tdl-A	40	6, 10	no	33	10
4	mMTC	700M	2	equal	CP-ofdm	fixed	Tdl-C	60	6, 8	no	32	9
5	mMTC	700M	2	equal	CP-ofdm	fixed	Tdl-A	75	4, 6	no	23	9
6	mMTC	700M	2	unequal	CP-ofdm	fixed	Tdl-A	20	6, 12	yes	13	6
7	mMTC	700M	2	unequal	CP-ofdm	fixed	Tdl-C	60	6, 8	no	19	7
8	mMTC	700M	2	unequal	DFT-s	fixed	Tdl-C	10	12, 24	yes	14	8
9	mMTC	700M	2	unequal	DFT-s	fixed	Tdl-C	20	6, 12	yes	13	7
10	mMTC	700M	2	unequal	CP-ofdm	random	Tdl-C	10	4	yes	15	4
11	mMTC	700M	2	unequal	CP-ofdm	random	Tdl-A	20	4	yes	14	4
12	mMTC	700M	2	unequal	DFT-s	random	Tdl-A	10	4	yes	11	3
13	mMTC	700M	2	unequal	DFT-s	random	Tdl-A	20	4	yes	12	3
14	URLLC	700M	4	equal	CP-ofdm	fixed	Tdl-C	10	6, 12	no	14	5
15	URLLC	700M	4	equal	CP-ofdm	fixed	Tdl-C	60	4, 6	no	14	5
16	URLLC	4GHz	4	equal	CP-ofdm	fixed	Tdl-A	10	6, 12	no	14	5
17	URLLC	4GHz	4	equal	CP-ofdm	fixed	Tdl-A	60	4, 6	no	13	4
18	eMBB	4GHz	4	equal	CP-ofdm	fixed	Tdl-A	20	12, 24	no	20	9
19	eMBB	4GHz	4	equal	CP-ofdm	fixed	Tdl-A	80	8, 16	no	18	8
20	eMBB	4GHz	4	equal	CP-ofdm	fixed	Tdl-A	150	4, 8	no	18	7
21	eMBB	4GHz	4	unequal	CP-ofdm	fixed	Tdl-C	20	12, 24	yes	10	5
22	eMBB	4GHz	4	unequal	CP-ofdm	fixed	Tdl-C	80	8, 16	yes	9	5
23	eMBB	4GHz	4	unequal	CP-ofdm	fixed	Tdl-C	150	4, 8	no	16	6
24	eMBB	4GHz	4	unequal	CP-ofdm	random	Tdl-A	40	4	yes	14	4
25	eMBB	4GHz	4	unequal	CP-ofdm	random	Tdl-A	80	4	yes	15	4
26	mMTC	700M	4	equal	CP-ofdm	fixed	Tdl-C	60	6, 8	no	16	6
27	mMTC	700M	4	equal	CP-ofdm	fixed	Tdl-A	75	4, 6	no	14	5
28	mMTC	700M	4	unequal	CP-ofdm	fixed	Tdl-C	60	6, 8	yes	7	3
29	mMTC	700M	2	unequal	DFT-s	fixed	Tdl-C	40	6, 10	yes	6	3
30	mMTC	700M	2	unequal	DFT-s	fixed	Tdl-C	60	6, 8	yes	6	3
31	mMTC	700M	2	unequal	DFT-s	fixed	Tdl-C	75	4, 6	yes	6	3
32	mMTC	700M Hz	2	5dB (see note)	CP-OFDM	Fixed	Tdl-C	20	{6, 12}	No	27	6
33	mMTC	700M Hz	2	4dB (see note)	CP-OFDM	Fixed	Tdl-C	60	{6, 8}	No	18	6
34	mMTC	700M Hz	4	4dB (see note)	CP-OFDM	Fixed	Tdl-A	60	{6, 8}	No	26	5
35	mMTC	700M Hz	4	5dB (see note)	CP-OFDM	Fixed	Tdl-A	20	{6, 12}	No	18	6

Note: The following options of SNR distribution can be considered for case 32-35:
- Opt 1: keep the current value with Gaussian distribution;
- Opt 2: 9dB for case 32 and 34;
- Opt 3: use CDF statistics in SLS;
- Opt 4: mixed Gaussian and Deterministic

Some examples of evaluation results and the code rate and receiver type corresponding to each of the reported curves are presented as below. More results can be found in the enclosed spreadsheet as below or in [40].

Template 1 - NOMA_LLS_BLER_

1) Case 1 with 12 UEs of ideal channel estimation:

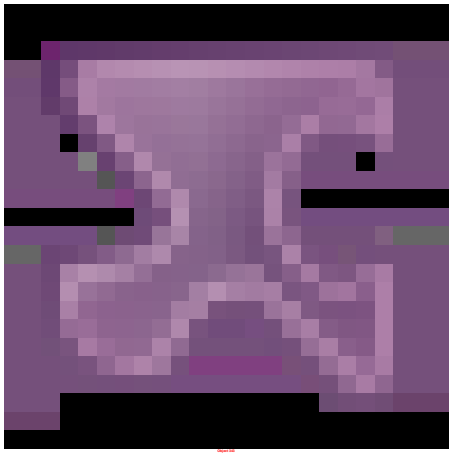

Figure 8.2-1: BLER vs. SNR results for Case 1 with 12 UEs

Table 8.2-2: Assumptions of code rate and receiver for each simulated scheme for Case 1 with 12 UEs

Company	Source 4	Source 11	Source 2		Source 3				Source 10				Source 6	
Scheme	RSMA	IDMA	PDMA	PDMA	UGMA	MUSA	SCMA	RSMA	IDMA	MUSA	IDMA	SCMA	LCRS	LCRS
Code rate	0.11	0.06	0.22	0.22	0.1	0.1	0.13	0.1	0.06	0.22	0.06	0.15	0.06	0.06
Receiver	MMSE - Hybrid IC	ESE-SISO	EPA	MMSE - hard SIC	MMSE -SIC	MMSE - hard SIC	EPA	MMSE - hard SIC	EPA	EPA	ESE	EPA	MMSE - hard SIC	EPA
Company	Source 1							Source 8	Source 13		Source 9			
Scheme	MUSA	WSMA	UGMA	RSMA	NOCA	NCMA	NCMAQ	NCMA	NCMA	Legacy BPSK	Legacy QPSK	IGMA	MUSA	
Code rate	0.22	0.22	0.22	0.22	0.22	0.22	0.22	0.111	0.0556	0.11	0.06	0.093	0.185	
Receiver	MMSE - hard SIC	MMSE - hard SIC	MMSE - hard SIC	MMSE - hard SIC	MMSE - hard SIC	MMSE - hard SIC	MMSE-hard SIC	MMSE - hard SIC	MMSE - hard SIC	MMSE - hard SIC	MMSE - hard SIC	ESE-SISO	ESE-SISO	
Company	Source 5										Source 7	Source 12	Source 14	
Scheme	SCMA	LCRS	MUSA	MUSA	SL-RSMA	SL-RSMA	ML-RSMA	ML-RSMA	SCMA	IGMA	NOCA	ACMA	LSSA	
Code rate	0.15	0.06	0.11	0.11	0.11	0.11	0.11	0.11	0.15	0.11		0.05	0.09	
Receiver	Chip EPA hybrid PIC	Chip EPA hybrid PIC	Block MMSE hard PIC	Chip EPA hybrid PIC	Block MMSE hard PIC	Chip EPA hybrid PIC	Block MMSE hard PIC	Chip EPA hybrid PIC	chip MMSE -hard PIC	Chip EPA hybrid PIC	MMSE - hard SIC	ESE-SISO	ESE	

Note: MMSE-Hybrid IC corresponds to MMSE - hybrid soft and hard IC conducted successively or in parallel

MMSE-hard SIC corresponds to MMSE - hard IC conducted successively

MMSE-hard PIC corresponds to MMSE - hard IC conducted in parallel

EPA hybrid PIC corresponds to EPA – hybrid soft and hard IC conducted in parallel.

2) Case 1 with 24 UEs of ideal channel estimation:

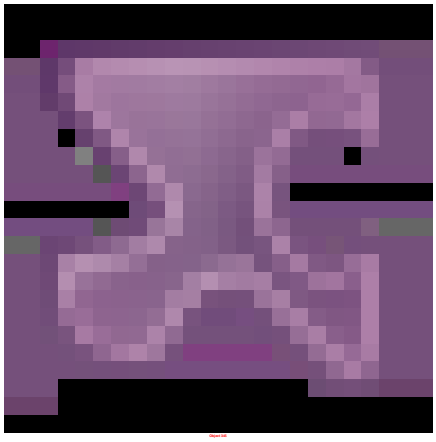

Figure 8.2-2: BLER vs. SNR results for Case 1 with 24 UEs

Table 8.2-3: Assumptions of code rate and receiver for each simulated scheme for Case 1 with 24 UEs

Company	Source 4	Source 11	Source 3			Source 8			Source 14	Source 2		
Scheme	RSMA	IDMA	UGMA	MUSA	SCMA	NCMA	NCMA	MUSA	LSSA	PDMA	MUSA	MUSA
Code rate	0.11	0.06	0.1	0.1	0.13	0.0556	0.111	0.222	0.09	0.22	0.22	0.11
Receiver	MMSE-Hybrid IC	ESE-SISO	MMSE-hard SIC	MMSE-hard SIC	EPA	MMSE-hard SIC	MMSE-hard SIC	MMSE-hard SIC	ESE	MMSE-hard SIC	MMSE-hard SIC	MMSE-hard SIC
Company	Source 5										Source 6	
Scheme	SCMA	LCRS	MUSA	MUSA	SL-RSMA	SL-RSMA	ML-RSMA	ML-RSMA	SCMA	IGMA	LCRS	LCRS
Code rate	0.15	0.06	0.11	0.11	0.11	0.11	0.11	0.11	0.17	0.11	0.06	0.06
Receiver	Chip EPA hybrid PIC	Chip EPA hybrid PIC	Block MMSE hard PIC	Chip EPA hybrid PIC	Block MMSE hard PIC	Chip EPA hybrid PIC	Block MMSE hard PIC	Chip EPA hybrid PIC	chip MMSE-hard PIC	Chip EPA hybrid PIC	MMSE-hard SIC	EPA
Company	Source 7	Source 13		Source 12	Source 9		Source 1	Source 10				
Scheme	NOCA	Legacy BPSK	Legacy QPSK	ACMA	IGMA	MUSA	MUSA	IDMA	MUSA	IDMA	SCMA	
Code rate		0.11	0.06	0.05	0.093	0.185	0.1	0.06	0.22	0.06	0.15	
Receiver	MMSE-hard SIC	MMSE-hard SIC	MMSE-hard SIC	ESE-SISO	ESE-SISO	ESE-SISO	MMSE-hard SIC	EPA	EPA	ESE	EPA	

Observations: with ideal channel estimation, the LLS results for Case 1 with 12 or 24 UEs show a similar performance for most of curves provided, at target BLER = 0.1, with appropriate configurations.

3) Case 2 with 6 UEs of ideal channel estimation:

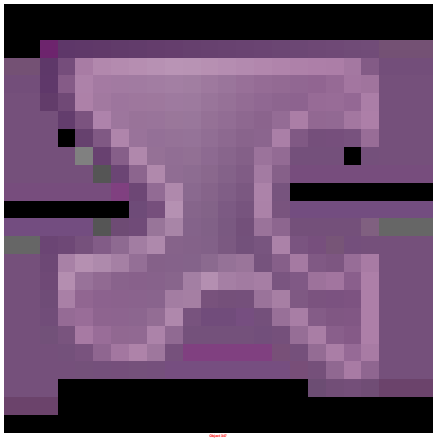

Figure 8.2-3: BLER vs. SNR results for Case 2 with 6 UEs

Table 8.2-4: Assumptions of code rate and receiver for each simulated scheme for Case 2 with 6 UEs

Company	Source 4	Source 11	Source 2		Source 3			Source 10			
Scheme	RSMA	IDMA	PDMA	PDMA	UGMA	MUSA	SCMA	IDMA	MUSA	IDMA	SCMA
Code rate	0.2	0.1	0.2	0.2	0.19	0.19	0.25	0.1	0.2	0.1	0.27
Receiver	MMSE - hybrid SIC	ESE-SISO	EPA	MMSE - hard SIC	MMSE-hard SIC	MMSE-hard SIC	EPA	EPA	EPA	ESE	EPA
Company	Source 6		Source 1	Source 8			Source 9		Source 12	Source 13	
Scheme	LCRS	LCRS	MUSA	NCMA	NCMA	MUSA	IGMA	MUSA	ACMA	Legacy BPSK	Legacy QPSK
Code rate	0.1	0.1	0.2	0.1	0.2	0.2	0.093	0.185	0.1	0.2	0.1
Receiver	MMSE - hard SIC	EPA	MMSE - hard SIC	MMSE - hard SIC	MMSE-hard SIC	MMSE-hard SIC	ESE-SISO	ESE-SISO	ESE-SISO	MMSE-hard SIC	MMSE-hard SIC
Company	Source 5									Source 14	Source 7
Scheme	SCMA	LCRS	MUSA	MUSA	SL-RSMA	SL-RSMA	SL-RSMA	ML-RSMA	SCMA	LSSA	NOCA
Code rate	0.1	0.1	0.2	0.2	0.2	0.2	0.2	0.2	0.2	0.1	
Receiver	Chip EPA hybrid PIC	Chip EPA hybrid PIC	Block MMSE hard PIC	Chip EPA hybrid PIC	Block MMSE hard PIC	Chip EPA hybrid PIC	Block MMSE hard PIC	Chip EPA hybrid PIC	chip MMSE-hard PIC	ESE	MMSE-hard PIC

4) Case 2 with 12 UEs of ideal channel estimation:

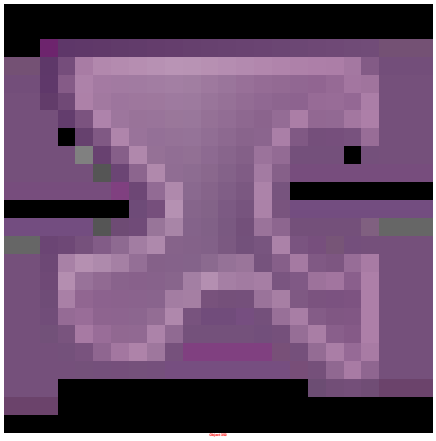

Figure 8.2-4: BLER vs. SNR results for Case 2 with 12 UEs

Table 8.2-5: Assumptions of code rate and receiver for each simulated scheme for Case 2 with 12 UEs

Company	Source 4	Source 11	Source 2		Source 3				Source 8		
Scheme	RSMA	IDMA	PDMA	PDMA	UGMA	MUSA	SCMA	RSMA	NCMA	NCMA	MUSA
Code rate	0.2	0.1	0.2	0.2	0.19	0.19	0.25	0.19	0.1	0.2	0.2
Receiver	MMSE - hybrid SIC	ESE-SISO	EPA	MMSE - hard SIC	MMSE - hard SIC	MMSE - hard SIC	EPA	MMSE - hard SIC	MMSE - hard SIC	MMSE - hard SIC	
Company	Source 1									Source 9	
Scheme	MUSA	WSMA	UGMA	RSMA	NOCA	NCMA	NCMA Q	MUSA		IGMA	MUSA
Code rate	0.2	0.41	0.41	0.41	0.41	0.41	0.41	0.41		0.093	0.185
Receiver	MMSE - hard SIC	MMSE - hard SIC	MMSE - hard SIC	MMSE - hard SIC	MMSE - hard SIC	MMSE - hard SIC	MMSE-hard SIC	MMSE - hard SIC		ESE-SISO	ESE-SISO
Company	Source 5										Source 14

Scheme	SCMA	LCRS	MUSA	MUSA	SL-RSMA	SL-RSMA	ML-RSMA	ML-RSMA	SCMA	IGMA	LSSA
Code rate	0.1	0.1	0.2	0.2	0.2	0.2	0.2	0.2	0.2	0.14	0.1
Receiver	Chip EPA hybrid PIC	Chip EPA hybrid PIC	Block MMSE hard PIC	Chip EPA hybrid PIC	Block MMSE hard PIC	Chip EPA hybrid PIC	Block MMSE hard PIC	Chip EPA hybrid PIC	chip MMSE-hard PIC	Chip EPA hybrid PIC	ESE
Company	Source 10				Source 7	Source 12	Source 10	Source 6		Source 13	
Scheme	IDMA	MUSA	IDMA	SCMA	PDMA	NOCA	ACMA	LCRS	LCRS	Legacy BPSK	Legacy QPSK
Code rate	0.1	0.2	0.1	0.27	0.2	0.37	0.1	0.1	0.1	0.2	0.1
Receiver	EPA	EPA	EPA	EPA	EPA	MMSE - hard PIC	ESE-SISO	MMSE - hard SIC	EPA	MMSE - hard SIC	MMSE - hard SIC

Observation: with ideal channel estimation, the LLS results for Case 2 with 6 or 12 UEs show a similar performance for most of curves provided for coding rates no more than 0.2, at target BLER = 0.1. With ideal channel estimation, the LLS results for Case 2 with 6 or 12 UEs show a similar performance for most of curves provided for coding rate ~0.4, at target BLER = 0.1.

5) Case 3 with 6 UEs of ideal channel estimation:

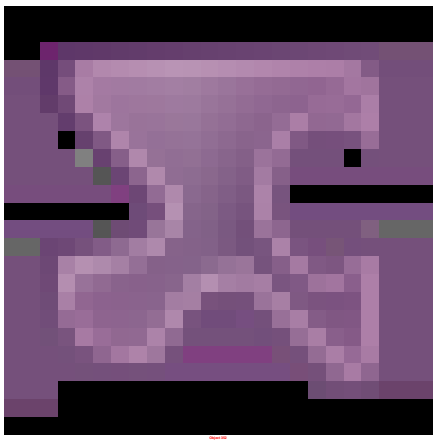

Figure 8.2-5: BLER vs. SNR results for Case 3 with 6 UEs

Table 8.2-6: Assumptions of code rate and receiver for each simulated scheme for Case 3 with 6 UEs

Company	Source 4	Source 8	Source 2		Source 3				Source 12	Source 13	
Scheme	RSMA	NCMA	PDMA	PDMA	UGMA	MUSA	SCMA	RSMA	ACMA	Legacy BPSK	Legacy QPSK
Code rate	0.19	0.19	0.39	0.39	0.37	0.37	0.37	0.37	0.19	0.39	0.19
Receiver	MMSE - hybrid SIC	MMSE-hard SIC	EPA	MMSE - hard SIC	MMSE-hard SIC	MMSE-hard SIC	EPA	MMSE-hard SIC	ESE-SISO	MMSE-hard SIC	MMSE-hard SIC
Company	Source 1			Source 9		Source 6		Source 10			
Scheme	MUSA	MUSA	SCMA	IGMA	MUSA	LCRS	LCRS	IDMA	IDMA	MUSA	SCMA
Code rate	0.39	0.39	0.39	0.37	0.74	0.19	0.19	0.19	0.19	0.39	0.39
Receiver	EPA	MMSE-hard SIC	EPA	ESE-SISO	ESE-SISO	MMSE-hard SIC	EPA	ESE	EPA	EPA	EPA
Company	Source 5										Source 14
Scheme	SCMA	LCRS	MUSA	MUSA	SL-RSMA	SL-RSMA	ML-RSMA	ML-RSMA	SCMA	IGMA	LSSA
Code rate	0.19	0.19	0.39	0.39	0.39	0.39	0.19	0.19	0.19	0.26	0.37
Receiver	Chip EPA hybrid PIC	Chip EPA hybrid PIC	Block MMSE hard PIC	Chip EPA hybrid PIC	Block MMSE hard PIC	Chip EPA hybrid PIC	Block MMSE hard PIC	Chip EPA hybrid PIC	chip MMSE-hard PIC	Chip EPA hybrid PIC	ESE

6) Case 3 with 10 UEs of ideal channel estimation:

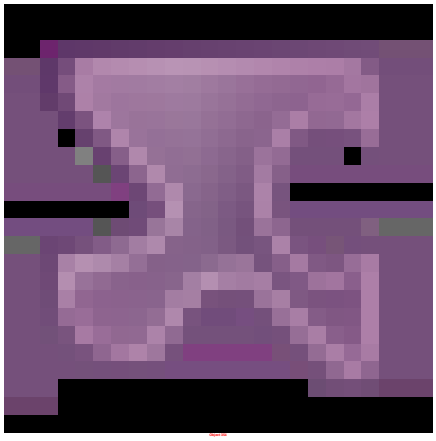

Figure 8.2-6: BLER vs. SNR results for Case 3 with 10 UEs

Table 8.2-7: Assumptions of code rate and receiver for each simulated scheme for Case 3 with 10 UEs

Company	Source 4	Source 12	Source 2		Source 3				Source 8	Source 13	
Scheme	RSMA	ACMA	PDMA	PDMA	UGMA	MUSA	SCMA	RSMA	NCMA	Legacy BPSK	Legacy QPSK
Code rate	0.19	0.19	0.39	0.39	0.37	0.37	0.37	0.37	0.39	0.39	0.19
Receiver	MMSE-hybrid SIC	ESE-SISO	EPA	MMSE-hard SIC	MMSE-hard SIC	MMSE-hard SIC	EPA	MMSE-hard SIC	MMSE-hard SIC	MMSE-hard SIC	MMSE-hard SIC
Company	Source 1			Source 6		Source 9		Source 10			
Scheme	MUSA	MUSA	SCMA	LCRS	LCRS	IGMA	MUSA	IDMA	IDMA	MUSA	SCMA
Code rate	0.39	0.39	0.39	0.19	0.19	0.37	0.74	0.1	0.19	0.39	0.39
Receiver	EPA	MMSE-hard SIC	EPA	MMSE-hard SIC	EPA	ESE-SISO	ESE-SISO	ESE-SISO	EPA	EPA	EPA
Company	Source 5										Source 14
Scheme	SCMA	LCRS	MUSA	MUSA	SL-RSMA	SL-RSMA	ML-RSMA	ML-RSMA	SCMA	IGMA	LSSA
Code rate	0.39	0.19	0.39	0.39	0.39	0.39	0.39	0.39	0.39	0.39	0.37
Receiver	Chip EPA hybrid PIC	Chip EPA hybrid PIC	Block MMSE hard PIC	Chip EPA hybrid PIC	Block MMSE hard PIC	Chip EPA hybrid PIC	Block MMSE hard PIC	Chip EPA hybrid PIC	chip MMSE-hard PIC	Chip EPA hybrid PIC	ESE

Observation: for Case 3 with 10 UEs and ideal channel estimation,

- the LLS results for simulated schemes with the Chip EPA hybrid PIC or MMSE-hybrid IC receiver or ESE-SISO receiver show a similar performance for most of curves provided with code rate up to 0.4, at target BLER = 0.1.
- the LLS results for simulated schemes with the MMSE-hard IC receiver show a similar performance for most of curves provided with code rate up to 0.4, at target BLER = 0.1.
- the LLS results with the Chip EPA hybrid PIC or MMSE-hybrid IC receiver or ESE-SISO receiver show better performance than the results with the MMSE-hard IC receiver.

7) Case 4 with 6 UEs of ideal channel estimation:

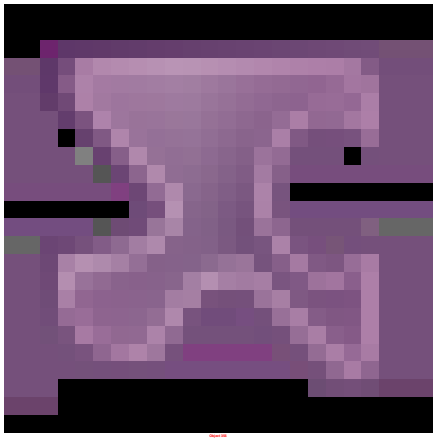

Figure 8.2-7: BLER vs. SNR results for Case 4 with 6 UEs

Table 8.2-8: Assumptions of code rate and receiver for each simulated scheme for Case 4 with 6 UEs

Company	Source 4		Source 2		Source 3				Source 10			
Scheme	RSMA	SCMA	PDMA	PDMA	UGMA	MUSA	SCMA		IDMA	IDMA	SCMA	
Code rate	0.29		0.57	0.57	0.55	0.55	0.69		0.29	0.15	0.57	
Receiver	MMSE - hybrid SIC	EPA	EPA	MMSE - hard SIC	MMSE - hard SIC	MMSE - hard SIC	EPA		EPA	ESE	EPA	
Company	Source 1			Source 8	Source 9			Source 6		Source 13		Source 12
Scheme	MUSA	MUSA	SCMA	NCMA	IGMA	MUSA	IGMA	LCRS	LCRS	Legacy BPSK	Legacy QPSK	ACMA
Code rate	0.57	0.57	0.57	0.57	0.56	0.56	0.56	0.29	0.29	0.57	0.29	0.287
Receiver	EPA	MMSE - hard SIC	EPA	MMSE - hard SIC	ESE-SISO	ESE-SISO	MMSE hybrid IC	MMSE - hard SIC	EPA	MMSE-hard SIC	MMSE - hard SIC	ESE-SISO
Company	Source 5										Source 14	
Scheme	MUSA	SL-RSMA	SL-RSMA	ML-RSMA	ML-RSMA	SCMA	SCMA	LCRS	MUSA	IGMA	LSSA	
Code rate	0.57	0.57	0.57	0.38	0.38	0.57	0.38	0.29	0.57	0.38	0.56	
Receiver	Chip EPA hybrid PIC	Block MMSE hard PIC	Chip EPA hybrid PIC	Block MMSE hard PIC	Chip EPA hybrid PIC	chip MMSE-hard PIC	Chip EPA hybrid PIC	Chip EPA hybrid PIC	Block MMSE hard PIC	Chip EPA hybrid PIC	ESE	

Observation: for Case 4 with 6 UEs and ideal channel estimation,

- the LLS results for simulated schemes with the Chip EPA hybrid PIC or MMSE-hybrid IC receiver show a similar performance for most of curves provided with code rate up to 0.6, at target BLER = 0.1.
- the LLS results for simulated schemes with the MMSE-hard IC receiver or ESE-SISO receiver show a similar performance for most of curves provided with code rate up to 0.6, at target BLER = 0.1.
- the LLS results with the Chip EPA hybrid PIC or MMSE-hybrid IC receiver show better performance than the results with the MMSE-hard IC receiver or ESE-SISO receiver.

8) Case 4 with 8 UEs of ideal channel estimation:

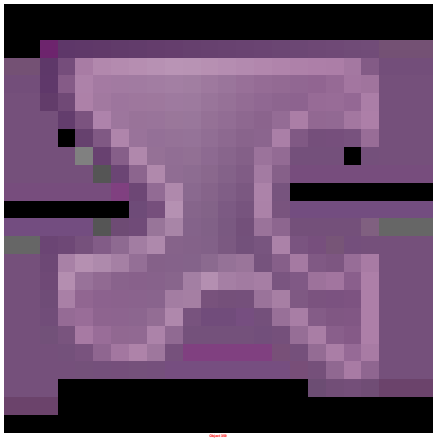

Figure 8.2-8: BLER vs. SNR results for Case 4 with 8 UEs

Table 8.2-9: Assumptions of code rate and receiver for each simulated scheme for Case 4 with 8 UEs

Company	Source 9				Source 3				Source 2	
Scheme	IGMA	MUSA	IGMA	MUSA	UGMA	MUSA	SCMA	RSMA	PDMA	PDMA
Code rate	0.56	0.56	0.56	0.56	0.55	0.55	0.69	0.55	0.57	0.57
Receiver	ESE-SISO	ESE- SISO	MMSE hybrid IC	Block MMSE	MMSE-hard SIC	MMSE-hard SIC	EPA	MMSE-hard SIC	EPA	MMSE-hard SIC
Company	Source 1									
Scheme	MUSA	WSMA	UGMA	RSMA	NOCA	NCMA	NCMAQ	MUSA	MUSA	SCMA
Code rate	0.43	0.57	0.57	0.57	0.57	0.57	0.57	0.57	0.43	0.57
Receiver	MMSE-hard SIC	MMSE-hard SIC	MMSE-hard SIC	MMSE-hard SIC	MMSE-hard SIC	MMSE-hard SIC	MMSE-hard SIC	MMSE-hard SIC	EPA	EPA
Company	Source 5									
Scheme	SCMA	LCRS	MUSA	MUSA	SL-RSMA	SL-RSMA	ML-RSMA	ML-RSMA	IGMA	
Code rate	0.57	0.29	0.43	0.43	0.43	0.57	0.43	0.57	0.57	
Receiver	Chip EPA hybrid PIC	Chip EPA hybrid PIC	Block MMSE hard PIC	Chip EPA hybrid PIC	Block MMSE hard PIC	Chip EPA hybrid PIC	Block MMSE hard PIC	Chip EPA hybrid PIC	Chip EPA hybrid PIC	
Company	Source 10			Source 13		Source 8	Source 12	Source 14	Source 4	
Scheme	IDMA	IDMA	SCMA	Legacy BPSK	Legacy QPSK	NCMA	ACMA	LSSA	RSMA	SCMA
Code rate	0.15	0.15	0.57	0.57	0.29	0.57	0.287	0.56	0.43	
Receiver	EPA	ESE	EPA	MMSE-hard SIC	MMSE-hard SIC	MMSE-hard SIC	ESE-SISO	ESE	MMSE-hybrid SIC	EPA

9) Case 5 with 4 UEs of ideal channel estimation:

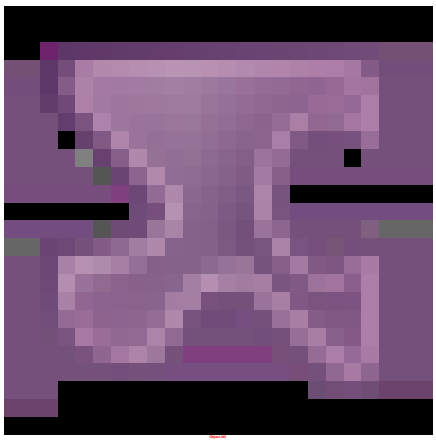

Figure 8.2-9: BLER vs. SNR results for Case 5 with 4 UEs

Table 8.2-10: Assumptions of code rate and receiver for each simulated scheme for Case 5 with 4 UEs

Company	Source 4		Source 2		Source 3			Source 10		Source 14	
Scheme	RSMA	SCMA	PDMA	PDMA	UGMA	MUSA	SCMA	IDMA	IDMA	LSSA	
Code rate	0.36	0.71	0.71	0.71	0.35	0.35	0.69	0.36	0.18	0.68	
Receiver	MMSE - hybard SIC	EPA	EPA	MMSE - hard SIC	MMSE - hard SIC	MMSE - hard SIC	EPA	EPA	ESE	ESE	
Company	Source 1			Source 8	Source 9		Source 12	Source 13		Source 6	
Scheme	MUSA	MUSA	SCMA	NCMA	IGMA	MUSA	ACMA	Legacy BPSK	Legacy QPSK	LCRS	LCRS
Code rate	0.36	0.71	0.71	0.36	0.7	0.7	0.38	0.71	0.36	0.36	0.36
Receiver	EPA	MMSE- hard SIC	EPA	MMSE - hard SIC	ESE-SISO	ESE-SISO	ESE-SISO	MMSE-hard SIC	MMSE-hard SIC	MMSE-hard SIC	EPA
Company	Source 5										
Scheme	SCMA	LCRS	MUSA	MUSA	SL-RSMA	SL-RSMA	ML-RSMA	ML-RSMA	SCMA	IGMA	
Code rate	0.36	0.36	0.71	0.71	0.71	0.71	0.36	0.36	0.36	0.48	
Receiver	Chip EPA hybrid PIC	Chip EPA hybrid PIC	Block MMSE hard PIC	Chip EPA hybrid PIC	Block MMSE hard PIC	Chip EPA hybrid PIC	Block MMSE hard PIC	Chip EPA hybrid PIC	chip MMSE-hard PIC	Chip EPA hybrid PIC	

Observation: for Case 5 with 4 UEs and ideal channel estimation,

- when the code rate is similar, the LLS results for simulated schemes with the Chip EPA hybrid PIC or MMSE-hybrid IC receiver show a similar performance for most of curves provided, at target BLER = 0.1.
- the LLS results for simulated schemes with the MMSE-hard IC receiver and ESE-SISO receiver show a similar performance for most of curves provided, at target BLER = 0.1.
- When the code rate is round 0.36, the LLS results with the Chip EPA hybrid PIC or MMSE-hybrid IC receiver show better performance than the results with the MMSE-hard IC receiver or ESE-SISO receiver.
- When the code rate is round 0.71, the LLS results with the Chip EPA hybrid PIC or MMSE-hybrid IC receiver show similar performance to the results with the MMSE-hard IC receiver or ESE-SISO receiver

10) Case 5 with 6 UEs of ideal channel estimation:

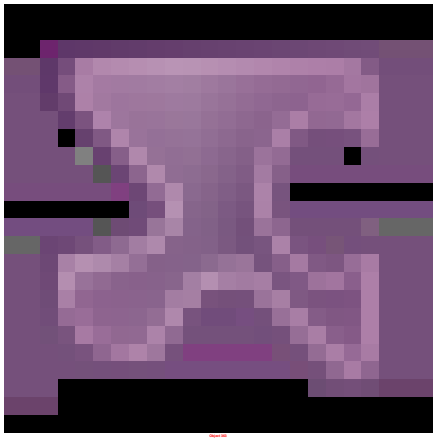

Figure 8.2-10: BLER vs. SNR results for Case 5 with 6 UEs

Table 8.2-11: Assumptions of code rate and receiver for each simulated scheme for Case 5 with 6 UEs

Compan	Source 4	Source	Source 3	Source 2	Source	

y				12							6	
Scheme	RSMA	RSMA	SCMA	ACMA	UGMA	MUSA	SCMA	RSMA	PDMA	PDMA	LCRS	
Code rate	0.36	2*0.19	0.71	0.38	0.35	0.35	0.69	0.35	0.71	0.71	0.36	
Receiver	MMSE -- hybrid SIC	MMSE -- hybrid SIC	EPA	ESE-SISO	MMSE -- hard SIC	MMSE -- hard SIC	EPA	MMSE -- hard SIC	EPA	MMSE -- hard SIC	MMSE -- hard SIC	
Company	Source 1			Source 8	Source 9				Source 14	Source 13		
Scheme	MUSA	MUSA	SCMA	NCMA	IGMA	MUSA	IGMA	MUSA	LSSA	Legacy BPSK	Legacy QPSK	
Code rate	0.71	0.71	0.46	0.36	0.7	0.7	0.7	0.7	0.68	0.71	0.36	
Receiver	EPA	MMSE -- hard SIC	EPA	MMSE -- hard SIC	ESE-SISO	ESE-SISO	MMSE hybrid IC	Block MMSE	ESE	MMSE - hard SIC	MMSE - hard SIC	
Company	Source 5										Source 10	
Scheme	MUSA	SL-RSMA	SL-RSMA	ML-RSMA	ML-RSMA	SCMA	LCRS	MUSA	IGMA	SCMA	IDMA	IDMA
Code rate	0.71	0.71	0.36	0.36	0.36	0.48	0.36	0.71	0.48	0.71	0.18	0.18
Receiver	Chip EPA hybrid PIC	Block MMSE hard PIC	Chip EPA hybrid PIC	Block MMSE hard PIC	Chip EPA hybrid PIC	Chip EPA hybrid PIC	Chip EPA hybrid PIC	Block MMSE hard PIC	Chip EPA hybrid PIC	chip MMSE -hard PIC	EPA	ESE

Observation: for Case 5 with 6 UEs and ideal channel estimation, the LLS results for linear-spreading based schemes (SF>1) with the MMSE-hard IC receiver show a similar performance, at target BLER = 0.1.

11) Case 14 with 6 UEs, ideal channel estimation

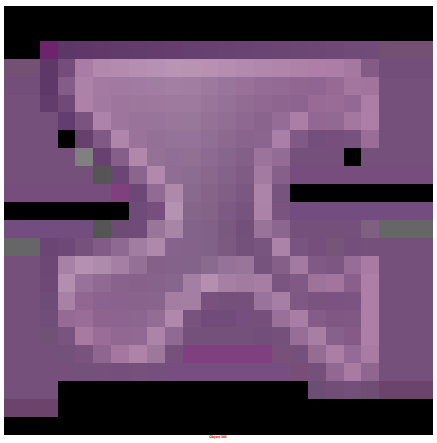

Figure 8.2-11: BLER vs. SNR results for Case 14 with 6 UEs

Table 8.2-12: Assumptions of code rate and receiver for each simulated scheme for Case 14 with 6 UEs

Company	Source 11	Source 3		Source 6	Source 1		Source 8		Source 4
Scheme	IDMA	UGMA	MUSA	LCRS	MUSA	MUSA	NCMA	NCMA2	RSMA
Code rate	0.055	0.1	0.1	0.06	0.11	0.11	0.056	0.11	0.1
Receiver	ESE-SISO	MMSE-hard SIC	MMSE-hard SIC	MMSE-hard SIC	EPA	MMSE-hard SIC	MMSE-hard SIC	MMSE-hard SIC	MMSE--hybrid SIC
Company	Source 5								
Scheme	SCMA	LCRS	MUSA	MUSA	SL-RSMA	SL-RSMA	ML-RSMA	ML-RSMA	SCMA
Code rate	0.06	0.06	0.11	0.11	0.11	0.11	0.06	0.06	0.06
Receiver	chip MMSE-hard PIC	Chip EPA hybrid PIC	Block MMSE hard PIC	Chip EPA hybrid PIC	Block MMSE hard PIC	Chip EPA hybrid PIC	Chip EPA hybrid PIC	Block MMSE hard PIC	Chip EPA hybrid PIC

12) Case 14 with 12 UEs, ideal channel estimation

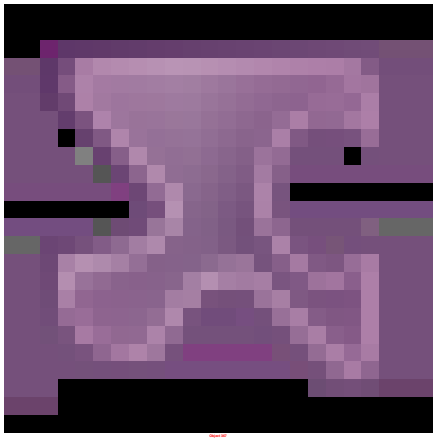

Figure 8.2-12: BLER vs. SNR results for Case 14 with 12 UEs

Table 8.2-13: Assumptions of code rate and receiver for each simulated scheme for Case 14 with 12 UEs

Company	Source 11	Source 3		Source 6	Source 1		Source 8		Source 4
Scheme	IDMA	UGMA	MUSA	LCRS	MUSA	MUSA	NCMA	NCMA2	RSMA
Code rate	0.055	0.1	0.1	0.06	0.11	0.11	0.056	0.11	0.1
Receiver	ESE-SISO	MMSE-hard SIC	MMSE-hard SIC	MMSE-hard SIC	EPA	MMSE-hard SIC	MMSE-hard SIC	MMSE-hard SIC	MMSE--hybrid SIC
Company	Source 5								
Scheme	SCMA	LCRS	MUSA	MUSA	SL-RSMA	SL-RSMA	ML-RSMA	ML-RSMA	SCMA
Code rate	0.06	0.06	0.11	0.11	0.11	0.11	0.06	0.06	0.06
Receiver	chip MMSE-hard PIC	Chip EPA hybrid PIC	Block MMSE hard PIC	Chip EPA hybrid PIC	Block MMSE hard PIC	Chip EPA hybrid PIC	Chip EPA hybrid PIC	Block MMSE hard PIC	Chip EPA hybrid PIC

Observation: Under ideal conditions for Case 14 with 6 or 12 UEs, the LLS results for simulated schemes show a similar performance for most of curves provided, at target BLER = 0.001, with appropriate configurations.

Note: "ideal conditions" means: equal SNR, zero TO/FO and fixed MA signature allocation.

13) Case 15 with 4 UEs, ideal channel estimation

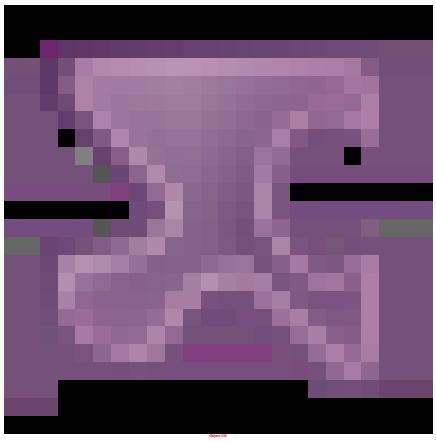

Figure 8.2-13: BLER vs. SNR results for Case 15 with 4 UEs

Table 8.2-14: Assumptions of code rate and receiver for each simulated scheme for Case 15 with 4 UEs

Company	Source 11	Source 3		Source 6	Source 1		Source 4	Source 8	
Scheme	IDMA	UGMA	MUSA	LCRS	MUSA	MUSA	RSMA	NCMA	NCMA2
Code rate		0.55	0.55	0.29	0.285	0.285	0.55	0.287	0.57

Receiver	ESE-SISO	MMSE-hard SIC	MMSE-hard SIC	MMSE-hard SIC	EPA	MMSE-hard SIC	MMSE--hybrid SIC	MMSE-hard SIC	MMSE-hard SIC
Company	Source 5								
Scheme	SCMA	LCRS	MUSA	MUSA	SL-RSMA	SL-RSMA	ML-RSMA	ML-RSMA	SCMA
Code rate	0.29	0.29	0.57	0.57	0.57	0.57	0.29	0.29	0.29
Receiver	chip MMSE-hard PIC	Chip EPA hybrid PIC	Block MMSE hard PIC	Chip EPA hybrid PIC	Block MMSE hard PIC	Chip EPA hybrid PIC	Chip EPA hybrid PIC	Block MMSE hard PIC	Chip EPA hybrid PIC

14) Case 15 with 6 UEs, ideal channel estimation

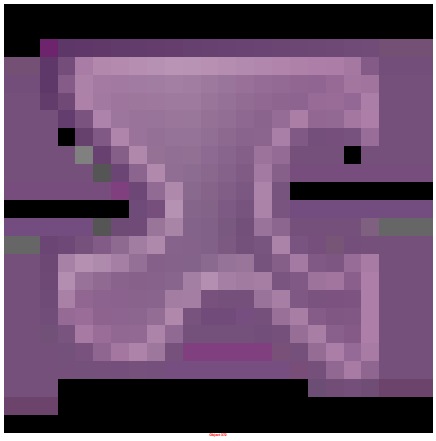

Figure 8.2-14: BLER vs. SNR results for Case 15 with 6 UEs

Table 8.2-15: Assumptions of code rate and receiver for each simulated scheme for Case 15 with 6 UEs

Company	Source 11	Source 3		Source 6	Source 1		Source 4		
Scheme	IDMA	UGMA	MUSA	LCRS	MUSA	MUSA	RSMA		
Code rate		0.55	0.55	0.29	0.285	0.285	0.55		
Receiver	ESE-SISO	MMSE-hard SIC	MMSE-hard SIC	MMSE-hard SIC	EPA	MMSE-hard SIC	MMSE--hybrid SIC		
Company	Source 5								
Scheme	SCMA	LCRS	MUSA	MUSA	SL-RSMA	ML-RSMA	ML-RSMA	SL-RSMA	SCMA
Code rate	0.29	0.29	0.57	0.57	0.57	0.29	0.29	0.57	0.29
Receiver	chip MMSE-hard PIC	Chip EPA hybrid PIC	Block MMSE hard PIC	Chip EPA hybrid PIC	Block MMSE hard PIC	Chip EPA hybrid PIC	Block MMSE hard PIC	Chip EPA hybrid PIC	Chip EPA hybrid PIC

Observation: Under ideal conditions for Case 15 with 4 or 6 UEs,

- the LLS results for simulated schemes with the code rate round 0.3 show a similar performance for most of curves, at target BLER = 0.001.
- the LLS results for simulated schemes with the code rate round 0.6 show a similar performance for most of curves, at target BLER = 0.001.
- the LLS results with the code rate round 0.3 show better performance than the results with the code rate round 0.6.

15) Case 16 with 6 UEs, ideal channel estimation

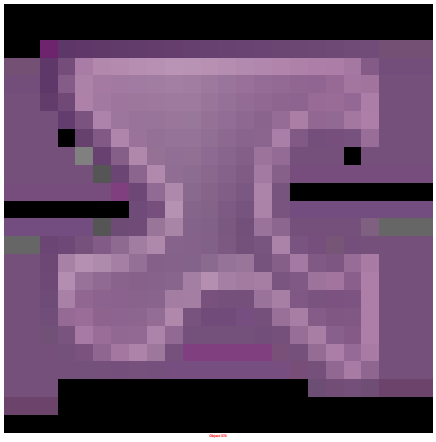

Figure 8.2-15: BLER vs. SNR results for Case 16 with 6 UEs

Table 8.2-16: Assumptions of code rate and receiver for each simulated scheme for Case 16 with 6 UEs

Company	Source 11	Source 9	Source 6	Source 1		Source 3			Source 8	
Scheme	IDMA	IGMA	LCRS	MUSA	MUSA	UGMA	MUSA	SCMA	NCMA	NCMA2
Code rate		0.11	0.06	0.11	0.11	0.1	0.1	0.125	0.055	0.11
Receiver	ESE-SISO	ESE-SISO	MMSE-hard SIC	EPA	MMSE-hard SIC	MMSE-hard SIC	MMSE-hard SIC	EPA	MMSE-hard SIC	MMSE-hard SIC
Company	Source 5									
Scheme	SCMA	LCRS	MUSA	MUSA	SL-RSMA	ML-RSMA	ML-RSMA	SL-RSMA	SCMA	
Code rate	0.06	0.06	0.11	0.11	0.11	0.06	0.06	0.11	0.06	
Receiver	chip MMSE-hard PIC	Chip EPA hybrid PIC	Block MMSE hard PIC	Chip EPA hybrid PIC	Block MMSE hard PIC	Block MMSE hard PIC	Chip EPA hybrid PIC	Chip EPA hybrid PIC	Chip EPA hybrid PIC	

16) Case 16 with 12 UEs, ideal channel estimation

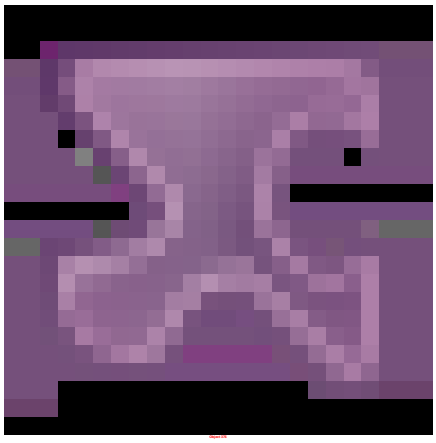

Figure 8.2-16: BLER vs. SNR results for Case 16 with 12 UEs

Table 8.2-17: Assumptions of code rate and receiver for each simulated scheme for Case 16 with 12 UEs

Company	Source 11	Source 9	Source 6	Source 1		Source 3			Source 8	
Scheme	IDMA	IGMA	LCRS	MUSA	MUSA	UGMA	MUSA	SCMA	NCMA	NCMA 2
Code rate		0.11	0.06	0.11	0.11	0.1	0.1	0.125	0.055	0.11
Receiver	ESE-SISO	ESE-SISO	MMSE-hard SIC	EPA	MMSE-hard SIC	MMSE-hard SIC	MMSE-hard SIC	EPA	MMSE- hard SIC	MMSE-hard SIC

Company	Source 5									
Scheme	SCMA	LCRS	MUSA	MUSA	SL-RSMA	ML-RSMA	ML-RSMA	SL-RSMA	SCMA	
Code rate	0.06	0.06	0.11	0.11	0.11	0.06	0.06	0.11	0.06	
Receiver	chip MMSE-hard PIC	Chip EPA hybrid PIC	Block MMSE hard PIC	Chip EPA hybrid PIC	Block MMSE hard PIC	Block MMSE hard PIC	Chip EPA hybrid PIC	Chip EPA hybrid PIC	Chip EPA hybrid PIC	

Observation: Under ideal conditions for Case 16 with 6 or 12 UEs, the LLS results for simulated schemes show a similar performance for most of curves provided, at target BLER = 0.001, with appropriate configurations.

17) Case 17 with 4 UEs, ideal channel estimation

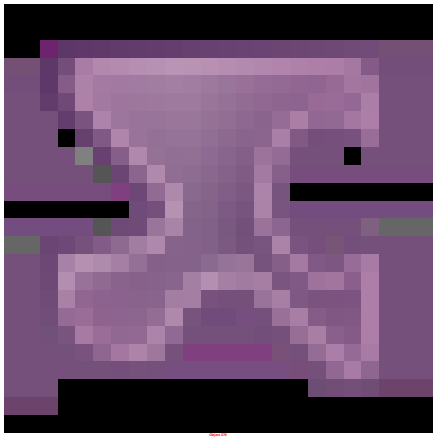

Figure 8.2-17: BLER vs. SNR results for Case 17 with 4 UEs

Table 8.2-18: Assumptions of code rate and receiver for each simulated scheme for Case 17 with 4 UEs

Company	Source 11	Source 9	Source 6	Source 1	Source 3			Source 8	
Scheme	IDMA	IGMA	LCRS	MUSA	UGMA	MUSA	SCMA	NCMA	NCMA2
Code rate	0.285		0.29	0.29	0.55	0.55	0.55	0.29	0.57
Receiver	ESE-SISO	ESE-SISO	MMSE-hard SIC	MMSE-hard SIC	MMSE-hard SIC	MMSE-hard SIC	EPA	MMSE-hard SIC	MMSE-hard SIC
Company	Source 5								
Scheme	SCMA	LCRS	MUSA	MUSA	SL-RSMA	ML-RSMA	ML-RSMA	SL-RSMA	SCMA
Code rate	0.29	0.29	0.57	0.57	0.57	0.29	0.29	0.57	0.29
Receiver	chip MMSE-hard PIC	Chip EPA hybrid PIC	Block MMSE hard PIC	Chip EPA hybrid PIC	Block MMSE hard PIC	Block MMSE hard PIC	Chip EPA hybrid PIC	Chip EPA hybrid PIC	Chip EPA hybrid PIC

18) Case 17 with 6 UEs, ideal channel estimation

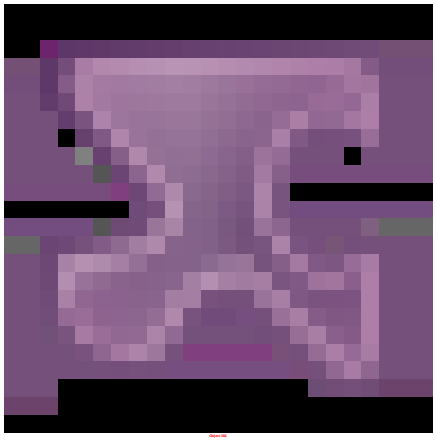

Figure 8.2-18: BLER vs. SNR results for Case 17 with 6 UEs

Table 8.2-19: Assumptions of code rate and receiver for each simulated scheme for Case 17 with 6 UEs

Company	Source 1	Source 9	Source 6	Source 3			Source 8		
Scheme	MUSA	IGMA	LCRS	UGMA	MUSA	SCMA	NCMA	NCMA2	
Code rate	0.29		0.29	0.55	0.55	0.55	0.29	0.57	
Receiver	MMSE-hard SIC	ESE-SISO	MMSE-hard SIC	MMSE-hard SIC	MMSE-hard SIC	EPA	MMSE-hard SIC	MMSE-hard SIC	
Company	Source 5								
Scheme	SCMA	LCRS	MUSA	MUSA	SL-RSMA	ML-RSMA	ML-RSMA	SL-RSMA	SCMA
Code rate	0.29	0.29	0.57	0.57	0.57	0.29	0.29	0.57	0.29
Receiver	chip MMSE-hard PIC	Chip EPA hybrid PIC	Block MMSE hard PIC	Chip EPA hybrid PIC	Block MMSE hard PIC	Block MMSE hard PIC	Chip EPA hybrid PIC	Chip EPA hybrid PIC	Chip EPA hybrid PIC

Observation: Under ideal conditions for Case 17 with 4 or 6 UEs,

- the LLS results for simulated schemes with the code rate round 0.3 show a similar performance for most of curves, at target BLER = 0.001.
- the LLS results for simulated schemes with the code rate round 0.6 show a similar performance for most of curves, at target BLER = 0.001.
- the LLS results with the code rate round 0.3 show better performance than the results with the code rate round 0.6.

19) Case 18 with 12 UEs, ideal channel estimation

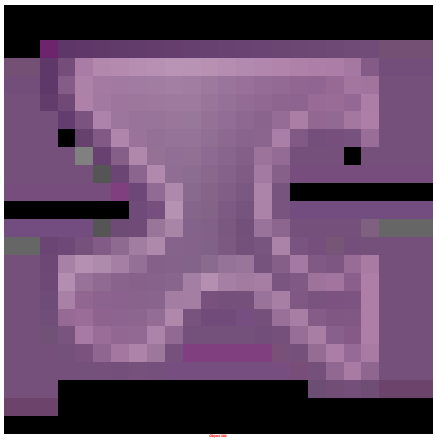

Figure 8.2-19: BLER vs. SNR results for Case 18 with 12 UEs

Table 8.2-20: Assumptions of code rate and receiver for each simulated scheme for Case 18 with 12 UEs

Company	Source 4	Source 11	Source 2		Source 3		Source 6	Source 8	
Scheme	RSMA	IDMA	PDMA	PDMA	UGMA	MUSA	LCRS	NCMA	NCMA2
Code rate	0.05	0.05	0.2	0.2	0.095	0.1	0.05	0.05	0.1
Receiver	MMSE-hybrid SIC	ESE-SISO	EPA	MMSE-hard SIC	MMSE-hard SIC	MMSE-hard SIC	MMSE-hard SIC	MMSE-hard SIC	MMSE-hard SIC
Company	Source 1		Source 9		Source 7	Source 13		Source 14	
Scheme	MUSA	MUSA	IGMA	MUSA	NOCA	Legacy BPSK	Legacy QPSK	LSSA	
Code rate	0.1	0.1	0.09	0.19	0.28	0.1	0.05	0,1	
Receiver	EPA	MMSE-hard SIC	ESE-SISO	ESE- SISO	MMSE-hard PIC	MMSE-hard SIC	MMSE-hard SIC	ESE	
Company	Source 5								
Scheme	SCMA	LCRS	MUSA	MUSA	SL-RSMA	SL-RSMA	ML-RSMA	ML-RSMA	SCMA
Code rate	0.14	0.05	0.1	0.1	0.2	0.2	0.2	0.2	0.14
Receiver	chip MMSE-hard PIC	Chip EPA hybrid PIC	Block MMSE hard PIC	Chip EPA hybrid PIC	Block MMSE hard PIC	Chip EPA hybrid PIC	Block MMSE hard PIC	Chip EPA hybrid PIC	Chip EPA hybrid PIC

20) Case 18 with 24 UEs, ideal channel estimation

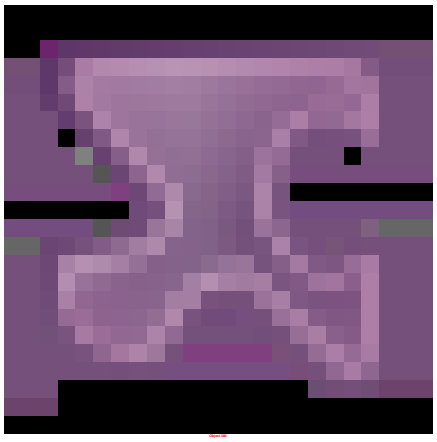

Figure 8.2-20: BLER vs. SNR results for Case 18 with 24 UEs

Table 8.2-21: Assumptions of code rate and receiver for each simulated scheme for Case 18 with 24 UEs

Company	Source 4	Source 11	Source 2		Source 3		Source 14	Source 8	
Scheme	RSMA	IDMA	PDMA	PDMA	UGMA	MUSA	LSSA	NCMA	NCMA2
Code rate	0.05	0.05	0.2	0.2	0.095	0.18	0,1	0.05	0.1
Receiver	MMSE-hybrid SIC	ESE-SISO	EPA	MMSE-hard SIC	MMSE-hard SIC	MMSE-hard SIC	ESE	MMSE-hard SIC	MMSE-hard SIC
Company	Source 1		Source 9		Source 7	Source 13			
Scheme	MUSA	MUSA	IGMA	MUSA	NOCA	Legacy BPSK	Legacy QPSK		
Code rate	0.1	0.1	0.09	0.19	0.28	0.1	0.05		
Receiver	EPA	MMSE-hard SIC	ESE-SISO	ESE- SISO	MMSE-hard PIC	MMSE-hard SIC	MMSE-hard SIC		
Company	Source 5								
Scheme	SCMA	LCRS	MUSA	MUSA	SL-RSMA	SL-RSMA	ML-RSMA	ML-RSMA	SCMA
Code rate	0.14	0.05	0.1	0.1	0.2	0.2	0.2	0.2	0.14
Receiver	chip MMSE-hard PIC	Chip EPA hybrid PIC	Block MMSE hard PIC	Chip EPA hybrid PIC	Block MMSE hard PIC	Chip EPA hybrid PIC	Block MMSE hard PIC	Chip EPA hybrid PIC	Chip EPA hybrid PIC

Observation: Under ideal conditions for Case 18 with 12 or 24 UEs, the LLS results for simulated schemes show a similar performance for most of curves provided, at target BLER = 0.1, with appropriate configurations.

21) Case 19 with 8 UEs, ideal channel estimation

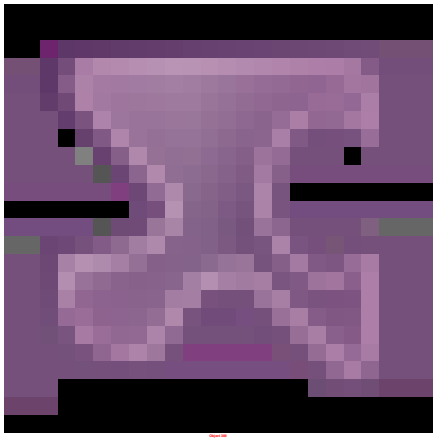

Figure 8.2-21: BLER vs. SNR results for Case 19 with 8 UEs

Table 8.2-22: Assumptions of code rate and receiver for each simulated scheme for Case 19 with 8 UEs

Company	Source 4	Source 6	Source 2		Source 3		Source 8		Source 14
Scheme	RSMA	LCRS	PDMA	PDMA	UGMA	MUSA	NCMA	NCMA2	LSSA
Code rate	0.19	0.19	0.38	0.38	0.37	0.37	0.19	0.37	0,19
Receiver	MMSE-hybrid SIC	MMSE-hard SIC	EPA	MMSE-hard SIC	MMSE-hard SIC	MMSE-hard SIC	MMSE-hard SIC	MMSE-hard SIC	ESE
Company	Source 1		Source 9			Source 13		Source 5	
Scheme	MUSA	MUSA	IGMA	MUSA	IGMA	Legacy BPSK	Legacy QPSK	SCMA	
Code rate	0.19	0.19	0.37	0.74	0.37	0.38	0.19	0.19	
Receiver	EPA	MMSE-hard SIC	ESE-SISO	ESE- SISO	MMSE-hybrid IC	MMSE-hard SIC	MMSE-hard SIC	Chip EPA hybrid PIC	
Company	Source 5								
Scheme	SCMA	LCRS	MUSA	MUSA	SL-RSMA	SL-RSMA	ML-RSMA	ML-RSMA	
Code rate	0.19	0.19	0.38	0.38	0.38	0.38	0.19	0.19	
Receiver	chip MMSE-hard PIC	Chip EPA hybrid PIC	Block MMSE hard PIC	Chip EPA hybrid PIC	Block MMSE hard PIC	Chip EPA hybrid PIC	Block MMSE hard PIC	Chip EPA hybrid PIC	

Observation: Under ideal conditions for Case 19 with 8 UEs, the LLS results for simulated schemes show a similar performance for most of curves provided, at target BLER = 0.1, with appropriate configurations.

22) Case 19 with 16 UEs, ideal channel estimation

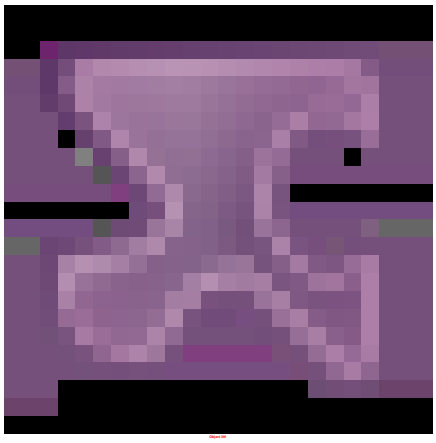

Figure 8.2-22: BLER vs. SNR results for Case 19 with 16 UEs

Table 8.2-23: Assumptions of code rate and receiver for each simulated scheme for Case 19 with 16 UEs

Company	Source 4	Source 14	Source 2		Source 3			
Scheme	RSMA	LSSA	PDMA	PDMA	UGMA	MUSA		
Code rate	0.38	0,19	0.76	0.76	0.37	0.37		
Receiver	MMSE-hybrid SIC	ESE	EPA	MMSE-hard SIC	MMSE-hard SIC	MMSE-hard SIC		
Company	Source 1		Source 9			Source 13		Source 5
Scheme	MUSA	MUSA	IGMA	MUSA	IGMA	Legacy BPSK	Legacy QPSK	SCMA
Code rate	0.19	0.38	0.37	0.74	0.37	0.38	0.19	0.25
Receiver	EPA	MMSE-hard SIC	ESE-SISO	ESE- SISO	MMSE-hybrid IC	MMSE-hard SIC	MMSE-hard SIC	Chip EPA hybrid PIC
Company	Source 5							
Scheme	SCMA	LCRS	MUSA	MUSA	SL-RSMA	SL-RSMA	ML-RSMA	ML-RSMA
Code rate	0.38	0.19	0.38	0.38	0.38	0.38	0.38	0.38
Receiver	chip MMSE-hard PIC	Chip EPA hybrid PIC	Block MMSE hard PIC	Chip EPA hybrid PIC	Block MMSE hard PIC	Chip EPA hybrid PIC	Block MMSE hard PIC	Chip EPA hybrid PIC

Observation: Under ideal conditions for Case 19 with 16 UEs, the LLS results for simulated schemes show a similar performance for most of curves provided for coding rates no more than 0.4, at target BLER = 0.1.

23) Case 20 with 4 UEs, ideal channel estimation

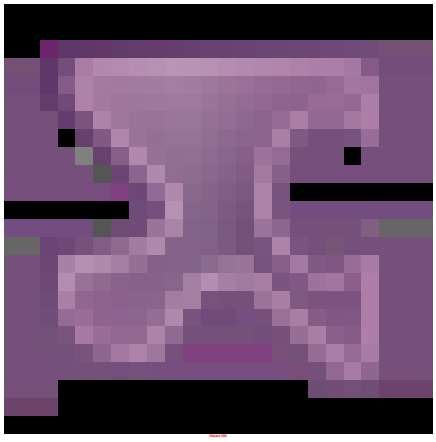

Figure 8.2-23: BLER vs. SNR results for Case 20 with 4 UEs

Table 8.2-24: Assumptions of code rate and receiver for each simulated scheme for Case 20 with 4 UEs

Company	Source 4	Source 1	Source 2		Source 3		Source 8	
Scheme	RSMA	MUSA	PDMA	PDMA	UGMA	MUSA	NCMA	NCMA2
Code rate	0.35	0.35	0.7	0.7	0.35	0.35	0.35	0.7
Receiver	MMSE-hybrid SIC	MMSE-hard SIC	EPA	MMSE-hard SIC	MMSE-hard SIC	MMSE-hard SIC	MMSE-hard SIC	MMSE-hard SIC
Company	Source 14	Source 9			Source 6	Source 13		Source 5
Scheme	LSSA	IGMA	MUSA	IGMA	LCRS	Legacy BPSK	Legacy QPSK	SCMA
Code rate	0.34	0.69	0.69	0.69	0.35	0.7	0.35	0.35
Receiver	ESE	ESE-SISO	ESE- SISO	MMSE-hybrid IC	MMSE-hard SIC	MMSE-hard SIC	MMSE-hard SIC	Chip EPA hybrid PIC
Company	Source 5							
Scheme	SCMA	LCRS	MUSA	MUSA	SL-RSMA	SL-RSMA	ML-RSMA	ML-RSMA
Code rate	0.35	0.35	0.7	0.7	0.7	0.7	0.35	0.35
Receiver	chip MMSE-hard PIC	Chip EPA hybrid PIC	Block MMSE hard PIC	Chip EPA hybrid PIC	Block MMSE hard PIC	Chip EPA hybrid PIC	Block MMSE hard PIC	Chip EPA hybrid PIC

24) Case 20 with 8 UEs, ideal channel estimation

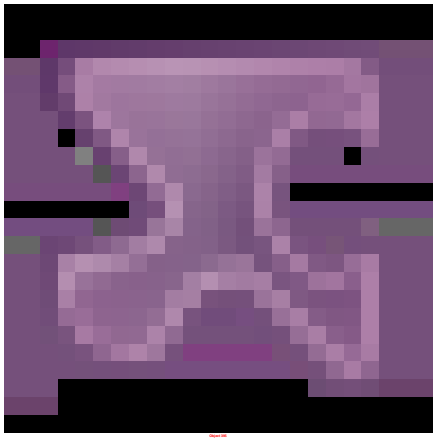

Figure 8.2-24: BLER vs. SNR results for Case 20 with 8 UEs

Table 8.2-25: Assumptions of code rate and receiver for each simulated scheme for Case 20 with 8 UEs

Company	Source 4		Source 2		Source 3		Source 1	
Scheme	RSMA	RSMA	PDMA	PDMA	UGMA	MUSA	MUSA	MUSA
Code rate	0.35	0.7	0.7	0.7	0.35	0.35	0.35	0.35
Receiver	MMSE-hybrid SIC	MMSE-hybrid SIC	EPA	MMSE-hard SIC	MMSE-hard SIC	MMSE-hard SIC	EPA	MMSE-hard SIC
Company	Source 14	Source 9			Source 6	Source 13		Source 5
Scheme	LSSA	IGMA	MUSA	IGMA	LCRS	Legacy BPSK	Legacy QPSK	SCMA
Code rate	0.34	0.69	0.69	0.69	0.35	0.7	0.35	0.35
Receiver	ESE	ESE-SISO	ESE- SISO	MMSE-hybrid IC	MMSE-hard SIC	MMSE-hard SIC	MMSE-hard SIC	Chip EPA hybrid PIC
Company	Source 5							
Scheme	SCMA	LCRS	MUSA	MUSA	SL-RSMA	SL-RSMA	ML-RSMA	ML-RSMA
Code rate	0.35	0.35	0.7	0.7	0.7	0.7	0.35	0.35
Receiver	chip MMSE-hard PIC	Chip EPA hybrid PIC	Block MMSE hard PIC	Chip EPA hybrid PIC	Block MMSE hard PIC	Chip EPA hybrid PIC	Block MMSE hard PIC	Chip EPA hybrid PIC

Observation: Under ideal conditions for Case 20 with 4 or 8 UEs,

- the LLS results for simulated schemes with the code rate round 0.35 show a similar performance for most of curves, at target BLER = 0.1.
- the LLS results for simulated schemes with the code rate round 0.7 show a similar performance for most of curves, at target BLER = 0.1.
- the LLS results with the code rate round 0.35 show better performance than the results with the code rate round 0.7.

25) Case 26 with 6 UEs, ideal channel estimation

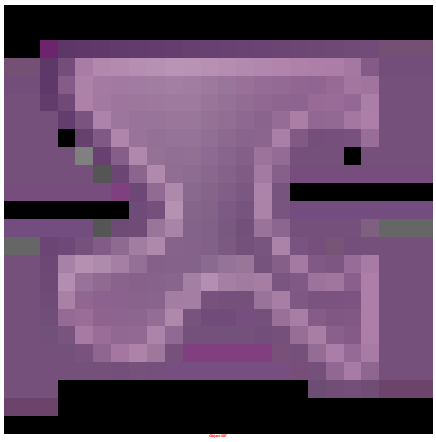

Figure 8.2-25: BLER vs. SNR results for Case 26 with 6 UEs

Table 8.2-26: Assumptions of code rate and receiver for each simulated scheme for Case 26 with 6 UEs

Company	Source 10		Source 6	Source 2		Source 1		Source 3		
Scheme	IDMA	IDMA	LCRS	PDMA	PDMA	MUSA	MUSA	UGMA	MUSA	SCMA
Code rate	0.29	0.29	0.29	0.57	0.57	0.29	0.29	0.55	0.55	0.55
Receiver	ESE-SISO	EPA	MMSE-hard SIC	EPA	MMSE-hard SIC	EPA	MMSE-hard SIC	MMSE-hard SIC	MMSE-hard SIC	EPA hybrid PIC
Company	Source 5									Source 4
Scheme	SCMA	LCRS	MUSA	MUSA	SL-RSMA	SL-RSMA	ML-RSMA	ML-RSMA	SCMA	SCMA
Code rate	0.29	0.29	0.57	0.57	0.57	0.57	0.29	0.29	0.29	0.29
Receiver	Chip EPA hybrid PIC	Chip EPA hybrid PIC	Block MMSE hard PIC	Chip EPA hybrid PIC	Block MMSE hard PIC	Chip EPA hybrid PIC	Block MMSE hard PIC	Chip EPA hybrid PIC	chip MMSE-hard PIC receiver	EPA

26) Case 26 with 8 UEs, ideal channel estimation

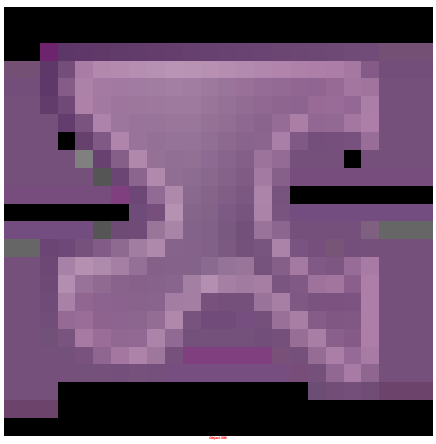

Figure 8.2-26: BLER vs. SNR results for Case 26 with 8 UEs

Table 8.2-27: Assumptions of code rate and receiver for each simulated scheme for Case 26 with 8 UEs

Company	Source 10		Source 6	Source 2		Source 1		Source 3		
Scheme	IDMA	IDMA	LCRS	PDMA	PDMA	MUSA	MUSA	UGMA	MUSA	SCMA
Code rate	0.29	0.29	0.29	0.57	0.57	0.29	0.29	0.55	0.55	0.55
Receiver	ESE-SISO	EPA	MMSE-hard SIC	EPA	MMSE-hard SIC	EPA	MMSE-hard SIC	MMSE-hard SIC	MMSE-hard SIC	EPA hybrid PIC
Company	Source 5									Source 4
Scheme	SCMA	LCRS	MUSA	MUSA	SL-	SL-	ML-	ML-	SCMA	SCMA

					RSMA	RSMA	RSMA	RSMA		
Code rate	0.29	0.29	0.57	0.57	0.57	0.57	0.29	0.29	0.29	0.29
Receiver	Chip EPA hybrid PIC	Chip EPA hybrid PIC	Block MMSE hard PIC	Chip EPA hybrid PIC	Block MMSE hard PIC	Chip EPA hybrid PIC	Block MMSE hard PIC	Chip EPA hybrid PIC	chip MMSE-hard PIC receiver	EPA

Observations: Under ideal conditions for Case 26 with 6 or 8 UEs,

- the LLS results for simulated schemes with the code rate round 0.3 show a similar performance for most of curves, at target BLER = 0.1.
- the LLS results for simulated schemes with the code rate round 0.6 show a similar performance for most of curves, at target BLER = 0.1.
- the LLS results with the code rate round 0.3 show better performance than the results with the code rate round 0.6.

27) Case 27 with 4 UEs, ideal channel estimation

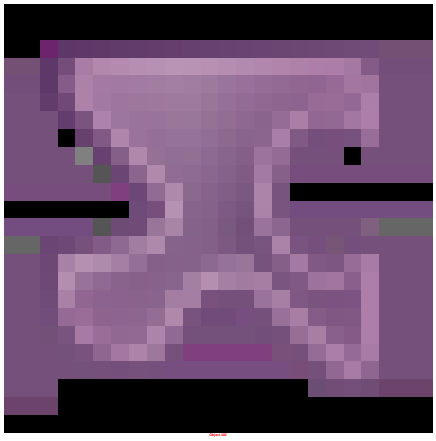

Figure 8.2-27: BLER vs. SNR results for Case 27 with 4 UEs

Table 8.2-28: Assumptions of code rate and receiver for each simulated scheme for Case 27 with 4 UEs

Company	Source 10		Source 6	Source 2		Source 1		Source 3		
Scheme	IDMA	IDMA	LCRS	PDMA	PDMA	MUSA	MUSA	UGMA	MUSA	SCMA
Code rate	0.36	0.36	0.36	0.71	0.71	0.36	0.36	0.69	0.69	0.69
Receiver	ESE-SISO	EPA	MMSE-hard SIC	EPA	MMSE-hard SIC	EPA	MMSE-hard SIC	MMSE-hard SIC	MMSE-hard SIC	EPA hybrid PIC
Company	Source 5									
Scheme	SCMA	LCRS	MUSA	MUSA	SL-RSMA	SL-RSMA	ML-RSMA	ML-RSMA	SCMA	
Code rate	0.36	0.36	0.71	0.71	0.71	0.71	0.36	0.36	0.36	
Receiver	Chip EPA hybrid PIC	Chip EPA hybrid PIC	Block MMSE hard PIC	Chip EPA hybrid PIC	Block MMSE hard PIC	Chip EPA hybrid PIC	Block MMSE hard PIC	Chip EPA hybrid PIC	chip MMSE-hard PIC receiver	

Observation: Under ideal conditions for Case 27 with 4 UEs,

- the LLS results for simulated schemes with the code rate round 0.35 show a similar performance for most of curves, at target BLER = 0.1.
- the LLS results for simulated schemes with the code rate round 0.7 show a similar performance for most of curves, at target BLER = 0.1.

- the LLS results with the code rate round 0.35 show better performance than the results with the code rate round 0.7.

28) Case 27 with 6 UEs, ideal channel estimation

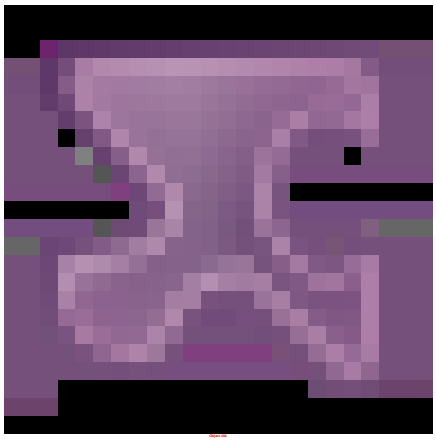

Figure 8.2-28: BLER vs. SNR results for Case 27 with 6 UEs

Table 8.2-29: Assumptions of code rate and receiver for each simulated scheme for Case 27 with 6 UEs

Company	Source 10		Source 6	Source 2		Source 1		Source 3		
Scheme	IDMA	IDMA	LCRS	PDMA	PDMA	MUSA	MUSA	UGMA	MUSA	SCMA
Code rate	0.36	0.36	0.36	0.71	0.71	0.36	0.36	0.69	0.69	0.69
Receiver	ESE-SISO	EPA	MMSE-hard SIC	EPA	MMSE-hard SIC	EPA	MMSE-hard SIC	MMSE-hard SIC	MMSE-hard SIC	EPA hybrid PIC
Company	Source 5									
Scheme	SCMA	LCRS	MUSA	MUSA	SL-RSMA	SL-RSMA	ML-RSMA	ML-RSMA	SCMA	
Code rate	0.36	0.36	0.71	0.71	0.71	0.71	0.36	0.36	0.36	
Receiver	Chip EPA hybrid PIC	Chip EPA hybrid PIC	Block MMSE hard PIC	Chip EPA hybrid PIC	Block MMSE hard PIC	Chip EPA hybrid PIC	Block MMSE hard PIC	Chip EPA hybrid PIC	chip MMSE-hard PIC receiver	

Observation: Under ideal conditions for Case 27 with 6 UEs,

- the LLS results for simulated schemes with the code rate round 0.35 show a similar performance for most of curves, at target BLER = 0.1.
- the LLS results for simulated schemes with the code rate round 0.7 show a similar performance for most of curves, at target BLER = 0.1.
- the LLS results with the code rate round 0.35 show better performance than the results with the code rate round 0.7.

29) Case 6,8,9,21, 32-35 with unequal SNR distribution

a) SNR offset is within +/-3dB

The following observations can be drawn from the case-by-case evaluation results under unequal SNR distributions:

- For Case 6 with 6 or 12 UEs, ideal channel estimation, unequal SNR (SNR offset is within +/-3dB), TO is within [0, 0.5*NCP], and non-zero FO, the LLS results for simulated schemes show a similar performance for most of curves provided, at target BLER = 0.1, with appropriate configurations.

- For Case 8 with 12 or 24 UEs, ideal channel estimation, unequal SNR (SNR offset is within +/-3dB), TO is within [0, 0.5*NCP], and non-zero FO, the LLS results for simulated schemes show a similar performance for most of curves provided, at target BLER = 0.1, with appropriate configurations.
- For Case 9 with 6 or 12 UEs, ideal channel estimation, unequal SNR (SNR offset is within +/-3dB), TO is within [0, 0.5*NCP], and non-zero FO, the LLS results for simulated schemes show a similar performance for most of curves provided, at target BLER = 0.1, with appropriate configurations.
- For Case 21 with 12 or 24 UEs, ideal channel estimation, unequal SNR (SNR offset is within +/-3dB), TO is within [0, 0.5*NCP], and non-zero FO, the LLS results for simulated schemes show a similar performance for most of curves provided, at target BLER = 0.1, with appropriate configurations.

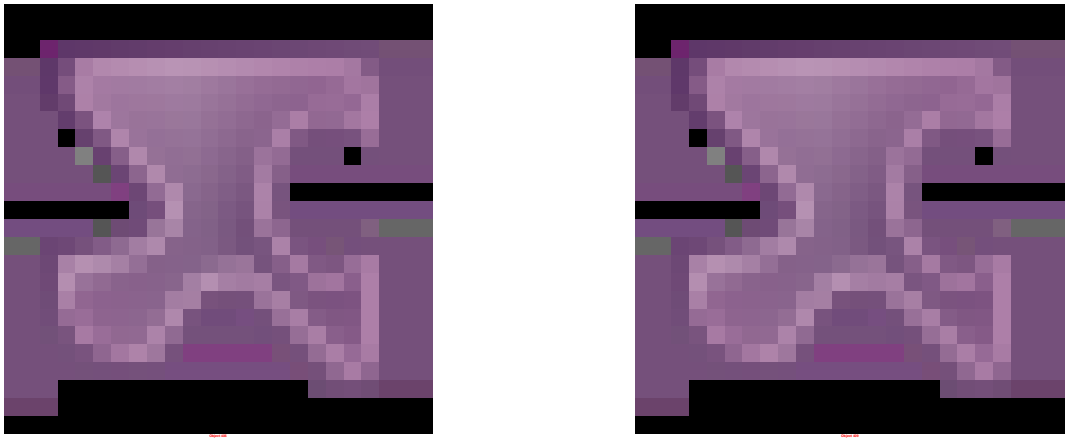

(a) 6 UEs (b) 12 UEs

Figure 8.2-29: BLER vs. SNR results for Case 6 with 6 or 12 UEs

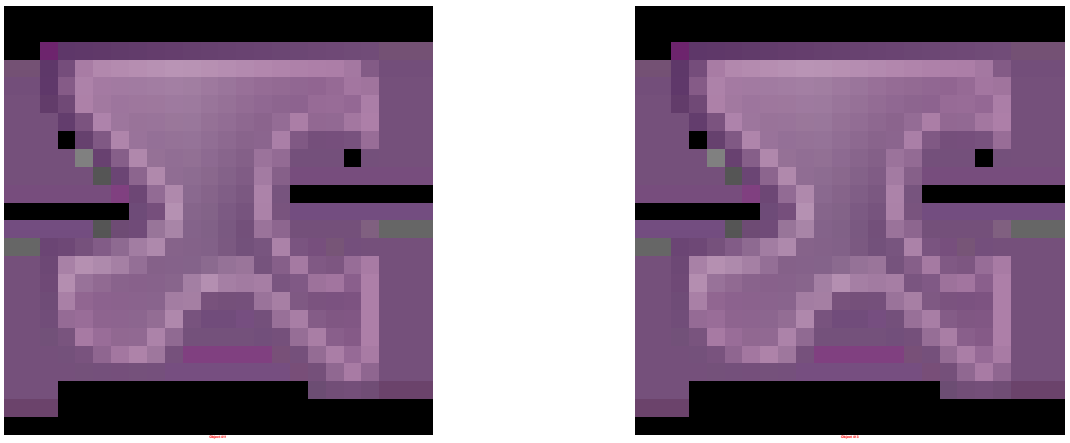

(a) 12 UEs (b) 24UEs

Figure 8.2-30: BLER vs. SNR results for Case 8 with 12 or 24 UEs

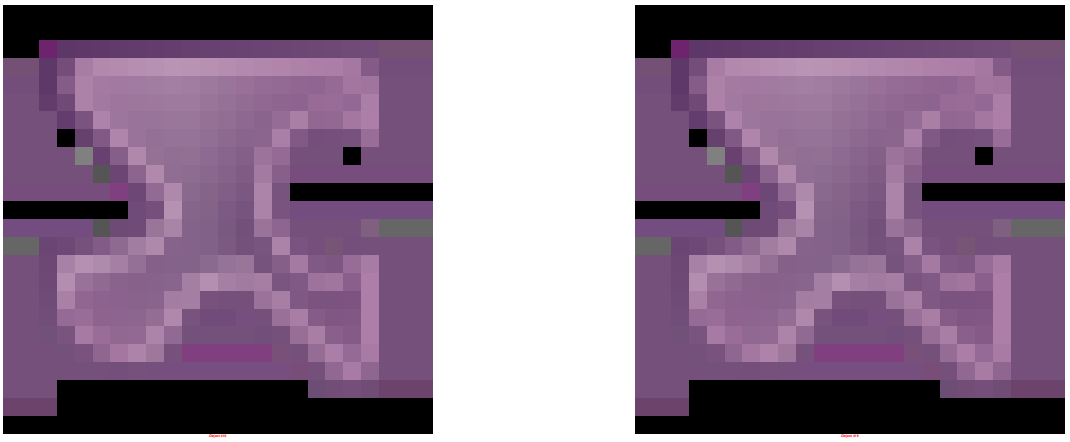

(a) 6 UEs (b) 12 UEs

Figure 8.2-31: BLER vs. SNR results for Case 9 with 6 or 12 UEs

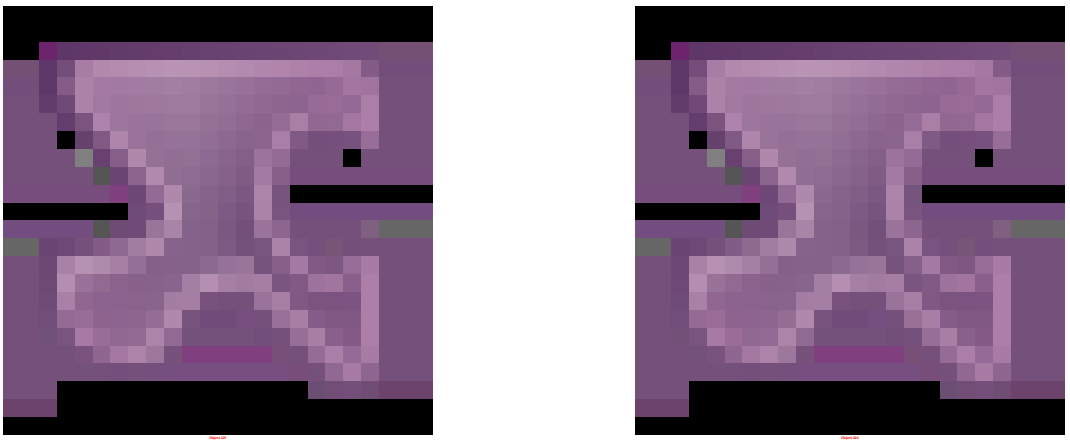

(a) 12 UEs (b) 24 UEs

Figure 8.2-32: BLER vs. SNR results for Case 21 with 12 or 24 UEs

b) SNR offset greater than +/-3dB

Observations:

- For LLS in the simulated cases 32/33/34/35 with ideal channel estimation, under unequal SNR, and fixed MA signature allocation, as long as the simulation configuration is appropriate, the performance difference between NOMA schemes/MA signatures is small, even when different receiver types are used.
- Performance loss of 1.1-3.2 dB can be observed with real channel estimation in multipath, where the losses are greater for the larger number of UEs or with greater SNR variation with for link level simulations in the simulated cases of 32 and 33 [41].

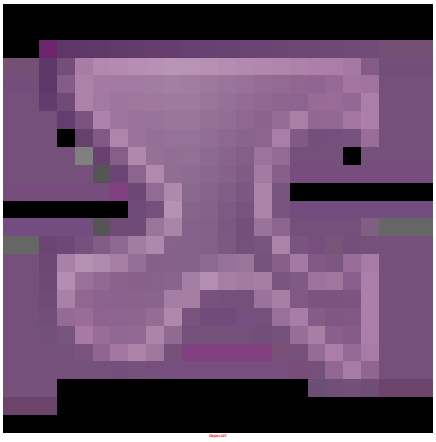

Figure 8.2-33: BLER vs. SNR results for Case 32 with 12 UEs

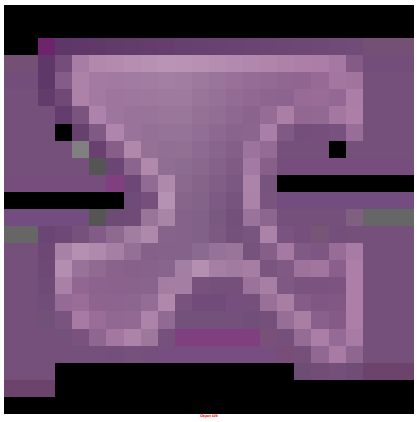

Figure 8.2-34: BLER vs. SNR results for Case 33 with 8 UEs

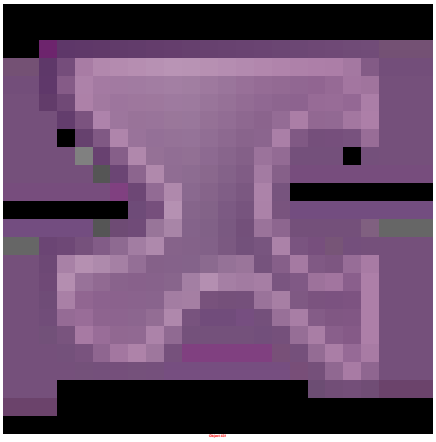

Figure 8.2-35: BLER vs. SNR results for Case 34 with 6 UEs

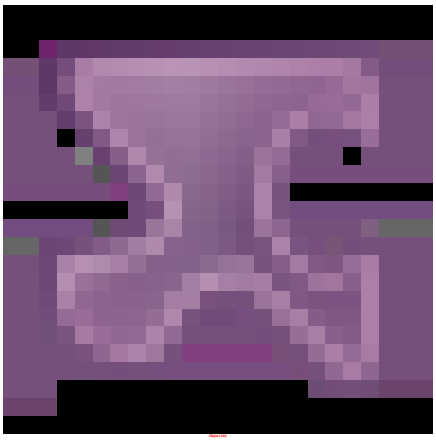

Figure 8.2-36: BLER vs. SNR results for Case 35 with 6 UEs

Table 8.2-30: Channel estimation loss statistics for Cases 32 and 33

Case No. & # of UEs	Channel estimation loss for 4 or 5dB	Channel estimation loss for 9dB
Case 32, N=6 (mMTC, TDL-C)	Median=1.1dB Mean=1.2dB Range: [1.0 … 2.1] dB	Median=1.8dB Mean=1.7 dB Range: [1.3 … 1.9] dB
Case 32, N=12 (mMTC, TDL-C)	Median=1.7dB Mean=2.3 dB Range: [1.7 … 4.6] dB	Median=3.2 dB Mean=3.1 dB Range: [2.4 … 3.4] dB
Case 33, N=6 (mMTC, TDL-C)	Median=0.9 dB Mean=1.1 dB Range: [0.8 … 3.1] dB	Median=1.9 dB Mean=1.9 dB Range: [1.8 … 2.1] dB
Case 33, N=8 (mMTC, TDL-C)	Median=1.2 dB Mean=1.5 dB Range: [1 … 3.6] dB	Median=2.8 dB Mean=2.8 dB Range: [2.1 … 3.5] dB

30) Case 11 with realistic channel estimation and random MA signature

a) 4UEs

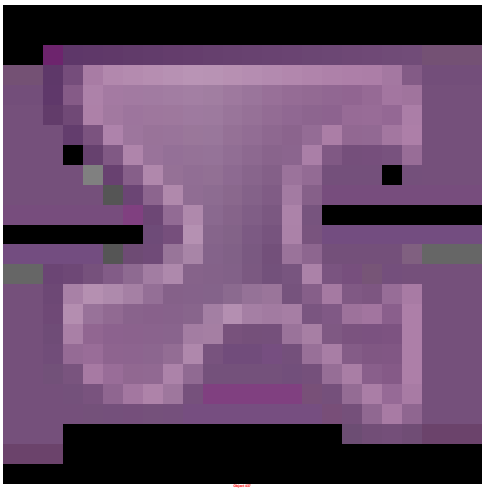

Figure 8.2-37: BLER vs. SNR results for Case 11 with 4 UEs

b) 6UEs

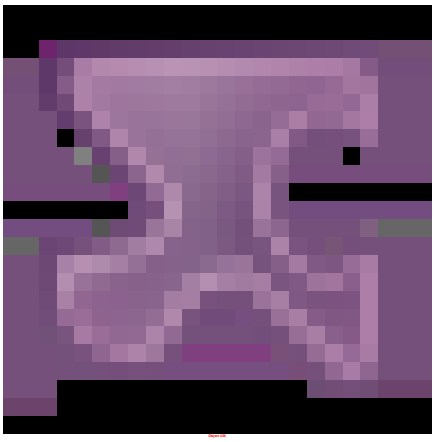

Figure 8.2-38: BLER vs. SNR results for Case 11 with 6 UEs

Table 8.2-31: Assumptions for each simulated scheme for Case 11 with 4 or 6 UEs

Company	Source 5					Source 1	Source 2	
Scheme	SCMA	LCRS	MUSA	SCMA	MUSA	MUSA	MUSA	
Code rate	0.2	0.1	0.2	0.14 for 4UEs / 0.2 for 6UEs	0.2	0.17	0.41	
Receiver	EPA	EPA	Block MMSE-hard PIC	Chip MMSE-hard PIC	EPA	MMSE-hard IC	MMSE-hard IC	
Max TO	0	0	0	0	0	1.5 CP	0.5 CP	
MA signature allocation / collision	Random activation / No	Random activation / No	Random activation / No	Random activation / No	Random activation / No	Random selection / Yes	Random selection / Yes	
RS overhead	1/7	1/7	1/7	1/7	1/7	1/2		
Company	Source 5							
Scheme	SCMA	SCMA	MUSA	MUSA	MUSA	MUSA	LCRS	LCRS
Code rate	0.27	0.33	0.2	0.24	0.2	0.24	0.1	0.12
Receiver	EPA	EPA	Block MMSE-hard PIC	Chip MMSE-hard PIC	EPA	EPA	EPA	EPA
Max TO	0.5 CP	1.5 CP	0.5 CP	1.5 CP	0.5 CP	1.5 CP	0.5 CP	1.5 CP
MA signature allocation / collision	Random selection / Yes	Random selection / Yes	Random selection / Yes	Random selection / Yes	Random selection / Yes	Random selection / Yes	Random selection / Yes	Random selection / Yes
RS overhead	1/7	2/7	1/7	2/7	1/7	2/7	1/7	2/7

Observations:

- For case 11 with realistic channel estimation and random selection with potential MA signature collision (timing offset is within [0, 1.5*NCP], non-zero FO, and SNR offset is within +/-3dB)

  - When the TBS is small (i.e. 20 bytes), with 6 simultaneous activated UEs, based on the realistic UE detection by using 2-slot transmission time (e.g., 50% overhead for legacy preamble as the RS, without DMRS, preamble and data have the same BW, without assuming guard-band, with the pool size of 48 and 64), there is around 3.5 dB performance loss at 10% BLER, compared to random activation with no DMRS/MA signature collision and timing offset is within [0, 0.5*NCP] and 1-slot transmission.

    Note: this observation is based on single company's results

- When the TBS is small (i.e. 20 bytes), 10% BLER cannot be achieved for 4 and 6 UEs, with random selection (DMRS overhead of 2/7 for pool size 24), for both realistic and ideal UE detection, with 1-slot transmission time.
- When the TBS is small (i.e. 20 bytes), with random activation (with realistic UE detection, DMRS overhead of 2/7 for pool size 24, without DMRS/MA signature collision) of 1-slot transmission, the performance degradation at 10% BLER for 4, 6 and 8 UEs is about 1 dB compared to random activation without timing offset (with realistic UE detection, DMRS overhead of 1/7 for pool size 24, without DMRS/MA signature collision)
- Note: this observation is based on single company's results

8.2.2 Observations from the LLS results

Some general observations can be drawn from the simulated cases:

- For LLS in mMTC/eMBB/URLLC scenarios with ideal channel estimation, equal SNR, zero TO/FO and fixed MA signature allocation
  - For low TBS (per UE SE is less than 0.15 bps/Hz and total SE is less than 1.8 bps/Hz), as long as the simulation configuration, e.g., reasonable code rate, is appropriate, the performance difference between NOMA schemes/MA signatures is small, even when different receiver types are used.
- For LLS in the simulated case 15/17/19/20/26/27 with ideal channel estimation, equal SNR, zero TO/FO and fixed MA signature allocation
  - For medium to high TBS (per UE SE is within [0.3, 0.55] bps/Hz, and total SE is less than 3.6 bps/Hz), as long as the simulation configuration, e.g., reasonable code rate, is appropriate, the performance difference between NOMA schemes/MA signatures is small.
    - Results with lower code rate (e.g. LDPC coding rate < 0.5) show better performance than the results with higher code rate (e.g. LDPC coding rate > 0.5).

By comparing the evaluation results between realistic channel estimation and ideal channel estimation based on cases 1~5 and 14~20, the following observations are made.

- For LLS with realistic channel estimation, equal SNR distribution, zero TO/FO and fixed MA signature allocation
  - Up to 2~4 dB performance degradation is observed compared to ideal channel estimation for mMTC/eMBB scenario.
  - Up to 5 dB performance degradation is observed compared to ideal channel estimation for URLLC scenario.
  - Different performance degradation levels may be due to different channel estimation algorithm and DMRS extension methods.
  - The lower the SNR operation point is, the larger the performance degradation due to realistic CE can be observed
  - Higher number of UEs have larger performance degradation than lower number of UEs under the same channel condition and the same TBS for each individual case.

9 System level performance evaluation

9.1 Performance metrics

The following performance metrics are used for NOMA study from system level point of view.

1) mMTC

Evaluation of NOMA in mMTC scenario should focus on normal coverage.

- The performance metrics for mMTC include the following:
  - Higher layer packet drop rate (PDR) vs. offered load. The definition of PDR is FFS:
    - Offered load can be at least
      - Higher layer packet arrival rate (PAR) per cell for massive connectivity
  - CDF of packet drop rate per UE is optional.
  - CDF of transmission latency is optional.
  - CDF of the inter-cell interference-over-thermal (IOT) is optional.
  - Note: companies are encouraged to provide the curve of resource utilization (RU) vs. offered load.
- The baseline for system-level performance comparison is
  - UL transmission with configured grant type 1 or type 2 in Rel.15 NR.
    - Companies to report the link adaptation assumptions, if any.
    - The DMRS collision, if any, should be taken into account.
- For the evaluation of NOMA schemes
  - UL transmission with configured grant type 1 or type 2 in Rel.15 NR as staring point
    - Companies to report the link adaptation assumptions, if any.
    - The MA signature (including DMRS) is semi-statically configured.
      - The MA signature collision, if any, should be taken into account.
  - FFS: to demonstrate the potential NOMA gain under grant-free transmission with random selection of MA signatures, where collision of MA signature should be considered.
    - The grant-free definition follows NR SI.

2) URLLC

- The performance metrics for URLLC include at least the following:
- Percentage of users satisfying reliability and latency requirements vs. packet arrival rate (PAR).
  - CDF of reliability per UE is optional.
  - CDF of the inter-cell interference-over-thermal (IOT) is optional.
    - Note: companies are encouraged to provide the curve of resource utilization (RU) vs. PAR.
- The baseline for performance comparison is UL transmission without dynamic link adaptation (i.e., using configured grant type 1 or type 2)
- Simplified system-level evaluations can be used for URLLC scenario as detailed as follows:
  - Mean BLER of a UE can be used to represent the reliability of the UE.
    - Note: Further considerations can be reviewed, e.g. the deviation of BLER about the mean BLER.

3) eMBB

- The performance metrics for eMBB include the following:
  - Metric 1: Higher layer packet drop rate (PDR) vs. offered load. The definition of PDR is FFS:
    - Offered load can be at least

        - Higher layer packet arrival rate (PAR) per cell
      - CDF of packet drop rate per UE is optional.
      - CDF of transmission latency is optional.
      - CDF of the inter-cell interference-over-thermal (IOT) is optional.
      - Note: companies are encouraged to provide the curve of resource utilization (RU) vs. offered load.
    - Metric 2: UPT vs. offered load.
      - CDF of the inter-cell interference-over-thermal (IOT) is optional.
      - CDF of UE perceived throughput is optional
    - FFS whether or not to have signalling overhead as one performance metric.
- The baseline for system-level performance comparison can be
    - Configured grant type 1 or type 2 in Rel.15 NR.
      - The DMRS collision, if any, should be taken into account.
      - Companies to report the link adaptation assumptions, if any.
    - UL transmission with dynamic grant
      - Details to be reported.
      - The signalling overhead should be reported.
- For the evaluation of NOMA schemes
    - Configured grant type 1 or type 2 in Rel.15 NR.
      - The MA signature (including DMRS) is semi-statically configured.
      - The MA signature collision, if any, should be taken into account.
      - Companies to report the link adaptation assumptions, if any.
    - UL transmission with dynamic grant
      - Details to be reported.
      - The signalling overhead should be reported.
    - FFS: to demonstrate the potential NOMA gain under grant-free transmission with random selection of MA signatures, where collision of MA signature should be considered.
      - The grant-free definition follows NR SI.

9.2 Evaluation results

9.2.1 Simulation results for mMTC

For mMTC scenario, under the system-level evaluation assumptions as detailed in Table 9.2-1, relative to the evaluated OFDM waveform (using configured grant with multiple users in the same time and frequency resources) with MMSE-IRC or advanced receiver, the evaluated NOMA schemes with configured grant (without DMRS collision) can provide the results in Table 9.2-1:

- In some simulated cases,
    - time and frequency resource configuration per UE for the baseline is different from that per UE for evaluated NOMA schemes;

- Receivers used for the baseline and for the evaluated NOMA schemes are in some cases different and in other cases the same.
- Resource utilization of simulated NOMA schemes is 3 to 5 times than baseline.

- In some other simulated cases,
  - the time and frequency resource configuration per UE for the baseline is the same as that per UE for the evaluated NOMA scheme
  - the same type of receiver is assumed for the baseline and the evaluated NOMA schemes
  - Resource utilization of simulated NOMA schemes is comparable to baseline.
- Different L2S mappings are used.
- Within source 1, the ideal assumptions of inter-cell interference covariance matrix (non-block diagonal and genie-known to the receiver) is assumed.
- Different baselines, different amount of optimization, and different choice of receiver types are used within different sources

Table 9.2-1: System simulation results for NOMA in mMTC scenario

Source	Source 1- Case 1[42]	Source 1 - Case 2[42]	Source 1 - Case 3[42]	Source 1 - Case 4[42]	Source 1 - Case 5[42]	Source 2 - Case 1[43]	Source 2- Case 2[43]	Source 2- Case 3[43]
Carrier frequency	700MHz, 1732m	700MHz, 1732m	700MHz, 1732m	700MHz, 1732m	700MHz, 1732m	700MHz, 1732m	700MHz, 1732m	700MHz, 1732m
Simulation bandwidth	6 PRBs	6 PRBs	6 PRBs	6 PRBs	6 PRBs	6 PRBs	6 PRBs	6 PRBs
BS antenna number	2Rx	2Rx	2Rx	2Rx	2Rx	2Rx	2Rx	2Rx
BS downtilt	92	92	92	92	92	92	92	92
Number of UEs per cell	100	100	100	100	100	100	100	100
UE power control	P0 = -100 dBm, alpha = 1	P0 = -100 dBm, alpha = 1	P0 = -95 dBm, alpha = 1	P0 = -100 dBm, alpha = 1	P0 = -95 dBm, alpha = 1	P0=-110 dBm, alpha = 1	P0=-110 dBm, alpha = 1	P0=-110 dBm, alpha = 1
HARQ/repetition	Maximum number of HARQ transmissions is 8; non-adaptive re-transmissions	Maximum number of HARQ transmissions is 8; non-adaptive re-transmissions	UEs are classified to 3 groups, different repetitions are assumed respectively	Maximum number of HARQ transmissions is 8 non-adaptive re-transmissions are assumed	4 repetitions	non-adaptive re-transmissions, maximum number of HARQ transmission=8, repetition dependents on coupling loss, can be 1,2	non-adaptive re-transmissions, maximum number of HARQ transmission=8, repetition dependents on coupling loss, can be 1,2	non-adaptive re-transmissions, maximum number of HARQ transmission=8, repetition dependents on coupling loss, can be 1,2
Channel estimation	Realistic	Realistic	Realistic	Realistic	Realistic	Realistic	Realistic	Realistic
BS advanced receiver	Baseline: MMSE-IRC or MMSE-PIC MUSA: MMSE-PIC	Baseline: MMSE-IRC or MMSE-PIC MUSA: MMSE-PIC	MMSE-IC for baseline and MUSA	MMSE-IC for baseline and MUSA	MMSE-IC for baseline and MUSA	EPA receiver for all schemes	EPA receiver for all schemes	EPA receiver for all schemes
TB size	25 bytes	25 bytes	25 bytes	25 bytes	20 bytes	20 bytes	60 bytes	40 bytes
Packet dropping criterion	If one TB is not received correctly after HARQ/repetition, the packet is dropped	If one TB is not received correctly after HARQ/repetition, the packet is dropped	If one TB is not received correctly after HARQ/repetition, the packet is dropped	If one TB is not received correctly after HARQ/ repetition, the packet is dropped;	If one TB is not received correctly after HARQ/ repetition, the packet is dropped;	8 HARQ transmissions or 1s latency	8 HARQ transmissions or 1s latency	8 HARQ transmissions or 1s latency
DMRS setting and allocation	24 DMRS each RB assumed, preconfigured, no collision	24 DMRS each RB assumed, preconfigured, no collision	Baseline: 24 DMRS, random selection MUSA: 64 DMRS, random selection	24 DMRS each RB assumed, preconfigured, no collision	No DM-RS; Baseline and MUSA: Preamble 64 Random selection	the DMRS pool size is 24 for each resource unit; no DMRS collision	the DMRS pool size is 24 for each resource unit; no DMRS collision	the DMRS pool size is 24 for each resource unit; no DMRS collision
MA signature and allocation	24 spreading codes of length 4 are used for MUSA, preconfigured	24 spreading codes of length 4 are used for MUSA, preconfigured	64 spreading codes of length 4 are used for MUSA, random selection	24 spreading codes of length 2, 4 and 6 are used for MUSA, preconfigured.	64 spreading codes of length 4 are used, random selection	spreading codes of length 2 are used for MUSA	spreading codes of length 2 are used for MUSA	spreading codes of length 2 are used for MUSA
Details on configured grant, e.g. periodicity, offset, and #of UEs assigned on the same resource	periodicity = 4 ms for baseline and MUSA	periodicity = 5 ms for baseline and MUSA	-	periodicity = 6 ms for baseline and MUSA	-	periodicity = 6 ms	periodicity = 6 ms	periodicity = 6 ms

Other assumptions for baseline	1 PRB+1ms per Tx for a UE ,	6 PRBs per Tx for a UE ,,	1 PRB per Tx for a UE; 1, 4 and 16 repetitions for the 3 groups respectively ,	1 PRB + 6 ms per Tx for a UE ,	Basic channel structure: 6 PRBs + 1ms for preamble, 6 PRBs + 1ms for data; TO belong to [0, 1.5*NCP]	a resource unit of 1 PRB+6 ms for each TB	a resource unit of 1 PRB+6 ms for each TB	a resource unit of 1 PRB+6 ms for each TB
Other assumptions for NOMA	1 PRB + 4 ms per Tx for a UE; the energy of spreading codes for MUSA is normalized to 1 Ideal assumptions of inter-cell interference covariance matrix, with both spatial and spreading code domain inter-cell interference covariance matrix	6 PRBs per Tx for a UE Ideal assumptions of inter-cell interference covariance matrix, with both spatial and spreading code domain inter-cell interference covariance matrix	1 PRB + 4 ms per Tx for a UE; 1, 1 and 4 repetitions for the 3 groups respectively, the energy of spreading codes used by UEs in the first group is normalized to 1 Ideal assumptions of inter-cell interference covariance matrix, with both spatial and spreading code domain inter-cell interference covariance matrix	1 PRB + 6 ms per Tx for a UE Ideal assumptions of inter-cell interference covariance matrix, with both spatial and spreading code domain inter-cell interference covariance matrix	Basic channel structure: 6 PRBs + 1ms for preamble, 6 PRBs + 1ms for data; TO belong to [0, 1.5*NCP] Ideal assumptions of inter-cell interference covariance matrix, with both spatial and spreading code domain inter-cell interference	a resource unit of 1 PRB+6 ms for each TB; Multi-layer transmission for SCMA; Single-layer or multi-layer transmission for RSMA	a resource unit of 1 PRB+6 ms for each TB; Multi-layer transmission for SCMA; Single-layer or multi-layer transmission for RSMA	a resource unit of 1 PRB+6 ms for each TB; Multi-layer transmission for SCMA; Single-layer or multi-layer transmission for RSMA
Supported PAR for baseline at PDR=1% (packet/s/cell)	300 for baseline with MMSE-IRC; 350 for baseline with MMSE-PIC	<100 for baseline with MMSE-IRC; <100 for baseline with MMSE-PIC	25	400	<50 for baseline with MMSE-SIC	590	740	860
Supported PAR for NOMA at PDR=1% (packet/s/cell)	600	200	50	700 for SF = 2 900 for SF = 4 1000 for SF = 6	100	590 for SCMA 580 for MUSA; 580 for SL-RSMA	740 for SCMA 620 for MUSA; 620 for SL-RSMA 720 for ML-RSMA	790 for MUSA, 780 for SL-RSMA, 860 for ML-RSMA,860 for SCMA
Gain (relative to baseline)	100% (baseline with MMSE-IRC) 71% (baseline with MMSE-PIC)	100%	100%	75% for SF = 2 125% for SF = 4 150% for SF = 6	100%	No gain	No gain	No gain

Source	**Source 2- Case 4[43]**	**Source 2- Case 5[43]**	**Source 2- Case 6[43]**	**Source 2[44]**	**Source 3[45]**	**Source 4[46]**	**Source 5[47]**	**Source 7[51]**
Carrier frequency	700MHz, 1732m	700MHz, 1732m	700MHz, 1732m	700MHz, 1732m	700MHz, 1732m	700MHz, 1732m	700MHz, 1732m	700MHz, 1732m
Simulation bandwidth	6 PRBs	6 PRBs	6 PRBs	6 PRBs	6 PRBs	6 PRBs	6 PRBs	6 PRBs
BS antenna number	2Rx	2Rx	2Rx	2Rx	2Rx	2Rx	2Rx	2Rx
BS downtilt	92	92	92	92	-	92	92	92
Number of UEs per cell	100	100	100	100	20	20	20	32
UE power control	P0=-110 dBm, alpha = 1	P0=-110 dBm, alpha = 1	P0=-110 dBm, alpha = 1	P0=-110 dBm, alpha = 1	P0=-90 dBm	P0=-110 dBm, alpha = 1	P0 = -110 dBm, alpha = 1	P0 = -105.4 dBm, α = 0.9
HARQ/repetition	non-adaptive re-transmissions, maximum number of HARQ transmission=8, repetition dependents on coupling loss, can be 1,2	non-adaptive re-transmissions, maximum number of HARQ transmission=8, repetition dependents on coupling loss, can be 1,2	non-adaptive re-transmissions, maximum number of HARQ transmission=8, repetition dependents on coupling loss, can be 1,2	non-adaptive re-transmissions, maximum number of HARQ transmission=8, repetition dependents on coupling loss, can be 1,2	HARQ combining with random back-off. The maximum number for transmissions is 8	Back off, max 8, no repetition	8 Chase combining	Max 8 HARQ attempts
Channel estimation	Realistic	Realistic	Realistic	Realistic	Ideal & Realistic	Realistic	Ideal & Realistic	Realistic
BS advanced receiver	SCMA/ LCRS: chip-wise MMSE hard IC receiver; MUSA and RSMA: block MMSE hard IC receiver	SCMA/ LCRS: chip-wise MMSE hard IC receiver; MUSA and RSMA: block MMSE hard IC receiver	SCMA/ LCRS: chip-wise MMSE hard IC receiver; MUSA and RSMA: block MMSE hard IC receiver	SCMA/ LCRS: chip-wise MMSE hard IC receiver; MUSA: block MMSE hard IC receiver	Baseline: MMSE-IRC IGMA: ESE receiver	Baseline: MMSE-IRC or MMSE-SIC NOCA: MMSE-SIC	EPA receiver for IDMA MMSE-IRC for baseline	MMSE with hard parallel IC
TB size	20 bytes	60 bytes	40 bytes	40 bytes	40 bytes	-	45 bytes (40 + 5 bytes)	16 bytes
Packet dropping criterion	8 HARQ transmissions or 1s latency	8 HARQ transmissions or 1s latency	8 HARQ transmissions or 1s latency	8 HARQ transmissions or 1s latency	8 HARQ transmissions	Max 8 transmissions	maximum number of HARQ transmissions	Packet is dropped after 8 HARQ attempts
DMRS setting and allocation	the DMRS pool size is 24 for each resource unit; no DMRS collision	the DMRS pool size is 24 for each resource unit; no DMRS collision	the DMRS pool size is 24 for each resource unit; no DMRS collision	the DMRS pool size is 24 for each resource unit; no DMRS collision	DMRS are semi-static configured	-	No DMRS collision	

MA signature and allocation	spreading codes of length 2 are used for MUSA	spreading codes of length 2 are used for MUSA	spreading codes of length 2 are used for MUSA	spreading codes of length 2/4 are used for MUSA	MA signatures are semi-static configured	spreading codes of length 6 are used for NOCA	Preconfigured UE specific interleavers	4 RSMA sequences of SF 2 preconfigured
Details on configured grant, e.g. periodicity, offset, and #of UEs assigned on the same resource	periodicity = 6 ms	periodicity = 6 ms	periodicity = 6 ms	periodicity = 6 ms	-	-	-	Periodicity: Every 8 UL slots (4 ms)
Other assumptions for baseline	a resource unit of 1 PRB+6 ms for each TB	a resource unit of 1 PRB+6 ms for each TB	a resource unit of 1 PRB+6 ms for each TB	a resource unit of 1 PRB+6 ms for each TB	one RB is allocated for each UE	each UE selects one PRB out of the allocated PRBs; QPSK 1/2 is used for all users	Each UE is configured with one PRB	3 PRBs assigned to a UE
Other assumptions for NOMA	a resource unit of 1 PRB+6 ms for each TB; Multi-layer transmission for SCMA; Single-layer or multi-layer transmission for RSMA	a resource unit of 1 PRB+6 ms for each TB; Multi-layer transmission for SCMA; Single-layer or multi-layer transmission for RSMA	a resource unit of 1 PRB+6 ms for each TB; Multi-layer transmission for SCMA; Single-layer or multi-layer transmission for RSMA	a resource unit of 1 PRB+6 ms for each TB; Multi/Single-layer transmission for SCMA;	all 6 RBs are occupied by each UE	each UE always occupies the whole allocated resources for transmission; QPSK 1/2 is used for all users	Each UE always occupies all 6 PRBs	6 PRBs assigned to a UE, SF = 2
Supported PAR for baseline at PDR=1% (packet/s/cell)	580	700	840	740	400 (ICE)	100 for baseline with MMSE-IRC or MMSE-SIC (5 packet/s/UE * 20 UE/cell) at PDR=1%	580	1200
Supported PAR for NOMA at PDR=1% (packet/s/cell)	580 for SCMA/MUSA/ML-RSMA/SL-RSMA	610 for MUSA, 610 for SL-RSMA, 700 for ML-RSMA,700 for SCMA	780 for MUSA, 770 for SL-RSMA, 840 for ML-RSMA,840 for SCMA	760 for 2-layer SCMA; 710 for SL-SCMA; 710 for MUSA with SF=4; 370 for MUSA with SF =2;	800 (ICE) 750 (RCE)	200 (10 packet/s/UE * 20 UE/cell) at PDR=1%	850	1850
Gain (relative to baseline)	No gain	No gain	No gain	2.7% for SCMA	100% (ICE) 87.5% (IGMA with RCE relative to baseline with ICE)	For low PAR: 100%; for medium to high PAR small to no gain	46%	54%

9.2.2 Simulation results for URLLC

For URLLC scenario, under the system-level evaluation assumptions as detailed in Table 9.2-2, relative to the evaluated OFDM waveform (using configured grant with multiple users in the same time and frequency resources) with MMSE-IRC or advanced receiver, the evaluated NOMA schemes with configured grant (without DMRS collision) can provide the results in Table 9.2-2:

- In some simulated cases
  - time and frequency resource configuration per UE for the baseline is different from that per UE for evaluated NOMA schemes;
  - Receivers used for the baseline and for the evaluated NOMA schemes are in some cases different and in other cases the same.
- In some other simulated cases,
  - the time and frequency resource configuration per UE for the baseline is the same as that per UE for the evaluated NOMA scheme
  - the same type of receiver is assumed for the baseline and the evaluated NOMA schemes
  - Resource utilization of simulated NOMA schemes is comparable to baseline.
- Different L2S mappings are used.
- Within source 1, the ideal assumptions of inter-cell interference covariance matrix (non-block diagonal and genie-known to the receiver) is assumed.

- Different baselines, different amount of optimization, and different choice of receiver types are used within different sources

Table 9.2-2: System simulation results for NOMA in URLLC scenario

Source	Source 1 - Case 1[42]	Source 1- Case 2[42]	Source 1- Case 3[42]	Source 1- Case 4[42]	Source 1- Case 5[42]	Source 2 - Case 1[48]	Source 2 Case 2[48]
Carrier frequency	4GHz, 200m	700MHz, 500m	4GHz, 200m	700MHz, 500m	4GHz, 200m	4GHz, 200m	4GHz, 200m
Simulation bandwidth	12 PRBs, SCS = 60kHz	12 PRBs, SCS = 60kHz	12 PRBs, SCS = 60kHz	12 PRBs, SCS = 60kHz	12 PRBs, SCS = 60kHz	12 PRBs, SCS = 60kHz, 7OS	12 PRBs, SCS = 60kHz, 7OS
BS antenna number	4 Rx	4 Rx	4 Rx	4 Rx	4 Rx	4 Rx	4 Rx
BS downtilt	102	98	102	98	102	102	102
Number of UEs per cell	20	20	20	20	20	10	10
UE power control	P0 = -90 dBm, alpha = 1	P0 = -90 dBm, alpha = 1	P0 = -90 dBm, alpha = 1	P0 = -90 dBm, alpha = 1	P0 = -90 dBm, alpha = 1	P0 = -85 dBm, alpha = 0.93	P0 = -85 dBm, alpha = 0.93
HARQ/repetition	Number of transmission(s) = 1, no HARQ/ repetition	Number of transmission(s) = 1, no HARQ/ repetition	Number of transmission(s) = 1, no HARQ/ repetition	Number of transmission(s) = 1, no HARQ/ repetition	Number of transmission(s) = 1, no HARQ/repetition	1 repetition, no retransmission	2 repetition, no retransmission
Channel estimation	Realistic	Realistic	Realistic	Realistic	Realistic	Realistic	Realistic
BS advanced receiver	Baseline: MMSE-IRC or MMSE-PIC (2 iterations) MUSA: same as baseline	Baseline: MMSE-IRC or MMSE-PIC (2 iterations) MUSA: same as baseline	Baseline: MMSE-IRC or MMSE-PIC (2 iterations) MUSA: same as baseline	Baseline: MMSE-IRC or MMSE-PIC (2 iterations) MUSA: same as baseline	Baseline: MMSE-IRC or MMSE-PIC (2 iterations) MUSA: same as baseline	EPA receiver for all schemes	EPA receiver for all schemes
TB size	60 bytes	60 bytes	200 bytes	200 bytes	60 bytes	60 bytes	60 bytes
Packet dropping criterion	-	-	-	-	-	-	-
DMRS setting and allocation	24 DMRS each RB assumed, preconfigured, no collision	24 DMRS each RB assumed, preconfigured, no collision	24 DMRS each RB assumed, preconfigured, no collision	24 DMRS each RB assumed, preconfigured, no collision	24 DMRS each RB assumed, preconfigured, no collision	the DMRS pool size is 12, no DMRS collision	the DMRS pool size is 12, no DMRS collision
MA signature and allocation	24 spreading codes of length 4 are used for MUSA, preconfigured	24 spreading codes of length 4 are used for MUSA, preconfigured	24 spreading codes of length 4 are used for MUSA, preconfigured	24 spreading codes of length 4 are used for MUSA, preconfigured	24 spreading codes of length 4 are used for MUSA, preconfigured	spreading codes of length 2 are used for MUSA	spreading codes of length 2 are used for MUSA
Details on configured grant, e.g. periodicity, offset, and #of UEs assigned on the same resource	periodicity = 0.5 ms for baseline and MUSA	periodicity = 0.5 ms for baseline and MUSA	periodicity = 2 ms for baseline and MUSA	periodicity = 2 ms for baseline and MUSA	periodicity = 0.5 ms for baseline and MUSA	7 OFDM symbols	7 OFDM symbols
Other assumptions for baseline	3 PRBs per Tx for a UE	3 PRBs per Tx for a UE	3 PRBs per Tx for a UE	3 PRBs per Tx for a UE	12 PRBs + 0.25ms per Tx for a UE	12PRBs per UE	12PRBs per UE
Other assumptions for NOMA	12 PRBs per Tx for a UE; Same power consumption as baseline Ideal assumptions of inter-cell interference covariance matrix, with both spatial and spreading code domain inter-cell interference covariance matrix,	12 PRBs per Tx for a UE; Same power consumption as baseline. Ideal assumptions of inter-cell interference covariance matrix, with both spatial and spreading code domain inter-cell interference covariance matrix,	12 PRBs per Tx for a UE; Same power consumption as baseline. Ideal assumptions of inter-cell interference covariance matrix, with both spatial and spreading code domain inter-cell interference covariance matrix,	12 PRBs per Tx for a UE; Same power consumption as baseline. Ideal assumptions of inter-cell interference covariance matrix, with both spatial and spreading code domain inter-cell interference covariance matrix,	12 PRBs + 0.25ms per Tx for a UE Ideal assumptions of inter-cell interference covariance matrix, with both spatial and spreading code domain inter-cell interference covariance matrix,	12PRBs per UE; Multi-layer transmission for SCMA; Single-layer or multi-layer transmission for RSMA	12PRBs per UE; Multi-layer transmission for SCMA; Single-layer or multi-layer transmission for RSMA
Supported PAR for baseline at PDR=1% (packet/s/cell)	750	1000	400	500	<500	2320	2810
Supported PAR for NOMA at PDR=1% (packet/s/cell)	2500	3500	1200	1200	2000	2350 for SCMA 1690 for MUSA 1690 for SL-RSMA 2290 for ML-RSMA	2930 for SCMA 2170 for MUSA 2170 for SL-RSMA 2810 for ML-RSMA

Gain (relative to baseline)	233%	250%	200%	140%	300%	1.3% for SCMA, no gain for other schemes	4.3% for SCMA, no gain for other schemes
Source	**Source 2 - Case 3[48]**	**Source 2 - Case 4[48]**	**Source 6[49]**				
Carrier frequency	4GHz, 200m	4GHz, 200m	4GHz, 200m				
Simulation bandwidth	12 PRBs, SCS = 60kHz, 7OS	12 PRBs, SCS = 60kHz, 7OS	12 PRBs				
BS antenna number	4 Rx	4 Rx	4 Rx				
BS downtilt	102	102	102				
Number of UEs per cell	10	10	20				
UE power control	P0 = -85 dBm, alpha = 0.93	P0 = -85 dBm, alpha = 0.93	P0 = -90 dBm, alpha = 1				
HARQ/repetition	1 repetition, no retransmission	2 repetition, no retransmission	No HARQ/repetition				
Channel estimation	Realistic	Realistic	Realistic				
BS advanced receiver	SCMA/LCRS: chip-MMSE hard IC MUSA/RSMA: block-MMSE hard IC	SCMA/LCRS: chip-MMSE hard IC MUSA/RSMA: block-MMSE hard IC	MMSE-SIC				
TB size	60 bytes	60 bytes	60 bytes				
Packet dropping criterion	-	-	-				
DMRS setting and allocation	the DMRS pool size is 12, no DMRS collision,	the DMRS pool size is 12, no DMRS collision	no DMRS collision				
MA signature and allocation	spreading codes of length 2 are used for MUSA	spreading codes of length 2 are used for MUSA	-				
Details on configured grant, e.g. periodicity, offset, and #of UEs assigned on the same resource	7 OFDM symbols	7 OFDM symbols	-				
Other assumptions for baseline	12PRBs per UE	12PRBs per UE	-				
Other assumptions for NOMA	12PRBs per UE; Multi-layer transmission for SCMA; Single-layer or multi-layer transmission for RSMA	12PRBs per UE; Multi-layer transmission for SCMA; Single-layer or multi-layer transmission for RSMA	-				
Supported PAR for baseline at PDR=1% (packet/s/cell)	2290	2810	1900				
Supported PAR for NOMA at PDR=1% (packet/s/cell)	2290 for SCMA 1690 for MUSA 1690 for SL-RSMA 2290 for ML-RSMA	2810 for SCMA 2150 for MUSA 2150 for SL-RSMA 2810 for ML-RSMA	2700 for MUSA 2950 for PDMA				

Gain (relative to baseline)	No Gain	No Gain	42.1% for MUSA 55.3% for PDMA				

9.2.3 Simulation results for eMBB

For eMBB scenario, under the system-level evaluation assumptions as detailed in Table 9.2-3, relative to the evaluated OFDM waveform (using configured grant with multiple users in the same time and frequency resources) with MMSE-IRC or advanced receiver, the evaluated NOMA schemes with configured grant (without DMRS collision) can provide the results in Table 9.2-3:

- In some simulated cases,
  - time and frequency resource configuration per UE for the baseline is different from that per UE for evaluated NOMA schemes;
  - Receivers used for the baseline and for the evaluated NOMA schemes are in some cases different and in other cases the same.
- In some other simulated cases,
  - the time and frequency resource configuration per UE for the baseline is the same as that per UE for the evaluated NOMA scheme
  - the same type of receiver is assumed for the baseline and the evaluated NOMA schemes
  - Resource utilization of simulated NOMA schemes is comparable to baseline.
- Different L2S mappings are used.
- Within source 1, the ideal assumptions of inter-cell interference covariance matrix (non-block diagonal and genie-known to the receiver) is assumed.
- Different baselines, different amount of optimization, and different choice of receiver types are used within different sources

Table 9.2-3: System simulation results for NOMA in eMBB scenario

Source	Source 1-Case 1[42]	Source 1- Case 2[42]	Source 2- Case 1[50]	Source 2- Case 2[50]	Source 2- Case 3[50]	Source 2- Case 4[50]	Source 6 [49]	Source 3[45]
Carrier frequency	4GHz, 200m	4GHz, 200m	4GHz, 200m	4GHz, 200m	4GHz, 200m	4GHz, 200m	4GHz, 200m	4GHz, 200m
Simulation bandwidth	12 PRBs	12 PRBs	12 PRBs	12 PRBs	12 PRBs	12 PRBs	12 PRBs	12 PRBs
BS antenna number	4 Rx	4 Rx	4 Rx	4 Rx	4 Rx	4 Rx	4 Rx	4 Rx
BS downtilt	102	102	102	102	102	102	102	-
Number of UEs per cell	100	100	20	20	20	20	40	20
UE power control	P0 = -95 dBm, alpha = 1	P0 = -95 dBm, alpha = 1	P0 = -90 dBm, alpha = 0.9	P0 = -90 dBm, alpha = 0.9	P0 = -90 dBm, alpha = 0.9	P0 = -90 dBm, alpha = 0.9	P0 = -90 dBm, alpha = 1	-
HARQ/repetition	Number of transmission(s) = 1, no HARQ/repetition	Number of transmission(s) = 1, no HARQ/repetition	Maximum number of retransmission=8, no repetition	Maximum number of retransmission=8, no repetition	Maximum number of retransmission=8, no repetition	Maximum number of retransmission=8, no repetition	Random back-off, max 4 HARQ, no repetition	HARQ combining with random back-off. The maximum number for transmissions is 8
Channel estimation	Realistic	Realistic	Realistic	Realistic	Realistic	Realistic	Realistic	Ideal & Realistic
BS advanced receiver	Baseline: MMSE-IRC or MMSE-PIC MUSA: MMSE-PIC	Baseline: MMSE-IRC or MMSE-PIC MUSA: MMSE-PIC	EPA receiver for all schemes	EPA receiver for all schemes	SCMA/LCRS: chip-MMSE hard IC MUSA/RSMA: block-MMSE hard IC	SCMA/LCRS: chip-MMSE hard IC MUSA/RSMA: block-MMSE hard IC	MMSE-SIC	Baseline: MMSE-IRC IGMA: ESE receiver
TB size	70 bytes	70 bytes	60 bytes	80 bytes	60 bytes	80 bytes	60 bytes	-

Packet dropping criterion	If one TB is not received correctly after HARQ/ repetition, the packet is dropped	If one TB is not received correctly after HARQ/ repetition, the packet is dropped	8 HARQ transmissions or 1s latency	8 HARQ transmissions or 1s latency	8 HARQ transmissions or 1s latency	8 HARQ transmissions or 1s latency	-	8 HARQ transmissions
DMRS setting and allocation	24 DMRS each RB assumed, preconfigured, no collision	24 DMRS each RB assumed, preconfigured, no collision	the DMRS pool size is 24, no DMRS collision	the DMRS pool size is 24, no DMRS collision	the DMRS pool size is 24, no DMRS collision	the DMRS pool size is 24, no DMRS collision	no DMRS collision	DMRS are semi-static configured
MA signature and allocation	24 spreading codes of length 4 are used for MUSA, preconfigured	24 spreading codes of length 4 are used for MUSA, preconfigured	spreading codes of length 2 are used for MUSA	spreading codes of length 2 are used for MUSA	spreading codes of length 2 are used for MUSA	spreading codes of length 2 are used for MUSA	-	MA signatures are semi-static configured
Details on configured grant, e.g. periodicity, offset, and #of UEs assigned on the same resource	periodicity = 5 ms for baseline and MUSA	periodicity = 5 ms for baseline and MUSA	periodicity = 1 ms	periodicity = 1 ms	periodicity = 1 ms	periodicity = 1 ms	-	-
Other assumptions for baseline	3 PRB per Tx for a UE	12 PRBs per Tx for a UE	12PRBs per UE	12PRBs per UE	12PRBs per UE	12PRBs per UE	-	2 RBs is allocated for each UE
Other assumptions for NOMA	12 PRBs per Tx for a UE; Same power consumption as baseline Ideal assumptions of inter-cell interference covariance matrix, with both spatial and spreading code domain inter-cell interference covariance matrix,	12 PRBs per Tx for a UE Ideal assumptions of inter-cell interference covariance matrix, with both spatial and spreading code domain inter-cell interference covariance matrix,	12PRBs per UE; Multi-layer transmission for SCMA; Single-layer or multi-layer transmission for RSMA	12PRBs per UE; Multi-layer transmission for SCMA; Single-layer or multi-layer transmission for RSMA	12PRBs per UE; Multi-layer transmission for SCMA; Single-layer or multi-layer transmission for RSMA	12PRBs per UE; Multi-layer transmission for SCMA; Single-layer or multi-layer transmission for RSMA	-	all 12 RBs are occupied by each UE
Supported PAR for baseline at PDR=1% (packet/s/cell)	800 for baseline with MMSE-IRC; 1200 for baseline with MMSE-PIC	400 for baseline with MMSE-IRC; 600 for baseline with MMSE-PIC	5050	-	4800	-	2100	450 (ICE)
Supported PAR for NOMA at PDR=1% (packet/s/cell)	2000	1500	5100 for SCMA 4950 for MUSA; 4900 for SL-RSMA 5050 for ML-RSMA	4850 for SCMA 4800 for MUSA; 4650 for SL-RSMA 4600 for ML-RSMA	4800 for SCMA/MUSA/RSMA	4500 for SCMA 4500 for MUSA; 4500 for SL-RSMA 4300 for ML-RSMA	2500 for MUSA 3000 for PDMA	900 (ICE) 860 (RCE)
Gain (relative to baseline)	150% (baseline with MMSE-IRC) 66.7% (baseline with MMSE-PIC)	275% (baseline with MMSE-IRC) 150% (baseline with MMSE-PIC)	0.99% for SCMA, no gain for other schemes	-	no gain	-	19.1% for MUSA 42.9% for PDMA	100% (ICE) 91.1% (IGMA with RCE relative to baseline with ICE)
Source	**Source 7- Case 1[51]**	**Source 7- Case 2[51]**	**Source 8[52]**					

Carrier frequency	4GHz, 200m	4GHz, 200m	4GHz, 200m					
Simulation bandwidth	12 PRBs	12 PRBs (grant based transmission, wherein DL SYS BW is assumed to be 80 MHz, and 25% is assumed for PDCCH, over 2 OFDM symbols)	12 PRBs					
BS antenna number	4 Rx	4 Rx	4Rx					
BS downtilt	102	102	102					
Number of UEs per cell	32	32	40					
UE power control	P0 = -99.4 dBm, alpha = 0.9	P0 = -99.4 dBm, alpha = 0.9	P0=-90 dBm, alpha = 1					
HARQ/repetition	Max 8 HARQ attempts	Max 8 HARQ attempts	maximum number of HARQ transmission=8, no repetition					
Channel estimation	Realistic	Realistic	Realistic					
BS advanced receiver	MMSE with hard parallel IC	MMSE with hard parallel IC	Baseline: MMSE-PIC UGMA: MMSE-SIC					
TB size	89 bytes	-	85 bytes					
Packet dropping criterion	Packet is dropped after 8 HARQ attempts	Packet is dropped after 8 HARQ attempts	8 HARQ transmissions or 1s latency					
DMRS setting and allocation	16 DMRS assumed, preconfigured, no collision	16 DMRS assumed, preconfigured, no collision	spreading codes of length 2 are used for UGMA					
MA signature and allocation	16 spreading codes of spreading factor 4, preconfigured	4 spreading codes of spreading factor 2	periodicity = 8 ms					
Details on configured grant, e.g. periodicity, offset, and #of UEs assigned on the same resource	TDD Config: 3 DL, 1UL Periodicity: Every 2 UL slots (i.e. every 8 slots = 4 ms) Overloading (# UEs per resource): Up to 4 for baseline; Up to 16 for NOMA	TDD Config: 3 DL, 1UL 2 PDCCH symbols used to convey UL grants for each UL slot	Inter-cell interference is treated as white Gaussian noise					
Other assumptions for baseline	3 PRBs assigned to a UE for each arrival rate, the best MCS is selected ensuring that the packet drop rate is within the 1% limit	Frequency-selective (Granularity: 4 sub-bands of 3 RBs each) PDCCH constrained to 18 CCEs for UL Grants	Inter-cell interference is treated as white Gaussian noise					

Other assumptions for NOMA	12 PRBs assigned to a UE, SF = 4 for each arrival rate, the best MCS is selected ensuring that the packet drop rate is within the 1% limit	Frequency-selective (Granularity: 4 sub-bands of 3 RBs each) PDCCH constrained to 18 CCEs for UL Grants	Inter-cell interference is treated as white Gaussian noise					
Supported PAR for baseline at PDR=1% (packet/s/cell)	supported PAR = 770 UPT (Mbps) at PAR = 770: 5%: 0.012 50%: 0.071 95%: 0.149	supported PAR = 1086 UPT (Mbps) at PAR = 1120: 5%: 0.0378 50%: 0.1115 95%: 0.3173	1000					
Supported PAR for NOMA at PDR=1% (packet/s/cell)	supported PAR = 840 UPT (Mbps) at PAR = 840: 5%: 0.018 50%: 0.081 95%: 0.157	supported PAR = 1165 UPT (Mbps) at PAR = 1120: 5%: 0.0142 50%: 0.0982 95%: 0.2619	1200					
Gain (relative to baseline)	Gain on PAR: 9.1% Gain on UPT at PAR = 770: 5%: 50% 50%: 25% 95%: 5%	Gain on PAR:7% No Gain on UPT at PAR = 1086	20%					

10 Conclusions

Non-orthogonal multiple access (NOMA) technology is studied from the aspects of transmitter side processing, receiver complexity, related procedure and performance evaluations. In transmitter side processing, schemes can be characterized by multiple access (MA) signatures. Both schemes supported by Rel-15 and those requiring specification enhancement have been studied. Several types of receivers for NOMA are analyzed and their complexities are estimated. For NOMA related procedure, both synchronous and asynchronous transmissions are studied and evaluated.

Performance evaluations are carried out at both link level and system level.

Some general observations can be drawn from the simulated/analyzed cases:

- For LLS in mMTC/eMBB/URLLC scenarios with ideal channel estimation, equal SNR, zero TO/FO and fixed MA signature allocation
  - For low TBS (per UE SE is less than 0.15 bps/Hz and total SE is less than 1.8 bps/Hz), as long as the simulation configuration, e.g., reasonable code rate, is appropriate, the performance difference between NOMA schemes/MA signatures is small, even when different receiver types are used.
- For LLS in some simulated cases (i.e., 15/17/19/20/26/27) with ideal channel estimation, equal SNR, zero TO/FO and fixed MA signature allocation
  - For medium to high TBS (per UE SE is within [0.3, 0.55] bps/Hz, and total SE is less than 3.6 bps/Hz), as long as the simulation configuration, e.g., reasonable code rate, is appropriate, the performance difference between NOMA schemes/MA signatures is small.
    - Results with lower code rate (e.g. LDPC coding rate < 0.5) show better performance than the results with higher code rate (e.g. LDPC coding rate > 0.5).

- Based simulations of some cases (i.e., cases 1~5, cases 14~20), for LLS with realistic channel estimation, equal SNR distribution, zero TO/FO and fixed MA signature allocation, it is observed that
  - Up to 2~4 dB performance degradation is observed compared to ideal channel estimation for mMTC/eMBB scenario.
  - Up to 5 dB performance degradation is observed compared to ideal channel estimation for URLLC scenario.
  - Different performance degradation levels may be due to different channel estimation algorithm and DMRS extension methods.
  - The lower the SNR operation point is, the larger the performance degradation due to realistic CE can be observed
  - Higher number of UEs have larger performance degradation than lower number of UEs under the same channel condition and the same TBS for each individual case.
- Based simulations of some cases (i.e., 32/33/34/35) with larger standard deviation of SNR difference, for LLS with ideal channel estimation, under unequal SNR, and fixed MA signature allocation, it is observed that as long as the simulation configuration is appropriate, the performance difference between NOMA schemes/MA signatures is small, even when different receiver types are used
  - Performance loss of 1.1-3.2 dB can be observed with real channel estimation in multipath, where the losses are greater for the larger number of UEs or with greater SNR variation with for link level simulations.
- For the case with realistic channel estimation and random selection with potential MA signature collision (timing offset is within [0, 1.5*NCP], non-zero FO, and SNR offset is within +/-3dB)
  - When the TBS is small (i.e. 20 bytes), with 6 simultaneous activated UEs, based on the realistic UE detection by using 2-slot transmission time (e.g., 50% overhead for legacy preamble as the RS, without DMRS, preamble and data have the same BW, without assuming guard-band, with the pool size of 48 and 64), there is around 3.5 dB performance loss at 10% BLER, compared to random activation with no DMRS/MA signature collision and timing offset is within [0, 0.5*NCP] and 1-slot transmission.

    Note: this observation is based on single company's results
  - When the TBS is small (i.e. 20 bytes), 10% BLER cannot be achieved for 4 and 6 UEs, with random selection (DMRS overhead of 2/7 for pool size 24), for both realistic and ideal UE detection, with 1-slot transmission time.
  - When the TBS is small (i.e. 20 bytes), with random activation (with realistic UE detection, DMRS overhead of 2/7 for pool size 24, without DMRS/MA signature collision) of 1-slot transmission, the performance degradation at 10% BLER for 4, 6 and 8 UEs is about 1 dB compared to random activation without timing offset (with realistic UE detection, DMRS overhead of 1/7 for pool size 24, without DMRS/MA signature collision)

    Note: this observation is based on single company's results

For system level performance evaluation of configured grant transmission (without DMRS collision and where different baselines, different amount of optimization, and different choice of receiver types are used by companies. The same set of contiguous PRBs, is configured and overlapped across cells for the baseline and the evaluated NOMA schemes, respectively):

- Under eMBB scenario,
  - Sources 1 [42], 3 [45], 6 [49] and 7 [51] assume that time and frequency resource configuration per UE for the baseline is different from that for evaluated NOMA schemes. Sources 1, 6 and 7 use Method 1 of L2S mapping, and Source 3 uses Method 2 of L2S mapping. For the baseline, Source 1 assumes spatial-only MMSE-PIC or MMSE-IRC receiver, Source 6 assumes spatial-only MMSE-SIC receiver and source 7 assumes spatial-only LMMSE hard IC receiver and Source 3 assumes spatial-only MMSE IRC receiver. For simulated NOMA schemes, Source 1 assumes joint spatial-spreading domain MMSE-PIC, Source 6 assumes joint spatial-spreading domain MMSE-SIC receiver and Source 7 assumes joint spatial-spreading domain LMMSE hard IC receiver, and Source 3 assumes e-ESE receiver. Source 1 assumes ideal inter-cell interference covariance matrix. Performance gains are demonstrated in these simulations as listed in Table 9.2-3.

  - Source 1 assumes that time and frequency resource configuration per UE for the baseline is the same as that per UE for evaluated NOMA schemes. Method 1 of L2S mapping is used. Spatial-only MMSE-IRC/PIC receivers are assumed for baseline, and joint spatial-spreading domain MMSE-PIC receiver is assumed for NOMA scheme. Ideal inter-cell interference covariance matrix is assumed. Performance gains are demonstrated in this simulation as listed in Table 9.2-3.

  - Source 8 [52] assumes that time and frequency resource configuration per UE for the baseline is the same as that per UE for evaluated NOMA schemes. Method 1 of L2S mapping is used. Spatial-only MMSE-P IC receiver is assumed for baseline and joint spatial-spreading domain MMSE-SIC receiver is assumed for the NOMA scheme. Performance gains are demonstrated in this simulation as listed in Table 9.2-3.

  - Source 2 [50] assumes that time and frequency resource configuration per UE for the baseline is the same as that per UE for evaluated NOMA schemes. Method 3 of L2S mapping is used. The same type of receiver, either spatial-only/joint spatial-spreading domain MMSE hard IC or EPA receiver is assumed for both baseline and NOMA. No performance gain is demonstrated in these simulations as listed in Table 9.2-3.

- Under uRLLC scenario,

  - Sources 1 and 6 assume that time and frequency resource configuration per UE for the baseline is different from that for evaluated NOMA schemes. They use Method 1 based L2S mapping. For the baseline, Source 1 assumes spatial-only MMSE-PIC or MMSE-IRC receiver, Source 6 assumes spatial-only MMSE-SIC receiver. For simulated NOMA schemes, Source 1 assumes joint spatial-spreading domain MMSE-PIC or MMSE-IRC, Source 6 assumes joint spatial-spreading domain MMSE-SIC receiver. Source 1 assumes ideal inter-cell interference covariance matrix. Performance gains are demonstrated in these simulations as listed in Table 9.2-2.

  - Source 1 assumes that time and frequency resource configuration per UE for the baseline is the same as that per UE for evaluated NOMA schemes. Method 1 of L2S mapping is used. Spatial-only MMSE-IRC/PIC receivers are assumed for the baseline and joint spatial-spreading domain MMSE-PIC is assumed for NOMA scheme. Ideal inter-cell interference covariance matrix is assumed. Performance gains are demonstrated in this simulation as listed in Table 9.2-2.

  - Source 2 [48] assumes that time and frequency resource configuration per UE for the baseline is the same as that per UE for evaluated NOMA schemes. Method 3 of L2S mapping are used. The same type of receiver, either spatial-only/ joint spatial-spreading domain MMSE hard IC or EPA receiver is assumed for both baseline and NOMA. No performance gain is demonstrated in these simulations as listed in Table 9.2-2.

- Under mMTC scenario,

  - Sources 1, 3, 4 [46], 5 [47] and 7 assume that time and frequency resource configuration per UE for the baseline is different from that for evaluated NOMA schemes. Resource utilization of simulated NOMA schemes is higher than that of baseline. Sources 1, 4 and 7 use Method 1 of L2S mapping, and Source 3 uses Method 2 of L2S mapping. For baseline, Source 1 assumes spatial-only MMSE-PIC or MMSE-IRC receiver, Source 7 assumes spatial-only LMMSE hard IC, Source 4 assume spatial-only MMSE SIC or MMSE IRC receiver and Source 3 assumes spatial-only MMSE IRC receiver. Source 5 assumes spatial-only MMSE-IRC receiver. For simulated NOMA schemes, Sources 1 assumes joint spatial-spreading domain MMSE-PIC or MMSE-IRC receiver, Source 7 assumes joint spatial-spreading domain LMMSE hard IC, Source 4 assumes joint spatial-spreading domain MMSE hard IC receiver, and Source 3 assumes e-ESE receiver. Source 5 assumes spatial-only EPA receiver. Source 1 assumes ideal inter-cell interference covariance matrix. Performance gains are demonstrated in these simulations as listed in Table 9.2-1.

  - Source 1 assumes that time and frequency resource configuration per UE for the baseline is the same as that per UE for evaluated NOMA schemes. Method 1 of L2S mapping is used. Spatial-only MMSE-IRC/PIC receivers are assumed for baseline, and joint spatial-spreading domain MMSE-PIC receiver is assumed for NOMA scheme. Ideal inter-cell interference covariance matrix is assumed. Performance gains are demonstrated in this simulation as listed in Table 9.2-1.

  - Source 2 [43][44] assumes that time and frequency resource configuration per UE for the baseline is the same as that per UE for evaluated NOMA schemes. Method 1 [44] and Method 3 [43] of L2S mapping are used. The same type of receiver, either spatial-only/ joint spatial-spreading domain MMSE hard IC or EPA receiver is assumed for both baseline and NOMA. No performance gain is demonstrated in these simulations as listed in Table 9.2-1.

Annex A: simulation scenarios and assumptions

A.1 Link level simulation assumptions

A.1.1 Simulation assumptions for link level evaluations.

Table A.1-1: Link-level evaluation assumptions

Parameters	mMTC	URLLC	eMBB	Further specified values
Carrier Frequency	700 MHz	700 MHz or 4 GHz	4 GHz, 700 MHz as optional	
Waveform (data part)	CP-OFDM and DFT-s-OFDM	CP-OFDM as starting point	CP-OFDM as starting point	
Channel coding	URLLC: NR LDPC eMBB: NR LDPC mMTC: NR LDPC			The choice of channel coding here is only for the performance evaluation purpose for NOMA study
Numerology (data part)	SCS = 15 kHz, #OS = 14	Case 1: SCS = 60 kHz, #OS = 7 (normal CP), optionally 6 (ECP) Case 2: SCS = 30 kHz, #OS = 4	SCS = 15 kHz #OS = 14	
Allocated bandwidth	6 as the starting point	12 for 60kHz SCS, and 24 for 30kHz SCS as the starting point	12 as the starting point	For high payload such as 75 bytes, larger number of RBs can be considered.
TBS per UE	At least five TBS that are [10, 20, 40, 60, 75] bytes. Other values higher than 10 bytes are not precluded. Lower than 0.1 bits/RE is optional	At least five TBS that are [10, 20, 40, 60, 75] bytes. Other values higher than 10 bytes are not precluded.	At least five TBS that are [20, 40, 80, 120, 150] bytes. Other values higher than 20 bytes are not precluded.	For ideal channel estimation, DMRS overhead is 1/7 for #OS 7 and 14, and 1/4 for #OS 4
Target BLER for one transmission	10%	0.1%	10%	
Number of UEs multiplexed in the same allocated bandwidth	To be reported by companies.			Companies are encouraged to perform evaluations with various number of UEs Note: refined set of numbers of UEs should be further discussed in the next meeting.
BS antenna configuration	2 Rx or 4 Rx for 700MHz, 4Rx or 8 Rx for 4 GHz 8Rx as optional			CDL model in 38.901 should be considered for 8Rx
UE antenna configuration	1Tx			
Propagation channel & UE velocity	TDL-A 30ns and TDL-C 300ns in TR38.901, 3km/h, CDL optional			
Max number of HARQ transmission	1 as starting point.	1 as starting point. More values, 2 for URLLC can be used.	1 as starting point.	
Channel estimation	Ideal channel estimation results should be reported for calibration			

	Realistic channel estimation Reuse the NR design for evaluation purpose for number of DMRS ports <= 12; (Other DMRS designs are not precluded for the NOMA study) For number of DMRS ports > 12, The DMRS overhead should not be less than NR design for evaluation purpose. (FFS extending DMRS design for the NOMA study)			
MA signature allocation (for data and DMRS)	Fixed/Random			Proponents report the details of random MA signature allocation (whether without or with collision)
Distribution of avg. SNR	Both equal and unequal	Equal	Both equal and unequal	Uniform discrete values for unequal case,, range [x - a, x + a] (dB) with 1 dB step, where x is the per UE average SNR in dB, and the deviation [a=3] SNR is defined as the mean received power over the allocated bandwidth per OFDM symbol carrying data, divided by noise power per OFDM symbol within the allocated bandwidth.
Timing offset	0 as starting point. For grant-free without perfect TA (asynchronous), value is within [0, y] as starting point, where y has two values at least for the purpose of evaluation: - Case 1: y = NCP/2 - Case 2: y = 1.5*NCP For all UEs in Case 1 or all UEs in Case 2, TO values for each UE for each transmission are i.i.d. from uniform distribution [0, y], and independent between UEs. For mixed sync and async, X% of UEs with zero TO and (100-X)% with non-zero TO - X = 80 - Other values are not precluded			
Frequency error	0 as starting point. Also evaluate uniform distribution between -70 and 70 Hz for 700MHz carrier frequency, and uniform distribution between -140 and 140 Hz for 4GHz carrier frequency.			
Traffic model for link level	Full buffer as starting point. Non-full-buffer model (like Poisson arrival of fixed packet size) is optional.			
For link level calibration purpose only	OMA single user whose spectral efficiency is the same as per UE SE in NOMA. AWGN curves can be provided also.			

Note: for the case when a parameter has a "OR" condition, companies are encouraged to evaluate all the corresponding

A.1.2 Link level evaluation assumptions for calibration purpose

Table A.1-2: LLS assumptions for calibration purpose

Implementation assumptions	Values
LDPC decoding algorithm (e.g. MaxLogMAP or LogMAP, fully parallel or row parallel)	Companies to report
Number of LDPC decoding iteration	Companies to report (e.g., 50 for flooding, 25 for layered)
Modulation for 10/20 bytes	QPSK
Modulation for 75/150 bytes	QPSK
Channel Estimation	Ideal
Channel Model	AWGN, TDL-A with 30ns (3km/h), TDL-C with 300ns

	(3km/h), no spatial correlation Initialize channel realization at each slot
Total number of slots	1000 for eMBB/mMTC AWGN 10000 for eMBB/mMTC fading channel [50000] for URLLC AWGN [100000] for URLLC fading channel
System bandwidth	10 MHz

Table A.1-3: Assumptions for decoding algorithm for LLS calibration

Additional assumptions	Source 1	Source 2	Source 3	Source 4	Source 5	Source 6	Source 7	Source 8	Source 9	Source 10
Number of LDPC decoding iteration	25	50	50	50	50	25	50	50	20	25
LDPC decoding algorithm	min_sum, layered	log map, Standard belief	min_sum, flooding	BP, flooding	BP, flooding	min_sum, layered	BP, flooding	BP, flooding	offset_min_sum, layered	offset_min_sum (offset=0.5) layered
Additional assumptions	Source 11	Source 12	Source 13	Source 14	Source 15	Source 16	Source 17	Source 18	Source 19	Source 20
Number of LDPC decoding iteration	50	50	50	50	50	50	25	50	50	50
LDPC decoding algorithm	BP, flooding	logBP	offset min_sum, layered	min_sum, flooding	BP, flooding	offset min_sum (offset=0.75) flooding	min_sum, layered	BP, flooding	BP, flooding	BP, flooding

In the following figures, for each simulation setting which is a combination of use scenario, TBS, channel and waveform, the results are presented in two groups: min_sum vs. log_BP.

1) mMTC 10 bytes, CP-OFDM, 1T2R

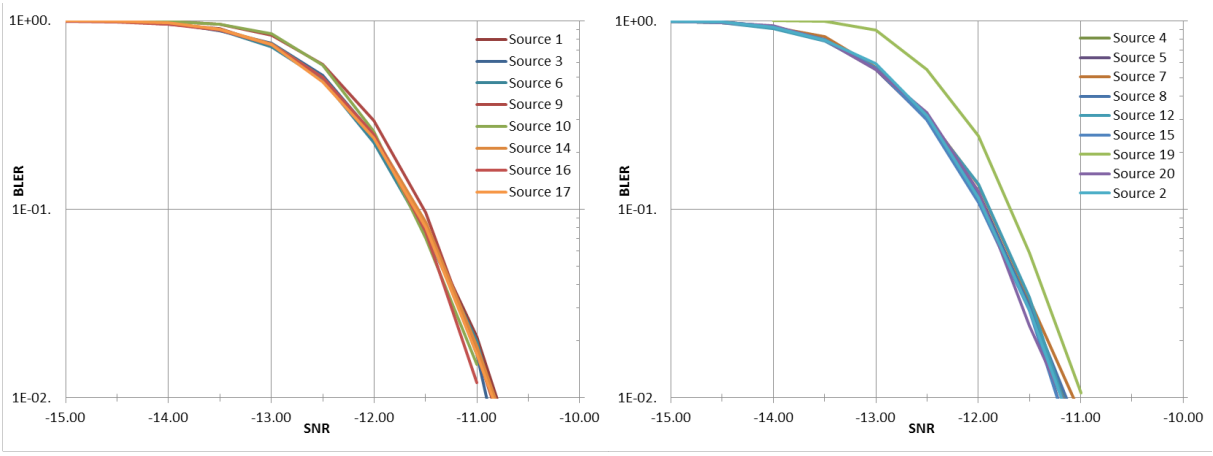

(a) min_sum, AWGN, 10 bytes, CP-OFDM (b) log_BP, AWGN, 10 bytes, CP-OFDM

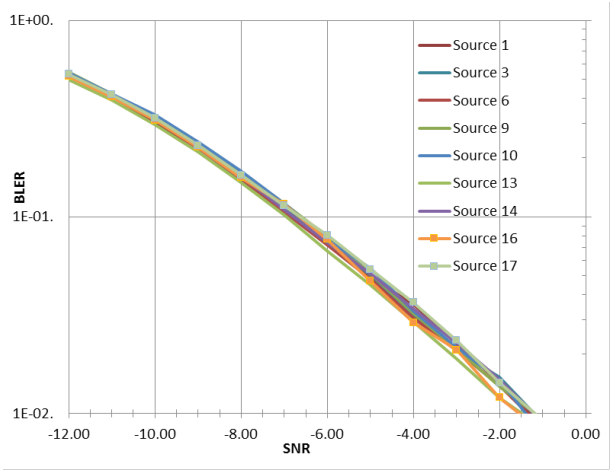

(c) min_sum, TDL-A, 10 bytes, CP-OFDM

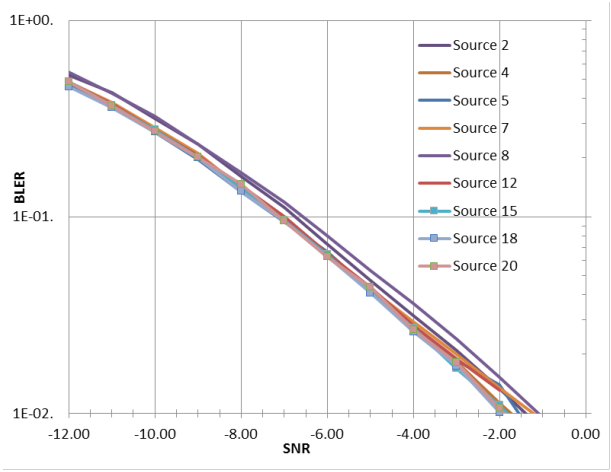

(d) log_BP, TDL-A, 10 bytes, CP-OFDM

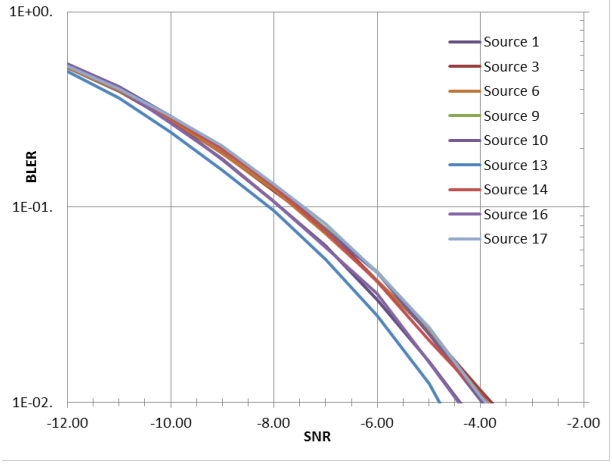

(e) min_sum, TDL-C, 10 bytes, CP-OFDM

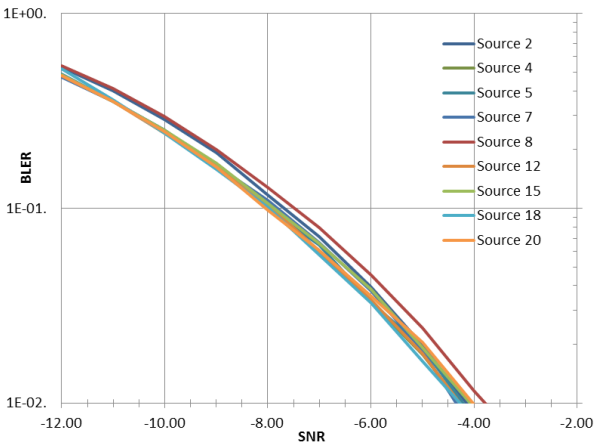

(f) log_BP, TDL-C, 10 bytes, CP-OFDM

Figure A.1-1: Calibration results for mMTC, 10bytes, CP-OFDM

2) mMTC 75 bytes, CP-OFDM, 1T2R

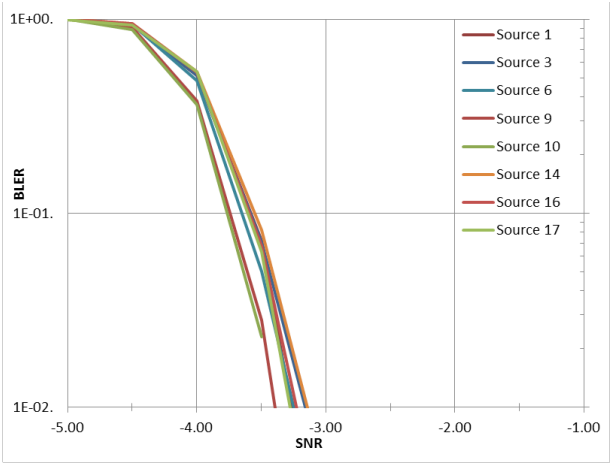

(a) min_sum, AWGN, 75 bytes, CP-OFDM

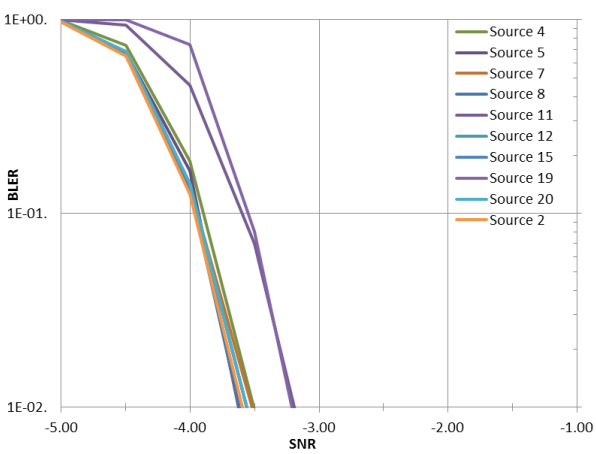

(b) log_BP, AWGN, 75 bytes, CP-OFDM

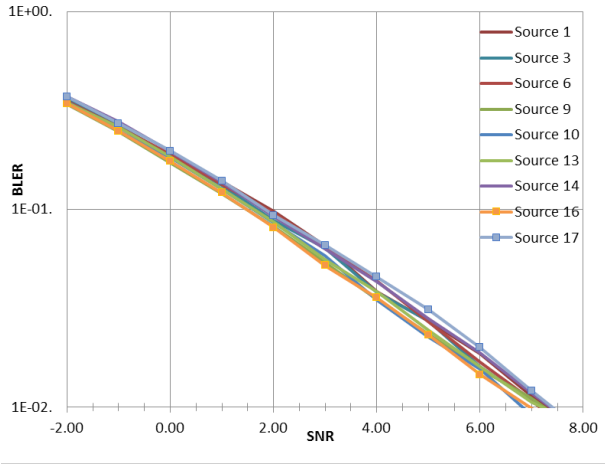

(c) min_sum, TDL-A, 75 bytes, CP-OFDM

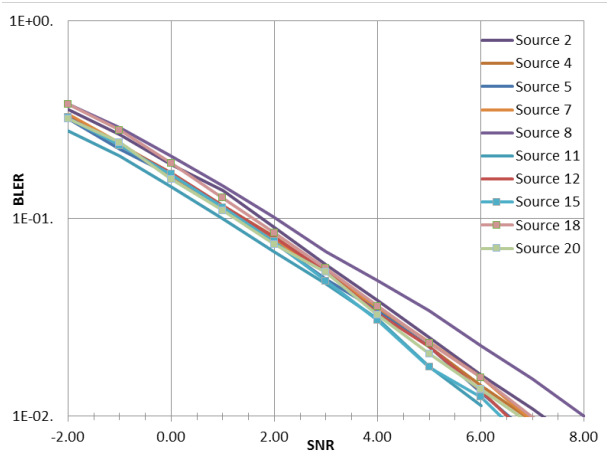

(d) log_BP, TDL-A, 75 bytes, CP-OFDM

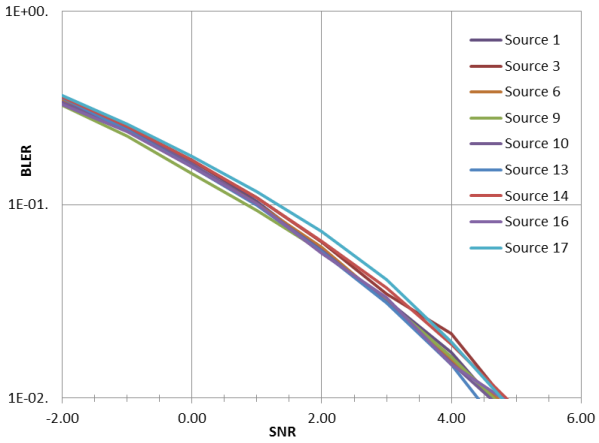

(e) min_sum, TDL-C, 75 bytes, CP-OFDM

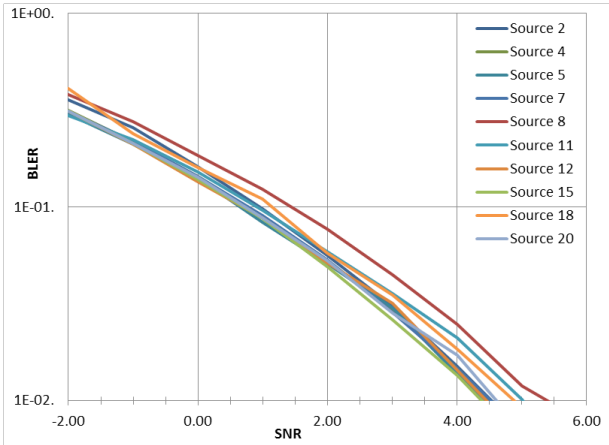

(f) log_BP, TDL-C, 75 bytes, CP-OFDM

Figure A.1-2: Calibration results for mMTC, 75bytes, CP-OFDM

3) mMTC 10 bytes, DFT-S-OFDM, 1T2R

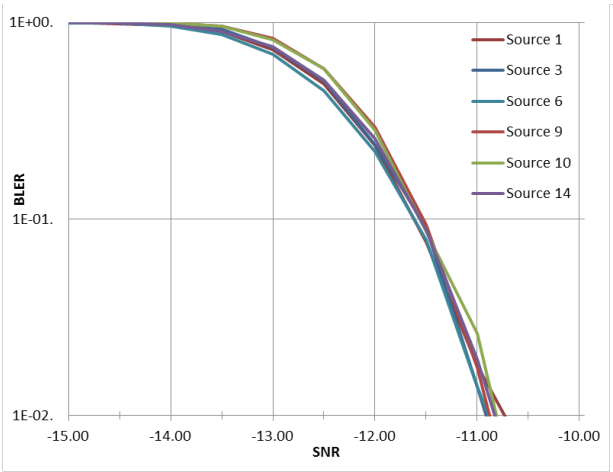

(a) min_sum, AWGN, 10 bytes, DFT-S-OFDM

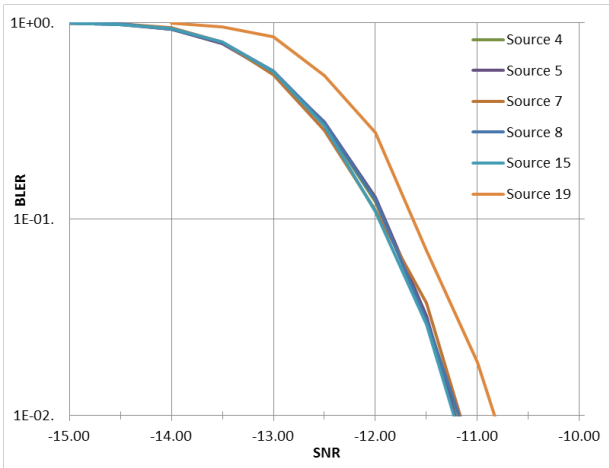

(b) log_BP, AWGN, 10 bytes, DFT-S-OFDM

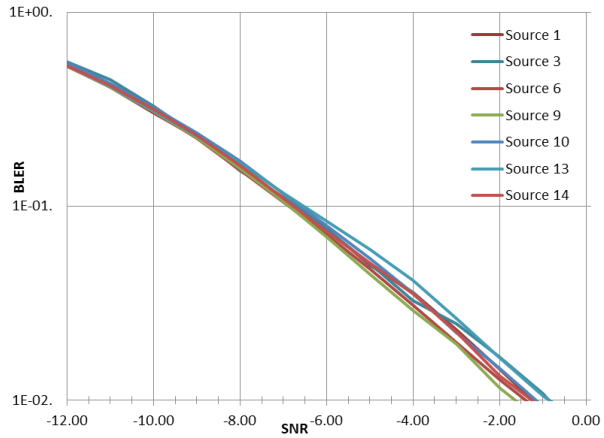

(c) min_sum, TDL-A, 10 bytes, DFT-S-OFDM

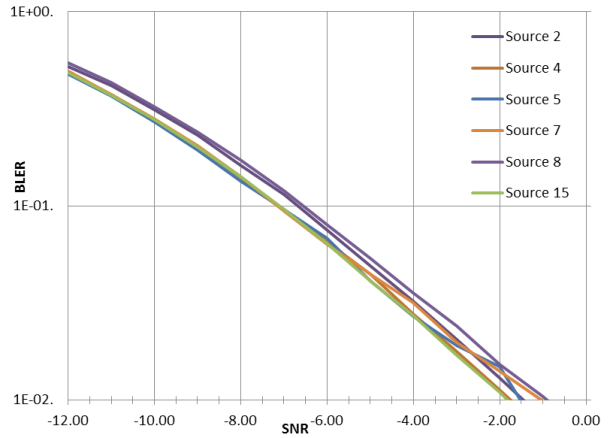

(d) log_BP, TDL-A, 10 bytes, DFT-S-OFDM

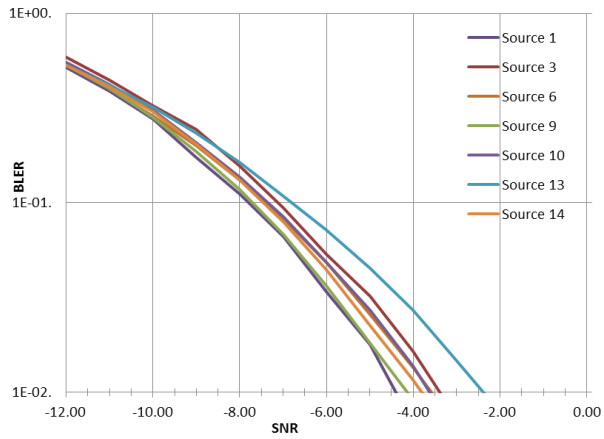

(e) min_sum, TDL-C, 10 bytes, DFT-S-OFDM

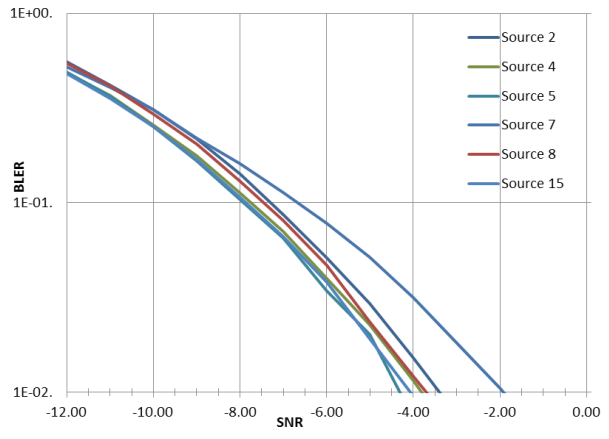

(f) log_BP, TDL-C, 10 bytes, DFT-S-OFDM

Figure A.1-3: Calibration results for mMTC, 10bytes, DFT-S OFDM

4) mMTC 75 bytes, DFT-S-OFDM, 1T2R

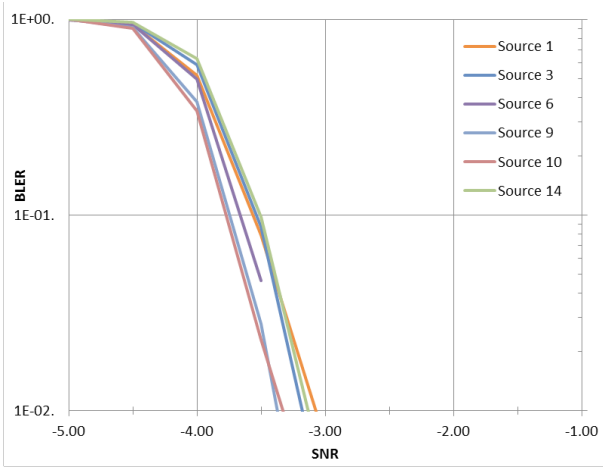

(a) min_sum, AWGN, 75 bytes, DFT-S-OFDM

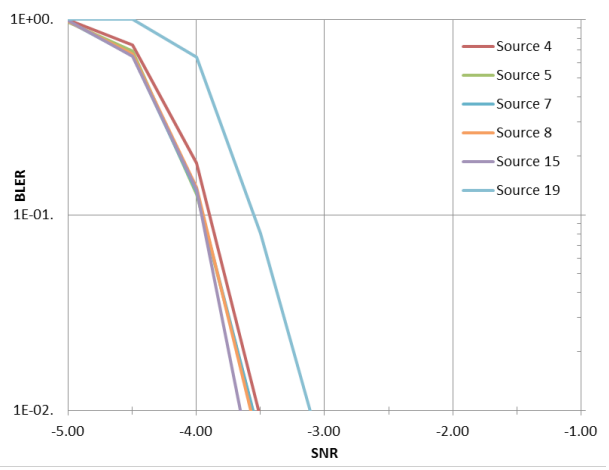

(b) log_BP, AWGN, 75 bytes, DFT-S-OFDM

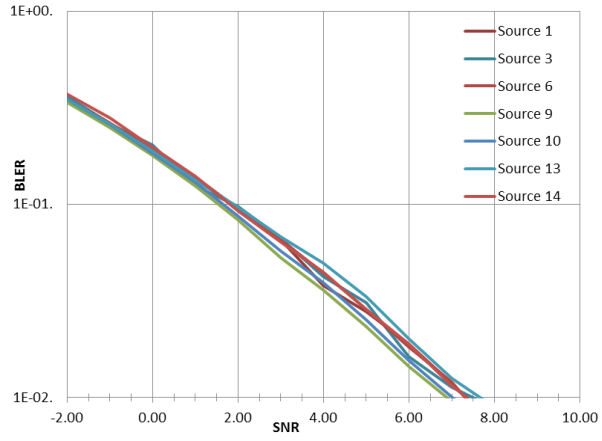

(c) min_sum, TDL-A, 75 bytes, DFT-S-OFDM

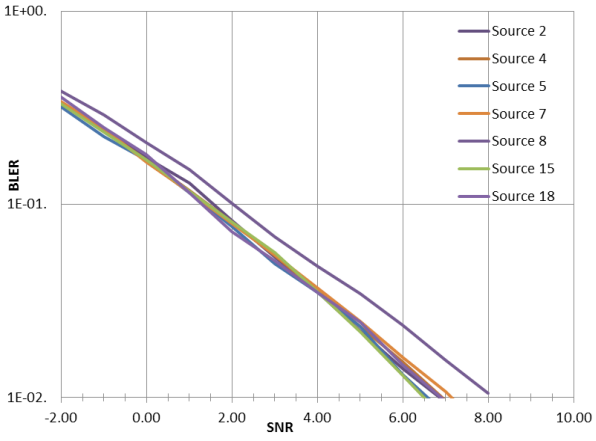

(d) log_BP, TDL-A, 75 bytes, DFT-S-OFDM

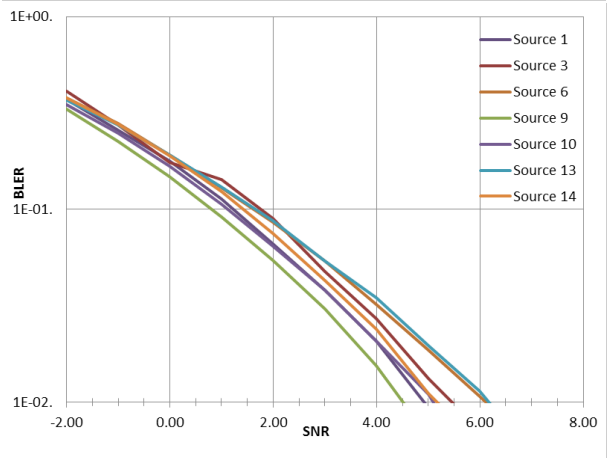

(e) min_sum, TDL-C, 75 bytes, DFT-S-OFDM

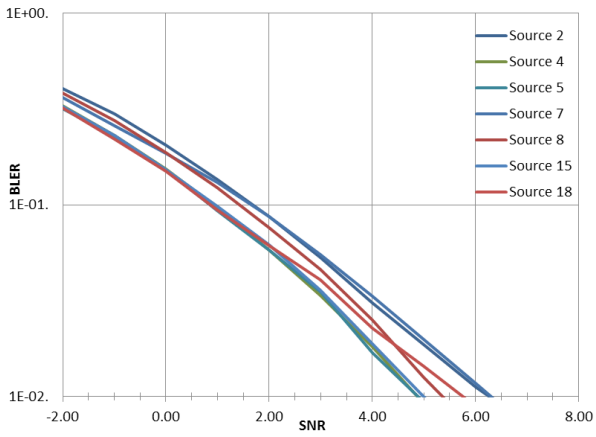

(f) log_BP, TDL-C, 75 bytes, DFT-S-OFDM

Figure A.1-4: Calibration results for mMTC, 75bytes, DFT-S-OFDM

5) eMBB, 20 bytes, 1T4R

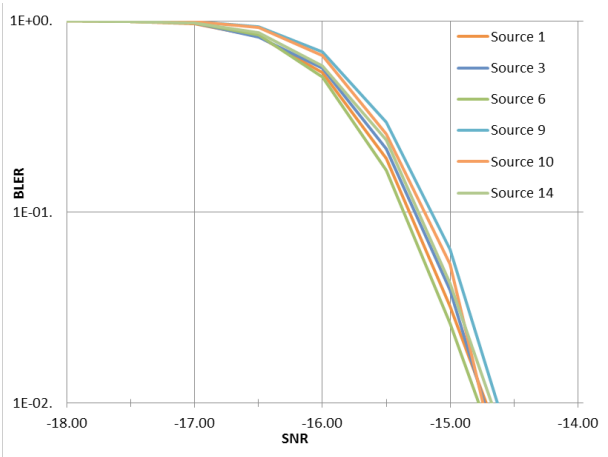

(a) min_sum, AWGN, 20 bytes

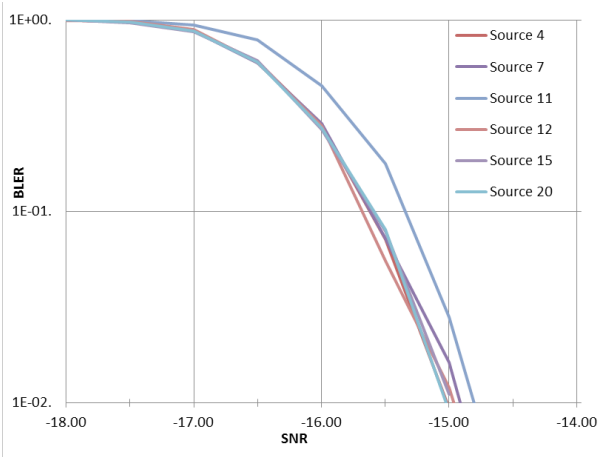

(b) log_BP, AWGN, 20 bytes

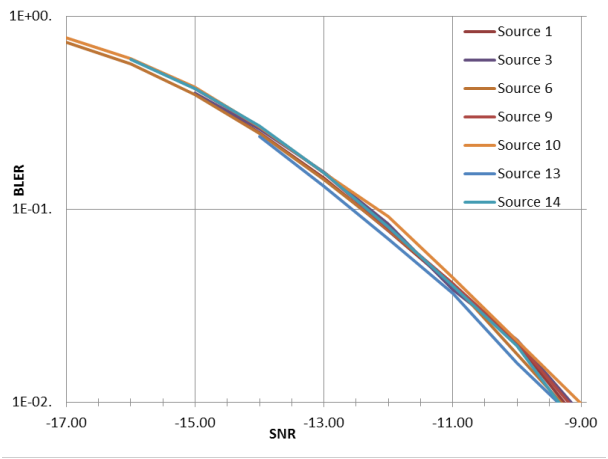

(c) min_sum, TDL-A, 20 bytes

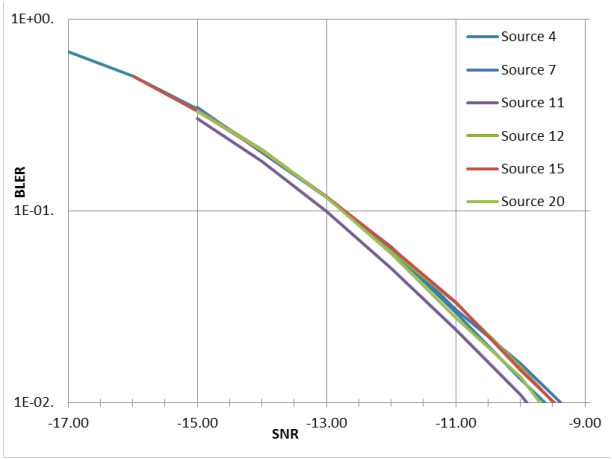

(d) log_BP, TDL-A, 20 bytes

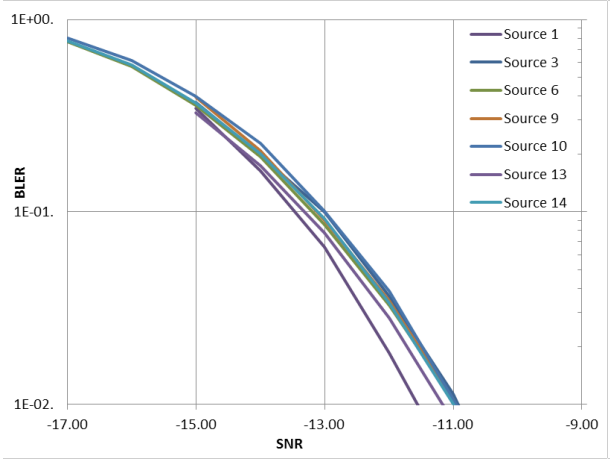

(e) min_sum, TDL-C, 20 bytes

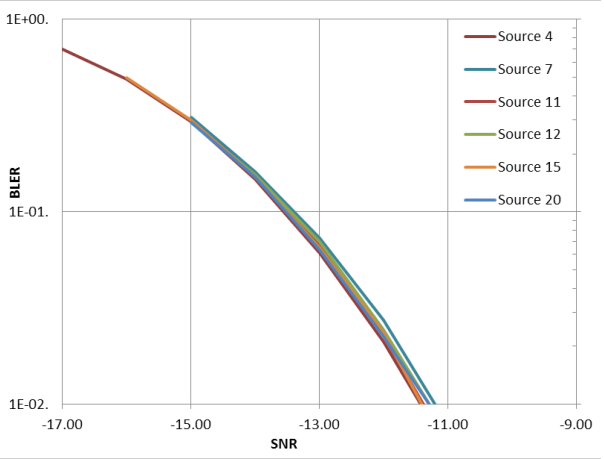

(f) log_BP, TDL-C, 20 bytes

Figure A.1-5: Calibration results for eMBB 20 bytes.

6) eMBB, 150 bytes, 1T4R

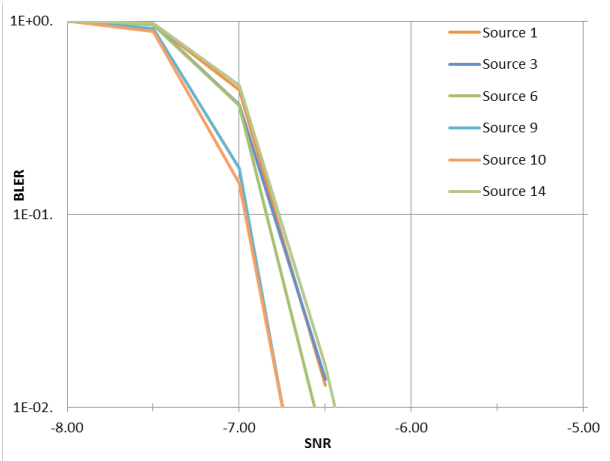

(a) min_sum, AWGN, 150 bytes

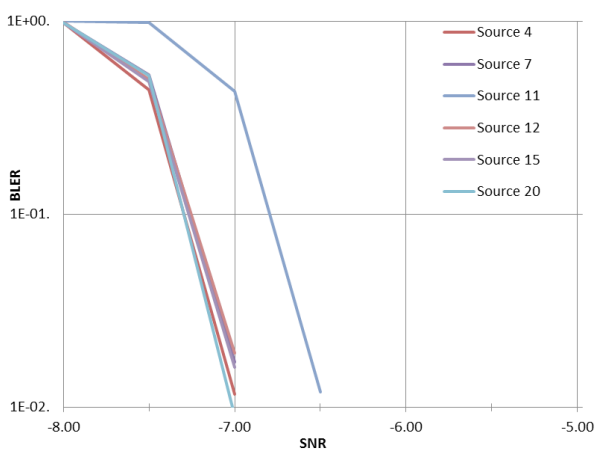

(b) log_BP, AWGN, 150 bytes

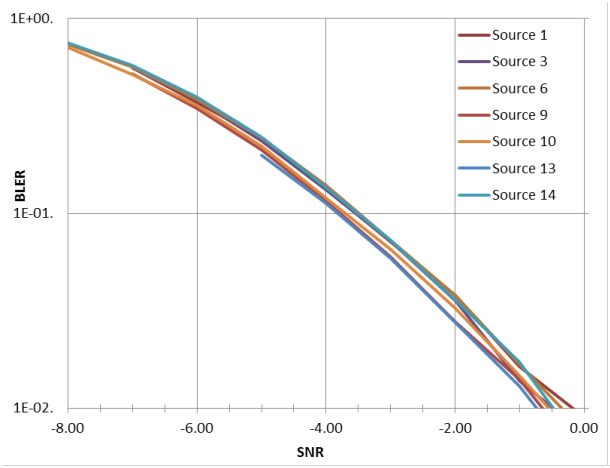

(c) min_sum, TDL-A, 150 bytes

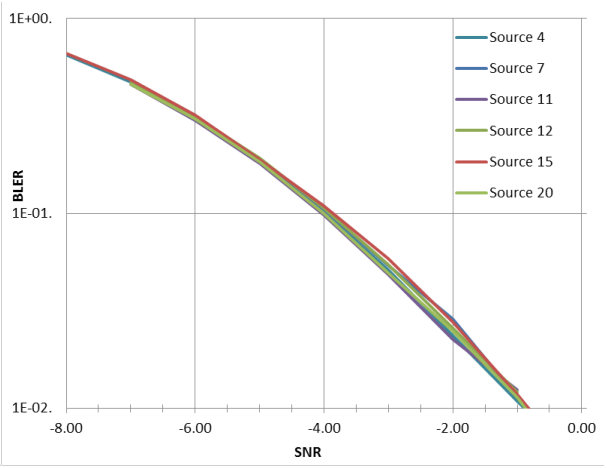

(d) log_BP, TDL-A, 150 bytes

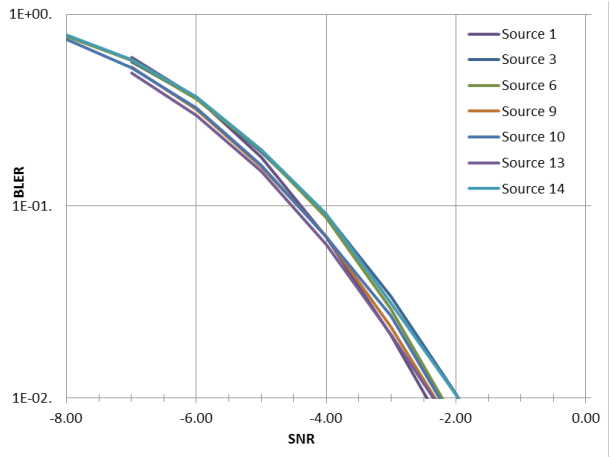

(e) min_sum, TDL-C, 150 bytes

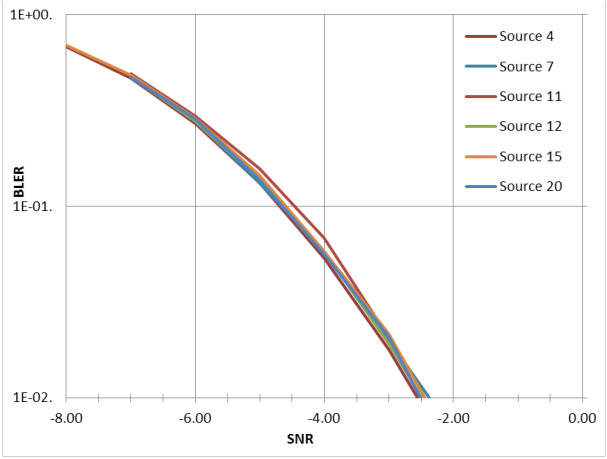

(f) log_BP, TDL-C, 150 bytes

Figure A.1-6: Calibration results for eMBB 150 bytes.

7) URLLC 10 bytes, 60kHz, 1T4R

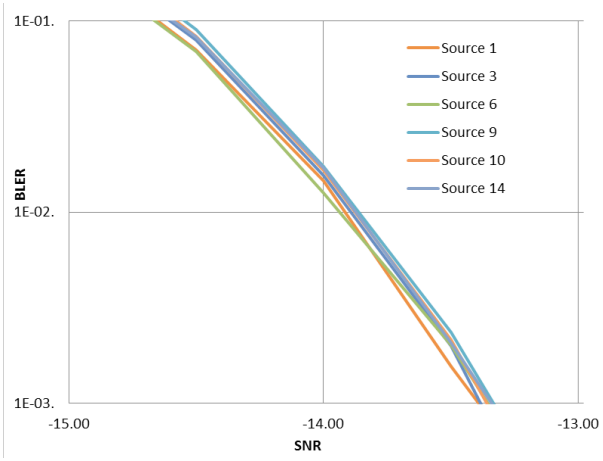

(a) min_sum, AWGN, 10 bytes, 60kHz

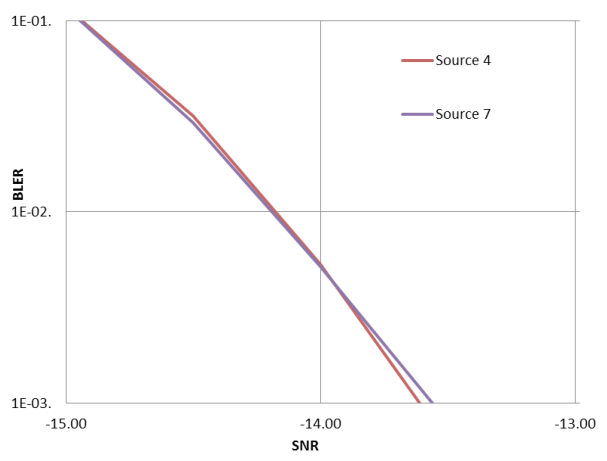

(b) log_BP, AWGN, 10 bytes, 60kHz

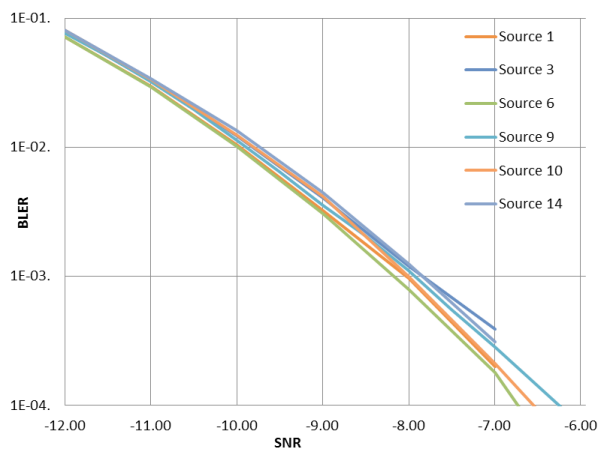

(c) min_sum, TDL-A, 10 bytes, 60kHz

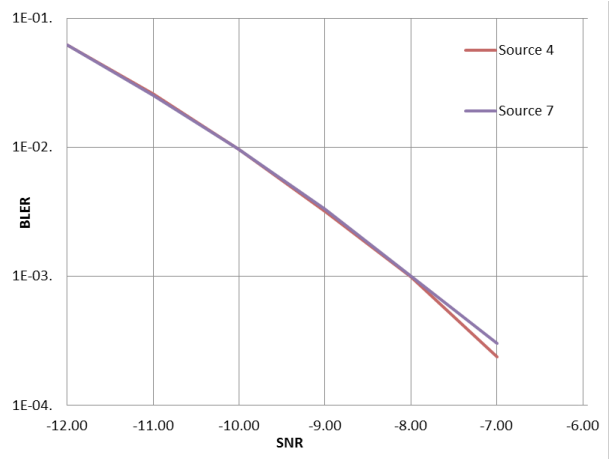

(d) log_BP, TDL-A, 10 bytes, 60kHz

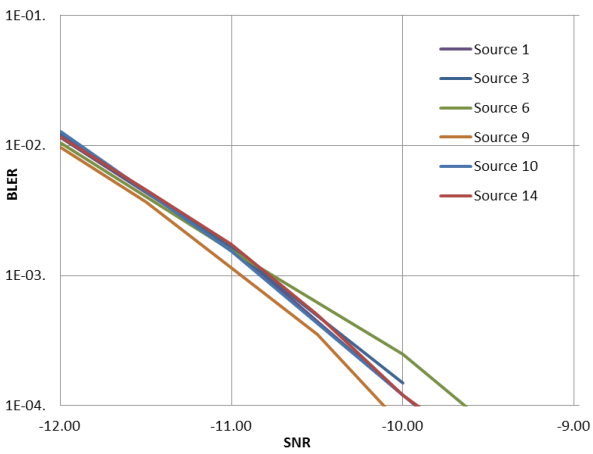

(e) min_sum, TDL-C, 10 bytes, 60kHz

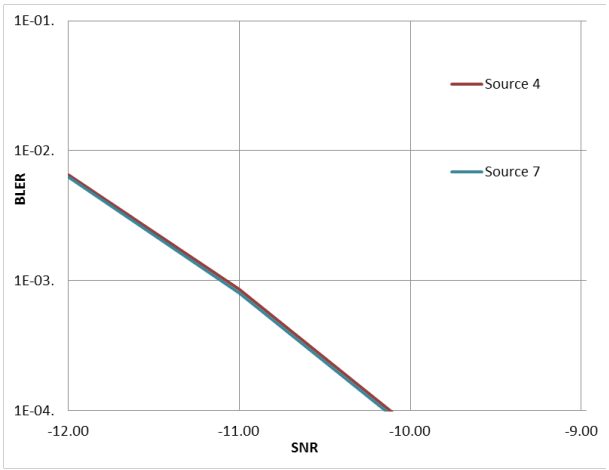

(f) log_BP, TDL-C, 10 bytes, 60kHz

Figure A.1-7: Calibration results for URLLC, 10bytes, 60kHz

8) URLLC 75 bytes, 60kHz, 1T4R

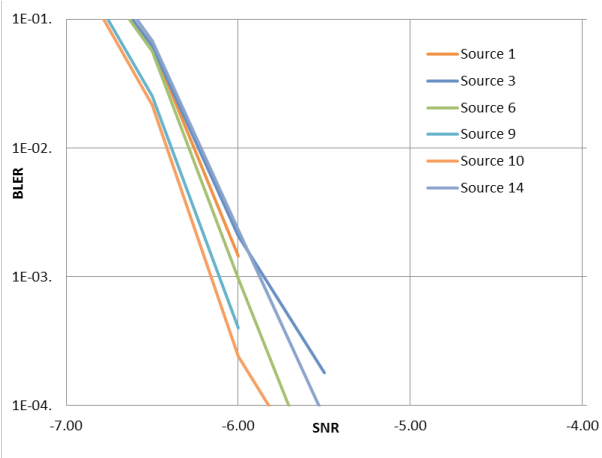

(a) min_sum, AWGN, 75 bytes, 60kHz

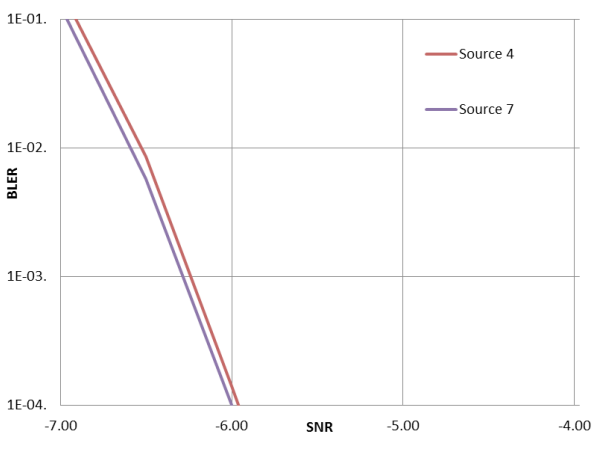

(b) log_BP, AWGN, 75 bytes, 60kHz

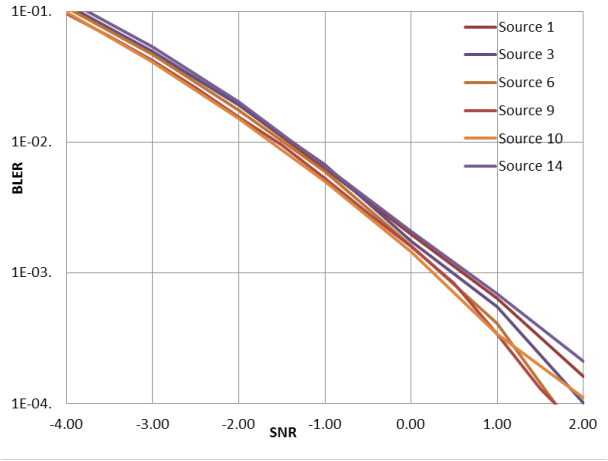

(c) min_sum, TDL-A, 75 bytes, 60kHz

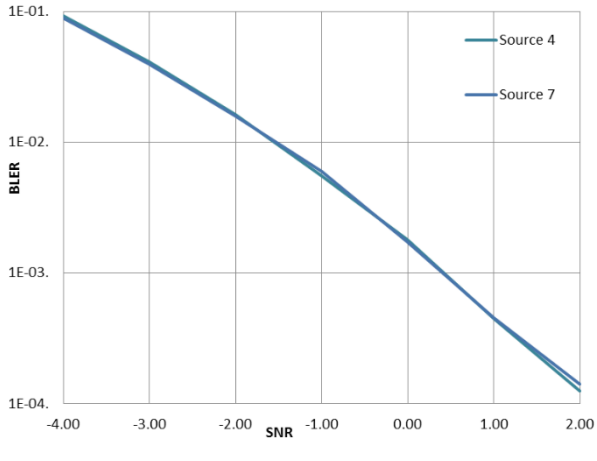

(d) log_BP, TDL-A, 75 bytes, 60kHz

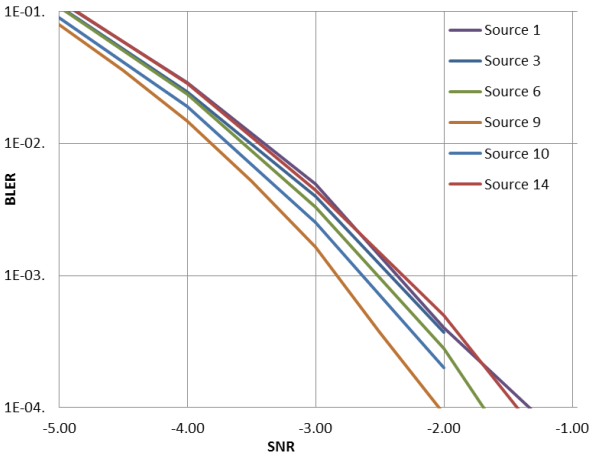

(e) min_sum, TDL-C, 75 bytes, 60kHz

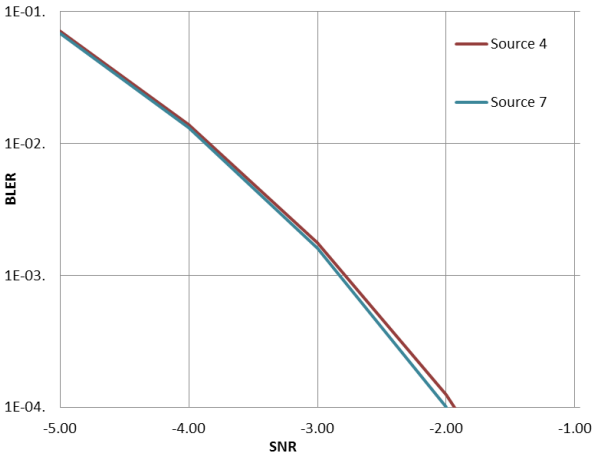

(f) log_BP, TDL-C, 75 bytes, 60kHz

Figure A.1-8: Calibration results for URLLC, 75bytes, 60kHz

9) URLLC 10 bytes, 30kHz, 1T4R

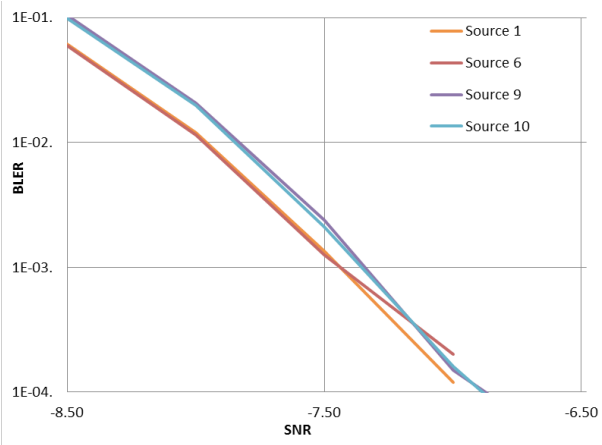

(a) min_sum, AWGN, 10 bytes, 30kHz

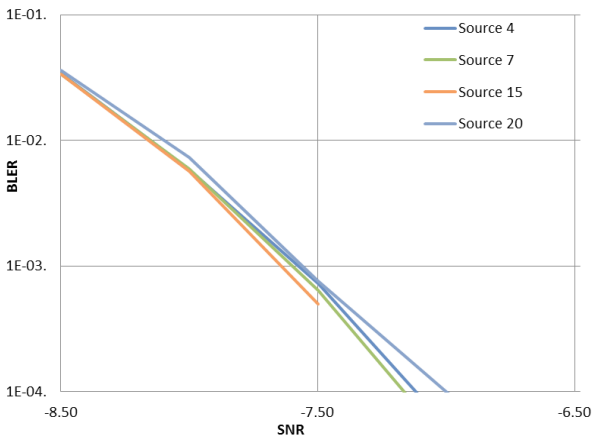

(b) log_BP, AWGN, 10 bytes, 30kHz

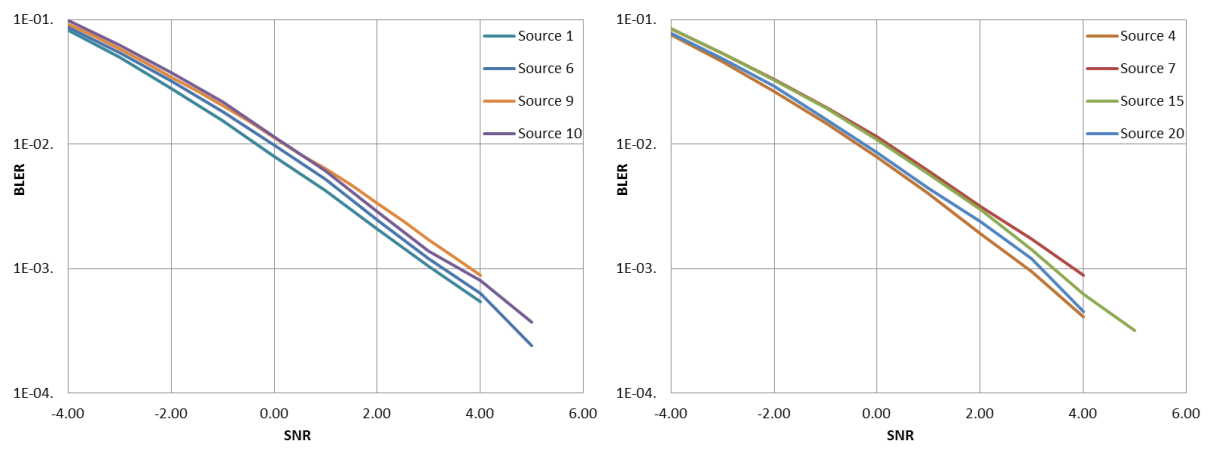

(c) min_sum, TDL-A, 10 bytes, 30kHz (d) log_BP, TDL-A, 10 bytes, 30kHz

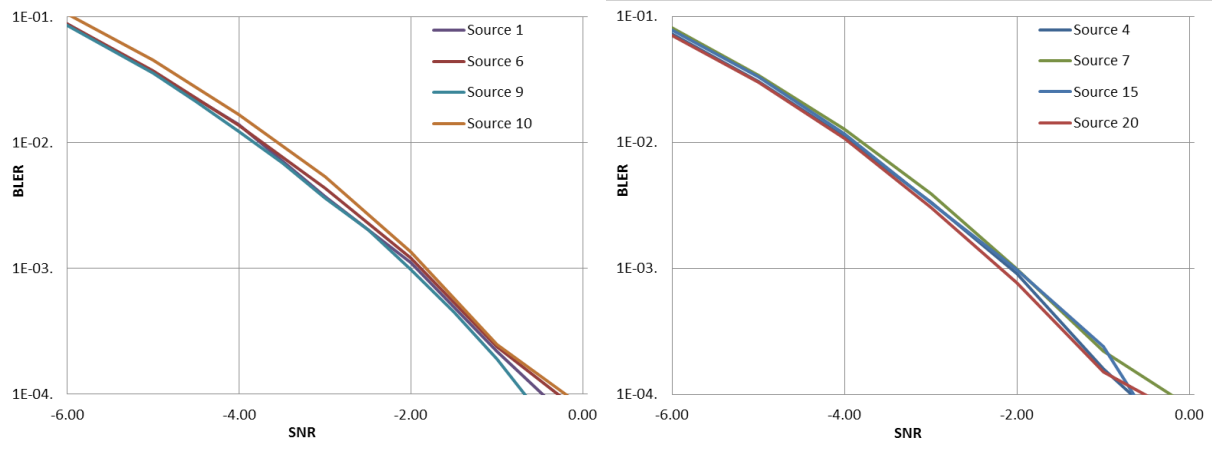

(e) min_sum, TDL-C, 10 bytes, 30kHz (f) log_BP, TDL-C, 10 bytes, 30kHz

Figure A.1-9: Calibration results for URLLC, 10bytes, 60kHz

10) URLLC 75 bytes, 30kHz, 1T4R

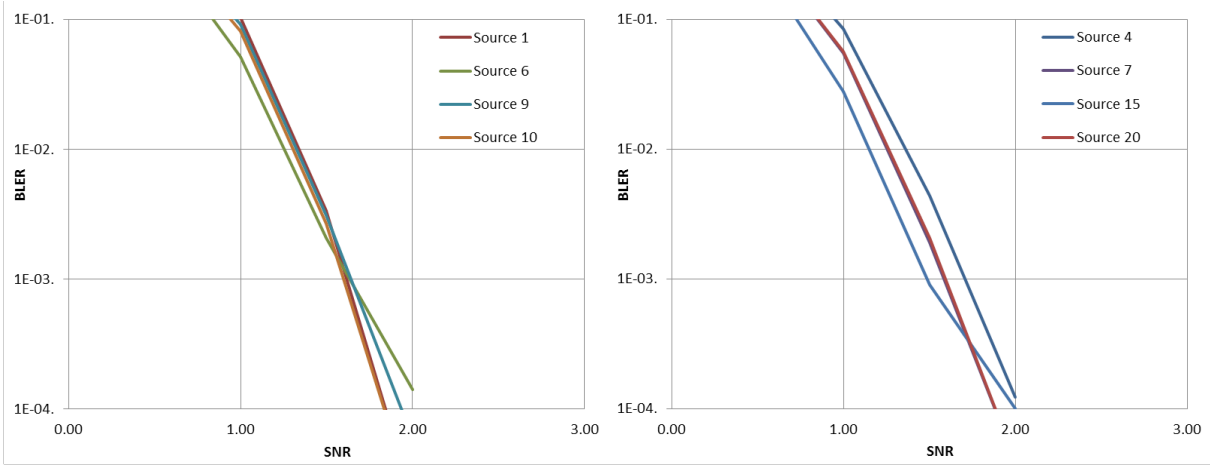

(a) min_sum, AWGN, 75 bytes, 30kHz (b) log_BP, AWGN, 75 bytes, 30kHz

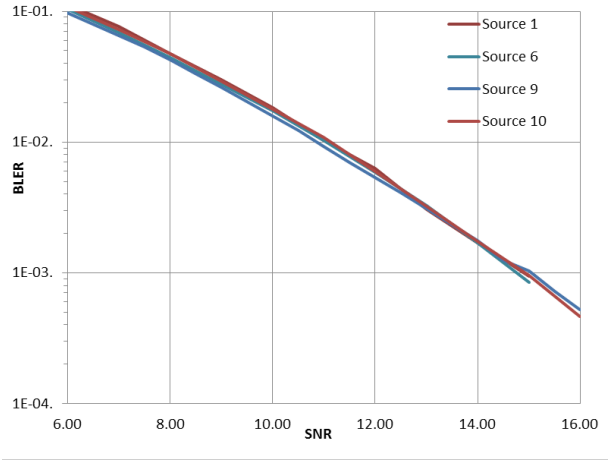

(c) min_sum, TDL-A, 75 bytes, 30kHz

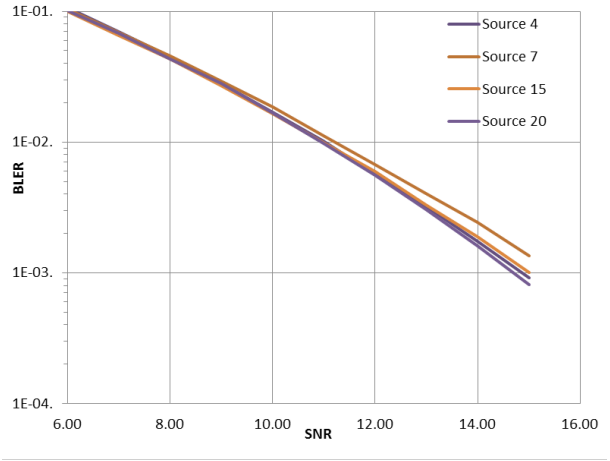

(d) log_BP, TDL-A, 75 bytes, 30kHz

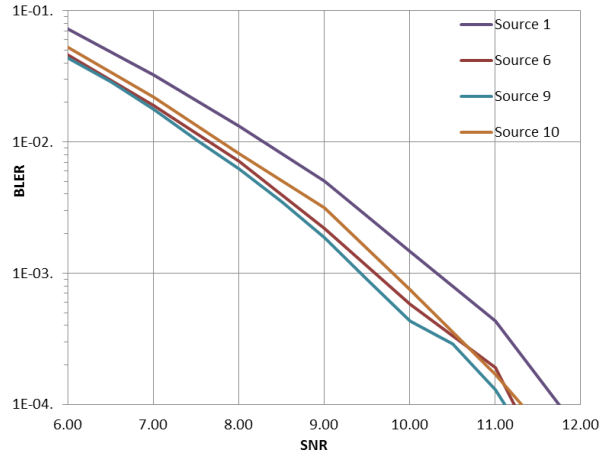

(e) min_sum, TDL-C, 75 bytes, 30kHz

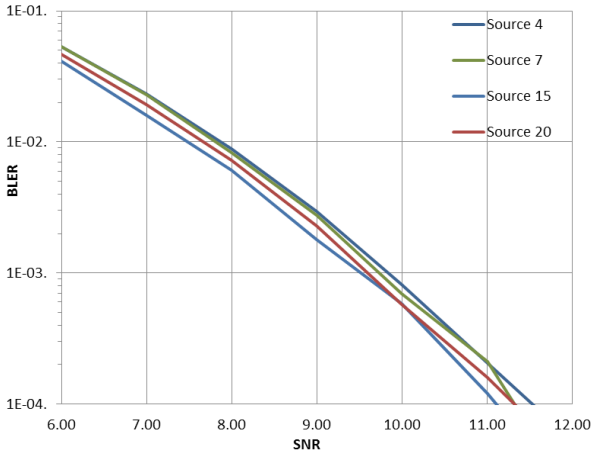

(f) log_BP, TDL-C, 75 bytes, 30kHz

Figure A.1-10: Calibration results for URLLC, 75bytes, 30kHz

A.2 Link-to-system modelling

Link-to-system modelling, also known as PHY abstraction, should reflect the key signal processing at the receiver, such as detection, channel decoding, channel estimation, etc. For NOMA study, multi-user link level simulations are needed to verify the validity of the PHY abstraction. The link-to-system modelling should also take into account of potential MA signature collision.

Alternatively, system-level evaluation can be based on using an embedded link-level receiver model. In such an approach, the system-level portion of the simulator generates the user traffic, corresponding channel model parameters, assigns users to cells, etc. The link level portion of the simulator is used for the explicit modeling of the actual packet transmission and reception for the generated interference environment.

A.2.1 Link-to-system mapping for MMSE-Hard IC receiver

1) Basic PHY abstraction method

PHY abstraction method for MMSE-Hard IC receiver is shown in Figure 2.1-1. The interference cancellation can be conducted successively (SIC), in parallel (PIC), or with hybrid process (HIC). The modeling adopts an iterative processing procedure and includes three steps, which are described as below.

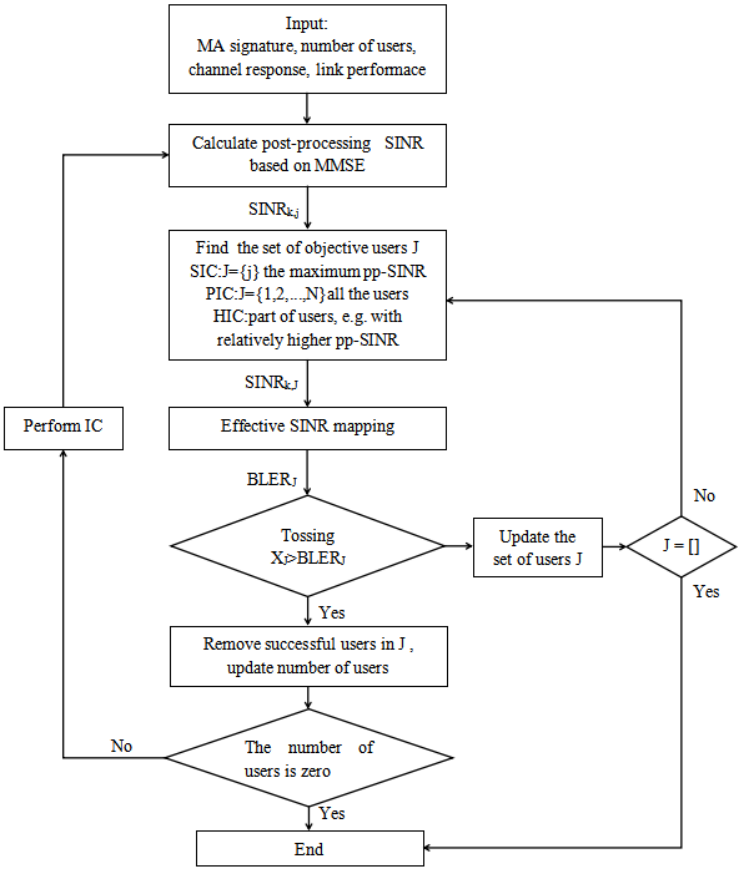

Figure A.2.1-1: PHY abstraction for MMSE-Hard IC receiver

Step 1: Calculation of post-processing (pp)-SINR

Assuming that N users share the same resource element group with the spreading factor of L, the received signal with R antenna ports can be written as

$$y_k = \sum_{i=1}^{N} \tilde{h}_{k,i} x_{k,i} + n_k \qquad \text{(A.2.1-1)}$$

where y_k with the size of $LR \times 1$ is the received symbol vector on the k^{th} resource element group, $x_k = [x_{1,k}, x_{2,k}, \cdots x_{N,k}]$ is a $N \times 1$ vector of transmitted symbols. $\tilde{h}_{k,i} = (\tilde{h}_{k,i,1}{}^T, \cdots, \tilde{h}_{k,i,r}{}^T, \cdots, \tilde{h}_{k,i,R}{}^T)^T$ denotes the effective channel of the i^{th} user, taking into account the transmitted power $P_{k,i}$, the channel response of each receive antenna $h_{k,i,r}$ and the $L*1$ spreading sequence s_i, as $\tilde{h}_{k,i,r} = \sqrt{P_{k,i}} h_{k,i,r} s_i$. n_k is the additive white Gaussian noise plus inter-cell interferences, with the power of σ^2 , and the covariance matrix of $R_{n_k n_k}$. For each of the i^{th} target user, the received signal in (A.2.1-1) can be rewritten as

$$y_k = \sum_{i=1}^{N} \tilde{h}_{k,i} x_{k,i} + n_k = \tilde{h}_{k,i} x_{k,i} + z_i \qquad \text{(A.2.1-2)}$$

where $z_i = \sum_{m=1, m \neq i}^{N} \tilde{h}_{k,m} x_{k,m} + n_k$ represents the noise plus intra-cell and inter-cell interferences experienced by the i^{th} user. The weight of linear MMSE receiver is then calculated as

$$w_i = R^{-1}\hat{h}_{k,i} = \left(\hat{h}_{k,i}\hat{h}_{k,i}^{*} + R_{z,i}\right)^{-1}\hat{h}_{k,i} \quad \text{(A.2.1-3)}$$

with the covariance of z_i

$$R_{z,i} = \sum_{m=1, m\neq i}^{N} \hat{h}_{k,m}\hat{h}_{k,m}^{*} + R_{n_k n_k} \quad \text{(A.2.1-4)}$$

where (.)* denotes Hermitian transpose and $R_{n_k n_k}$ is the covariance matrix of noise plus inter-cell interference. It should be noticed that the real estimated channel should be used in (A.2.1-3), as described in (A.2.1-7). The corresponding pp-SINR of the i^{th} user can be calculated as

$$SINR_{k,i} = \frac{\left|w_i^{*}\hat{h}_{k,i}\right|^2}{\sum_{j=1, j\neq i}^{N}\left|w_i^{*}\hat{h}_{k,j}\right|^2 + w_i^{*}R_{n_k n_k}w_i} \quad \text{(A.2.1-5)}$$

The j^{th} user's data with the highest averaged pp-SINR over K resource elements, i.e., $j = \underset{i}{\operatorname{argmax}}\left\{\frac{1}{K}\sum_{k=1}^{K} SINR_{k,i}\right\}$ will be treated in each loop of the MMSE-SIC receiver. Therefore, the analytical SINR mapping in SLS starts from the j^{th} user.

Step 2: Effective SINR mapping

As link level curves are normally generated assuming frequency flat channel at given SINR, an effective SINR, $SINR^{eff}$ is required to accurately map SINR at system level onto the link level curves to determine the BLER, when the actual channel at system level is frequency selective. Assuming that the j^{th} user has the highest pp-SINR. The effective SINR is calculated as

$$SINR_j^{eff} = \varphi^{-1}\left(\frac{1}{K}\sum_{k=1}^{K}\varphi\left(SINR_{k,j}\right)\right) \quad \text{(A.2.1-6)}$$

where K is the number of modulation symbols (or resource elements) in a code block, $\varphi(\cdot)$ is a non-linear invertible function that defines Received Bit Mutual Information Rate (RBIR). The block error rate value of the j^{th} user is determined by looking up the BLER vs. SNR tables for AWGN channel, with the input of the effective SINR.

Step 3: Interference cancellation

Since the BLER of the user with highest pp-SINR has been calculated, a random variable X~Uniform [0 1] is generated to decide whether the user's data is decoded correctly or not. If the user's data is considered as correctly decoded, then the interference cancellation procedure is performed.

2) Modeling for realistic channel estimation

In the case with realistic channel estimation, channel estimation error can be modelled for link-to-system mapping.

Channel estimation error, denoted as ΔH, is the difference between the realistic channel estimation (RCE) and the ideal channel estimation (ICE). It can be modelled as a Gaussian distributed random variable with the mean value of 0 and the variance as σ_e^2.

$$H_R = H + \Delta H \cdot |H| \quad \text{(A.2.1-7)}$$

$$\sigma_e^2 = \frac{1}{a \cdot N_s \cdot SNR} \quad \text{(A.2.1-8)}$$

In Eq. (A.2.1-7), SNR is the instantaneous received SNR (per RE DMRS power divided by per RE noise power plus DMRS contamination from other cell on the active transmission bandwidth of the UE) and can be time-varying in fading channels. N_s is the total number of DMRS samples used for estimating a channel coefficient, which is equal to 4

for the NR DMRS design. And *a* is a scaling factor that takes into account the effect of interpolation and smoothing for different channel coefficients, which can be tuned differently for different fading channel and channel estimation algorithms.

Figure A.2.1-2 shows the channel estimation error validation results in a single-user simulation case, for different channel conditions and DMRS types, where the solid curves show the statistics of collected normalized channel estimation error which is calculated is $\frac{|H_R - H|^2}{|H|^2}$. It can be observed that the variance predicted by the error model matches well the variance of the actual estimation.

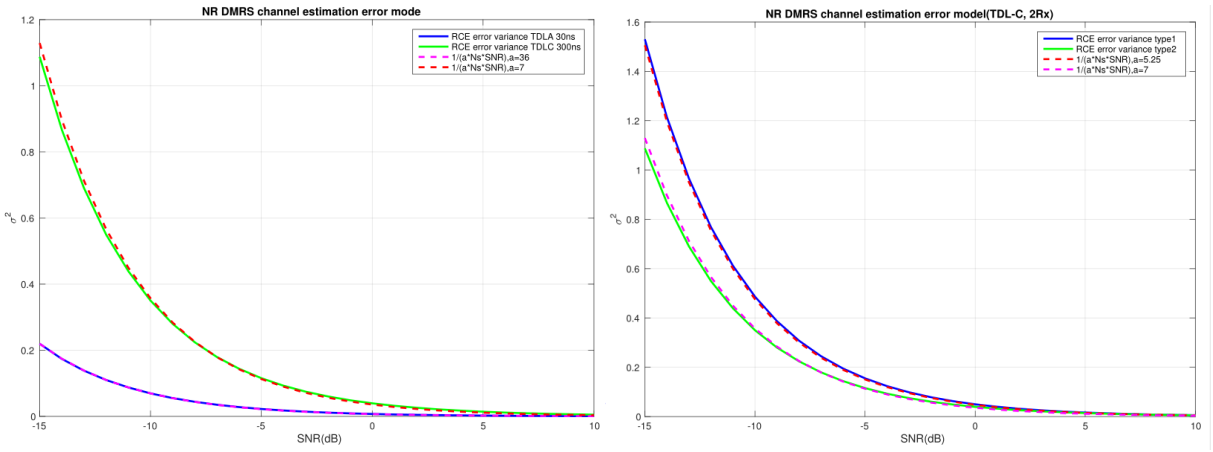

Figure A.2.1-2: Channel estimation error model (TDL-C 300ns)

So for PHY abstraction for realistic channel estimation, we can replace the channel $h_{k,i,r}$ by H_R in Eq. (A.2.1-7), where the channel estimation error is modelled based on Eq. (A.2.1-8). Then we can use H_R to calculate the weight of the linear MMSE receiver with Eq. (A.2.1-3). Finally the corresponding pp-SINR can be calculated based on Eq. (A.2.1-5), where ideal channel is still used for the target signal and the interfering signal.

The H_R should also be used in the interference cancellation(IC) procedure to model the non-perfect IC, which is described as follows assuming a receiver using codeword IC:

If the j^{th} user's data is correctly decoded, channel estimation error of jth user $\Delta H_j = H_{R,j} - H_{I,j}$ is used as residual interference, where $H_{R,j}$ and $H_{I,j}$ refers the modelled realistic channel estimation and the ideal channel estimation value of jth user, respectively, and ΔH_j is modelled based on Eq. (A.2.1-8).

3) Validation results

In Figure 2.1-4, BLER performances of DMRS-based realistic channel estimation (RCE) are compared with the BLERs of above PHY abstraction with fixed MA signature allocation. The results indicate that the proposed PHY abstraction can closely match the performance of actual MMSE-SIC receiver with realistic channel estimation. For the number of UE larger than 12, larger FDM comb is applied for DMRS extension.

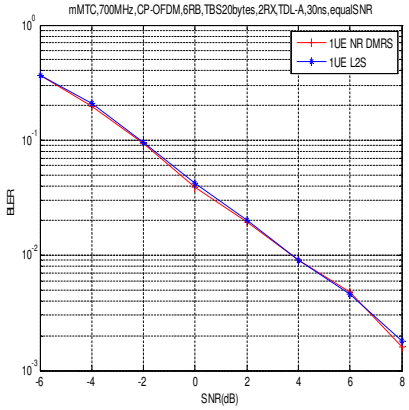

(a) 1 UE, TDL-A 30ns, mMTC, equal SNR

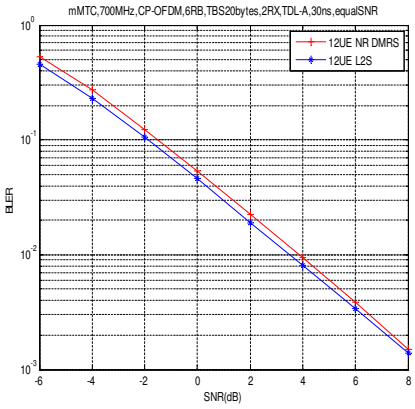

(b) 12 UEs, TDL-A 30ns, mMTC, equal SNR

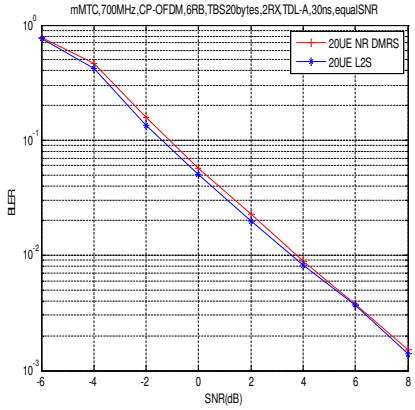

(c) 20 UEs, TDL-A 30ns, mMTC, equal SNR

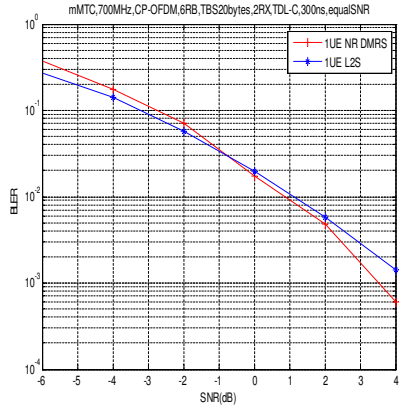

(d) 1 UE, TDL-C 300ns, mMTC, equal SNR

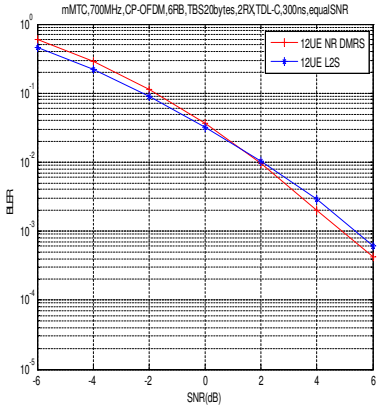

(e) 12 UEs, TDL-C 300ns, mMTC, equal SNR

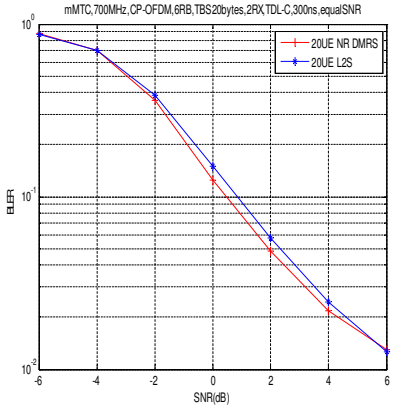

(f) 20 UEs, TDL-C 300ns, mMTC, equal SNR

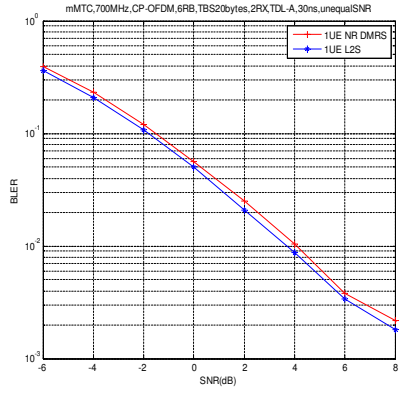

(g) mMTC, 1 UE, TDL-A 30ns, unequal SNR, uniform [-3, 3]

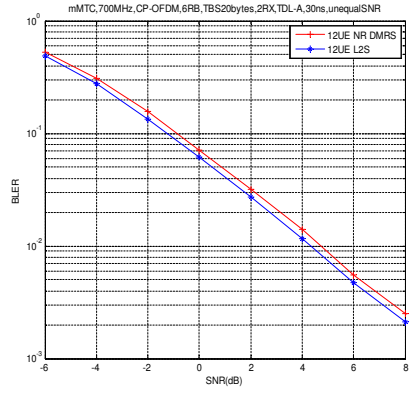

(h) mMTC, 12 UE, TDL-A 30ns, unequal SNR, uniform [-3, 3]

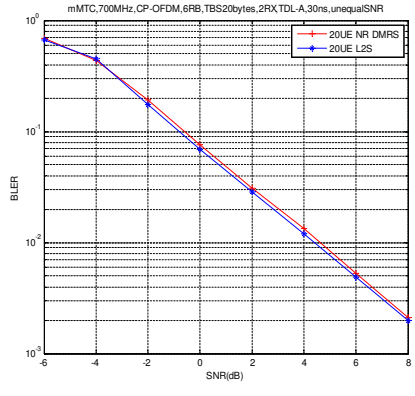

(i) mMTC, 20 UE, TDL-A 30ns, unequal SNR, uniform [-3, 3]

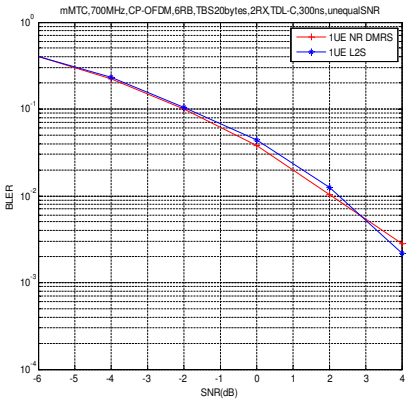

(j) mMTC, 1 UE, TDL-C 300ns, unequal SNR, uniform [-3, 3]

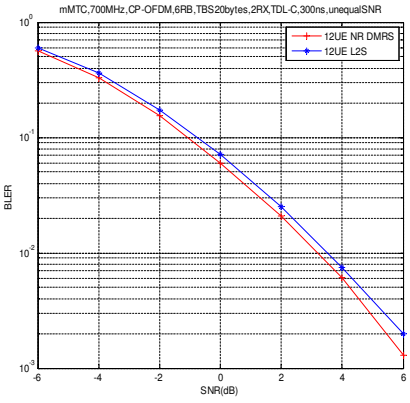

(k) mMTC, 12 UE, TDL-C 300ns, unequal SNR, uniform [-3, 3]

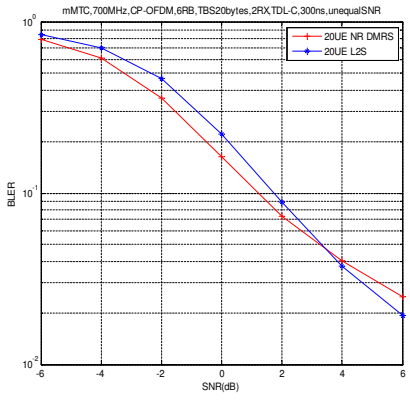

(l) mMTC, 20 UE, TDL-C 300ns, unequal SNR, uniform [-3, 3]

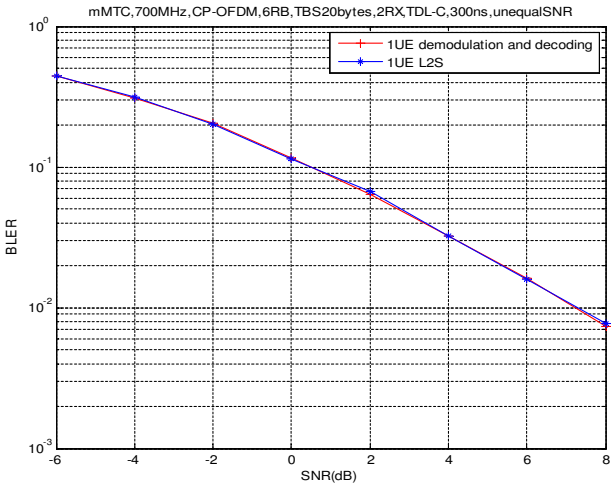

(m) mMTC, 1 UE, TDL-C 300ns, unequal SNR, Gaussian distribution, $\sigma = 5dB$

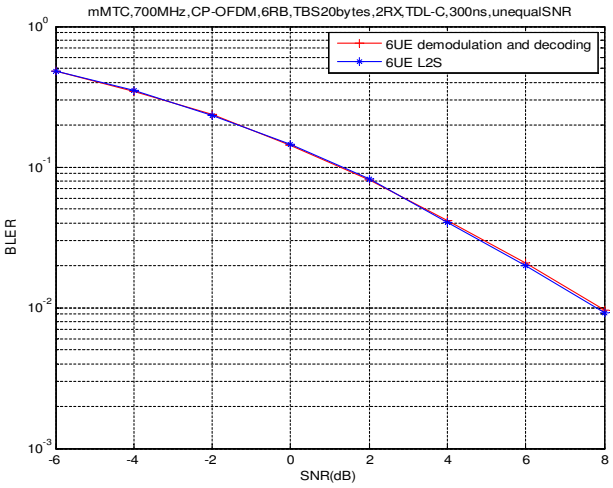

(n) mMTC, 6 UE, TDL-C 300ns, unequal SNR, Gaussian distribution, $\sigma = 5dB$

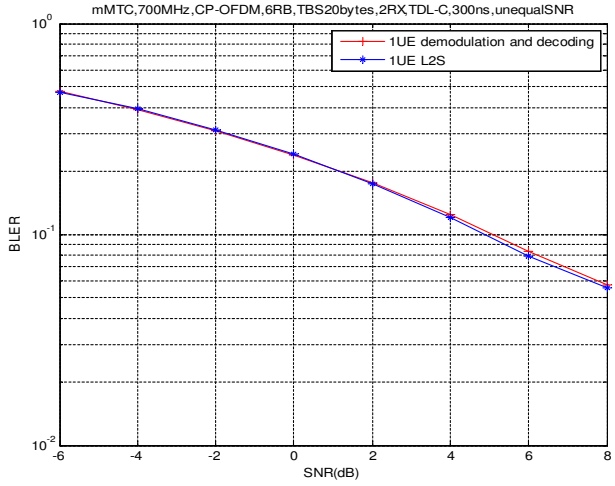

(o) mMTC, 1 UE, TDL-C 300ns, unequal SNR, Gaussian distribution, $\sigma = 9dB$

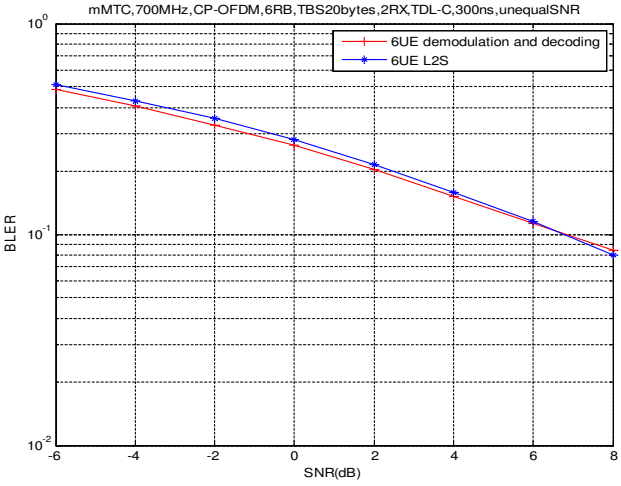

(p) mMTC, 6 UE, TDL-C 300ns, unequal SNR, Gaussian distribution, $\sigma = 9dB$

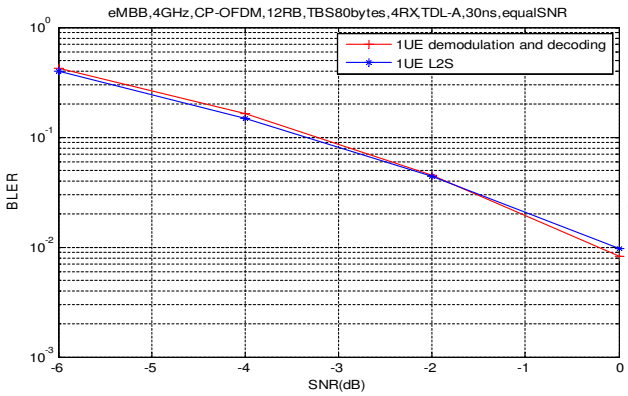

(q) eMBB, 1 UE, TDL-A 30ns, equal SNR

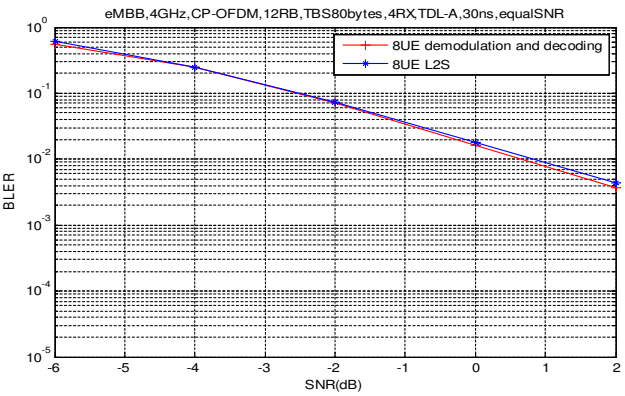

(r) eMBB, 8 UE, TDL-A 30ns, equal SNR

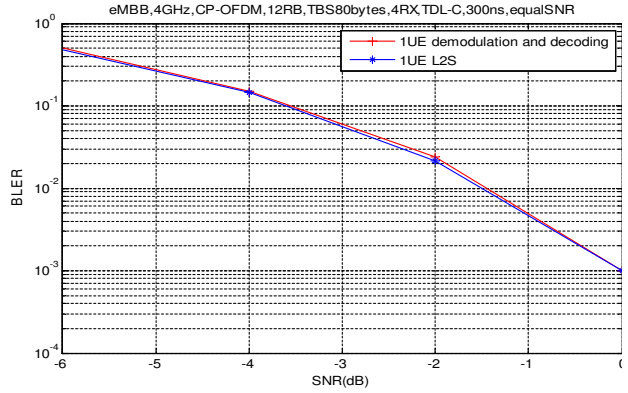

(s) eMBB, 1 UE, TDL-C 300ns, equal SNR

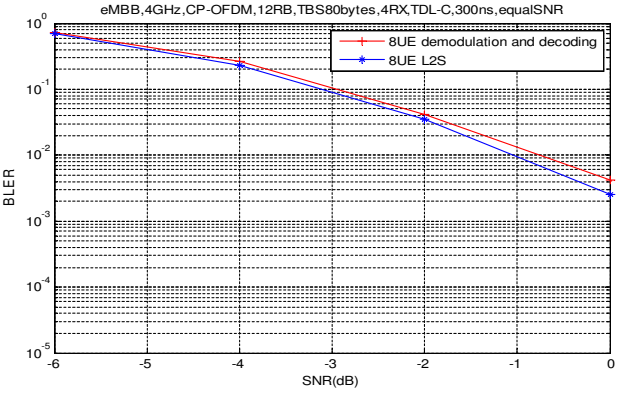

(t) eMBB, 8 UE, TDL-C 300ns, equal SNR

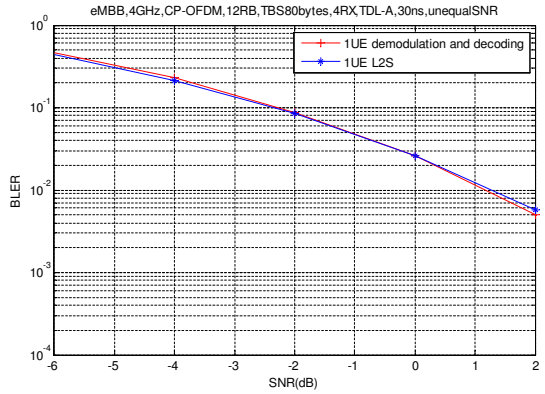

(u) eMBB, 1 UE, TDL-A 30ns, unequal SNR, uniform [-3, 3]

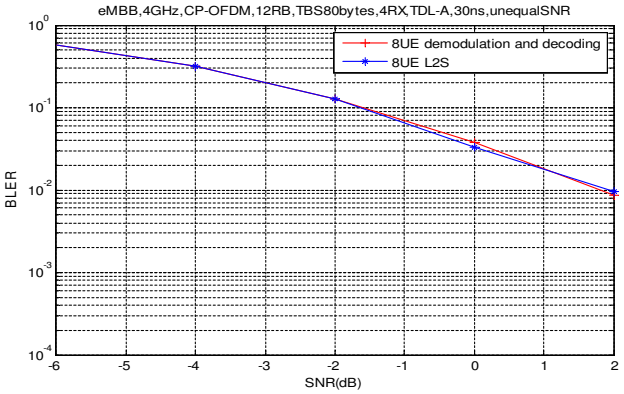

(v) eMBB, 8 UE, TDL-A 30ns, unequal SNR, uniform [-3, 3]

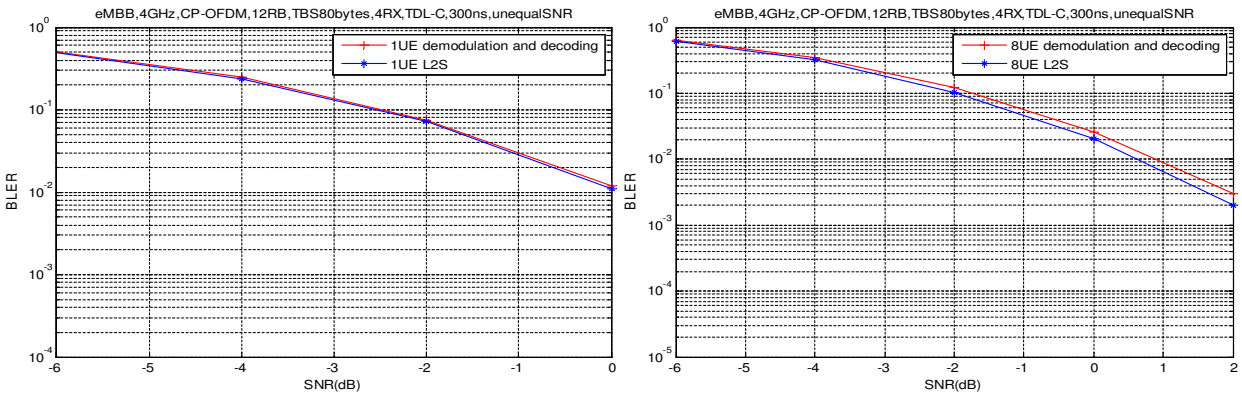

(w) eMBB, 1 UE, TDL-C 300ns, unequal SNR, uniform [-3, 3]

(x) eMBB, 8 UE, TDL-C 300ns, unequal SNR, uniform [-3, 3]

Figure A.2.1-4: BLER of realistic channel estimation (RCE) vs BLER of PHY abstraction for MMSE-SIC receiver

A.2.2 Link-to-system mapping for ESE-SISO receiver

1) PHY abstraction method

The effective SNR mapping (ESM) PHY abstraction is used in SLS. Generally, for ESM, the effective SNR is calculated as

$$SNR_{eff} = f^{-1}\left(\frac{1}{N}\sum_{n=0}^{N-1} f\left(\sin R_n\right)\right) \quad \text{(A.2.2-1)}$$

where N is the symbol block size, $\sin R_n$ is the SINR for the *n*-th sub-carrier, SNR_{eff} is the effective SNR for the entire block and function $f(\cdot)$ is an invertible function. Based on this effective SNR, the corresponding BLER can be obtained based on SNR-BLER mapping table under AWGN channel for specific MCS.

To facilitate the PHY abstraction and avoid receiver modeling, an approximation approach is applied and is summarized as follows:

Step 1: Calculate the upper bound post-processing SINR.

For non-orthogonal multiple access, the optimal performance can be achieved if the signals from multiple UEs can be separated completely. In this sense, the post-processing SINR of PIC detector is regarded as upper bound. If per-RE power of transmitted signal is normalized to 1, the post-processing SINR after PIC detection for the *n*-th sub-carrier of the *k*-th UE is expressed as

$$SINR_{k,n}^{PIC} = \frac{\left|h_{k,n}\right|^2}{\sigma^2 + I_n} \quad \text{(A.2.2-2)}$$

where $h_{k,n}$ denotes the frequency domain channel coefficient vector of the *n*-th sub-carrier of the *k*-th UE, σ^2 denotes the noise power and I_n denotes the power of inter-cell interference on the *n*-th sub-carrier.

Step 2: Approximate the real post-processing SINR based the upper bound.

Although by using advanced receiver, such as chip-by-chip MAP detector, multi-user interference can be mitigated or even eliminated, there still will be some performance degradation, especially when the number of serviced UEs is large. A scaling factor β is used to emulate this performance degradation. Denote $C_{PIC}^{k,n} = \log_2\left(1 + SINR_{k,n}^{PIC}\right)$ as the capacity for PIC detector and for non-orthogonal multiple access, the achievable capacity is a scaled version which is expressed as follows

$$C_{NoMA}^{k,n} = \log_2(1+\sin R_{k,n}) = \beta C_{PIC}^{k,n} \quad \text{(A.2.2-3)}$$

where $\sin R_{k,n}$ denotes the approximated SINR for *n*-th sub-carrier of the *k*-th UE and based on this scaled capacity, $\sin R_{k,n}$ can be calculated as

$$\sin R_{k,n} = \left(1+SINR_{k,n}^{PIC}\right)^{\beta} - 1 \quad \text{(A.2.2-4)}$$

The parameter β can describe the capacity loss due to the superposition of multiple UEs and should be optimized by off-line link level simulations for different number of UEs under different cases.

Step 3: Calculate the effective SNR.

The approximated SINR for *n*-th sub-carrier of the *k*-th UE obtained in step 2 is used for the mapping of effective SNR. Several methods can be applied and the received-bit information rate (RBIR) for SNR mapping is used due to its simplicity. The effective SNR is expressed as

$$SNR_{eff,k} = RBI\,R^{-1}\left(\frac{1}{N}\sum_{n} RBIR\left(\sin R_{k,n}, Q\right)\right) \quad \text{(A.2.2-5)}$$

where $SNR_{eff,k}$ denotes the effective SNR for the *k*-th UE and *Q* denotes the modulation order. The function $RBIR(SNR, Q)$ denotes the RBIR metric given *SNR* and modulation order *Q* and $RBI\,R^{-1}(\cdot)$ is its inverse function given RBIR metric to find corresponding SNR. The RBIR metric function is pre-calculated off-line and stored as a look-up table.

Step 4: Obtain BLER according to the SNR-BLER mapping.

After getting the effective SNR for the *k*-th UE, the corresponding BLER is obtained according to the SNR-BLER mapping relationship which is pre-calculated for given MCS under AWGN channel.

The only parameter that should be optimized is the scaling factor β and the optimization can be completed by solving a minimum mean square error problem.

2) Validation results

In Fig. A.2.2-1, the performance comparison between the L2S mapping and LLS evaluation under ideal channel estimation. mMTC scenario with TDL-C channel is considered. TBS is set as 40 bytes. As can be observed from Fig. A.2.2-1, by chosing appropriate β value, the performance obtained by L2S mapping method described above is quite aligned with evaluation results, especially for high SNR region.

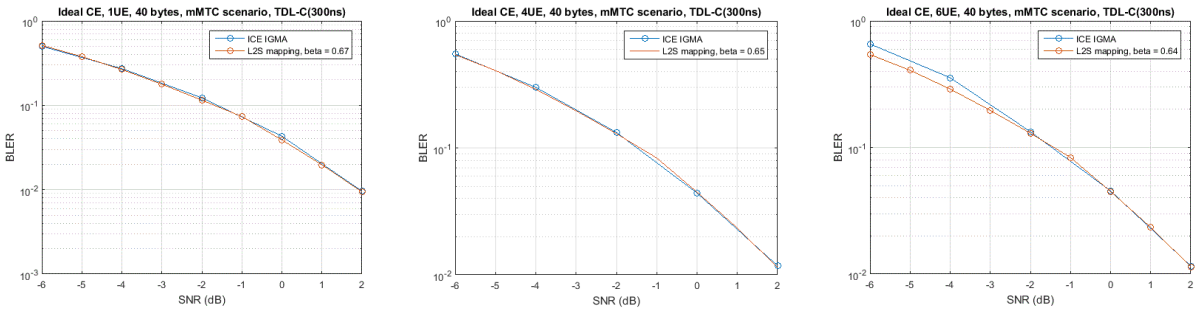

(a) 1 UE (b) 4 UEs (c) 6 UEs

Figure A.2.2-1: BLER based on L2S mapping vs evaluated BLER, mMTC scenario, CP-OFDM, ICE, 6 RBs, TBS = 40 bytes, TDL-C 300 ns

Fig. A.2.2-2 shows the performance comparison between L2S mapping and LLS results for realistic channel estimation. Similary with Fig. A.2.2-1, mMTC scenario with TDL-C channel is considered and TBS is set as 40 bytes. For channel estimation, LMMSE is applied. We can observe that even with larger number of UEs, the L2S mapping can still match the LLS results with realistic channel estimation, if proper β value is selected.

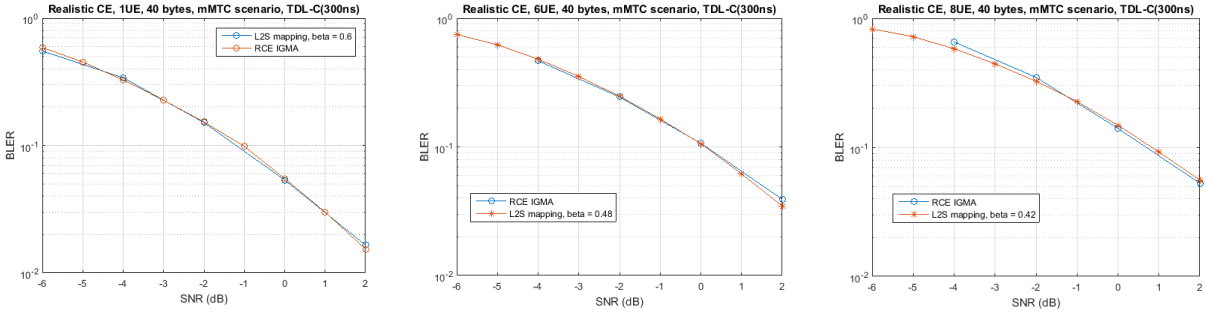

(a) 1 UE (b) 6 UEs (c) 8 UEs

Figure A.2.2-2: BLER based on L2S mapping vs evaluated BLER, mMTC scenario, CP-OFDM, RCE, 6 RBs, TBS = 40 bytes, TDL-C 300 ns

A.2.3 Link-to-system mapping for EPA-hybrid IC and MMSE-Hard IC receiver

1) PHY abstraction method

Step 1: Calculation of post-processing (pp)-SINR

Let N_r denote the receiver antenna number and S_n be the signature of the n^{th} user. The UL transmission model with *N* non-orthogonal users of the k^{th} RE group (each group contains N_F REs, where N_F is the spreading factor, i.e. for spreading-based NOMA transmission schemes, $N_F>1$; for other NOMA transmission schemes, $N_F=1$) is as below:

$$y_k=\sum_{n=1}^{N}\hat{h}_{k,n}x_{k,n}+w_k=H_k x_k+w_k, \qquad \text{(A.2.3-1)}$$

where y_k is a $N_F N_r\times 1$ received symbol vector and x_k is a $N\times 1$ vector of transmitted symbols. $\hat{h}_{k,n}$ denotes the effect channel of the n^{th} user, taking into account both channel realizations and MA signatures such that $\hat{h}_{k,n}=\left(\hat{h}_{k,n,1}^T,\cdots,\hat{h}_{k,n,N_r}^T\right)^T$, where $\hat{h}_{k,n,r}=¿\quad h_{k,n,r}\odot S_n\wedge\odot$ denotes the component-wise multiplication, and therefore $H_k=[\hat{h}_{k,1},\cdots,\hat{h}_{k,N}]$. w_k represents the AWGN noise plus inter-cell interference vector with covariance matrix $R_{k,ww}$.

The post-processing pp-SINR of the k^{th} RE group with perfect interference cancellation (PIC) bound for the n^{th} user/data layer is as follows

$$\gamma_{k,n}^{PIC}=\hat{h}_{k,n}^H R_{k,ww}^{-1}\hat{h}_{k,n} \qquad \text{(A.2.3-2)}$$

Step 2: Effective SINR mapping

The effective SNR can be obtained by using the pp-SINRs and the curve fitting parameter α and β , as following

$$\gamma_n^{eff}=f^{-1}\left(\frac{1}{K}\sum_{k=1}^{K}f\left(\left(\beta\gamma_{k,n}^{PIC}\right)^{\alpha}\right)\right) \qquad \text{(A.2.3-3)}$$

where f(•) is the model specific function, which can be e.g. Shannon capacity formula, Received bit mutual information rate (RBIR), etc., and f^{-1}(•) is its inverse. The curve fitting parameters $\alpha=10^{\delta}$ represents the slope bias between

multi-user and single-user performance, while β represents the SNR loss from the multi-user to single-user performance. Generally, when the multiplexed UE number is not very large, only the fitting parameter β is required, i.e. $\alpha=1$. The effective SNR mapping formula in this case can be rewritten as below, which is the one as agreed and captured in TR 38.802

$$\gamma_n^{eff}=f^{-1}\left(\frac{1}{K}\sum_{k=1}^{K}f\left(\beta\gamma_{k,n}^{PIC}\right)\right) \quad \text{(A.2.3-4)}$$

The fitting parameter(s) α_{opt} and β_{opt} should be chosen to minimize the mean square errors (MSE) between the BLERs derived from real multi-user UL LLS evaluation and the ones from the PHY abstraction prediction, under given number of active users and given MCSs.

Step 3: Lookup AWGN table

Get the BLER value by looking up the SISO AWGN link performance table with the derived effective SINR value in step 2 as the input.

2) Validation results

Equal SNR

The BLER performance comparisons between real UL LLS evaluation based on realistic channel estimation and the BLER based on the described PHY abstraction method are shown in Figures A.2.3-1 to A.2.3-9 for different NOMA schemes, TB size and active users. The best fitting parameters δ_{opt} , β_{opt} , and the corresponding MSE are given in Tables A.2.3-1,2,3.

It should be noted that, the best fitting parameter(s) δ_{opt} and β_{opt} given in Tables A.2.3-1,2,3 may vary with each company's simulation platform. Therefore, each company may optimize the fitting parameters δ_{opt} and β_{opt} based on their own implementation of the simulation platform.

In addition, it is noted that realistic channel estimation error has already been considered in the PHY abstraction since the real LLS with realistic channel estimation is used. Therefore, channel estimation error does not need to be remodeled in SLS.

Table A.2.3-1: TB size-20 Bytes

	UE number	2	4	6	8	10	12	14	16	18
SCMA	δ	0	0	0	0	0	0	0.5	0.5	0.5
	β	0.82	0.8	0.74	0.72	0.66	0.6	0.56	0.52	0.46
	MSE	0.0007	0.0001	0.0001	0.001	0.002	0.0057	0.002	0.0047	0.005
MUSA	δ	0	0	0	0	0	0	0.5	0.5	0.5
	β	0.84	0.8	0.76	0.72	0.68	0.62	0.58	0.51	0.44
	MSE	0.0007	0.0001	0.0001	0.001	0.002	0.0057	0.002	0.0047	0.01
LCRS	δ	0	0	0	0	0	0	0.5	0.5	0.5
	β	0.86	0.82	0.76	0.72	0.68	0.62	0.58	0.5	0.43
	MSE	0.0007	0.0001	0.0001	0.001	0.002	0.0057	0.002	0.0047	0.01

Table A.2.3-2: TB size-40 Bytes

	UE number	2	4	6	8	10
SCMA	δ	0	0	0	0	0.5
	β	0.86	0.78	0.72	0.62	0.34
	MSE	0.0004	0.0001	0.0019	0.007	0.0045
MUSA	δ	0	0	0	0.5	0.5
	β	0.86	0.78	0.72	0.42	0.3
	MSE	0.0002	0.0014	0.0038	0.009	0.0038
LCRS	δ	0	0	0	0.5	0.5
	β	0.86	0.8	0.74	0.4	0.26
	MSE	0.0001	0.0007	0.0043	0.008	0.0022

Table A.2.3-3 TB: size-60 Bytes

	UE number	2	4	6
SCMA	δ	0	0	0.25
	β	0.86	0.76	0.38
	MSE	0.0004	0.0038	0.0065
MUSA	δ	0	0	0.25
	β	0.82	0.7	0.32
	MSE	0.0005	0.001	0.002
LCRS	δ	0	0	0.25
	β	0.86	0.76	0.38
	MSE	0.0003	0.0031	0.006

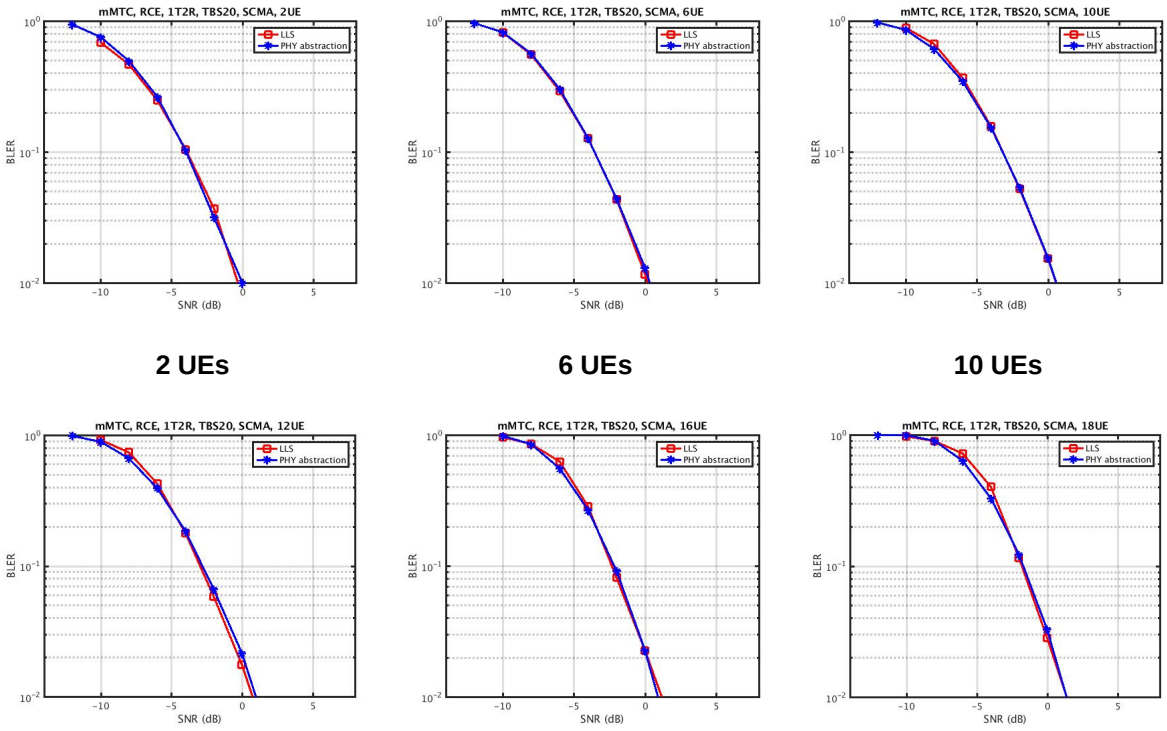

2 UEs **6 UEs** **10 UEs**

12 UEs **16 UEs** **18 UEs**

Figure A.2.3-1: TB size=20 Bytes, SCMA, EPA- hybrid IC receiver

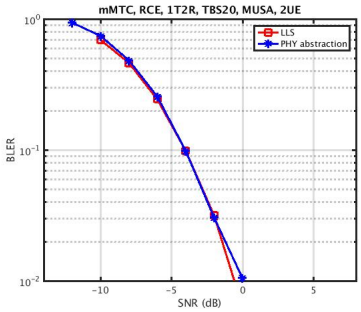

2 UEs

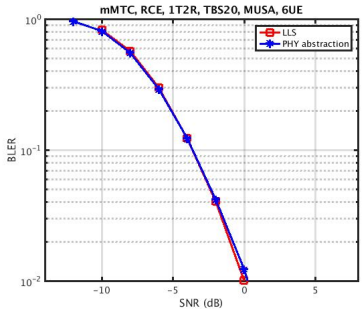

6 UEs

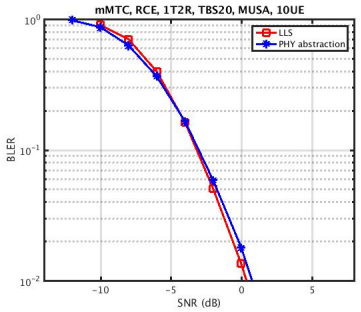

10 UEs

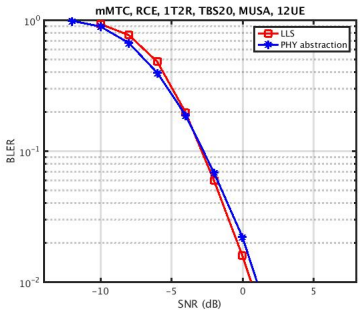

12 UEs

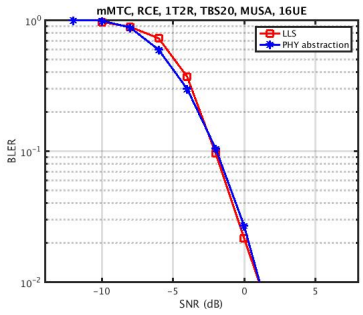

16 UEs

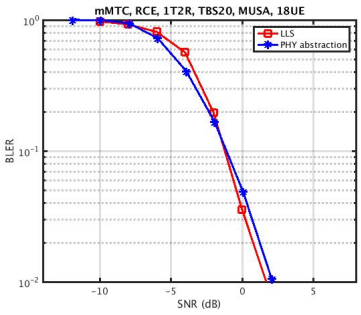

18 UEs

Figure A.2.3-2: TB size=20 Bytes, MUSA, MMSE-Hard IC receiver

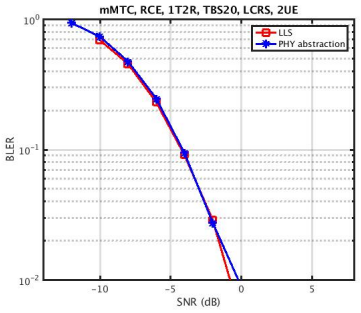

2 UE

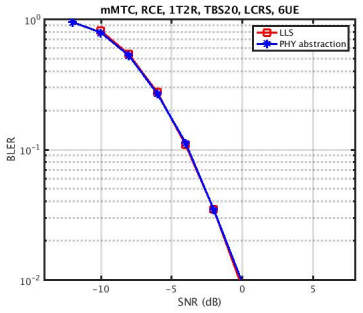

6 UEs

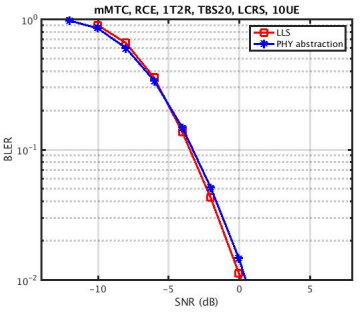

10 UEs

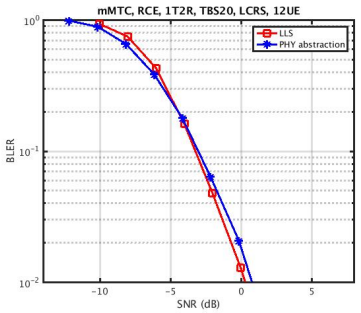

12 UEs

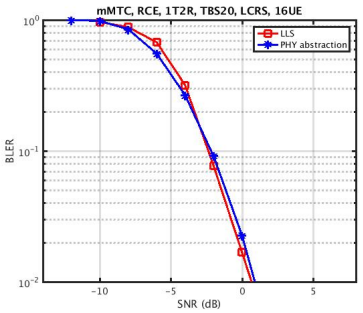

16 UEs

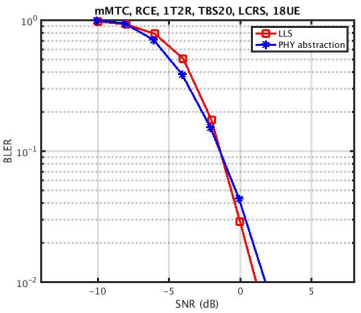

18 UEs

Figure A.2.3-3: TB size=20 Bytes, LCRS, EPA- hybrid IC receiver

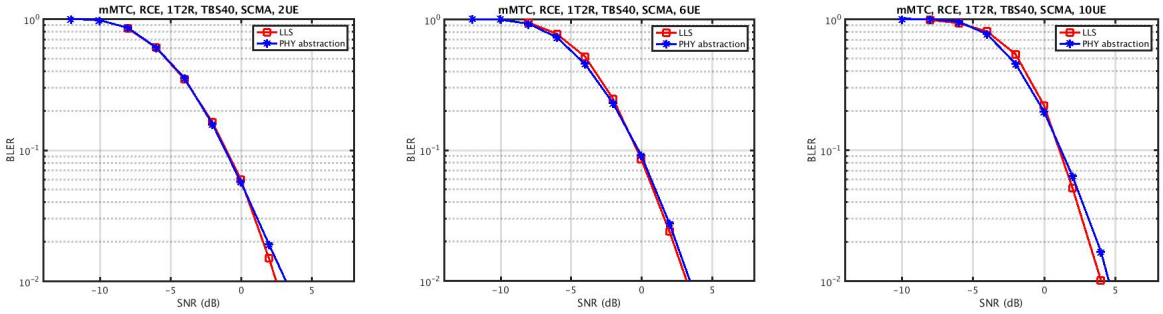

2 UEs **6 UEs** **10 UEs**

Figure A.2.3-4: TB size=40 Bytes, SCMA, EPA- hybrid IC receiver

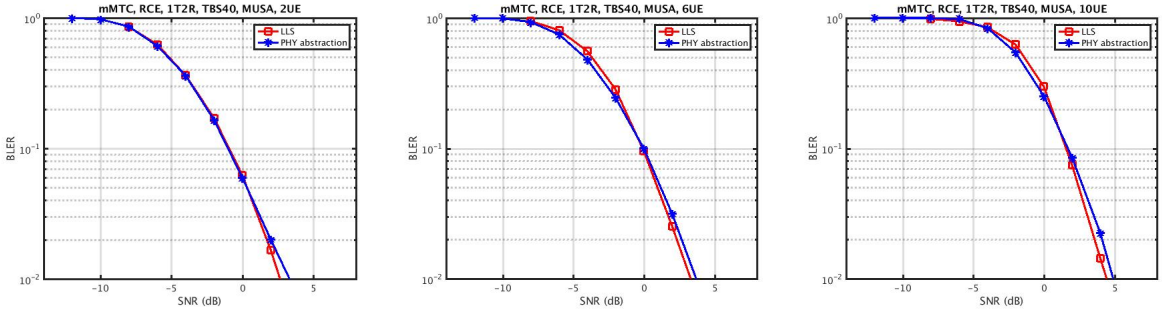

2UEs **6 UEs** **10 UEs**

Figure A.2.3-5: TB size=40 Bytes, MUSA, MMSE-Hard IC receiver

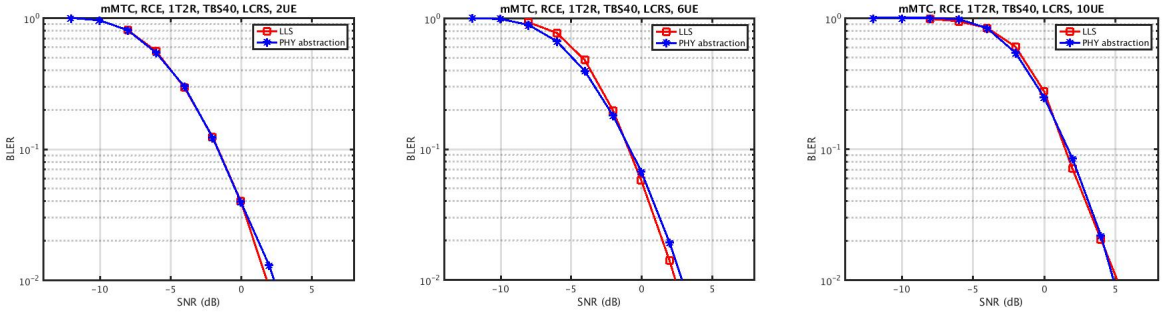

2 UEs **6 UEs** **10 UEs**

Figure A.2.3-6: TB size=40 Bytes, LCRS, EPA- hybrid IC receiver

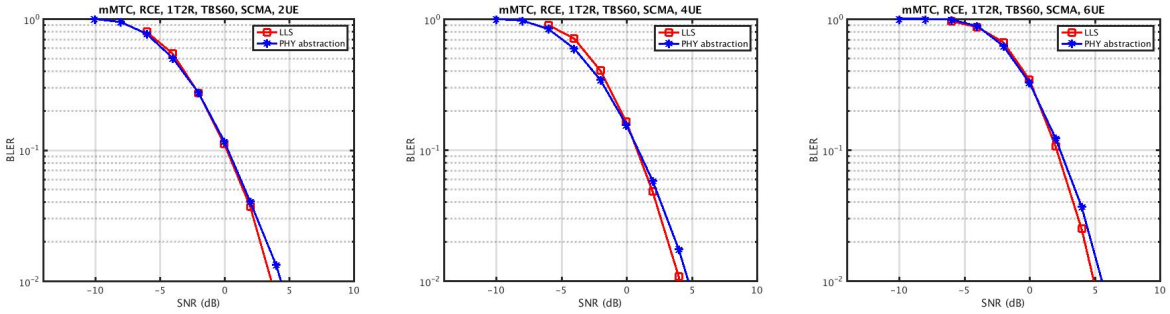

2 UEs **4 UEs** **6 UEs**

Figure A.2.3-7: TB size=60 Bytes, SCMA, EPA- hybrid IC receiver

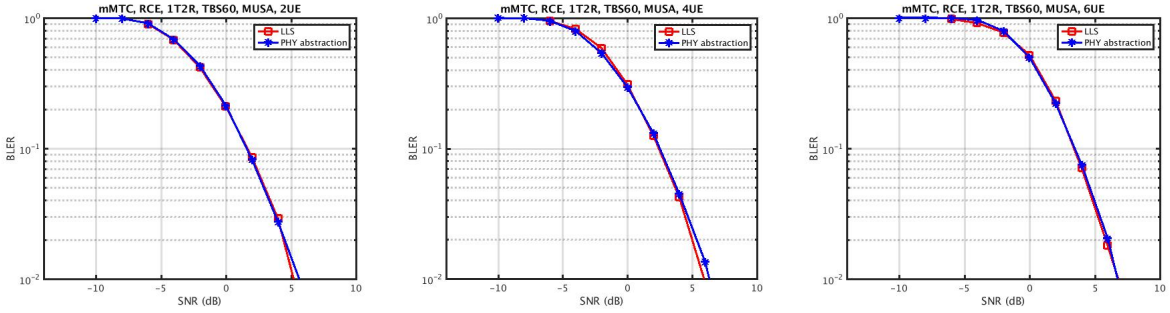

2 UEs **4 UEs** **6 UEs**

Figure A.2.3-8: TB size=60 Bytes, MUSA, MMSE-Hard IC receiver

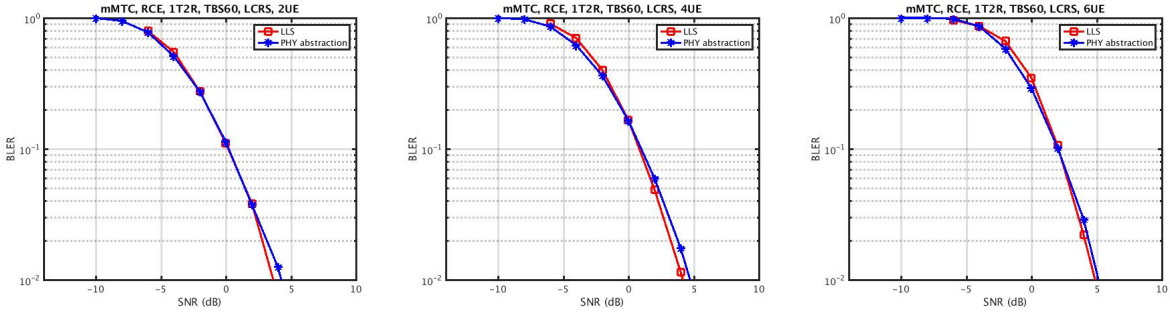

2 UEs **4 UEs** **6 UEs**

Figure A.2.3-9: TB size=60 Bytes, LCRS, EPA- hybrid IC receiver

Unequal SNR

With unequal SNR of different SNR variations, the BLER performance comparisons between real UL LLS evaluation with realistic channel estimation and the BLER obtained from the described PHY abstraction method for different TBSs are shown in Figure A.2.3-10, Figure A.2.3-11 and Figure A.2.3-12 respectively.

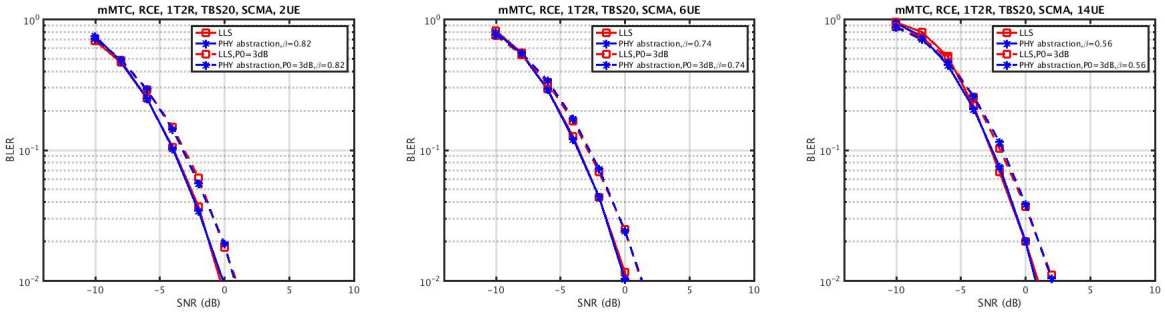

2UE **6UE** **14UE**

Figure A.2.3-10: TB size=20 Bytes, SCMA

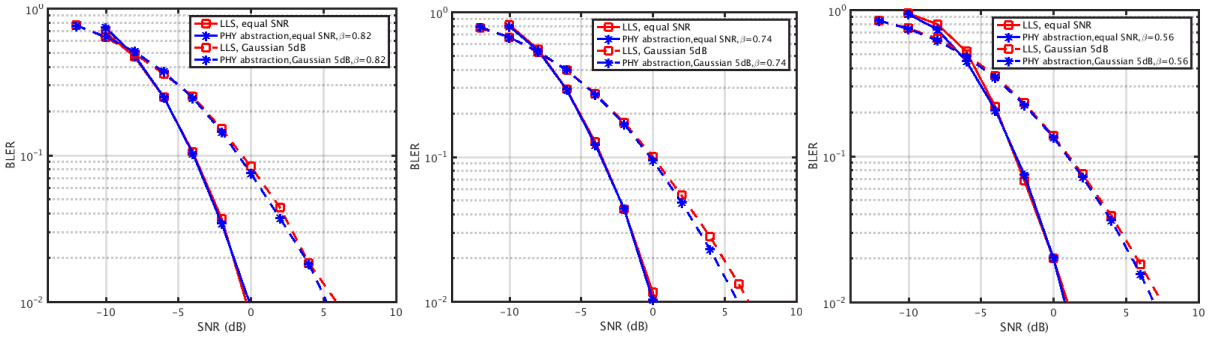

2UE **6UE** **14UE**

Figure A.2.3-11: TB size=20 Bytes, SCMA, Gaussian, 5dB

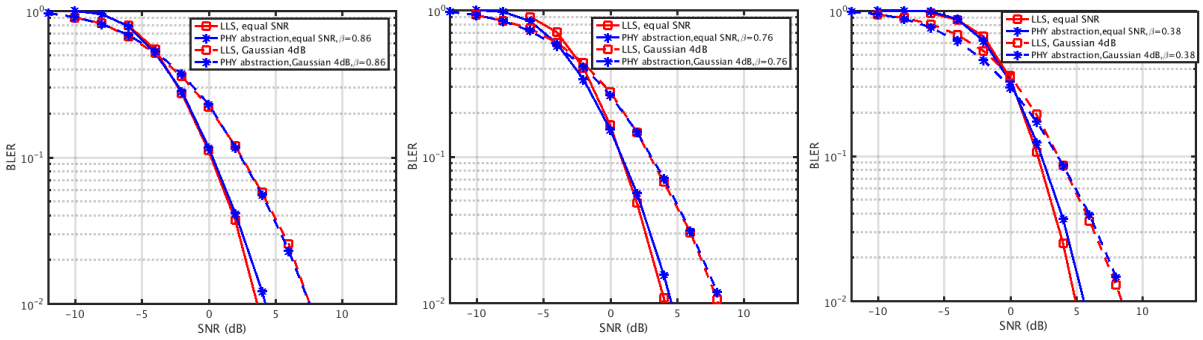

2UE **4UE** **6UE**

Figure A.2.3-12: TB size=60 Bytes, SCMA, Gaussian, 4dB

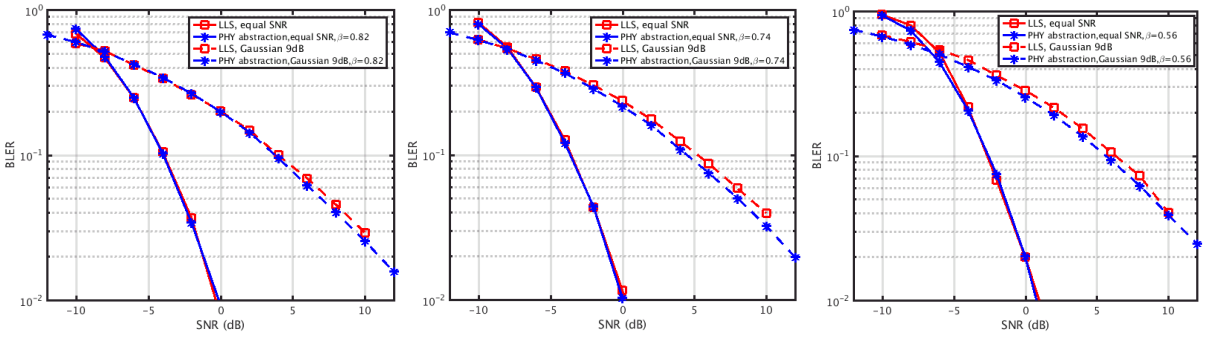

2UE **6UE** **14UE**

Figure A.2.3-13: TB size=20 Bytes, SCMA, Gaussian, 9dB

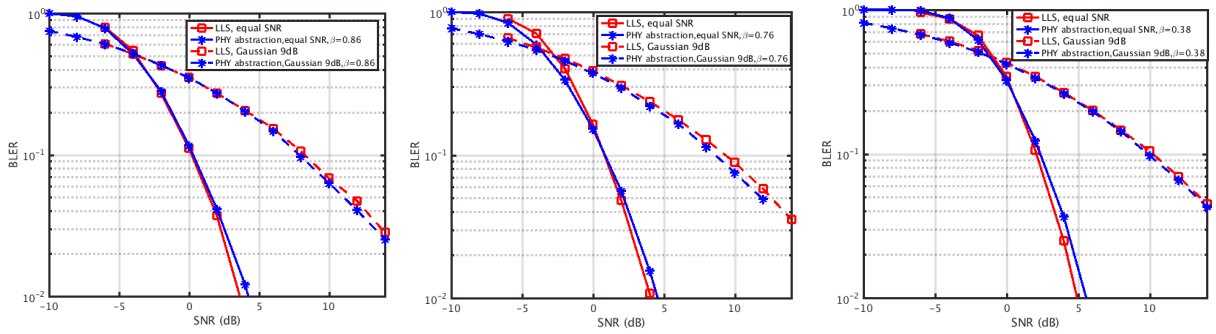

2UE **4UE** **6UE**

Figure A.2.3-14: TB size=60 Bytes, SCMA, Gaussian, 9dB

A.3 System level simulation assumptions

A.3.1 Simulation assumptions for system level evaluations.

Table A.3-1: System-level evaluation assumptions

Parameters	mMTC	URLLC	eMBB	Further specified values
Layout	Single layer - Macro layer: Hex. Grid			
Inter-BS distance	1732m	200m for 4GHz or 500m for 700MHz	200m	
Carrier frequency	700MHz	4GHz or 700MHz	4GHz	
Simulation bandwidth	6 PRBs as starting point	12 PRBs	12 PRBs	Bandwidth for uplink transmission FFS whether or not to introduce system bandwidth in SLS
Number of UEs per cell	Companies report			
Channel model	UMa in TR 38.901 The building penetration model defined in Table 7.4.3-3 in TR 38.901 is used for SLS with frequencies below 6 GHz.			
UE Tx power	Max 23 dBm			

BS antenna configurations	2 Rx or 4 Rx for 700MHz; 2 ports: (M, N, P, Mg, Ng) = (10, 1, 2, 1, 1), 2 TXRU; 4 ports: (M, N, P, Mg, Ng) = (10, 2, 2, 1, 1), 4 TXRU; dH = dV = 0.5λ; BS antenna downtilt: companies to report, FFS a single value 4 Rx or 16 Rx for 4GHz; 4 ports: (M, N, P, Mg, Ng) = (10, 2, 2, 1, 1), 4 TXRU; 16 ports: (M, N, P, Mg, Ng) = (10, 8, 2, 1, 1), 16 TXRU; dH = 0.5λ, dV = 0.8λ; BS antenna downtilt: companies to report, FFS a single value	
BS antenna height	25m	
BS antenna element gain + connector loss	8 dBi, including 3dB cable loss	
BS receiver noise figure	5dB	
UE antenna configuration	1Tx as starting point	
UE antenna height	Follow the modelling of TR 38.901	
UE antenna gain	0dBi as starting point	
UE distribution	For mMTC: 20% of users are outdoors (3km/h), 80% of users are indoor (3km/h); Users dropped uniformly in entire cell Companies are encouraged to check whether the percentage of UEs whose CL > 144 dB is significant (e.g., 5%) and the CDF of the CL. Further discuss the percentage of outdoor UEs, to be finalized in May meeting. For URLLC with 4GHz and 200m ISD 20% of users are outdoors (3km/h), 80% of users are indoor (3km/h); Users dropped uniformly in entire cell. For URLLC with 700MHz and 500m ISD 20% of users are outdoors (3km/h), 80% of users are indoor (3km/h); Users dropped uniformly in entire cell. Other option(s) not precluded, e.g., 80% of users are outdoors (3km/h), 20% of users are indoor (3km/h). For eMBB 20% of users are outdoors (3km/h), 80% of users are indoor (3km/h); Users dropped uniformly in entire cell	
UE power control	Open loop PC for mMTC. Companies report the PC mechanisms used for eMBB and URLLC.	
HARQ/repetition	Companies report (including HARQ mechanisms).	
Channel estimation	Realistic	
BS receiver	Advanced receiver, with baseline scheme is MU-MIMO (e.g., has the capability of spatial differentiation) Companies to provide analysis of complexity between baseline vs. advanced receivers	

Note: other values can be considered.

- For SLS in mMTC and eMBB, the packet drop rate (PDR) is defined as (the number of packets in outage) / (the number of packets generated), where a packet is in outage if this packet failed to be successfully decoded by the receiver beyond
  - "packet dropping timer", or
    - The packet dropping timer can be set to 1 second as the starting point.
  - "maximum number of HARQ transmission(s)"
    - 1 and 8 as starting point
    - The HARQ timing is FFS

    - The target higher layer system PDR to be used to evaluate the supported system capability in terms of high layer system PAR for mMTC or eMBB scenarios is 1%

- For URLLC, the target reliability is 99.999% and the target delay requirement is 1ms (for 60 bytes) and 4ms (for 200bytes) as starting point.
    - The target percentage of users satisfying reliability and latency requirements to be used to evaluate the supported system capability in terms per UE PAR for URLLC scenario is 95%

A.3.2 Traffic model for system-level evaluations

- For mMTC scenario
    - Packet arrival per UE: Poisson arrival with arrival rate λ;
    - Packet size: 20~200 bytes Pareto + higher layer protocol overhead of 29 bytes, as defined in TR 45.820 to be the starting point
        - Other packet sizes are not precluded.
- For URLLC scenario:
    - Packet arrival per UE can be based on either option 1 or option 2
        - Option 1: FTP Model 3 with Poisson arrival;
        - Option 2: Periodic packet arrivals.
    - Packet size:
        - Single fixed value per simulation: 60 bytes and 200 bytes
            - higher layer protocol overhead included
- For eMBB scenario:
    - Packet arrival per UE: FTP Model 3 with Poisson arrival
    - Packet size:
        - 50~ 600 bytes Pareto distribution, with shaping parameter alpha = 1.5 as starting point.
        - In the case of packet segmentation, use 5 bytes packet segmentation overhead for each TB

A.3.3 System-level assumptions for calibration purpose

For calibration of the CDFs of coupling loss and downlink geometry averaged over two antenna ports, use the assumption in the following Table.

Table A.3-2: System-level assumptions for calibration purpose

Parameters	Case 1	Case 2	Case 3
Layout	Single layer - Macro layer: Hex. Grid		
Wrapping method	Geographical distance based wrapping		
Inter-BS distance	1732m	500m	200m
UE-BS min. distance	35m	10m	10m
Carrier frequency	700MHz	700MHz	4GHz
Channel model	UMa in TR 38.901		
UE Tx power	Max 23 dBm		
BS Tx power	46 dBm	46 dBm	41 dBm
Bandwidth	10MHz		
BS antenna configurations	2 ports: (M, N, P, Mg, Ng) = (10, 1, 2, 1, 1), +-45 Polarization dH = dV = 0.8λ; One TXRU per vertical dimension per polarization. TXRU virtualization only in the vertical dimension, i.e., sub-array partition model with ID virtualization, refer to TR 36.897		

Polarized antenna modeling	Model-2 in TR 36.873		
BS antenna downtilt	92	98	102
BS antenna height	25m		
BS antenna element gain + connector loss	8 dBi, including 3dB cable loss		
BS receiver noise figure	5dB		
UE receiver noise figure	9dB		
UE antenna configuration	1 (vertical polarization)		
UT array orientation	Uniformly distributed on [0, 360] degree		
UE antenna height	Follow the modelling of TR 38.901		
UE antenna gain	0dBi		
UE distribution	Follow the evaluation assumptions		
UE power control	Open loop PC, P0 = [-90] dBm, alpha = 1.		
HARQ/repetition	1		
UE attachment	Based on RSRP		
Handover margin	0dB		

Figures A.3-1, A.3-3 and A.3-5 are the coupling loss calibration for Case 1, Case 2 and Case 3, respectively. Figures A.3-2, A.3-4 and A.3-6 are the downlink geometry calibration for Case 1, Case 2 and Case 3, respectively.

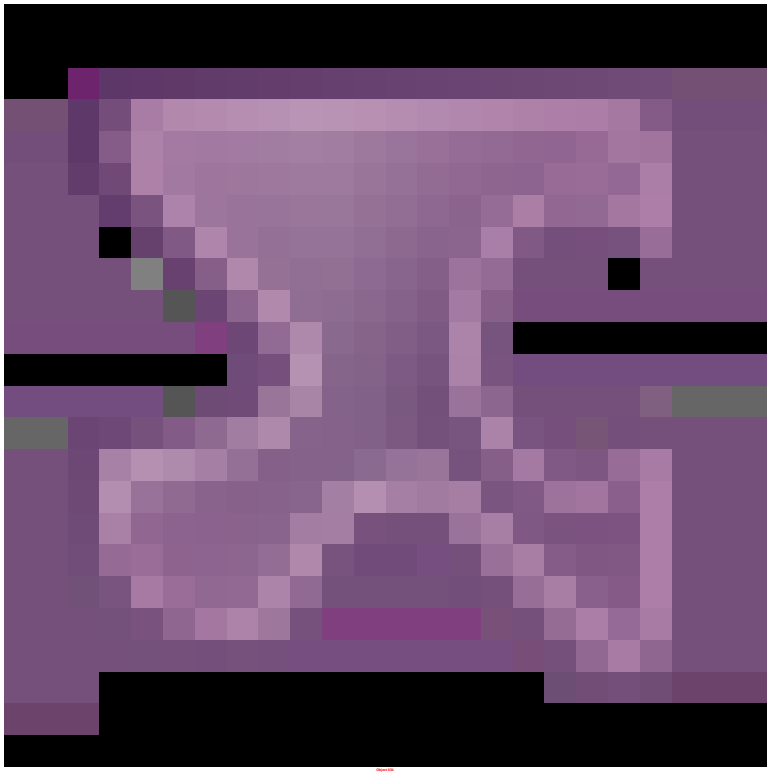

Figure A.3-1: Coupling loss for SLS calibration Case 1

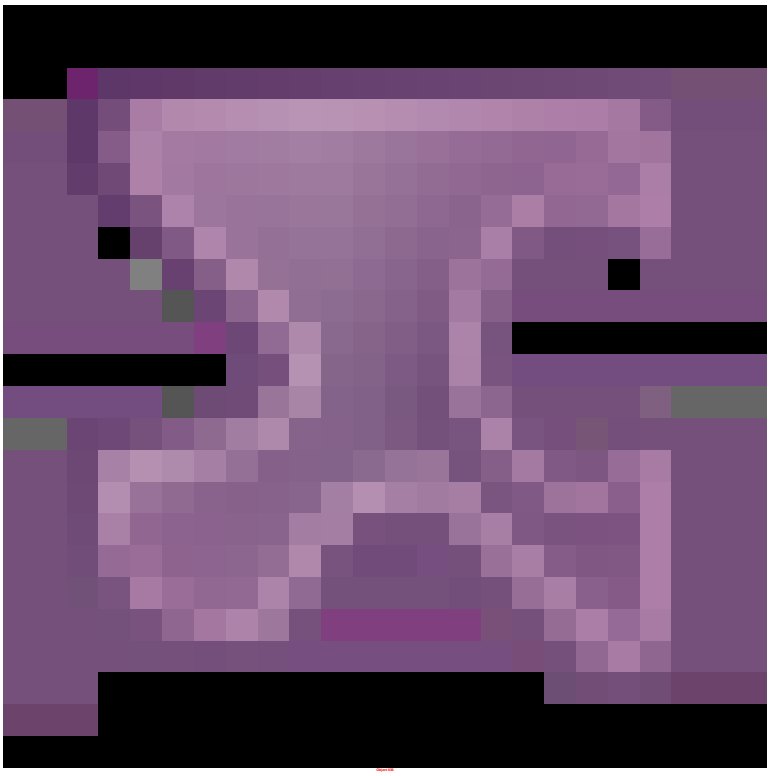

Figure A.3-2: Geometry for SLS calibration Case 1

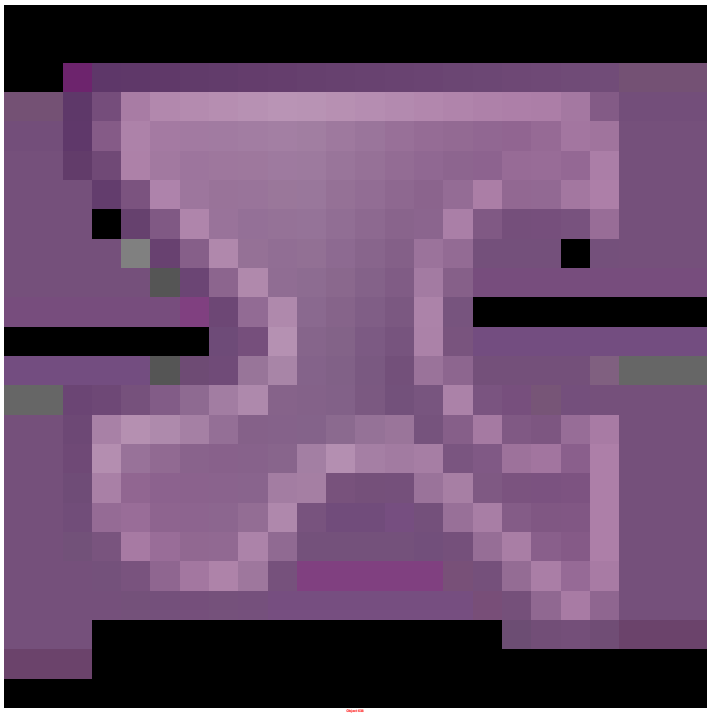

Figure A.3-3: Coupling loss for SLS calibration Case 2

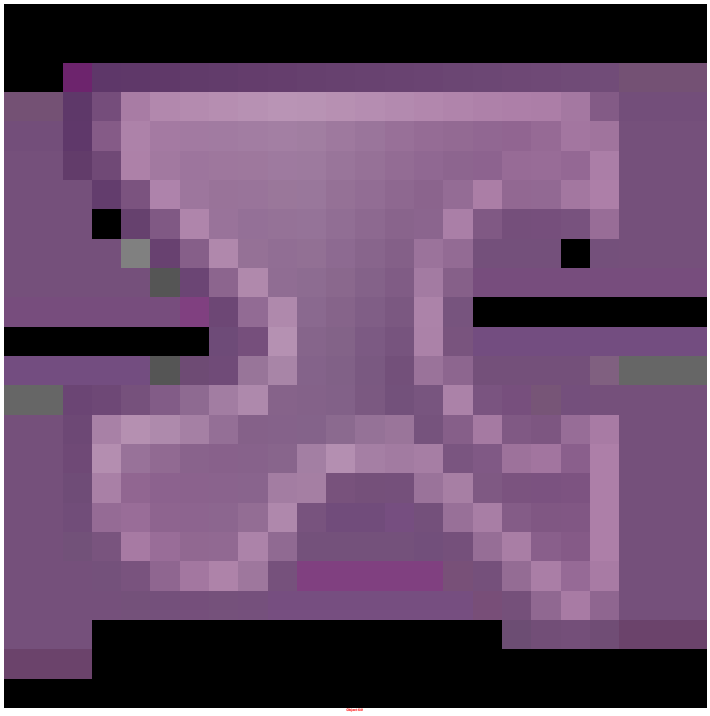

Figure A.3-4: Geometry for SLS calibration Case 2

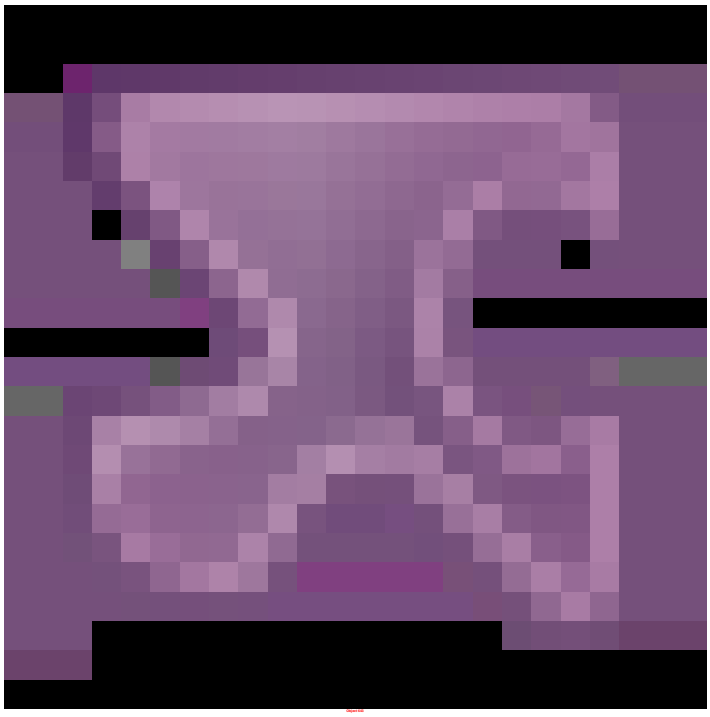

Figure A.3-5: Coupling loss for SLS calibration Case 3

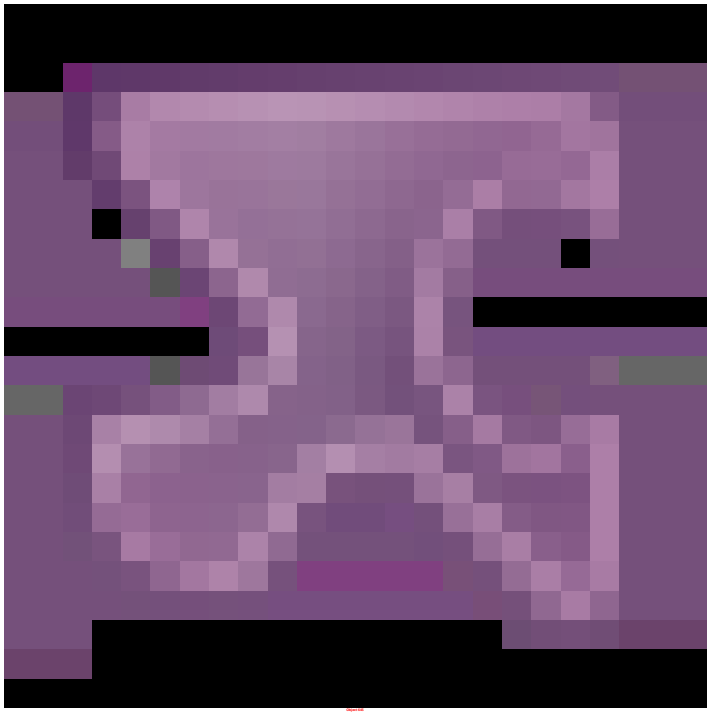

Figure A.3-6: Geometry for SLS calibration Case 3

A.4 MA signature designs for NOMA schemes

A.4.1 Generation method for the construction of WBE spreading sequences

For a user k, let b_k be the transmitted symbol that modulates a unit norm spreading sequence (SS) vector s_k. The Additive White Gaussian Noise (AWGN) signal model may be given as $y = Sb + z$, where z is the zero-mean AWGN vector with a covariance matrix I, i.e., an Identity matrix. the overall SS matrix with an SS codeword (CW) in each of its columns is S, the transmit symbol vector is b. The transmit power of each user is set to unity, so the power control problem is not addressed here. A unit norm receive filter f_k, such as a Matched Filter (MF) or a linear Minimum Mean Squared Error (MMSE) filter, may be employed by the receiver to obtain an estimate $\hat{b}_k$ for the transmitted symbol b_k. The post processed SINR γ_k of a user k is given as

$$\gamma_k = \frac{\left|f_k^H s_k\right|^2}{\sum_{j=1, j\neq k}^{K} \left|f_k^H s_j\right|^2 + \left|f_k^H z\right|^2} = \frac{f_k^H (s_k s_k^H) f_k}{f_k^H \left(\sum_{j=1, j\neq k}^{K} s_j s_j^H + I\right) f_k} \Rightarrow f_k = s_k \frac{1}{trace\left(\left(S S^T\right)^2\right) - 1 + v_k},$$

where $trace(\cdot)$ is the trace operator, v_k is the noise component in the SINR γ_k. The $trace(\cdot)$ term in the denominator is the total squared correlation (TSC), which also contains the desired unit signal power. So an additional unity term arises in the denominator. If the post processed noise is white, i.e., the noise power of each v_k is the same, then the TSC can directly be used as a performance metric.

From the center part of the SINR equation, let $R_k = \left(\sum_{j=1, j\neq k}^{K} s_j s_j^H + I\right)$, which is the correlation matrix of the interference plus noise. It can be identified that minimizing the denominator (or equivalently maximizing γ_k) is a well known Rayleigh-Quotient problem. From this, the Eigen vector corresponding to the minimum Eigen value of R_k may be considered as CW for UE k, if it is assumed that f_k is matched to s_k.

The fixed-point iterations start from the users choosing a random CW, preferably with a unit norm. In a given sequential user order, say $k=1,2,\ldots K$, each user updates its SS s_k by solving the Eigen value problem while other SS, $s_j, j \neq k,$ are kept fixed, i.e. After user k , the next user updates it's CW in the same way by assuming the other CWs to be fixed. The iterations progress up to the final user in the given order, such that in each iteration there are K updates, one for each CW (a signature vector) in S . After the final update in the given iteration, the first user in the order restarts the updates. This repeats until convergence. Note that matrices that minimize the TSC are not unique.

Again, from the center part of the SINR equation, the solution to f_k can also be identified as the well known Generalized Eigen Value Problem (GEVP), i.e., finding a common Eigen value for the matrix pair (I, R_k). The solution to which is the linear MMSE vector given as $\frac{R_k^{-1} s_k}{\left(s_k^H R_k^{-2} s_k\right)^{1/2}}$, in its normalized form. Sequential iterations as mentioned before can be used, except that instead of solving the Eigen value problem, the normalized linear MMSE expression is used during updates. For this SINR maximization problem (or equivalently a TSC minimization), the obtained solution for S from both the MMSE iterations and the Eigen vector iterations is the same fixed-point. These methods are classified as Interference Avoidance (IA) techniques.

The obtained TSC value is bounded from below by the Welch Bound (WB). For theoretically optimal system performance in certain conditions, it is required that the bound be satisfied by equality, in which case it is called the Welch Bound Equality (WBE). At the WBE, various metrics (such as the System Capacity, Sum MSE) in the system are simultaneously optimized. So the main objective of the IA technique here is to obtain a matrix S, such that the TSC from the constituent vectors achieve the WBE.

A Kronecker product based approach may be employed to obtain (or construct) higher dimensional Welch bound equality (WBE) SS, i.e., higher N values, from lower dimensional WBE SS.

Signature grouping can also be applied to have low or no correlation between signature sequences within the group targeting to reduce the complexity of the receiver while not decreasing the performance. One such approach is to have orthogonality between certain subset of vectors within a given Welch Bond (WB) set. Such a set of vectors are said to form a subspace-packing based codebook. In addition, these vectors also satisfy the Welch Bound (WB). So, the codebook is a subset of general WB codebook.

Table A.4.1-1: An instance of a (4x8) WSMA spreading matrix (codebook) from an ensemble of (4x8) WBE complex codebooks with spreading factor *L*=4, supporting *K*=8 active users. Overloading factor (*K*/*L*)=2. Each 4x1 column is a unit norm complex vector assigned to a single user. [14]

	Sequence #	1	2	3	4
Sequence Sample #	1	-0.6617 + 0.1004i	-0.0912 + 0.4191i	0.4151 - 0.3329i	0.2736 - 0.4366i
	2	0.0953 + 0.4784i	-0.4246 - 0.0859i	0.2554 - 0.3140i	0.5452 + 0.2068i
	3	-0.4233 - 0.1399i	-0.4782 + 0.3752i	-0.3808 - 0.1569i	-0.4690 - 0.2225i
	4	-0.1265 + 0.3153i	0.4936 + 0.1233i	0.6130 - 0.0873i	-0.3399 + 0.0974i
	Sequence #	5	6	7	8
Sequence Sample #	1	-0.4727 - 0.1234i	-0.3413 + 0.1257i	0.4216 + 0.1187i	0.4603 + 0.2142i
	2	0.0592 - 0.6432i	0.3671 - 0.1430i	-0.0241 - 0.5620i	0.0048 - 0.4244i
	3	0.3493 - 0.1988i	0.6514 - 0.0660i	-0.4507 + 0.0958i	0.4047 + 0.1601i
	4	-0.0975 - 0.4161i	0.2174 + 0.4864i	-0.5167 + 0.1116i	-0.4908 + 0.3629i

Table A.4.1-2: An instance of a (4x12) WSMA spreading matrix (codebook) from an ensemble of (4x12) WBE complex codebooks with spreading factor *L*=4, supporting *K*=12 active users. Overloading factor (*K*/*L*)=3. Each 4x1 column is a unit norm complex vector assigned to a single user. [14]

	Sequence #	1	2	3	4
Sequence Sample #	1	-0.2221 + 0.3220i	-0.0690 - 0.5020i	-0.4866 + 0.3090i	0.4007 - 0.3034i
	2	0.1709 - 0.3679i	-0.2222 - 0.2729i	-0.4148 - 0.2589i	-0.3206 - 0.0231i
	3	0.4335 - 0.4253i	0.0875 - 0.3912i	0.5181 + 0.0067i	-0.6714 - 0.0514i
	4	-0.2877 + 0.4804i	0.6669 - 0.1183i	-0.3439 - 0.2048i	-0.2117 - 0.3819i
	Sequence #	**5**	**6**	**7**	**8**
Sequence Sample #	1	0.0525 - 0.6492i	-0.3121 + 0.4136i	0.1887 - 0.5138i	0.3628 - 0.5556i
	2	0.2786 + 0.2173i	-0.5533 + 0.2843i	-0.5603 + 0.0403i	-0.2496 - 0.3482i
	3	0.4058 - 0.3688i	-0.3497 + 0.2042i	0.3714 - 0.0660i	0.4539 - 0.0605i
	4	-0.0586 - 0.3831i	0.4123 + 0.1027i	0.3124 + 0.3807i	-0.2014 - 0.3549i
	Sequence #	**9**	**10**	**11**	**12**
Sequence Sample #	1	-0.4067 - 0.0166i	-0.2969 - 0.2084i	0.3160 + 0.0753i	0.3612 - 0.2061i
	2	0.5821 - 0.2559i	-0.5414 - 0.1665i	-0.7029 - 0.1267i	0.3525 - 0.0158i
	3	0.1316 - 0.2310i	-0.1075 + 0.6412i	0.3540 - 0.2274i	-0.4880 - 0.1396i
	4	0.5222 - 0.2944i	0.2613 - 0.2380i	-0.3490 - 0.2925i	-0.5884 - 0.3142i

Table A.4.1-3: An instance of a (6x12) WSMA spreading matrix (codebook) from an ensemble of (6x12) WBE complex codebooks with spreading factor *L*=6, supporting *K*=12 active users. Overloading factor (*K*/*L*)=2. Each 6x1 column is a unit norm complex vector assigned to a single user. [14]

	Sequence #	1	2	3	4
Sequence Sample #	1	0.2077 + 0.3793i	0.3451 + 0.1338i	0.2279 - 0.4659i	0.1552 + 0.3036i
	2	-0.0242 - 0.2918i	0.1832 + 0.1258i	0.2007 + 0.0517i	-0.0691 - 0.2333i
	3	0.0033 + 0.4259i	-0.0068 - 0.5688i	-0.0117 + 0.1839i	0.3280 - 0.0232i
	4	0.2805 + 0.2018i	-0.2553 + 0.1472i	-0.3232 - 0.4850i	-0.4418 - 0.1054i
	5	0.4517 - 0.1700i	-0.4087 + 0.4122i	-0.0183 - 0.2256i	-0.0676 - 0.2340i
	6	-0.1248 + 0.4218i	0.1703 - 0.1931i	-0.5000 - 0.1145i	-0.4826 - 0.4668i
	Sequence #	**5**	**6**	**7**	**8**
Sequence Sample #	1	-0.1673 - 0.3954i	-0.4380 + 0.0177i	-0.4180 + 0.0654i	-0.4587 + 0.0503i
	2	-0.4059 + 0.0635i	0.3095 + 0.1809i	0.2950 + 0.0247i	-0.1975 - 0.3656i
	3	0.3157 - 0.1566i	0.1062 - 0.1523i	0.4446 + 0.1407i	-0.4910 - 0.0302i
	4	-0.3762 - 0.0444i	0.0795 - 0.4774i	-0.2827 + 0.1945i	0.2100 - 0.4170i
	5	0.4927 + 0.0365i	-0.0625 + 0.2372i	0.5409 - 0.1294i	-0.0451 - 0.3571i
	6	0.1134 + 0.3497i	-0.3099 + 0.5045i	-0.1071 - 0.2781i	-0.0360 - 0.1536i
	Sequence #	**9**	**10**	**11**	**12**
Sequence Sample #	1	-0.2025 - 0.2054i	-0.2957 + 0.0742i	0.4714 - 0.2817i	-0.0674 + 0.1996i
	2	0.2475 - 0.7093i	0.1213 - 0.1690i	-0.0943 - 0.5046i	-0.5072 + 0.2784i
	3	0.2462 - 0.0514i	-0.3848 + 0.5111i	-0.2767 + 0.1296i	-0.3987 - 0.0943i
	4	0.2286 + 0.2661i	-0.2398 + 0.1706i	-0.4046 + 0.1132i	-0.2844 + 0.2621i
	5	-0.2812 + 0.0005i	-0.5698 + 0.0562i	0.1131 - 0.2679i	0.2862 - 0.0408i
	6	-0.2472 - 0.1609i	0.1745 + 0.0979i	0.2413 + 0.1491i	-0.3883 - 0.2626i

Table A.4.1-4: An instance of a (6x18) WSMA spreading matrix (codebook) from an ensemble of (6x18) WBE complex codebooks with spreading factor *L*=6, supporting *K*=18 active users. Overloading factor (*K*/*L*)=3. Each 6x1 column is a unit norm complex vector assigned to a single user. [14]

	Sequence #	1	2	3	4
Sequence Sample #	1	0.0127 - 0.4081i	0.4044 + 0.0562i	-0.2851 + 0.2922i	-0.4006 + 0.0789i
	2	-0.3376 + 0.2295i	-0.3739 + 0.1639i	-0.1569 + 0.3769i	-0.2290 + 0.3380i
	3	-0.1792 - 0.3668i	-0.3488 - 0.2121i	-0.2767 + 0.3001i	-0.3467 - 0.2155i
	4	0.1812 + 0.3658i	-0.1718 - 0.3704i	-0.3815 + 0.1454i	-0.3994 + 0.0846i
	5	0.2566 + 0.3176i	0.2490 - 0.3235i	-0.3897 - 0.1217i	0.3421 + 0.2228i
	6	0.0764 - 0.4010i	0.3607 - 0.1912i	-0.2157 - 0.3466i	0.4079 - 0.0172i
	Sequence #	**5**	**6**	**7**	**8**
Sequence Sample #	1	0.4065 - 0.0374i	0.2661 + 0.3096i	0.2941 - 0.2831i	-0.2765 + 0.3003i
	2	0.4008 + 0.0779i	-0.4068 + 0.0347i	-0.2459 - 0.3259i	-0.3970 - 0.0953i
	3	0.3497 - 0.2106i	0.3137 - 0.2613i	-0.2331 + 0.3352i	-0.3400 + 0.2260i
	4	-0.2905 + 0.2869i	0.3796 + 0.1502i	0.1112 - 0.3928i	0.0136 - 0.4080i
	5	0.4072 + 0.0287i	-0.0430 - 0.4060i	0.2744 + 0.3023i	-0.0933 - 0.3974i
	6	-0.0089 + 0.4082i	-0.2751 + 0.3017i	0.1705 + 0.3709i	-0.1029 + 0.3951i
	Sequence #	**9**	**10**	**11**	**12**
Sequence Sample #	1	-0.3326 + 0.2367i	-0.3130 - 0.2621i	0.3478 - 0.2137i	-0.1482 - 0.3804i
	2	0.3399 - 0.2261i	0.3567 - 0.1986i	-0.3279 + 0.2432i	0.3409 + 0.2246i
	3	-0.4045 - 0.0552i	-0.2184 - 0.3449i	-0.3677 - 0.1773i	0.2542 - 0.3195i
	4	-0.3645 - 0.1839i	-0.0414 + 0.4061i	-0.3691 + 0.1744i	-0.3072 - 0.2688i
	5	0.3338 - 0.2351i	0.0992 - 0.3960i	0.2238 - 0.3414i	-0.3323 - 0.2371i
	6	-0.1345 - 0.3854i	-0.1021 + 0.3953i	-0.4039 + 0.0595i	-0.1442 + 0.3819i
	Sequence #	**13**	**14**	**15**	**16**
Sequence Sample #	1	0.3503 + 0.2097i	0.3966 + 0.0968i	-0.0718 - 0.4019i	0.1103 - 0.3931i
	2	0.2704 + 0.3059i	-0.3121 - 0.2631i	-0.1017 - 0.3954i	0.3154 + 0.2592i
	3	-0.3382 - 0.2286i	0.0828 - 0.3998i	-0.3402 + 0.2257i	0.3827 - 0.1420i
	4	0.2216 - 0.3429i	-0.3867 - 0.1310i	-0.4068 - 0.0340i	-0.0265 - 0.4074i
	5	-0.2380 - 0.3317i	-0.3579 + 0.1964i	-0.3580 + 0.1963i	-0.4082 - 0.0055i
	6	-0.3926 + 0.1118i	0.0940 + 0.3973i	-0.3610 - 0.1906i	-0.1204 - 0.3901i
	Sequence #	**17**	**18**		
Sequence Sample #	1	-0.1234 - 0.3891i	-0.0403 - 0.4063i		
	2	-0.3884 + 0.1257i	-0.0692 + 0.4023i		
	3	0.3979 - 0.0914i	0.0233 + 0.4076i		
	4	-0.3194 - 0.2543i	-0.2744 - 0.3022i		
	5	-0.3812 + 0.1461i	0.2992 - 0.2777i		
	6	0.0883 + 0.3986i	-0.0814 - 0.4000i		

A.4.2 WBE based on modified Chirp sequence

Assuming the spreading factor is *K* and the number of distinct spreading codes is *N*, the *n*-th spreading code can be denoted by

$$S_n \triangleq \left[s_n(1) s_n(2) \cdots s_n(K) \right]; 1 \le n \le N, N > K \ge 2 \qquad \text{(A.4.2-1)}$$

One example of closed-form construction would be

$$s_n(k) \triangleq \frac{1}{\sqrt{K}} \exp\left(j\pi \left(\frac{(k+n)^2}{N} \right) \right) w(k) \quad ; \quad 1 \le k \le K, 1 \le n \le N \qquad \text{(A.4.2-2)}$$

where $w(k)$ is a perfect sequence of period *K*, that is

$$\sum_{k=1}^{K} w(k) w^{*}(k+l) = K\delta(l). \qquad \text{(A.4.2-3)}$$

It can be shown that the spreading code generated above is a WBE set, which achieves the WB on sum squared correlations for arbitrary *K* and *N* satisfying $N > K \ge 2$.

A.4.3 Examples of complex-valued sequences with quantized elements

Table A.4.3-1 Example of MUSA sequences with SF = 2, pool size = 6 (before normalization).

No.	c1	c2
1	1	1
2	1	-1
3	1	j
4	1	-j
5	1	0
6	0	1

Table A.4.3-2 MUSA sequences for SF = 3:

$$\frac{1}{\sqrt{2}}\begin{bmatrix}1 & \omega^2 & \omega & 1 & \omega^2 & \omega & 0 & 0 & 0\\ 1 & \omega & \omega^2 & 0 & 0 & 0 & 1 & \omega^2 & \omega\\ 0 & 0 & 0 & 1 & \omega & \omega^2 & 1 & \omega & \omega^2\end{bmatrix}, \omega = e^{j\frac{2\pi}{3}}$$

Table A.4.3-3 Example of MUSA sequence with SF = 4, pool size = 64 (before normalization).

No.	c1	c2	c3	c4	No.	c1	c2	c3	c4
1	1	1	1	1	**33**	1	1	1	-j
2	1	1	-1	-1	**34**	1	1	-1	j
3	1	-1	1	-1	**35**	1	-1	1	j
4	1	-1	-1	1	**36**	1	-1	-1	-j
5	1	1	-j	j	**37**	1	1	-j	1
6	1	1	j	-j	**38**	1	1	j	-1
7	1	-1	-j	-j	**39**	1	-1	-j	-1
8	1	-1	j	j	**40**	1	-1	j	1
9	1	-j	1	j	**41**	1	-j	1	1
10	1	-j	-1	-j	**42**	1	-j	-1	-1
11	1	j	1	-j	**43**	1	j	1	-1
12	1	j	-1	j	**44**	1	j	-1	1
13	1	-j	-j	-1	**45**	1	-j	-j	j
14	1	-j	j	1	**46**	1	-j	j	-j
15	1	j	-j	1	**47**	1	j	-j	-j
16	1	j	j	-1	**48**	1	j	j	j
17	1	1	1	-1	**49**	1	1	1	j
18	1	1	-1	1	**50**	1	1	-1	-j
19	1	-1	1	1	**51**	1	-1	1	-j
20	1	-1	-1	-1	**52**	1	-1	-1	j
21	1	1	-j	-j	**53**	1	1	-j	-1
22	1	1	j	j	**54**	1	1	j	1
23	1	-1	-j	j	**55**	1	-1	-j	1
24	1	-1	j	-j	**56**	1	-1	j	-1
25	1	-j	1	-j	**57**	1	-j	1	-1
26	1	-j	-1	j	**58**	1	-j	-1	1
27	1	j	1	j	**59**	1	j	1	1
28	1	j	-1	-j	**60**	1	j	-1	-1
29	1	-j	-j	1	**61**	1	-j	-j	-j
30	1	-j	j	-1	**62**	1	-j	j	j
31	1	j	-j	-1	**63**	1	j	-j	j
32	1	j	j	1	**64**	1	j	j	-j

Table A.4.3-4: Example of BPSK or {+1/-1} sequence with SF = 6, pool size = 16 (before normalization).

No.	c1	c2	c3	c4	c5	c6
1	1	1	1	1	1	1
2	1	1	1	1	-1	-1
3	1	1	1	-1	1	-1
4	1	1	1	-1	-1	1
5	1	1	-1	1	1	-1
6	1	1	-1	1	-1	1
7	1	1	-1	-1	1	1
8	1	1	-1	-1	-1	-1
9	1	-1	1	1	1	-1
10	1	-1	1	1	-1	1
11	1	-1	1	-1	1	1
12	1	-1	1	-1	-1	-1
13	1	-1	-1	1	1	1
14	1	-1	-1	1	-1	-1
15	1	-1	-1	-1	1	-1
16	1	-1	-1	-1	-1	1

A.4.4 Examples of Grassmannian sequences

- Examples of Grassmannian Sequence based spreading codebook

Table A.4.4-1: Grassmannian Sequence based codebook for Spreading Factor: *N* = 2

# of sequences (*K*)	Examples of spreading codebook $\left[C^{(1)} \quad \cdots \quad C^{(K)}\right]$
2	0.5+0.5i 0.5+0.5i 0.5+0.5i -0.5-0.5i
3	-0.6263+0.7075i -0.573-0.0791i -0.5129+0.0638i -0.0133+0.3272i 0.673+0.4609i -0.455-0.7251i
4	-0.332+0.5287i -0.4097+0.8563i -0.1019-0.3184i -0.7084-0.3089i 0.2967+0.7227i -0.3059+0.0722i 0.9012-0.2757i 0.4757+0.42i
6	-0.3216+0.1994i -0.6835-0.3756i -0.0804-0.5006i -0.4603+0.3705i -0.1868-0.9794i -0.8377+0.1357i 0.8477-0.3719i -0.5584+0.2827i -0.084-0.8579i -0.5978-0.5418i -0.0455-0.0625i 0.3387-0.4064i
8	-0.4355-0.8256i -0.8275-0.133i -0.2565-0.2043i -0.1369-0.5129i -0.1733-0.3142i 0.0924-0.5376i -0.1633+0.9305i -0.4608-0.7112i … -0.316-0.094i -0.9512+0.0838i -0.3073-0.7312i -0.1059+0.6197i 0.0767-0.941i 0.2937+0.0432i -0.5853+0.1684i -0.1573-0.7615i
12	-0.4674-0.5448i -0.389-0.3685i -0.9054-0.4138i -0.2598-0.2783i -0.258+0.1298i -0.1395-0.7374i 0.6583-0.2265i 0.0489+0.8429i 0.0506+0.0802i -0.1676-0.9094i 0.1195-0.9499i -0.6574-0.0676i … -0.9257+0.0341i -0.709-0.2363i -0.2001-0.2789i -0.789-0.3244i -0.2703+0.6757i -0.1207-0.8743i -0.0837-0.3674i -0.3586-0.5594i -0.9337+0.1017i 0.199+0.4823i 0.069-0.6823i -0.2052-0.423i

Table A.4.4-2 Grassmannian Sequence based codebook for Spreading Factor: *N* = 4

# of sequences (*K*)	Examples of spreading codebook $\left[C^{(1)} \quad \cdots \quad C^{(K)}\right]$
4	0.3536+0.3536i 0.3536+0.3536i 0.3536+0.3536i 0.3536+0.3536i 0.3536+0.3536i -0.3536-0.3536i 0.3536+0.3536i -0.3536-0.3536i 0.3536+0.3536i 0.3536+0.3536i -0.3536-0.3536i -0.3536-0.3536i 0.3536+0.3536i -0.3536-0.3536i -0.3536-0.3536i 0.3536+0.3536i
6	-0.5659+0.2301i -0.2438+0.0689i -0.0199-0.8583i -0.0756+0.1161i -0.4797+0.3517i -0.1779+0.0383i -0.3658+0.0035i -0.0102-0.3345i -0.3024+0.0388i 0.2302+0.3263i -0.2896-0.5898i 0.3838+0.5954i 0.1548+0.1412i -0.0633-0.693i -0.0159-0.2511i -0.1419+0.7303i 0.2695+0.2056i 0.4001-0.4804i 0.1012-0.6625i -0.5252+0.2524i -0.3086+0.1071i -0.406+0.3209i -0.112+0.2949i 0.073+0.2622i
8	-0.3769-0.1993i -0.4946+0.0729i -0.0349-0.1744i -0.4983-0.2361i 0.0071-0.4246i 0.0484+0.2172i -0.4864+0.5118i 0.3678-0.0002i -0.7438-0.2074i 0.1526-0.5642i -0.1478+0.1545i 0.6445+0.1123i 0.0662-0.1932i 0.1281-0.5852i -0.3512+0.5484i -0.1883+0.3118i … -0.0589-0.2775i -0.3141-0.2162i -0.3118-0.2513i -0.6128+0.4861i 0.6654-0.2483i 0.2752+0.0869i -0.0147+0.3864i -0.3671+0.3724i -0.4067+0.4932i -0.2122-0.4038i -0.3986+0.2848i -0.1428-0.0632i 0.072+0.0362i -0.5858+0.4691i 0.5659-0.3604i 0.282+0.104i
12	-0.1211 + 0.1742i -0.1864 + 0.1486i -0.4450 - 0.2565i -0.1650 + 0.3506i -0.4503 + 0.2070i -0.3310 - 0.2575i 0.5284 - 0.0028i 0.5630 - 0.0523i -0.5537 + 0.0264i 0.2754 + 0.1722i 0.0650 - 0.1528i -0.5335 + 0.6004i 0.1518 - 0.5314i 0.2665 - 0.4503i 0.3965 + 0.2446i -0.2259 + 0.3311i -0.1173 + 0.3294i -0.1120 - 0.2999i 0.3043 + 0.5270i 0.2024 - 0.5556i 0.3116 - 0.3387i -0.3280 - 0.6900i 0.6983 + 0.3420i -0.1290 + 0.2449i … -0.2344 - 0.1865i -0.4251 + 0.0869i -0.2091 - 0.5656i -0.8263 - 0.3684i -0.5363 - 0.1981i -0.6964 - 0.1831i 0.1663 - 0.2439i 0.6626 - 0.4120i -0.1403 - 0.1177i 0.1024 + 0.0356i 0.3090 - 0.5397i 0.1029 + 0.2755i 0.7183 - 0.0739i -0.0365 - 0.0355i -0.0380 - 0.3106i 0.2040 - 0.3275i -0.1106 + 0.2210i -0.0585 + 0.6228i -0.4388 - 0.3303i -0.3826 + 0.2322i -0.1052 - 0.7027i 0.1073 + 0.0961i 0.2328 - 0.4136i -0.0382 - 0.0488i

24	-0.4830 - 0.2050i -0.6615 - 0.0671i -0.6259 + 0.0369i -0.3959 - 0.0233i -0.1603 - 0.2521i -0.6038 + 0.4112i -0.2624 - 0.1541i 0.4989 + 0.1979i 0.4263 + 0.1862i 0.2071 + 0.0445i -0.4414 - 0.4468i -0.0881 - 0.4998i 0.1666 + 0.6409i -0.1865 + 0.1094i 0.2179 - 0.0776i 0.1435 + 0.2335i 0.4663 + 0.1111i -0.4010 - 0.1035i 0.4013 - 0.1805i 0.1638 + 0.4431i -0.2700 - 0.5139i -0.7073 + 0.4716i -0.0505 + 0.5329i 0.0192 - 0.1919i … -0.1635 - 0.1720i -0.1179 + 0.0788i -0.1956 + 0.0307i -0.2600 + 0.2399i -0.2038 - 0.6405i -0.4881 - 0.5159i 0.7563 + 0.0361i -0.4599 - 0.1309i -0.1232 - 0.6046i -0.3615 - 0.4122i -0.2539 + 0.0586i -0.1130 - 0.4476i -0.2782 - 0.2679i -0.1685 + 0.6825i 0.6386 - 0.1426i -0.2622 - 0.5184i -0.0735 - 0.5538i 0.2439 + 0.0633i -0.4506 + 0.1348i -0.3230 + 0.3907i 0.3472 - 0.1775i 0.1503 + 0.4628i 0.1120 - 0.3945i -0.1279 - 0.4501i … -0.3285 - 0.2600i -0.0493 - 0.1783i -0.0727 + 0.7759i -0.1140 - 0.0059i -0.4202 + 0.0846i -0.1926 - 0.5845i -0.2321 + 0.4945i -0.0936 - 0.1371i -0.0051 - 0.0993i 0.8473 - 0.2674i -0.6712 + 0.0690i 0.4597 + 0.1189i -0.3453 + 0.6286i 0.0050 - 0.5683i -0.0618 - 0.5636i 0.1556 + 0.0334i -0.2547 + 0.0501i -0.5381 + 0.1646i -0.0900 - 0.0602i -0.7617 - 0.1871i 0.2389 - 0.0656i 0.1766 - 0.3756i 0.1964 - 0.5051i 0.0392 - 0.2784i … -0.1330 + 0.5960i -0.0860 + 0.0279i -0.1848 - 0.7667i -0.4759 - 0.0853i -0.5030 - 0.1257i -0.3274 + 0.1413i 0.6664 + 0.3456i -0.2417 - 0.5119i -0.0172 - 0.4039i 0.1071 - 0.0115i -0.0097 + 0.3024i 0.1559 + 0.1646i -0.0779 - 0.2098i -0.1963 + 0.4415i -0.2174 - 0.1382i 0.2280 - 0.1530i -0.5637 + 0.0694i -0.4217 - 0.7887i 0.0142 + 0.1150i -0.0101 - 0.6617i -0.3424 + 0.1762i 0.7979 - 0.2064i 0.5591 - 0.0670i -0.0345 + 0.1433i

Table A.4.4-3: Grassmannian Sequence based codebook for Spreading Factor: *N* = 6

# of sequences (*K*)	Examples of spreading codebook $\left[c^{(1)} \quad \cdots \quad c^{(K)}\right]$
6	-0.0067 + 0.1511i -0.4237 - 0.3591i -0.1953 - 0.0263i -0.2925 - 0.4896i -0.0118 + 0.0830i -0.1683 + 0.5188i 0.1368 + 0.4258i -0.0108 + 0.2746i 0.7358 + 0.1501i 0.1518 - 0.1068i 0.0716 - 0.0748i -0.1933 + 0.2792i -0.5648 - 0.1014i -0.0970 + 0.4963i -0.1376 - 0.2277i 0.3041 - 0.1107i -0.3406 - 0.1132i 0.0733 + 0.3244i 0.1170 + 0.1862i -0.4994 + 0.2468i 0.0429 - 0.3209i -0.0097 - 0.1937i -0.1889 + 0.3199i -0.1491 - 0.5819i 0.0510 + 0.5028i -0.1730 - 0.1237i -0.2822 - 0.3193i 0.3790 + 0.4902i 0.3024 + 0.0765i 0.0360 + 0.1876i -0.2469 - 0.2882i -0.0678 + 0.0059i 0.1937 - 0.0511i 0.2007 - 0.2713i 0.6612 + 0.4253i 0.2814 - 0.0048i
9	-0.1750 - 0.4216i -0.0946 + 0.1509i -0.4759 - 0.1498i -0.4398 - 0.4474i -0.3105 + 0.3168i -0.3774 + 0.2254i 0.3676 - 0.5634i -0.0470 + 0.0828i -0.1229 - 0.2901i -0.0986 - 0.2838i 0.2603 - 0.2223i 0.1551 - 0.1842i -0.0355 - 0.6399i 0.1221 + 0.4573i -0.1649 + 0.3555i 0.3240 - 0.1133i 0.3985 + 0.1683i 0.1904 - 0.0575i -0.2519 + 0.1605i 0.3528 + 0.1098i 0.2924 + 0.2830i 0.0595 - 0.1749i -0.3949 - 0.1124i -0.3052 + 0.1304i 0.5112 - 0.2972i -0.0755 - 0.4383i 0.3266 - 0.3604i -0.3949 - 0.1124i -0.1440 + 0.2510i -0.0049 + 0.2705i … -0.1162 - 0.3727i -0.0648 - 0.2974i -0.0177 - 0.2267i -0.2034 + 0.0548i -0.0352 - 0.3251i 0.0709 - 0.0592i -0.3009 + 0.3806i -0.1825 - 0.4514i -0.4636 + 0.1430i 0.0111 + 0.0995i -0.4061 - 0.0636i -0.1006 - 0.4420i 0.1034 - 0.2690i 0.7401 - 0.0802i -0.0695 + 0.1943i -0.3844 + 0.4339i 0.2077 + 0.0577i -0.1192 - 0.1341i 0.2391 - 0.6253i -0.1846 - 0.2280i 0.6084 - 0.0748i -0.5224 + 0.1717i 0.2217 + 0.0637i -0.2966 + 0.0553i
12	-0.1799 + 0.0182i -0.3752 - 0.0780i -0.0550 + 0.5153i -0.6672 + 0.0053i -0.4456 + 0.2529i -0.1911 + 0.0966i 0.2918 + 0.4154i 0.3932 - 0.2216i 0.0912 + 0.2021i -0.2390 - 0.5541i 0.0746 + 0.1821i -0.4875 + 0.0236i -0.3001 + 0.3627i -0.0245 + 0.1734i -0.0135 + 0.0519i 0.0633 + 0.0018i 0.0004 - 0.1361i 0.0218 + 0.1235i 0.2107 - 0.0750i -0.0247 + 0.1896i 0.3250 + 0.4860i 0.0870 - 0.2467i -0.4553 + 0.1958i 0.2442 - 0.4576i -0.4704 + 0.0977i -0.2204 - 0.5670i 0.1762 + 0.0893i 0.2063 + 0.2215i 0.2710 + 0.0832i -0.4821 - 0.3798i -0.4475 + 0.0829i 0.0399 - 0.4588i -0.3544 - 0.4159i 0.0116 - 0.1629i 0.0416 + 0.5937i 0.2329 - 0.0193i … -0.1602 - 0.2034i -0.0230 - 0.0010i -0.3547 + 0.4951i -0.1954 - 0.0178i -0.5962 - 0.0794i -0.2205 + 0.3040i 0.0053 - 0.3703i -0.2725 + 0.1803i 0.1958 + 0.0695i 0.1745 + 0.2030i 0.4328 + 0.4512i -0.2995 - 0.1768i 0.2836 + 0.2482i 0.5987 - 0.4278i 0.5229 + 0.2682i 0.2627 - 0.0545i 0.0088 - 0.2753i -0.6204 + 0.2082i -0.2787 + 0.6350i -0.2270 + 0.3232i 0.3061 - 0.1277i -0.0315 + 0.0366i 0.1001 - 0.2319i -0.2803 + 0.1567i -0.2379 + 0.0987i -0.0976 + 0.0064i 0.1490 - 0.2797i -0.2829 - 0.6616i -0.1003 + 0.1802i -0.3775 - 0.1088i -0.0326 + 0.3247i -0.4007 - 0.1584i 0.1727 - 0.0154i -0.2890 + 0.4628i 0.2504 - 0.0492i 0.0224 + 0.2275i

18	-0.0536 + 0.2198i -0.2693 - 0.4333i -0.6187 - 0.3042i -0.3505 + 0.2617i -0.1589 + 0.2300i -0.1636 + 0.6216i 0.1610 + 0.2080i 0.0330 - 0.0319i -0.2020 + 0.0123i 0.0084 - 0.0715i 0.4481 - 0.4723i 0.0572 + 0.3221i -0.1757 - 0.3555i -0.1606 + 0.0675i -0.3890 - 0.1223i -0.1811 - 0.1130i 0.2193 + 0.0070i 0.0979 - 0.0995i 0.1967 - 0.2453i 0.3753 - 0.4278i -0.1664 + 0.1142i 0.4995 + 0.3997i 0.1433 + 0.1017i 0.1512 - 0.0650i -0.3967 - 0.6296i -0.3954 - 0.2248i -0.1870 + 0.4162i -0.3456 - 0.0821i 0.1803 + 0.5078i -0.3314 + 0.4116i 0.2579 - 0.0575i -0.0923 + 0.4099i -0.2609 - 0.0201i 0.1127 + 0.4580i 0.2118 + 0.2895i -0.2658 - 0.2887i … -0.0836 - 0.0713i -0.1902 + 0.2305i -0.1258 - 0.3152i -0.0598 - 0.0660i -0.0416 - 0.6963i -0.2187 + 0.0966i 0.2830 + 0.0819i 0.2434 + 0.5321i 0.1513 + 0.2619i -0.0409 - 0.3969i -0.1199 + 0.4086i -0.3253 - 0.6174i -0.2828 + 0.4158i 0.5634 + 0.1299i 0.3199 - 0.3650i -0.0537 - 0.1960i 0.0041 - 0.2080i 0.0488 - 0.3033i -0.6601 + 0.2903i -0.2645 + 0.2004i 0.2574 + 0.1827i -0.1445 + 0.3869i 0.2050 - 0.2825i -0.0355 - 0.1696i 0.1783 + 0.0362i 0.0462 - 0.2951i 0.0834 + 0.3910i -0.4705 + 0.2520i 0.3482 + 0.0103i -0.2860 - 0.4483i 0.1443 + 0.2727i -0.0046 - 0.1861i -0.5331 - 0.1190i 0.5797 - 0.0054i 0.1597 - 0.1420i -0.1695 + 0.1414i … -0.3305 - 0.1589i -0.3229 - 0.1153i -0.3847 - 0.2045i -0.2858 + 0.0966i -0.0293 - 0.3977i -0.3220 - 0.2467i -0.0072 - 0.1362i 0.0003 + 0.1612i -0.0727 + 0.2529i -0.4430 - 0.4194i -0.4484 - 0.0575i 0.4686 - 0.0367i 0.2791 - 0.6295i -0.1596 + 0.0026i 0.3451 + 0.3977i -0.1290 + 0.3090i 0.6156 + 0.1897i -0.2436 - 0.0584i -0.0907 + 0.2319i 0.1119 + 0.1202i 0.5727 - 0.0428i -0.3128 + 0.3001i 0.0484 - 0.3115i 0.5536 + 0.0751i 0.2236 - 0.0605i 0.3439 + 0.1623i 0.0183 + 0.3426i 0.1422 - 0.1277i -0.0379 - 0.2246i -0.2479 + 0.1114i 0.1836 - 0.4726i 0.7750 + 0.2425i 0.0941 + 0.0857i -0.2265 - 0.3859i -0.2611 + 0.0467i 0.0434 - 0.4048i
24	-0.1205 - 0.0906i -0.2429 + 0.0101i -0.1958 + 0.0334i -0.5558 - 0.3450i -0.0762 - 0.2053i -0.1104 + 0.1181i 0.2126 - 0.1759i 0.0735 + 0.2287i -0.0088 - 0.1481i -0.0654 - 0.0106i -0.2058 - 0.6040i -0.3184 + 0.2838i 0.2841 + 0.1491i -0.5703 + 0.1454i -0.0281 - 0.6488i -0.0644 - 0.1848i -0.0863 + 0.1620i 0.5370 + 0.1881i -0.6343 - 0.0281i -0.1898 + 0.2781i 0.5698 - 0.2672i -0.0118 - 0.2547i 0.1953 - 0.6045i 0.1292 - 0.1513i 0.2070 + 0.2441i -0.0429 + 0.1770i 0.0323 + 0.2969i -0.5527 + 0.3919i 0.0008 - 0.2196i -0.2188 - 0.4891i 0.2647 - 0.4717i -0.2798 + 0.5585i -0.1664 - 0.0624i 0.0639 - 0.0334i 0.2386 + 0.0484i 0.1780 + 0.3312i … -0.1405 + 0.7400i -0.3438 + 0.3117i -0.2251 + 0.1306i -0.1659 + 0.5745i -0.0835 - 0.7271i -0.3349 + 0.1225i 0.3308 - 0.1548i -0.0342 - 0.1486i 0.1171 - 0.0360i 0.0376 + 0.3678i 0.2232 + 0.2730i 0.5830 + 0.4476i 0.1930 - 0.2437i -0.0099 - 0.1051i -0.4569 - 0.0981i -0.3908 + 0.2070i -0.0484 - 0.2027i -0.3928 - 0.1026i 0.0669 + 0.3682i 0.4912 + 0.0310i 0.5227 + 0.2637i -0.1248 - 0.0970i -0.0507 + 0.3744i 0.0820 - 0.1718i -0.1003 - 0.0071i 0.5636 - 0.2794i -0.2933 + 0.3081i -0.5188 + 0.0279i 0.0441 - 0.0585i 0.2717 + 0.0624i 0.1977 - 0.1158i 0.1010 - 0.3195i 0.4177 - 0.0264i 0.0819 - 0.0917i -0.1485 - 0.3556i 0.2313 + 0.0170i … -0.3658 + 0.3791i -0.3840 - 0.1457i -0.2731 - 0.0015i -0.1237 - 0.4324i -0.4458 - 0.3228i -0.3369 - 0.2023i -0.2440 + 0.3924i 0.3868 - 0.5010i 0.1135 - 0.0866i -0.0334 + 0.2990i -0.3695 - 0.2152i -0.0237 - 0.0792i 0.1990 + 0.2832i 0.0352 - 0.3687i 0.1787 + 0.1482i 0.1434 + 0.1604i 0.2443 + 0.1392i 0.2139 + 0.2847i 0.4762 + 0.3122i 0.0183 - 0.0049i -0.0222 - 0.4405i 0.7431 - 0.2009i 0.1677 - 0.1024i -0.1170 - 0.0208i -0.0914 + 0.2299i -0.1498 - 0.2164i 0.6446 + 0.0964i 0.1748 - 0.1145i 0.1808 + 0.2664i -0.1995 - 0.6235i -0.0604 + 0.0091i 0.3436 - 0.3252i 0.1246 + 0.4651i 0.0934 - 0.1258i -0.3477 - 0.4148i -0.2578 - 0.4502i …

	-0.2107 - 0.0633i	-0.2499 - 0.0492i	-0.1906 + 0.0636i	-0.0005 - 0.2597i	-0.4153 + 0.0351i	-0.1159 + 0.2327i
	0.3673 + 0.2826i	0.2659 - 0.2545i	0.1698 + 0.4714i	0.1146 + 0.3938i	0.0363 + 0.3590i	-0.2075 - 0.1135i
	0.2240 + 0.5811i	-0.1207 + 0.2402i	-0.1359 + 0.1650i	0.6185 + 0.0954i	0.0692 - 0.0723i	0.6153 + 0.2655i
	0.0808 + 0.1921i	-0.2030 - 0.1218i	0.2503 + 0.4427i	-0.0807 - 0.2431i	0.1282 + 0.0604i	-0.2904 + 0.2418i
	0.4247 + 0.0662i	-0.4125 - 0.5222i	0.0571 - 0.6091i	-0.1775 + 0.3962i	-0.1271 + 0.0215i	0.1794 + 0.3055i
	-0.2556 - 0.2355i	0.1366 + 0.4580i	0.1723 - 0.0152i	-0.2674 - 0.2171i	0.2468 - 0.7671i	-0.0960 + 0.3870i

NOTE: All of spreading codebooks are normalized by multiplying $P_{no,N,K}$, which is ($K \times K$) normalized matrix for the power constraints, $P_{no,N,K} = \begin{bmatrix} P_{no,1} & 0 & 0 & 0 \\ 0 & P_{no,2} & 0 & 0 \\ 0 & 0 & \ddots & 0 \\ 0 & 0 & 0 & P_{no,K} \end{bmatrix}$. Here, $P_{no,k} = \left(1/\left|c^{(k)}\right|\right) \times \sqrt{N}, for\ k = 1, \ldots, K$.

Above tables A.4.4-1, A.4.4-2 and A.4.4-3 can be quantized via coefficients from 64QAM modulation as follows.

- Examples of 64QAM-quantized Grassmannian Sequence based spreading codebook

Table A.4.4-4: 64QAM-quantized Grassmannian Sequence based codebook for Spreading Factor: *N* = 2

# of sequence (*K*)	Examples of spreading codebook $\left[c^{(1)} \quad \cdots \quad c^{(K)}\right]$											
2						5+5i	5+5i					
						5+5i	-5-5i					
3					-5+7i		-5-1i		-5+1i			
					-1+3i		7+5i		-5-7i			
4				-3+5i		-3+7i		-1-3i		-7-3i		
				3+7i		-3+1i		7-3i		5+3i		
6		-3+1i		-7-3i		-1-5i		-5+3i		-1-7i	-7+1i	
		7-3i		-5+3i		-1-7i		-5-5i		-1-1i	3-3i	
8	-3-7i		-7-1i		-3-1i		-1-5i		-3-1i	-7+1i	-3-7i	-1+5i
	-1-3i		1-5i		-1+7i		-5-7i		1-7i	3+1i	-5+1i	-1-7i
12	-5-5i	-3-3i	-7-3i	-3-3i	-3+1i	-1-7i	-7+1i	-7-3i	-1-3i	-7-3i	-3+7i	-1-7i
	7-3i	1+7i	1+1i	-1-7i	1-7i	-7-1i	-1-3i	-3-5i	-7+1i	1+5i	1-7i	-1-3i

Table A.4.4-5: 64QAM-quantized Grassmannian Sequence based codebook for Spreading Factor: *N* = 4

# of sequence (*K*)	Examples of spreading codebook $\left[C^{(1)} \quad \cdots \quad C^{(K)}\right]$
4	5+5i 5+5i 5+5i 5+5i 5+5i -5-5i 5+5i -5-5i 5+5i 5+5i -5-5i -5-5i 5+5i -5-5i -5-5i 5+5i
6	-7+3i -3+1i -1-7i -1+1i -7+5i -3+1i -5+1i -1-5i -3+1i 3+5i -3-7i 5+7i 3+1i -1-7i -1-3i -1+7i 3+3i 5-7i 1-7i -7+3i -3+1i -5+5i -1+3i 1+3i
8	-5-3i -7+1i -1-3i -7-3i -1-3i -5-3i -5-3i -7+7i 1-5i 1+3i -7+7i 5-1i 7-3i 3+1i -1+5i -5+5i -7-3i 1-7i -1+3i 7+1i -5+7i -3-5i -5+3i -1-1i 1-3i 1-7i -5+7i -3+5i 1+1i -7+7i 7-5i 3+1i
12	-1+3i -3+1i -5-3i -3+5i -5+3i -5-3i -3-3i -5+1i -3-7i -7-5i -7-3i -7-3i 7-1i 7-1i -7+1i 3+3i 1-1i -7+7i 3-3i 7-5i -1-1i 1+1i 5-7i 1+3i 1-7i 3-5i 5+3i -3+5i -1+5i -1-3i 7-1i -1-1i -1-5i 3-5i -1+3i -1+7i 3+7i 3-7i 5-5i -5-7i 7+5i -1+3i -5-5i -5+3i -1-7i 1+1i 3-5i -1-1i
24	-7-3i -7-1i -7+1i -5-1i -3-3i -7+5i -3-3i -1+1i -3+1i -3+3i -3-7i -7-7i -3-1i 7+3i 5+3i 3+1i -5-5i -1-7i 7+1i -5-1i -1-7i -5-5i -3+1i -1-5i 3+7i -3+1i 3-1i 1+3i 7+1i -5-1i -3-3i -3+7i 7-1i -3-7i -1-7i 3+1i 5-3i 3+5i -3-7i -7+7i -1+7i 1-3i -5+1i -5+5i 5-3i 1+5i 1-5i -1-5i … -5-3i -1-3i -1+7i -1-1i -5+1i -3-7i -1+7i -1+1i -3-7i -7-1i -7-1i -5+1i -3+7i -1-1i -1-1i 7-3i -7+1i 5+1i 7+5i -3-7i -1-5i 1-1i -1+3i 3+3i -5+7i 1-7i -1-7i 3+1i -3+1i -7+3i -1-3i -3+5i -3-1i 3-1i -7+1i -5-7i -1-1i -7-3i 3-1i 3-5i 3-7i 1-3i 1+1i -1-7i -5+3i 7-3i 7-1i -1+1i

Table A.4.4-6: 64QAM-quantized Grassmannian Sequence based codebook for Spreading Factor: *N* = 6

# of sequence (*K*)	Examples of spreading codebook $\left[c^{(1)} \quad \cdots \quad c^{(K)}\right]$
6	-1+3i -7-5i -3-1i -5-7i -1+1i -3+7i 3+7i -1+5i 7+3i 3-1i 1-1i -3+5i -7-1i -1+7i -3-3i 5-1i -5-1i 1+5i 1+3i -7+3i 1-5i -1-3i -3+5i -3-7i 1+7i -3-1i -5-5i 7+7i 5+1i 1+3i -3-5i -1+1i 3-1i 3-5i 7+7i 5-1i
9	-3-7i -1+3i -7-3i -7-7i -5+5i -1-5i -1-5i -1-3i -3+1i -5+3i 5-7i -1+1i -1-5i -1-5i -1-5i 1-1i -5+7i -3-7i 5-3i 3-3i -1-7i 1+7i -3+5i -7+3i 1+1i -7-1i -1-7i 5-1i 7+3i 3-1i -3+3i 5+1i 1-5i 7-1i -1+3i -7+7i 5+5i 1-3i -7-1i -5+3i 7-5i 3+1i -1-3i 3-7i -3-3i -1-7i 5-5i 5-1i -3+3i -1+5i 7-1i -7+3i 3+1i -5+1i
12	-3+1i -5-1i -1+7i -7+1i -7+5i -3+1i -3-3i -1-1i -5+7i -3-1i -7-1i -3+5i 5+7i 7-3i 1+3i -3-7i 1+3i -7+1i 1-5i -5+3i 3+1i 3+3i 7+7i -5-3i -5+5i -1+3i -1+1i 1+1i 1-3i 1+1i 5+3i 7-7i 7+5i 5-1i 1-5i -7+3i 3-1i -1+3i 5+7i 1-3i -7+3i 3-7i -5+7i -3+5i 5-3i -1+1i 1-3i -5+3i -7+1i -3-7i 3+1i 3+3i 5+1i -7-7i -3+1i -1+1i 3-5i -5-7i -1+3i -5-1i -7+1i 1-7i -5-7i 1-3i 1+7i 3-1i -1+5i -7-3i 3-1i -5+7i 3-1i 1+3i
18	-1+3i -5-7i -7-5i -5+5i -3+3i -3+7i -1-1i -3+3i -1-5i 3+3i 1-1i -3+1i 1-1i 7-7i 1+5i 5+1i 3+7i 3+5i -3-5i -3+1i -7-1i -3-1i 3+1i 1-1i -5+7i 7+3i 5-5i 3-3i 5-7i -3+1i 7+7i 3+1i 3-1i -7+5i -5+3i 5+3i -7-7i -7-3i -3+7i -5-1i 3+7i -5+7i 3+1i 1-5i 1+7i 5-1i -1+7i -5-1i 1+7i 3+5i -5-5i 3+5i -1-3i -7-1i … -1-1i -1-7i -3+1i -5-3i -5-1i -7-3i -5+1i -1-7i -5-3i -1-7i -1+7i -5-7i -1-3i 1+3i -1+5i -7-7i -7-1i 7-1i -1-3i 1-3i 1-5i 5-7i -3+1i 5+7i -3+5i 7+3i -3-1i -3+7i 3-5i -1-3i -1+3i 1+1i 7-1i -5+5i 1-5i 7+1i -7+5i 5+1i -5-7i 3-1i 5+3i 1+5i 3-3i -1-3i -3+1i 7-1i 3-3i -3+3i 3-7i 7+3i 1+1i -3-7i -5+1i 1-7i

24	-1-1i -3+1i -3+1i -7-5i -1-3i -1+1i -3+7i -5+5i -3+3i -3+7i -1-7i -5+1i 3-3i 1+3i -1-3i -1-1i -3-7i -5+5i 5-3i -1-3i 1-1i 1+5i 3+5i 7+7i 5+3i -7+3i -1-7i -1-3i -1+3i 7+3i 3-3i -1-1i -7-1i -7+3i -1-3i -7-1i -7-1i -3+5i 7-5i -1-5i 3-7i 3-3i 1+5i 7+1i 7+5i -1-1i -1+5i 1-3i 3+3i -1+3i 1+5i -7+7i 1-3i -3-7i -1-1i 7-5i -5+5i -7+1i 1-1i 5+1i 5-7i -5+7i -3-1i 1-1i 3+1i 3+5i 3-1i 1-5i 7-1i 1-1i -3-5i 3+1i … -5+7i -7-3i -5-1i -1-7i -7-5i -5-3i -3-1i -3-1i -3+1i -1-5i -7+1i -1+3i -3+7i 7-7i 1-1i -1+5i -5-3i -1-1i 5+5i 5-5i 3+7i 1+7i 1+5i -3-1i 3+5i 1-5i 3+3i 3+3i 3+3i 3+5i 3+7i -1+3i -3+3i 7+1i 1-1i 7+5i 7+5i 1-1i -1-7i 7-3i 3-1i -1-1i 1+3i -3-1i 3+7i -1-3i 3+1i -5+3i -1+3i -3-3i 7+1i 3-1i 3+5i -3-7i 7+1i -7-7i 1-7i -3+7i -3+1i 3+5i -1+1i 5-5i 1+7i 1-1i -5-7i -5-7i -5-3i 3+7i 3-1i -5-3i '3-7i' -1+7i

NOTE: All of spreading codebooks are normalized by multiplying $P_{no,N,K}$, which is ($K \times K$) normalized matrix for the power constraints, $P_{no,N,K}=\begin{bmatrix} P_{no,1} & 0 & 0 & 0 \\ 0 & P_{no,2} & 0 & 0 \\ 0 & 0 & \ddots & 0 \\ 0 & 0 & 0 & P_{no,K} \end{bmatrix}$. Here, $P_{no,k}=\left(1/\left|c^{(k)}\right|\right)\times\sqrt{N}, for\ k=1,\ldots,K$.

NOTE: Tables A.4.4-1, A.4.4-2 and A.4.4-3 can be quantized by other coefficients, e.g., QPSK, 9QAM, 16QAM.

A.4.5 Algorithms of constructing GWBE sequences

Table A.4.5-1: Algorithms of constructing GWBE sequences S for any spreading factor *N*, number of users *K*, received powers $\{P_1,\ldots,P_K\}$

1: Find the set of oversized users K satisfying $P_k > \frac{\sum_{i=1}^{K} P_i \cdot sign\{P_i > P_k\}}{N - \sum_{i=1}^{K} sign\{P_i \geq P_k\}}$ for $k \in K$
2: Construct a matrix $Q \in C^{(K-\lvert K\rvert)\times(K-\lvert K\rvert)}$ with diagonal elements $\{P_i \vee i \notin K\}$ and eigenvalues $\left[\frac{\sum_{i\notin K} P_i}{N-\lvert K\rvert}1_{N-\lvert K\rvert}^{T}, 0_{(K-N)\times 1}^{T}\right]^{T}$ with "Generalized Chan-Li" or "Generalized Bendel-Mickey" algorithms in [37]
3: Decompose $Q=UV U^{H}$, where U is the matrix of eigenvectors
4: Denote the eigenvectors in U corresponding to the non-zero eigenvalues as $\breve{U} \in C^{(K-\lvert K\rvert)\times(K-\lvert K\rvert)}$ and the non-zero eigenvalues as $\breve{\Lambda}=\frac{\sum_{i\notin K} P_i}{N-\lvert K\rvert} I_{N-\lvert K\rvert}$
5: Construct sequences $\breve{S}=\breve{\Lambda}\breve{U}\breve{P}^{\frac{-1}{2}}$, where $\breve{P}=diag\{P_i \vee i \in K\}$

6: Construct $S=C_{orth}\begin{bmatrix} I_{|K|} & 0_{|K|\times(K-|K|)} \\ 0_{(N-|K|)\times|K|} & \breve{S} \end{bmatrix}$, where $C_{orth}\in C^{N\times N}$ is any orthogonal matrix satisfying $C_{orth}C_{orth}^{H}=I_N$.

Table A.4.5-2: Example for GWBE sequences with unit norm before quantization (Spreading factor = 4, Number of users = 8, Number of groups = 2, Received power offset = 6dB)

Sequences for group with high power	Sequences for group with low power
-0.3068-0.4002i -0.1823-0.2575i 0.2787+0.4238i 0.5287-0.3308i	-0.5 -0.5 -0.5 -0.5
-0.0229+0.3563i 0.869-0.2734i 0.0574+0.021i -0.0142-0.1965i	-0.8869-0.2366i 0.1684-0.0164i 0.1991+0.2087i -0.1898+0.0979i
-0.1936-0.4658i 0.2822-0.0885i -0.0736+0.3716i -0.7151+0.0569i	-0.118-0.1499i -0.0994-0.2647i 0.377-0.381i -0.6336-0.4415i
-0.3066+0.3717i -0.2369-0.2155i -0.7377+0.2445i 0.0236-0.2465i	0.5835-0.2329i -0.407+0.0047i 0.3753-0.453i -0.2874+0.1048i

Table A.4.5-3: Example for GWBE sequences quantized by {-2, -1, 0, 1, 2} before normalization (Spreading factor = 4, Number of users = 8, Number of groups = 2, Received power offset = 6dB)

Sequences for group with high power	Sequences for group with low power
-1- i - i 1+ i 2- i	-1 -1 -1 -1
i 2- i 0 - i	-2-i 1 1+i -1
-1- i 1 i -2	0 -i 1-i -2-i
-1+i -1-i -2+i -i	2-i -1 1- i -1

Table A.4.5-4: Example for GWBE sequences with unit norm before quantization (Spreading factor = 4, Number of users = 12, Number of groups = 2, Received power offset = 6dB)

Sequences for group with high power	Sequences for group with low power
0.1904+0.0145i 0.7272-0.514i -0.2103-0.2594i 0.2418-0.024i	-0.5 0.5 0.5 -0.5
0.3224-0.3367i -0.0836+0.6834i -0.1767+0.375i 0.3294-0.1684i	-0.4686-0.1212i -0.3517-0.4534i -0.059+0.1422i 0.5211-0.3757i
0.1415+0.2701i 0.3498+0.0601i -0.5172+0.3126i 0.1143-0.6347i	0.1485+0.1008i -0.0978-0.1169i -0.5555+0.3244i -0.5181+ 0.5121i
0.0739+0.3791i 0.4316+0.0877i -0.4466+0.191i -0.1158+0.6383i	-0.7443+0.2562i -0.0277-0.3199i -0.017+0.0495i 0.4254-0.3058i
-0.4567+0.3433i 0.0599+0.0521i 0.5939+0.4209i 0.2542+0.2697i	-0.3393-0.0337i -0.0657-0.1985i 0.1794-0.4201i -0.4464-0.6574i
0.0308 - 0.8351i 0.0303 - 0.0103i 0.026 - 0.4612i 0.0799+ 0.2843i	0.3945-0.0972i 0.3061+0.5307i -0.1173-0.2804i 0.0612-0.6028i

Table A.4.5-5 Example for GWBE sequences quantized by {-2, -1, 0, 1, 2} before normalization (Spreading factor = 4, Number of users = 12, Number of groups = 2, Received power offset = 6dB)

Sequences for group with high power	Sequences for group with low power
1 2-i -1-i 1	-1 2 2 -1
1-i 2i i 1	-1 -1-i i 2-i
1+i 1 -1+i 1-2i	1 0 -2+i -1+2i
i 2 -1+i 2i	-2+i -i 0 2-i
-1+i 0 2+2 i 1+ i	-1 0 1-i -1-2 i
-2i 0 -i i	1 1+2i -i -2i

Table A.4.5-6: Example for GWBE sequences with unit norm before quantization (Spreading factor = 4, Number of users = 16, Number of groups = 2, Received power offset = 6dB)

Sequences for group with high power	Sequences for group with low power
0.5747-0.3408i -0.2554+0.4933i -0.0064-0.3592i 0.1565-0.3023i	-0.5 -0.5 -0.5 -0.5
0.3786-0.2143i 0.0064-0.5928i -0.4637+0.2793i 0.0282-0.4069i	-0.4321+0.3191i -0.031-0.1271i -0.5079-0.1491i -0.4844-0.4237i
-0.0439+0.3734i 0.2209-0.0687i -0.3654+0.7617i 0.1165-0.279i	0.682+0.3864i -0.4349+0.1979i -0.3113-0.0085i 0.1355+0.2046i
0.2663-0.3807i -0.0548-0.1704i -0.1334+0.6523i 0.527+0.176i	-0.0278+0.654i -0.5421+0.2316i -0.4443+0.0596i 0.1428-0.0523i
0.3714+0.1164i -0.2134+0.3388i 0.1225+0.2758i -0.7398+0.2234i	-0.1467+0.6878i -0.2674+0.1785i -0.1723+0.3663i 0.1277+0.4711i
0.1216-0.537i -0.0764-0.2757i -0.3015+0.0669i -0.7202+0.0299i	0.4229-0.576i 0.411+0.0295i 0.1824+0.2432i 0.417-0.2307i
0.212+0.2656i -0.633-0.5417i 0.1693-0.398i 0.0549+0.0147i	-0.1062-0.3379i -0.1145-0.1416i 0.7577+0.0774i 0.4096-0.3057i
-0.148+0.4161i 0.1072+0.5946i 0.1729+0.301i -0.1189-0.5525i	-0.3009-0.4003i -0.5465+0.6044i 0.1188+0.1732i 0.1014-0.1756i

Table A.4.5-7: Example for GWBE sequences quantized by {-2, -1, 0, 1, 2} before normalization (Spreading factor = 4, Number of users = 16, Number of groups = 2, Received power offset = 6dB)

Sequences for group with high power	Sequences for group with low power
2-i -1+2i -i -i	-2 -2 -2 -2
1-i -2i -2+i -i	-1+i 0 -2-i -2-i
i 1 -1+2i -i	2+i -1+i -1 i
1-i -i 2i 2+i	2i -2+i -2 0
1 -1+i i -2+i	-1+2i -1+1 i -1+1 i 2i
-2i -i -1 -2	1-2i 1 1+ i 1-i
1+i -2-2i 1-i 0	-i -i 2 1-i
-1+i 2i 1+i -2 i	-1-i -2+2i i -i

A.4.6 Examples of QPSK based sequences

Table A.4.6-1: $\varphi(n)$ for SF=4

u	$\varphi(0),...,\varphi(3)$			
0	3	3	1	3
1	-3	-3	-3	1
2	-3	-1	-1	-1
3	-1	-1	-3	-3
4	1	3	-1	-1
5	1	-1	-1	-3
6	-3	1	-1	-3
7	1	1	3	-3
8	1	3	1	-3
9	-1	3	1	-3

Table A.4.6-2: $\varphi(n)$ for SF=6

u	$\varphi(0),..., \varphi(5)$					
0	-1	-3	3	-	3	-3
1	-1	3	-1	1	1	1
2	3	-1	-3	-	1	3
3	3	-1	-1	1	-1	-1
4	-1	-1	-3	1	-3	-1
5	1	3	-3	-	-3	3
6	-3	3	-1	-	1	-3
7	-1	-3	-3	1	3	3
8	3	-1	-1	3	1	3
9	3	-3	3	1	-1	1
10	-3	1	-3	-	-3	-3
11	-3	-3	-3	1	-3	-3
12	3	-3	1	-	-3	-3
13	3	-3	3	-	-1	-3
14	3	-1	1	3	3	1
15	-1	1	-1	-	1	1
16	-3	-1	-3	-	3	3
17	1	-1	3	-	3	3
18	1	3	1	1	-3	3
19	-1	-3	-1	-	3	-3
20	3	-1	-3	-	-1	-3
21	3	1	3	-	-3	1
22	1	3	-1	-	1	-1
23	-3	1	-3	3	3	3
24	1	3	-3	3	-3	3
25	-1	-1	1	-	1	-1
26	1	-3	-1	-	3	1
27	-3	-1	-1	3	1	1
28	-1	3	-3	-	-3	3
29	3	1	-1	1	3	1

Table A.4.6-3: $\varphi(n)$ for SF=12.

u	$\varphi(0),..., \varphi(11)$											
0	-1	1	3	-3	3	3	1	1	3	1	-3	3
1	1	1	3	3	3	-1	1	-3	-3	1	-3	3
2	1	1	-3	-3	-3	-1	-3	-3	1	-3	1	-1
3	-1	1	1	1	1	-1	-3	-3	1	-3	3	-1
4	-1	3	1	-1	1	-1	-3	-1	1	-1	1	3
5	1	-3	3	-1	-1	1	1	-1	-1	3	-3	1
6	-1	3	-3	-3	-3	3	1	-1	3	3	-3	1
7	-3	-1	-1	-1	1	-3	3	-1	1	-3	3	1
8	1	-3	3	1	-1	-1	-1	1	1	3	-1	1
9	1	-3	-1	3	3	-1	-3	1	1	1	1	1
10	-1	3	-1	1	1	-3	-3	-1	-3	-3	3	-1
11	3	1	-1	-1	3	3	-3	1	3	1	3	3
12	1	-3	1	1	-3	1	1	1	-3	-3	-3	1
13	3	3	-3	3	-3	1	1	3	-1	-3	3	3
14	-3	1	-1	-3	-1	3	1	3	3	3	-1	1
15	3	-1	1	-3	-1	-1	1	1	3	1	-1	-3
16	1	3	1	-1	1	3	3	3	-1	-1	3	-1
17	-3	1	1	3	-3	3	-3	-3	3	1	3	-1
18	-3	3	1	1	-3	1	-3	-3	-1	-1	1	-3
19	-1	3	1	3	1	-1	-1	3	-3	-1	-3	-1
20	-1	-3	1	1	1	1	3	1	-1	1	-3	-1
21	-1	3	-1	1	-3	-3	-3	-3	-3	1	-1	-3
22	1	1	-3	-3	-3	-3	-1	3	-3	1	-3	3
23	1	1	-1	-3	-1	-3	1	-1	1	3	-1	1
24	1	1	3	1	3	3	-1	1	-1	-3	-3	1
25	1	-3	3	3	1	3	3	1	-3	-1	-1	3
26	1	3	-3	-3	3	-3	1	-1	-1	3	-1	-3
27	-3	-1	-3	-1	-3	3	1	-1	1	3	-3	-3
28	-1	3	-3	3	-1	3	3	-3	3	3	-1	-1
29	3	-3	-3	-1	-1	-3	-1	3	-3	3	1	-1

A.4.7 Examples of unequal weighted sparse spreading pattern

Table A.4.7-1: Examples of different sparse spreading pattern with elements selected from {0, 1}

Overloading factor	Sparse spreading pattern
150%	$G_{PDMA,Type1}^{[4,6]} = \begin{bmatrix} 1 & 0 & 1 & 1 & 0 \\ 0 & 1 & 1 & 0 & 1 \\ 1 & 1 & 0 & 1 & 1 \\ 1 & 1 & 0 & 0 & 0 \end{bmatrix}$
200%	$G_{PDMA,type1}^{[4,8]} = \begin{bmatrix} 0 & 0 & 1 & 1 & 0 & 0 & 0 \\ 1 & 1 & 0 & 0 & 1 & 0 & 0 \\ 1 & 0 & 1 & 0 & 0 & 1 & 0 \\ 0 & 1 & 0 & 0 & 0 & 0 & 1 \end{bmatrix}$
300%	$G_{PDMA,type1}^{[4,12]} = \begin{bmatrix} 0 & 1 & 1 & 1 & 0 & 0 & 0 & 1 & 0 & 0 & 0 \\ 1 & 1 & 0 & 0 & 1 & 1 & 0 & 0 & 1 & 0 & 0 \\ 1 & 0 & 1 & 0 & 1 & 0 & 1 & 0 & 0 & 1 & 0 \\ 1 & 0 & 0 & 1 & 0 & 1 & 1 & 0 & 0 & 0 & 1 \end{bmatrix}$

Table A.4.7-2: Examples of different sparse spreading pattern with elements selected from {0, 1, -1, j, -j}

k	g_k				k	g_k				k	g_k			
0	1	j	-1	-j	**32**	1	1	j	-1	**64**	1	-1	-j	0
1	1	-j	-1	j	**33**	1	j	-1	-1	**65**	1	j	-j	1
2	1	-1	1	-1	**34**	1	0	0	-1	**66**	1	-1	j	0
3	1	-1	-j	j	**35**	1	1	-j	-1	**67**	0	1	-j	j
4	1	-1	j	-j	**36**	1	-j	-1	-1	**68**	0	1	-1	j
5	1	-1	-1	1	**37**	0	1	0	j	**69**	1	-j	j	0
6	1	j	-j	-1	**38**	1	0	j	0	**70**	1	-1	1	1
7	1	-j	j	-1	**39**	1	1	0	-1	**71**	1	1	-1	1
8	1	j	-j	j	**40**	1	0	-1	-1	**72**	1	-j	j	1
9	1	-1	1	j	**41**	1	j	j	-1	**73**	1	-1	j	-1
10	1	j	0	-1	**42**	1	j	-1	j	**74**	1	j	1	-1
11	1	0	j	-1	**43**	1	-j	1	j	**75**	1	-j	1	-1
12	1	-j	j	-j	**44**	1	-1	0	1	**76**	1	-1	-j	-1
13	1	-1	1	-j	**45**	1	0	-1	1	**77**	1	1	-1	j
14	1	0	-1	j	**46**	1	j	1	-j	**78**	1	-j	j	j
15	1	-j	0	j	**47**	1	-j	-1	-j	**79**	1	-1	0	-j
16	1	j	-1	0	**48**	0	1	0	-j	**80**	1	0	j	-j
17	0	1	j	-1	**49**	1	0	-j	0	**81**	1	1	-j	0
18	1	j	-1	1	**50**	1	-j	-j	-1	**82**	0	1	1	-j
19	1	-1	-j	1	**51**	1	-j	0	0	**83**	1	-j	-j	0
20	0	1	-1	1	**52**	0	0	1	-j	**84**	0	1	-j	-j
21	1	-1	1	0	**53**	0	1	-j	0	**85**	1	-1	-1	-j
22	1	0	-j	-1	**54**	0	1	-j	1	**86**	1	j	j	-j
23	1	-j	0	-1	**55**	0	1	j	1	**87**	0	1	j	j
24	1	j	0	-j	**56**	1	j	1	0	**88**	1	j	j	0
25	0	1	-j	-1	**57**	1	-j	1	0	**89**	1	1	j	0
26	1	0	-1	-j	**58**	0	0	1	j	**90**	1	1	j	-j
27	1	-j	-1	0	**59**	0	1	j	0	**91**	0	1	1	j
28	1	0	-1	0	**60**	1	j	0	0	**92**	1	-1	-j	-j
29	0	1	0	-1	**61**	0	1	j	-j	**93**	0	1	-1	0
30	1	-j	-1	1	**62**	0	1	-1	-j	**94**	1	-1	0	0
31	1	-1	j	1	**63**	1	j	-j	0	**95**	0	0	1	-1

Table A.4.7-3: Examples of different sparse spreading pattern with elements selected from {0, 1, -1, j, -j}

k	g_k				k	g_k			
0	1	j	-1	-j	**32**	1	1	j	-1
1	1	-j	-1	j	**33**	1	j	-1	-1
2	1	-1	1	-1	**34**	1	0	0	-1
3	1	-1	-j	j	**35**	1	1	-j	-1
4	1	-1	j	-j	**36**	1	-j	-1	-1
5	1	-1	-1	1	**37**	0	1	0	j
6	1	j	-j	-1	**38**	1	0	j	0
7	1	-j	j	-1	**39**	1	1	0	-1
8	1	j	-j	j	**40**	1	0	-1	-1
9	1	-1	1	j	**41**	1	j	j	-1
10	1	j	0	-1	**42**	1	j	-1	j
11	1	0	j	-1	**43**	1	-j	1	j
12	1	-j	j	-j	**44**	1	-1	0	1
13	1	-1	1	-j	**45**	1	0	-1	1
14	1	0	-1	j	**46**	1	j	1	-j
15	1	-j	0	j	**47**	1	-j	-1	-j
16	1	j	-1	0	**48**	0	1	0	-j
17	0	1	j	-1	**49**	1	0	-j	0
18	1	j	-1	1	**50**	1	-j	-j	-1
19	1	-1	-j	1	**51**	1	-j	0	0
20	0	1	-1	1	**52**	0	0	1	-j
21	1	-1	1	0	**53**	0	1	-j	0
22	1	0	-j	-1	**54**	0	1	-j	1
23	1	-j	0	-1	**55**	0	1	j	1
24	1	j	0	-j	**56**	1	j	1	0
25	0	1	-j	-1	**57**	1	-j	1	0
26	1	0	-1	-j	**58**	0	0	1	j
27	1	-j	-1	0	**59**	0	1	j	0
28	1	0	-1	0	**60**	1	j	0	0
29	0	1	0	-1	**61**	0	1	j	-j
30	1	-j	-1	1	**62**	0	1	-1	-j
31	1	-1	j	1	**63**	1	j	-j	0

A.4.8 MUI based sequence generation method

MUI is calculated using Equation 1. Where M represents the number of code words in a pool, v_i is a single code word that MUI parameter is evaluated toward. N is the length of the codeword.

$$MU\,I_i = \frac{N \cdot M}{\sum_{j=0,\, j \neq i}^{M-1} \left| \langle v_i, v_j \rangle \right|} \qquad \text{(A.4.8-1)}$$

To create a spreading code, it is first required to set the length of the spreading code. For an N -length code, we can create N orthogonal sequences. This will span the space of the spreading code. We will generate the code using complex Hadamard codes in normalized de-phased form. The construction equation is showed as Eq. (A.4.8-2) below.

$$\left[F_N\right] = e^{\frac{jk2\pi}{N}} \qquad \text{(A.4.8-2)}$$

After we create the orthogonal base, we start the creation of the non-orthogonal set.

First, we construct the hereby defined *hyperplanes* – we choose pairs of orthogonal vectors from the base set F_N . Each pair of orthogonal vectors defines a hyperplane. Therefore, for a set of N vectors we can define $K \equiv \binom{N}{2}$ orthogonal hyperplanes, as seen in Eq. (A.4.8-3).

$$K=\binom{N}{2}=\frac{N!}{2!(N-2)!}=\frac{N}{2}\cdot(N-1) \quad \text{(A.4.8-3)}$$

Second, we construct non-orthogonal vectors in each hyperplane. To do so, we need to decide how many non-orthogonal vectors we would like to create. Considering K hyperplanes, N orthogonal sequences and M required sequence pool size, the number of non-orthogonal vectors per hyperplanes L is calculated by Eq. (A.4.8-4). Looking at Eq. (A.4.8-4) it is seen that there is a flexibility at the size of the sequence pool that is dependent on L.

$$L=\lceil \frac{M-N}{K} \rfloor \quad \text{(A.4.8-4)}$$

To generate the new sequences, we will generate linear combination in each hyperplane by setting minimum cross correlation between the new vector and its building hyperplanes. This is called the *constraint of least projection* which is defined by $min(A,B)$.

Let us see an example of such an operation. Assume two orthogonal vectors $\vec{A},\vec{B}$ defined as in Eq. (A.4.8-5). It is possible to see that using α and β we create a linear combination to generate the new spreading sequence. To generate α and β we use $\theta_s := \frac{\pi * s}{2(L+1)}$ for $s=\{1,\ldots,L\}$ so that: $\alpha_s=\cos(\theta_s)$ and $\beta_s=\sin(\theta_s)$.

$$\vec{A}=\vec{a_1}+\vec{a_2}+\ldots+\vec{a_N}$$
$$\vec{B}=\vec{b_1}+\vec{b_2}+\ldots+\vec{b_N}$$
$$V^s_{non-orthogonal}=\alpha_s\cdot\vec{A}+i\cdot\beta_s\cdot\vec{B} \quad \text{(A.4.8-5)}$$

Last, we assign the MUI quality figure for each sequence by using Eq. (A.4.8-1). We will also look at the standard deviation as a comparison tool. An example sequence can be viewd in Table A.4.8-1.

Table A.4.8-1: N = 4, L = 2 proposed sequence pool

a_1	a_2	a_3	a_4
1	1	1	1
1	0+1i	-1	-0-1i
1	-1	1	-1
1	-0-1i	-1	0+1i
1.366	0.866+0.5i	0.366	0.866-0.5i
1.366	0.5+0.866i	-0.366	0.5-0.866i
1.366	0.366	1.366	0.366
1.366	-0.366	1.366	-0.366
1.366	0.866-0.5i	0.366	0.866+0.5i
1.366	0.5-0.866i	-0.366	0.5+0.866i
1.366	-0.5+0.866i	-0.366	-0.5-0.866i
1.366	-0.866+0.5i	0.366	-0.866-0.5i
1.366	-0+0.366i	-1.366	-0-0.366i
1.366	-0-0.366i	-1.366	-0+0.366i
1.366	-0.866-0.5i	0.366	-0.866+0.5i
1.366	-0.5-0.866i	-0.366	-0.5+0.866i

A.4.9 Examples of bits-to-symbols mapping function for symbol-level spreading with modified modulation

Table A.4.9-1: Mapping function for the 8-point modulated symbol sequence of length 2

Sequence index	1	2	3	4	5	6	7	8
Corresponding bit sequence	000	001	010	011	100	101	110	111
Output symbol sequence	$\begin{bmatrix} -a_8+jb \\ -a_8+jb \end{bmatrix}$	$\begin{bmatrix} a_8+j \\ a_8+j \end{bmatrix}$	$\begin{bmatrix} -a_8- \\ -a_8+ \end{bmatrix}$	$\begin{bmatrix} a_8- \\ a_8+ \end{bmatrix}$	$\begin{bmatrix} -a_8+ \\ -a_8- \end{bmatrix}$	$\begin{bmatrix} a_8+ \\ a_8- \end{bmatrix}$	$\begin{bmatrix} -a_8- \\ -a_8- \end{bmatrix}$	$\begin{bmatrix} a_8- \\ a_8- \end{bmatrix}$

with $a_8 = 0.5774$ and $b_8 = 0.8165$.

Table A.4.9-2: Mapping function for the 16-point modulated symbol sequence of length 2

Sequence index	1	2	3	4	5	6	7	8
Corresponding bit sequence	0000	0001	0010	0011	0100	0101	0110	0111
Output Symbol sequence	$\begin{bmatrix} 3+3j \\ 1+j \end{bmatrix}$	$\begin{bmatrix} -1+3 \\ 3+j \end{bmatrix}$	$\begin{bmatrix} 1+3j \\ -3+j \end{bmatrix}$	$\begin{bmatrix} -3+3 \\ -1+ \end{bmatrix}$	$\begin{bmatrix} 3-j \\ 1+3j \end{bmatrix}$	$\begin{bmatrix} -1-j \\ 3+3j \end{bmatrix}$	$\begin{bmatrix} 1-j \\ -3+3 \end{bmatrix}$	$\begin{bmatrix} -3-j \\ -1+3j \end{bmatrix}$
Sequence index	9	10	11	12	13	14	15	16
Corresponding bit sequence	1000	1001	1010	1011	1100	1101	1110	1111
Output Symbol sequence	$\begin{bmatrix} 3+j \\ 1-3j \end{bmatrix}$	$\begin{bmatrix} -1+j \\ 3-3j \end{bmatrix}$	$\begin{bmatrix} 1+j \\ -3-3 \end{bmatrix}$	$\begin{bmatrix} -3+ \\ -1-3 \end{bmatrix}$	$\begin{bmatrix} 3-3j \\ 1-j \end{bmatrix}$	$\begin{bmatrix} -1-3 \\ 3-j \end{bmatrix}$	$\begin{bmatrix} 1-3j \\ -3-j \end{bmatrix}$	$\begin{bmatrix} -3-3j \\ -1-j \end{bmatrix}$

Table A.4.9-3: Mapping function for the 64-point modulated symbol sequence of length 2

Sequence index	1	2	3	4	5	6	7	8
Corresponding bit sequence	000 000	000 001	000 01	000 011	000 10	000 101	000 11	000 111
Output symbol sequence	$\begin{bmatrix}1+j\\1+j\end{bmatrix}$	$\begin{bmatrix}1+3j\\1+3j\end{bmatrix}$	$\begin{bmatrix}1-j\\1+j\end{bmatrix}$	$\begin{bmatrix}1-3j\\1+3j\end{bmatrix}$	$\begin{bmatrix}3+j\\3+j\end{bmatrix}$	$\begin{bmatrix}3+3j\\3+3j\end{bmatrix}$	$\begin{bmatrix}3-j\\3+j\end{bmatrix}$	$\begin{bmatrix}3-3j\\3+3j\end{bmatrix}$
Sequence index	9	10	11	12	13	14	15	16
Corresponding bit sequence	001 000	001 001	001 01	001 011	001 10	001 101	001 11	001 111
Output symbol sequence	$\begin{bmatrix}-1+j\\1+j\end{bmatrix}$	$\begin{bmatrix}-1+3\\1+3j\end{bmatrix}$	$\begin{bmatrix}-1-\\1+j\end{bmatrix}$	$\begin{bmatrix}-1-3\\1+3j\end{bmatrix}$	$\begin{bmatrix}-3+j\\3+j\end{bmatrix}$	$\begin{bmatrix}-3+3\\3+3j\end{bmatrix}$	$\begin{bmatrix}-3-\\3+j\end{bmatrix}$	$\begin{bmatrix}-3-3\\3+3j\end{bmatrix}$
Sequence index	17	18	19	20	21	22	23	24
Corresponding bit sequence	010 000	010 001	010 01	010 011	010 10	010 101	010 11	010 111
Output symbol sequence	$\begin{bmatrix}1+j\\1-j\end{bmatrix}$	$\begin{bmatrix}1+3j\\1-3j\end{bmatrix}$	$\begin{bmatrix}1-j\\1-j\end{bmatrix}$	$\begin{bmatrix}1-3j\\1-3j\end{bmatrix}$	$\begin{bmatrix}3+j\\3-j\end{bmatrix}$	$\begin{bmatrix}3+3j\\3-3j\end{bmatrix}$	$\begin{bmatrix}3-j\\3-j\end{bmatrix}$	$\begin{bmatrix}3-3j\\3-3j\end{bmatrix}$
Sequence index	25	26	27	28	29	30	31	32
Corresponding bit sequence	011 000	011 001	011 01	011 011	011 10	011 101	011 11	011 111
Output symbol sequence	$\begin{bmatrix}-1+j\\1-j\end{bmatrix}$	$\begin{bmatrix}-1+3\\1-3j\end{bmatrix}$	$\begin{bmatrix}-1-\\1-j\end{bmatrix}$	$\begin{bmatrix}-1-3\\1-3\end{bmatrix}$	$\begin{bmatrix}-3+\\3-j\end{bmatrix}$	$\begin{bmatrix}-3+3\\3-3\end{bmatrix}$	$\begin{bmatrix}-3-\\3-j\end{bmatrix}$	$\begin{bmatrix}-3-3\\3-3j\end{bmatrix}$
Sequence index	33	34	35	36	37	38	39	40
Corresponding bit sequence	100 000	100 001	100 01	100 011	100 10	100 101	100 11	100 111
Output Symbol sequence	$\begin{bmatrix}1+j\\-1+j\end{bmatrix}$	$\begin{bmatrix}1+3j\\-1+3\end{bmatrix}$	$\begin{bmatrix}1-j\\-1+\end{bmatrix}$	$\begin{bmatrix}1-3\\-1+3\end{bmatrix}$	$\begin{bmatrix}3+j\\-3+\end{bmatrix}$	$\begin{bmatrix}3+3j\\-3+3\end{bmatrix}$	$\begin{bmatrix}3-j\\-3+\end{bmatrix}$	$\begin{bmatrix}3-3j\\-3+3\end{bmatrix}$
Sequence index	41	42	43	44	45	46	47	48
Corresponding bit sequence	101 000	101 001	101 01	101 011	101 10	101 101	101 11	101 111
Output Symbol sequence	$\begin{bmatrix}-1+j\\-1+j\end{bmatrix}$	$\begin{bmatrix}-1+3\\-1+3\end{bmatrix}$	$\begin{bmatrix}-1-\\-1+\end{bmatrix}$	$\begin{bmatrix}-1-3\\-1+3\end{bmatrix}$	$\begin{bmatrix}-3+\\-3+\end{bmatrix}$	$\begin{bmatrix}-3+3\\-3+3\end{bmatrix}$	$\begin{bmatrix}-3-\\-3+\end{bmatrix}$	$\begin{bmatrix}-3-3\\-3+3\end{bmatrix}$
Sequence index	49	50	51	52	53	54	55	56
Corresponding bit sequence	110 000	110 001	110 01	110 011	110 10	110 101	110 11	110 111
Output Symbol sequence	$\begin{bmatrix}1+j\\-1-j\end{bmatrix}$	$\begin{bmatrix}1+3\\-1-3\end{bmatrix}$	$\begin{bmatrix}1-j\\-1-\end{bmatrix}$	$\begin{bmatrix}1-3\\-1-3\end{bmatrix}$	$\begin{bmatrix}3+j\\-3-\end{bmatrix}$	$\begin{bmatrix}3+3\\-3-3\end{bmatrix}$	$\begin{bmatrix}3-j\\-3-\end{bmatrix}$	$\begin{bmatrix}3-3j\\-3-3\end{bmatrix}$
Sequence index	57	58	59	60	61	62	63	64
Corresponding bit sequence	111 000	111 001	111 01	111 011	111 10	111 101	111 11	111 111
Output Symbol sequence	$\begin{bmatrix}-1+j\\-1-j\end{bmatrix}$	$\begin{bmatrix}-1+3\\-1-3\end{bmatrix}$	$\begin{bmatrix}-1-\\-1-\end{bmatrix}$	$\begin{bmatrix}-1-3\\-1-3\end{bmatrix}$	$\begin{bmatrix}-3+\\-3-\end{bmatrix}$	$\begin{bmatrix}-3+3\\-3-3\end{bmatrix}$	$\begin{bmatrix}-3-\\-3-\end{bmatrix}$	$\begin{bmatrix}-3-3\\-3-3\end{bmatrix}$

Table A.4.9-4: Three mapping functions with 4-point low PAPR modulated symbol of length 4 (no sparsity is applied, only used when transform precoding is enabled in coverage limited case)

Sequence index	1	2	3	4
Corresponding bit sequence	00	01	10	11
Output symbol sequence	$\begin{bmatrix}1\\1\\1\\1\end{bmatrix}$	$\begin{bmatrix}1\\-j\\-1\\j\end{bmatrix}$	$\begin{bmatrix}-1\\j\\1\\-j\end{bmatrix}$	$\begin{bmatrix}-1\\-1\\-1\\-1\end{bmatrix}$
Sequence index	1	2	3	4
Corresponding bit sequence	00	01	10	11
Output symbol sequence	$\begin{bmatrix}1\\1\\1\\1\end{bmatrix}$	$\begin{bmatrix}1\\j\\-1\\-j\end{bmatrix}$	$\begin{bmatrix}-1\\-j\\1\\j\end{bmatrix}$	$\begin{bmatrix}-1\\-1\\-1\\-1\end{bmatrix}$
Sequence index	1	2	3	4
Corresponding bit sequence	00	01	10	11
Output symbol sequence	$\begin{bmatrix}1\\j\\-1\\-j\end{bmatrix}$	$\begin{bmatrix}1\\-j\\-1\\j\end{bmatrix}$	$\begin{bmatrix}-1\\j\\1\\-j\end{bmatrix}$	$\begin{bmatrix}-1\\-j\\1\\j\end{bmatrix}$

A.4.10 Examples of scalable MA signature design by multi-branch transmission

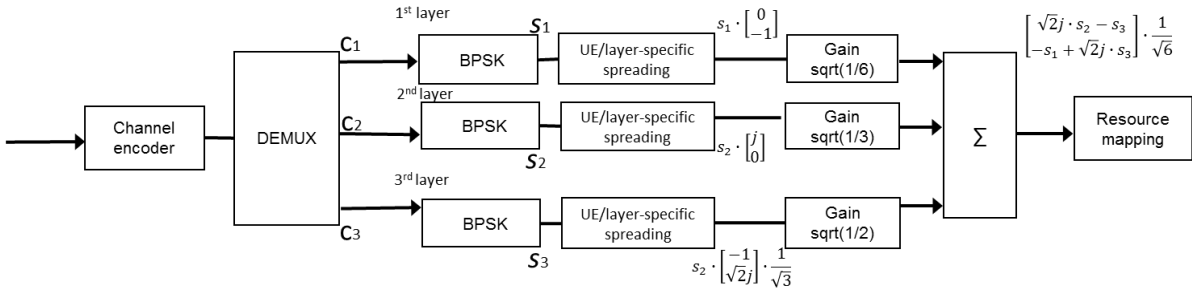

Figure A.4.10-1: Example of three branches transmissiton for symbol-level spreading with BPSK.

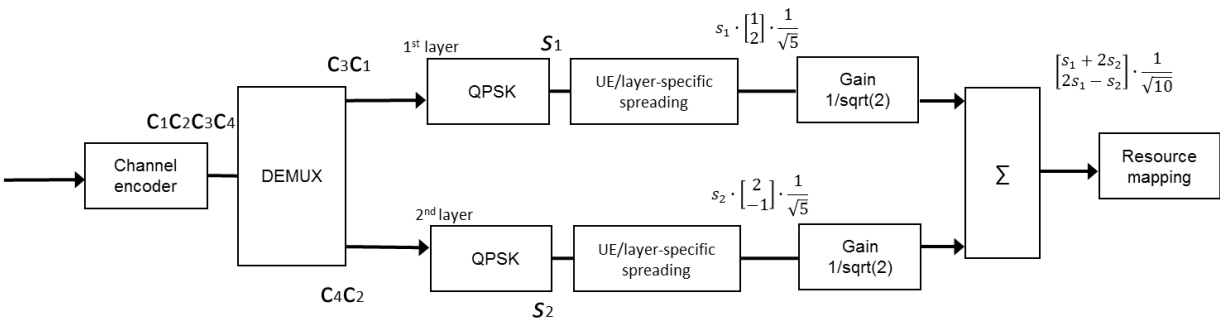

Figure A.4.10-2: Example of two branches transmission for symbol-level spreading with QPSK.

A.4.11 Method of bit level interleaving and symbol level interleaving with zero padding

- ***UE specific bit level interleaving***

The data matrix has X column(s) and Y row(s), the input bit sequence is $\boldsymbol{a}$ and output bit sequence $\boldsymbol{x}$, the starting position of the bit level interleaving for k_{th} UE is configured as $CS_{k\text{-}bit,}$

b=0;

for j = 0 to X-1

for i = 0 to Y-1

$$x_{i+j\cdot Y}=a_{b\cdot X+mod(j+CS_{k-bit},X)}$$

$b=b+1$

end for

end for

- ***UE specific symbol level interleaving with zero padding***

The zero row index set is $I=\{i_0,..,i_z\}$, e.g., if the zero pattern is [1,0,1,0], then the I={1,3}. The data symbol matrix has X column(s) and Y row(s) , the input symbol sequence is $\boldsymbol{S}$ and output symbol sequence $\boldsymbol{S'}$, and the interleaver starting position of the symbol level interleaving for k_{th} UE is configured as $CS_{k\text{-}symbol}$ (in addition, $CS_{k\text{-}symbol}$ can be equal to $CS_{k\text{-}bit}$),

b=0

for j = 0 to X-1

for i = 0 to Y-1

if $i\in I$

$$S'_{i+j\cdot Y}=0$$

else

$$S'_{i+j\cdot Y}=S_{b\cdot X+mod(j+CS_{k-symbol},X)}$$

b= b+1

end for

end for

A.4.12 Sequence grouping method

For any sequences pool with L sequences, the sequences pool can be divided into G groups for interference reduction and performance enhancement. For unequal received powers, only the cross-correlations among sequences in groups with lower received powers matter. Therefore, the optimal sequences in group g should satisfy

$$\min_{S_g} \sum_{m,n\geq g} \sum_{i\in K_m} \sum_{j\in K_n} \widetilde{P}_m \widetilde{P}_n \left| s_i^H s_j \right|^2 \quad , \qquad \text{(A.4.12-1)}$$

where S_g is composed by sequences for group g, K_m and $\widetilde{P}_m$ denote the set of sequences indices and average received power of group *m*, respectively, and $\widetilde{P}_1 \geq \cdots \geq \widetilde{P}_G$ without loss of generality. Based on Eq. (A.4.12-1), the sequences for the *G* groups can be obtained from the original sequence pool $S=\left[s_1, \cdots, s_L\right]$.

Considering the complexity of implementation and large storage requirement of optimal sequence grouping for any multi-level received powers, sub-optimal sequence grouping algorithm ignoring the exact power setup shown in Table A.4.12-1 and Table A.4.12-2 can be considered.

Table A.4.12-1: Algorithm for sequence grouping (For small power offset between adjacent groups)

1: Let $g=1$ and $S^{(1)}=S$ //Initialization

2: **loop**

3: **if** $g<G$ **then**

4: Compute matrix $C=\left|\left(S^{(g)}\right)^H S^{(g)}\right|$ //Cross-correlation matrix

5: Compute vector $c=\left[\sum_{j=1}^{L-\sum_{m=1}^{g-1} L_m} C_{1j}^2, \cdots, \sum_{j=1}^{L-\sum_{m=1}^{g-1} L_m} C^2_{\left(L-\sum_{m=1}^{g-1} L_m\right)j}\right]$, where C_{ij} is the element at the *i*-th row and *j*-th column of C //Sum cross-correlations of sequences in groups with the same or lower powers

6: Find the L_g smallest values in c and denote the index set as I_g //Find the index of sequences for group g

7: Define $S_g=\left[S^{(g)}\right]_{I_g}$ as sequences for group g, where $\left[\cdot\right]_j$ denotes the *j*-th column of a matrix.

8: Update $g=g+1$ and $S^{(g)}=S^{(g-1)}\backslash S_{g-1}$, where $S^{(g-1)}\backslash S_{g-1}$ denotes sequences in $S^{(g-1)}$ except S_{g-1}

9: **end if**

10: **end loop**

Table A.4.12-2: Algorithm for sequence grouping (For large power offset between adjacent groups)

1: Let $g=1$ and $S^{(1)}=S$ //Initialization

2: **loop**

3: **if** $g<G$ **then**

4: Find all $A=\begin{pmatrix} L-\sum_{m=1}^{g-1} L_m \\ L_g \end{pmatrix}$ combinations of L_g sequences from sequence pool $S^{(g)}$. Denote L_g sequences in the *a*-th combination as $S_a^{(g)}$

5: Find the index a^* of optimal combination for group g satisfying $\min\limits_{1\leq a\leq A} \sum\limits_{s_i, s_j \in S_a^{(g)}} \left|s_i^H s_j\right|^2$

6: The sequences for group g are $S_g=S_{a^*}^{(g)}$

7: Update $g=g+1$ and $S^{(g)}=S^{(g-1)}\{S¿_{g-1}$, where $S^{(g-1)}\{S¿_{g-1}$ denotes sequences in $S^{(g-1)}$ except S_{g-1}

8: **end if**

9: **end loop**

A.4.13 DM-RS designs for evaluation

For the evaluation of NOMA, the Rel.15 NR DMRS design is reused for the evaluation purpose for number of DMRS ports <= 12. In addition, different DM-RS designs to increase the number of DMRS ports compared to Rel.15 DM-RS have been considered by different sources. The following approaches are used in evaluations:

1) OCC code in both time and frequency domain, e.g.,
   - Same pattern as Rel-15 DMRS Type 2 with extended OCC code, i.e., length-4 FD OCC and length-2 TD OCC [53][58][60]; or length-2 FD OCC and length-4 TD OCC for 24 ports [53]; or length-4 FD OCC, and length-4 TD OCC for 48 ports [54];
2) Different numerologies, e.g.,
   - Two OFDM symbols overhead and ZC sequences with up to 3 roots and 24 CSs [55] for up to 72 ports.
3) Sparse frequency domain structure, e.g.,
   - Same pattern as Rel-15 DMRS Type 2 with 6 CDM group (length-2 FD-OCC and length-2 TD-OCC) for 24 ports [56][57][60];
   - Same pattern as Rel-15 DM-RS Type 1 with Comb 4 with 2 CSs and length-2 TD-OCC for 16 ports [57];
   - Same pattern as Rel-15 DM-RS Type 1 with Comb 6 with 2 CSs and length-2 TD-OCC for 24 ports.
4) Enlarged resources, e.g.,
   - Same pattern as Rel-15 DMRS Type 2 with additional resource by setting dmrs-AdditionalPosition = 1 for 24 ports [59][61].
5) More cyclic shifts, e.g.
   - Same pattern as NR DMRS Type 1 with ZC sequence, 2 symbol overhead, cyclic shift = 6, Comb-2, and length-2 TD OCC for 24 ports [51][62].
   - The cyclic shift gap depends on the total number of UEs, e.g. with 18 users, NR Type 2 DMRS with 1 symbol and cyclic shift = 4.
6) Quasi-orthogonal design using (up to) all roots of ZC sequences and all cyclic shifts, e.g. 70*72 ports supported for 6 PRB. This can be applied in conjunction with enlarged resources. [72]

A.5 Receiver complexity for MMSE-hybrid IC receiver

A complexity summary for the LMMSE receiver with hybrid interference cancellation can be found in the following table.

Table A.5-1: Total complexity of the LMMSE MUD with hybrid IC across all iterations

Receiver component	Detailed component	Computation in parametric number of usages, O(.) analysis, [impact factor]
		LMMSE with Hybrid IC
Detector	UE detection	$O\left(N_{AP}^{DMRS}\cdot N_{\Re}^{DMRS}\cdot N_{rx}\right)$
	Channel estimation	$O\left(N_{UE}\cdot N_{\Re}^{CE}\cdot N_{\Re}^{DMRS}\cdot N_{rx}\right)$
	Rx combining, if any	
	Covariance matrix calculation, if any	$O\left(N_{SF}^{2}.N_{rx}^{2}.N_{UE}.N_{\Re}^{data}/N_{\Re}^{adj}\right)$ $N_{UE}^{+¿}.N_{\Re}^{data}/N_{SF}$ $\left(N_{iter}^{'IC}-1\right)N_{SF}^{2}.N_{rx}^{2}.¿$ $+O¿$
	Demodulation weight computation, if any	$O\left(N_{SF}^{2}.N_{rx}^{2}.N_{UE}.N_{\Re}^{data}/N_{\Re}^{adj}\right)+O\left(N_{SF}^{3}.N_{rx}^{3}.N_{\Re}^{data}/N_{\Re}^{adj}\right)$ $N_{UE}^{+¿}.N_{\Re}^{data}/N_{SF}$ $\left(N_{iter}^{'IC}-1\right).N_{SF}^{2}.N_{rx}^{2}.¿+O\left(\left(N_{iter}^{'IC}-1\right).N_{SF}^{3}N_{rx}^{3}.N_{\Re}^{data}/N_{SF}\right)$ $+O¿$
	UE ordering, if any	
	Demodulation, if any	$O\left(N_{SF}.N_{rx}.N_{UE}.N_{\Re}^{data}/N_{\Re}^{adj}\right)$ $N_{UE}^{'+¿\,2}.N_{\Re}^{data}/N_{SF}$ $\left(N_{iter}^{'IC}-1\right).N_{SF}.N_{rx}.¿$ $+O¿$ $N_{UE}^{+¿}.N_{\Re}^{data}/N_{SF}$ $\left(N_{iter}^{'IC}-1\right).N_{SF}.N_{rx}.¿$ $+O¿$
	Soft information generation, if any	$N_{UE}^{+¿}.N^{bit}$ $N_{iter}^{'IC}.¿$ $O¿$
	Soft symbol reconstruction, if any	$O\left(N_{iter}^{'IC}.N_{UE}^{'S}.N_{\Re}^{data}.N_{rx}\right)$
	Soft symbol reconstruction, if any	
	Message passing, if any	
	Others	
Decoder	LDPC decoding	A: $N_{iter}^{'IC}.N_{UE}^{'}.N_{iter}^{LDPC}.\left(d_{v}N^{bit}+2\left(N^{bit}-K^{bit}\right)\right)$ C: $N_{iter}^{'IC}.N_{UE}^{'}.N_{iter}^{LDPC}.\left(2d_{c}-1\right)\cdot\left(N^{bit}-K^{bit}\right)$
Interference cancellation	Symbol reconstruction(Including FFT operations for DFT-S-OFDM waveform), if any	
	LLR to probability conversion, if any	$O\left(N_{iter}^{'IC}.N_{UE}^{'F}.2^{Q_{m}}.N_{\Re}^{data}/N_{SF}\right)$

	Interference cancellation	Complexity of addition ignored
	LDPC encoding, if any	Buffer shifting: $N_{iter}^{'IC} \cdot N_{UE}^{'S} \cdot (N^{bit} - K^{bit})/2$ Addition: $N_{iter}^{'IC} \cdot N_{UE}^{'S} \cdot (d_c - 1)(N^{bit} - K^{bit})$

Note: The following notation is used in Table A.5-1.

- $N_{iter}^{'IC}$ average number of IC iterations.
- $N_{UE}^{'}$ average number of UEs processed per iteration.
- $N_{UE}^{'+}$ average number of UEs per IC iteration excluding the first iteration.
- $N_{UE}^{'S}$ average number of successfully decoded UE per IC iteration.
- $N_{UE}^{'F}$ average number of UEs that were not successfully decoded per IC iteration.

A.6 Impact of $N_{\Re}^{adj}$ on the BLER performance

The impact of $N_{\Re}^{adj}$ on the BLER performance for MMSE hard IC receiver is analysed by Source 1 [64], Source 2 [65], Source 4 [69], and in [70] and [71].

- The analysis from Source 1 indicates the BLER performance can be similar between $N_{\Re}^{adj}$ = *4* and $N_{\Re}^{adj}$ = *48* for different packet sizes, when the UE speed is 3km/h;
- The analysis from Source 2 indicates when $N_{\Re}^{adj}$ > *N*_SF, *N*_SF = *2 or 4*,
  - the value of $N_{\Re}^{adj}$ as large as 24, 48 at UE speed higher than 3 km/h, e.g. 60km/h or 120 km/h, can cause significant BLER performance degradation for larger TBS, e.g. 75 bytes or 150 bytes;
  - the value of $N_{\Re}^{adj}$ as large as 144, can cause significant BLER performance degradation even for 20 bytes TBS at 3km/h;
- The analysis from Source 4 indicates that for $N_{\Re}^{adj}$ =*48* and *N*_SF = *4*, negligible or 0.15 dB performance loss is observed for 20 bytes TBS at 30 km/h or 120km/h respectively;
- The analysis in [70] indicates that the impact of $N_{\Re}^{adj}$ on BLER performance depends on both time and frequency selectivity of the channel, and the evaluation shows that
  - no clear performance degradation is observed for $N_{\Re}^{adj}$ = *24 or 144* at UE speed of 3km/h
  - 0.3 dB ~0.9 dB loss is observed for $N_{\Re}^{adj}$ = *24 or 144*, respectively at UE speed of 30 km/h
  - severe performance degradation is observed at UE speed of 60 km/h
- The analysis in [71] indicates that the practical implementation should consider to use $N_{\Re}^{adj}$ =*N*_SF

Annex B:
Change history

Change history							
Date	**Meeting**	**TDoc**	**CR**	**Rev**	**Cat**	**Subject/Comment**	**New version**
2018-02	RAN1#92	R1-1801413				Initial draft skeleton	0.0.0
2018-02	RAN1#92	R1-1803329				Endorsed draft skeleton	0.0.1
2018-04	RAN1#92b	R1-1803613				Text proposal for LLS parameters in TR 38.812 (NOMA)	0.0.2
2018-08	RAN1#94	RP-1808150				Text proposal to capture agreements made in RAN1#93 to TR 38.812 (NOMA)	0.0.3
2018-08	RAN1#94	R1-1810046				MCC clean-up based on endorsed version in R1-1808150	0.1.0
2018-11	RAN1#95	R1-1814006				Text proposal to capture agreements made in RAN1#94 and RAN1#94bis to TR 38.812 (NOMA)	0.2.0
2018-11	RAN1#95	R1-1814347				Text proposal to capture agreements made in RAN1#95 to TR 38.812 (NOMA)	0.3.0
2018-11	RAN1#95	R1-1814407				Adding missing table and some link-level calibration results in Subclause A.1.2	0.4.0
2018-12	RAN#82	RP-182478				MCC clean up – version for one-step approval	1.0.0
2018-12	RAN#82					Following RAN#82 decision, Rel-16 specification goes under change control	16.0.0